A SPECTROSCOPIC STUDY OF SQUARE PLANAR RHODIUM(I) COMPLEXES

A thesis submitted to the

UNIVERSITY OF CAPE TOWN

in fulfilment of the requirements for the degree of

DOCTOR OF PHILOSOPHY

by

PHILIP SIMON HALL

M.Sc. (University of Cape Town)

Department of Inorganic Chemistry
University of Cape Town
Rondebosch 7700
South Africa

August 1989

" IMAGINATION

IS MORE IMPORTANT

THAN KNOWLEDGE "

EINSTEIN

ACKNOWLEDGEMENTS

My sincere thanks and appreciation are to be extended to:

- My supervisors, Professors G.E. Jackson, J.R. Moss and D.A. Thornton for their interest, encouragement and discussion in directing this study.

- Professor K.R. Koch, for his invaluable assistance and interest in recording the ^{15}N nmr spectra.

- Dr. P.F.M. Verhoeven for recording the Raman spectral data, and for assistance provided for the normal coordinate analysis study.

- My colleagues and friends in the School of Chemistry, especially Ms. I. Nel for her valued friendship and moral support.

- The University of Cape Town and The South African Council for Scientific and Industrial Research for financial assistance.

ABSTRACT

Ninety square planar Rh(I) complexes of the type *cis*-$[Rh(CO)_2(X)(L)]$, $[Rh(COD)(X)(L)]$, $[Rh(CO)_2(L)_2]ClO_4$ and $[Rh(COD)(L)_2]ClO_4$ (X is Cl or Br; COD is 1,5-cyclooctadiene; L is aniline, pyridine, pyridine *N*-oxide, imidazole and ammonia), as well as their isotopically labelled derivatives (^{13}CO, ^{2}H and ^{15}N) were prepared, characterized by microanalysis and melting point, and investigated by the following spectroscopic techniques: infrared, Raman, ultraviolet, mass spectrometry, and ^{1}H, ^{13}C and ^{15}N nmr spectroscopy.

The comprehensive isotopic labelling studies allowed unambiguous assignment of the infrared modes in the 4000-50 cm^{-1} region. The infrared assignments are discussed with reference to their ν^D/ν^H ratios, the various ligands and halogens used, the charges on the complexes, and are compared to similar compounds.

The ^{1}H, ^{13}C and ^{15}N nmr runs were performed at room and low temperatures. Fluxionality of the ligands (L) was observed and the exchange process was monitored by variable temperature nmr. The enthalpy and entropy values for the *inter*molecular exchange of L in the complexes *cis*-$[Rh(CO)_2(X)(L)]$ were obtained by a complete computer simulated band shape analysis of the carbonyl region of the ^{13}C nmr spectra.

The non-equivalence, and specific assignment of the carbonyl groups in the *cis*-$[Rh(CO)_2(X)(L)]$ complexes were determined by recording the variable temperature ^{13}C nmr spectra of the doubly enriched species *cis*-$[Rh(^{13}CO)_2(X)(^{15}N\text{-ligand})]$. $^{2}J(^{13}C\text{-}Rh\text{-}^{15}N)$ values are reported for the first time. The $^{1}J(^{15}N\text{-}^{103}Rh)$ coupling constants are rationalized in terms of the metal-

nitrogen bonding, and correlate with the *s*-character of the bonding electron on nitrogen.

While the solution electronic spectra reveal that the complexes are discrete monomeric entities in solution, there are indications of metal-metal interactions in the solid-state.

The normal coordinate analysis study of the complexes *cis*-$[Rh(CO)_2(X)(L)]$ involved the calculation of a general valence force field by applying the eigenvector method of Becher and Mattes. The results show that point-mass-modelling and simplified force field, as assumed in our treatment, describes, to a good approximation, the vibrational properties of the complexes. The potential energy distribution provided further support for the proposed infrared assignments of the complexes.

ABBREVIATIONS

an	=	aniline
py	=	pyridine
pyO	=	pyridine *N*-oxide
imid	=	imidazole
COD	=	1,5-cyclooctadiene

ν	=	stretch
δ, α	=	in-plane bend
γ, π	=	out-of-plane bend
τ	=	twist
ω	=	wag
ρ	=	rock

Subscripts s and as denote symmetric and antisymmetric modes, respectively.

Although the dimensions of ν (frequency) and $\tilde{\nu}$ (wavenumber) differ, it is traditional to use them interchangeably. All the spectral data in this thesis are given in terms of $\tilde{\nu}$ (cm^{-1}).

TABLE OF CONTENTS

CHAPTER 1

INTRODUCTION

1. General

Rhodium was first isolated by W.H. Wollaston in 1804. He named the new element rhodium (Greek *rhodos* - a rose) "from the rose colour of a dilute solution of the salts containing it" [1]. However, progress in rhodium complex chemistry was slow and it was not until 1912 that Werner established the stereochemistry of rhodium (III) complexes [2,3].

The mundane chemistry of rhodium began a new life with the discovery of the remarkable catalytic properties of $[Rh(Cl)(PPh_3)_3]$ by Wilkinson and co-workers in the 1960's [4,5]. Since then the chemistry of rhodium has rapidly diversified and expanded and its use is now commonplace in many industrial and practical applications. Approximately 70% of the total western world demand for rhodium last year arose in the autocatalyst sector for the control of exhaust emissions. The main other uses are in the chemical (nitric acid industry), glass (glass fibre production) and electrical (manufacture of thermocouples) sectors [6].

Although rhodium has various oxidation states, almost all of its complexes involve either the tri- or mono- valent states. Almost all rhodium (III) species are octahedral while the rhodium (I) species are mainly square planar.

To understand the preferential formation of square planar rhodium (I) complexes, it is necessary to consider the crystal field splitting of the various geometries, see Figures 1.1 and 1.2. The essence of this crystal field theory [7] is that the five *d* orbitals, which are degenerate and equal in energy in the gaseous metal ion, become differentiated in the presence of the electrostatic field due to the ligands. Those

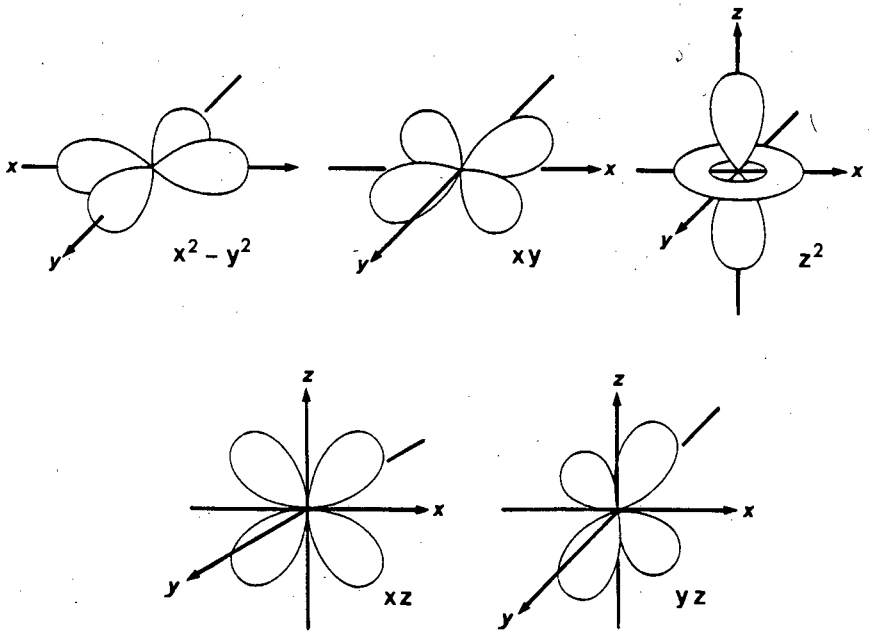

Figure 1.1 Spatial arrangement of the five *d* orbitals.

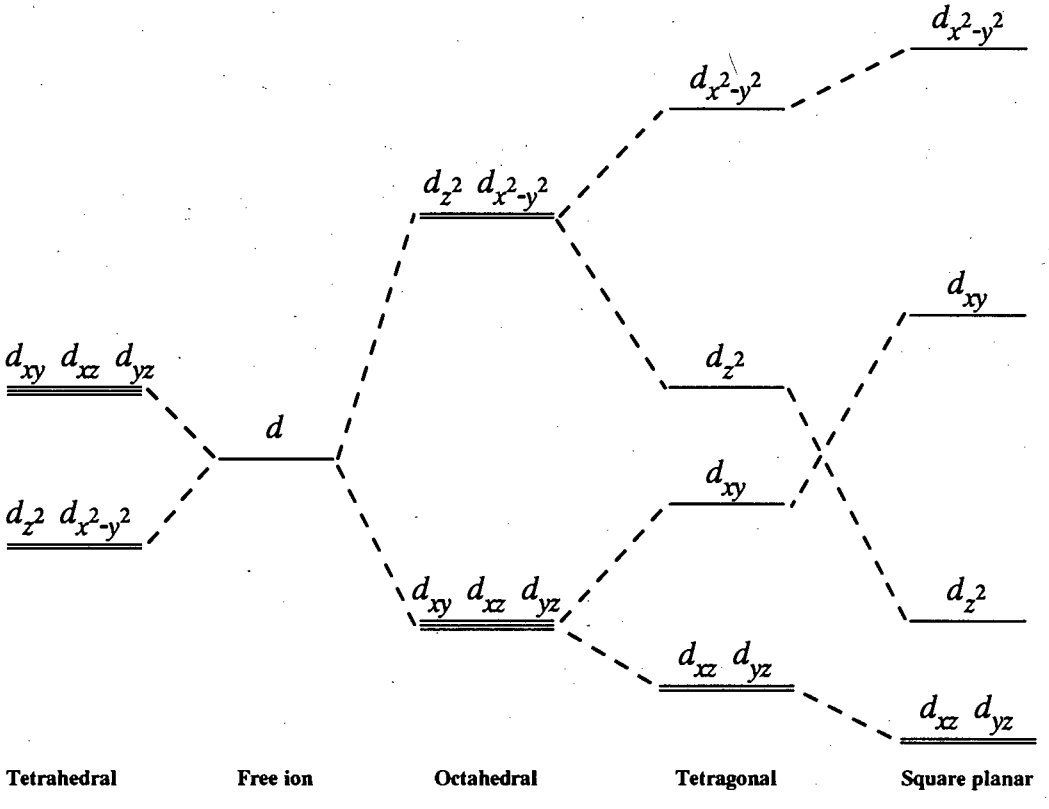

Figure 1.2 Crystal field splittings of the *d* orbitals of a central ion in regular complexes of various structures.

orbitals lying in the direction of the ligands are raised in energy with respect to those orbitals lying away from the ligands. By preferentially filling the low-lying orbital levels, the *d* electrons can stabilize the system, as compared to the case of random filling of the *d* orbitals. The gain in bonding energy achieved in this way may be called the crystal field stabilization energy (CFSE).

With the above in mind, and the fact that Rh^{+1} has eight *d* electrons, it is quite apparent why square planar geometry is the most favoured, since it is possible to leave the antibonding $d_{x^2-y^2}$ orbital empty.

2. Application of Group Theory to Molecular Vibrations

The concept of symmetry is important to almost every aspect of life in our universe. For instance, when molecules and ions conglomerate into crystals they do so to give extensive structures with well-defined symmetry. The quantitative discussion of symmetry is called Group Theory. The symmetry elements of a molecule determine the point group to which it belongs. These point groups, with their specific symmetry elements, constitute the character tables and may be found in many vibrational spectroscopy texts [8-10].

Consider a molecule composed of *N* atoms. All the movements (translational, rotational and vibrational) of the atoms within the molecule may be resolved into components along the *x*-, *y*- and *z*- axes. Thus, there are a total of $3N$ possible movements in the molecule of which six are translational and rotational, while the remaining $3N-6$ ($3N-5$ for a linear molecule) are internal molecular vibrations. The symmetries of these vibrational modes are categorized by labelling each atom of the molecule with three Cartesian coordinates representing unit displacement vectors. These vectors represent all the $3N$ degrees of freedom, and on performing the

symmetry operations we can relate new vector positions to old vector positions by [3*N* x 3*N*] matrices, whose character, χ, forms a reducible representation, Γ_{total}.

The application of Group Theory is best seen by example. Consider more specifically complexes of the type *cis*-[$Rh(CO)_2(X)(L)$], (see Figure 1.3) which will be examined in Chapters 3 and 6.

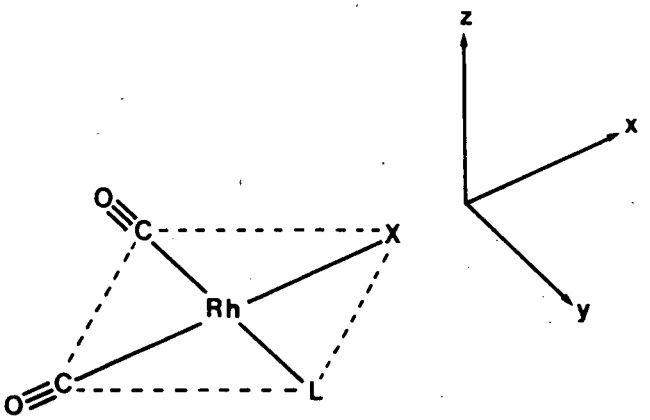

Figure 1.3 Square planar structure of *cis*-[$Rh(CO)_2(X)(L)$]

By regarding the ligand (L), as a point mass, the molecule has an inherent C_s symmetry for which Γ_{total} is

C_s	E	$\sigma(xy)$
Γ_{total}	21	7

To determine the symmetry species of all the possible molecular motions, the following reduction formula is applied:

$$N_i = 1/h \left(\Sigma \chi_R \chi_I N \right)$$

where N_i = the number of times each irreducible representation appears in the reducible representation,

h = the order of the group

χ_R = character of the reducible representation

χ_I = character of the irreducible representation

N = number of symmetry operations in each class.

Thus the 21 possible molecular motions for *cis*-[Rh(CO)$_2$(X)(L)] are:

$$\Gamma_{3N} = 14A' + 7A''$$

The molecular translations and rotations are obtained from the character table of the molecule. These are tables of the irreducible representations containing information regarding the nature of these representations and their properties. Thus for *cis*-[Rh(CO)$_2$(X)(L)] we have:

Symmetries for all molecular motions	$14A' + 7A''$
Symmetries for translations	$2A' + 1A''$
Symmetries for rotations	$1A' + 2A''$
Symmetries for vibrations (Γ_{vib})	$11A' + 4A''$

To determine the number of stretches and bends which constitute Γ_{vib}, internal displacement vectors are chosen on a new basis for the point group representation. To determine the reducible representation for the stretches, vectors are drawn along the bonds. Any vector unshifted by a symmetry operation will contribute +1 to the character of the matrix, while any vector shifted will contribute zero. For *cis*-[Rh(CO)$_2$(X)(L)] this yields:

C_s	E	$\sigma(xy)$
$\Gamma_{stretch}$	6	6

which reduces to

$$\Gamma_{stretch} = \quad 6A'$$

and the bends are obtained by subtracting $\Gamma_{stretch}$ from Γ_{vib}, yielding

$$\Gamma_{bend} = \quad 5A' \quad + \quad 4A''$$

Another aspect that can be determined from the symmetry elements is whether fundamentals, that is, stretches and bends, are infrared or Raman active. A fundamental will be infrared active if during vibration there is a resultant change in dipole moment. The dipole moment changes in a similar manner as the *x*-, *y*- and *z*-coordinates, hence a vibration will be infrared active if it belongs to the same representation as any of the internal displacement vectors. This can be read directly from the character table. Similarly, a fundamental will be Raman active, depending on the polarizability of the bond, if the mode involved belongs to the same representation as any of the components of the polarizability tensor of the molecule. Any irreducible representation having the transformation properties of x^2, y^2, z^2, xy, xz or yz is therefore Raman active. Thus for *cis*-[$Rh(CO)_2(X)(L)$] all the stretches and bends are both infrared and Raman active. The in-plane and out-of-plane modes are shown in Figures 1.4 and 1.5, respectively.

The above discussion only applies when one considers the molecule to be an isolated unit [8-10], for instance, as in the gaseous phase where the vibrations of the molecule are restricted only by its own point symmetry. In the solid state the molecule can no longer be regarded as a separate entity and is subject to the symmetry restrictions of its crystalline environment. Any rigorous vibrational analysis would need to consider the entire array of molecules, which for all practical purposes is an impossible task. Fortunately, site group and factor group analyses make certain assumptions that provide valid approximations. However, for both approximations a full x-ray crystal structure with atomic coordinates is necessary.

STRETCHES

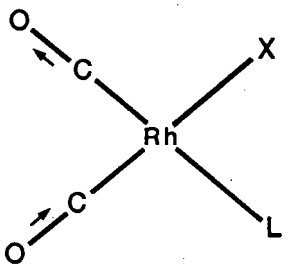

ν_{as}(CO)

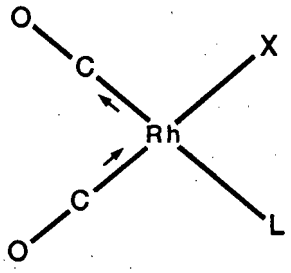

ν_{as}(RhC)

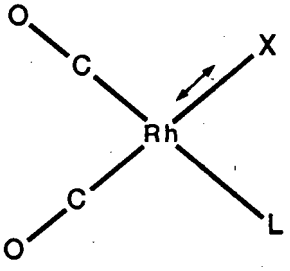

ν(RhX)

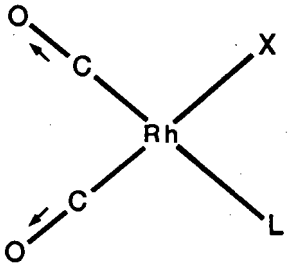

ν_{s}(CO)

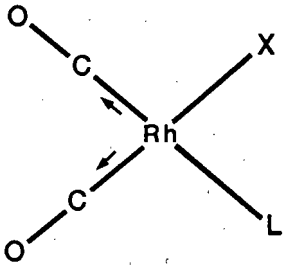

ν_{s}(RhC)

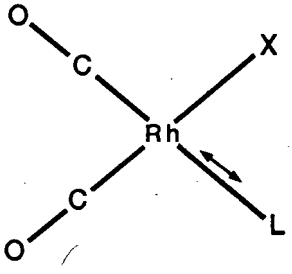

ν(RhL)

BENDS

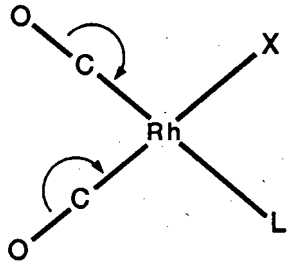

δ_{as}(RhCO)

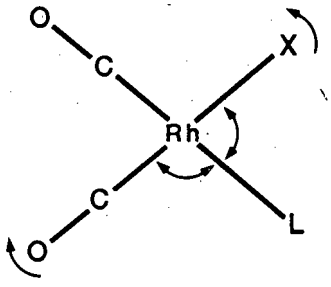

δ(RhX)

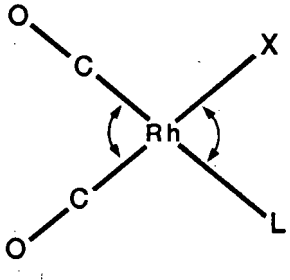

δ(CRhC)

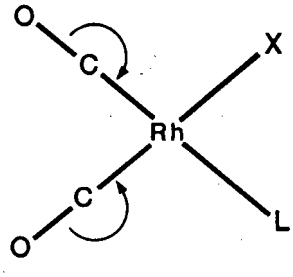

δ_{s}(RhCO)

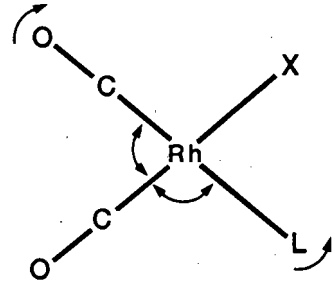

δ(RhL)

Figure 1.4 The in-plane modes of *cis*-[Rh(CO)$_2$(X)(L)].

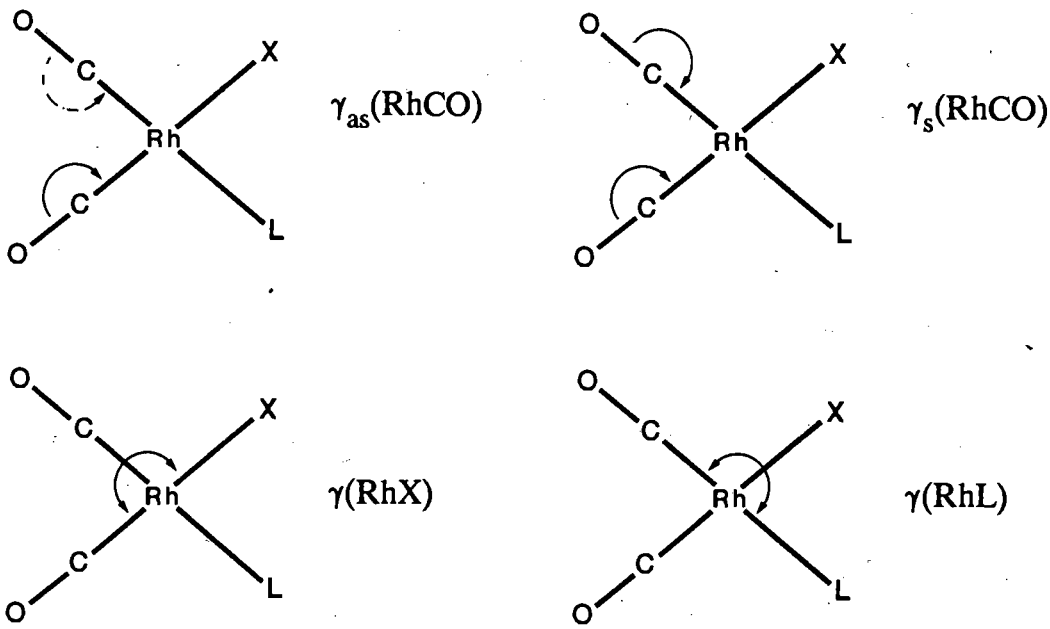

Figure 1.5 The out-of-plane modes of *cis*-[Rh(CO)$_2$(X)(L)].

Factor group analysis is the more rigorous of the two approximations since it accounts for lattice modes and solid state splitting of nondegenerate vibrations of the free molecule. Halford [11], and Adams and Newton [12] list useful information for the use of these two group analyses.

Hence, Group Theory can provide useful information regarding the expected number and types of infrared (and Raman) bands in molecules. This data is helpful for the assignment of bands in the vibrational spectra.

3. Techniques Applied to the Assignment Problem

Among the many vibrations of metal complexes, the assignments of the metal-ligand vibrations are the most important since their frequencies, species and number provide direct information regarding the structure of the complex and the nature of the metal-ligand bond. These vibrations generally appear below 600 cm^{-1} in the

infrared spectrum because of the high mass of the metal ion and the relatively weak nature of the metal-ligand bond. However, their assignments are often difficult to make because the infrared spectrum is complicated by intermolecular interactions, lattice modes, lowering of symmetry, vibrational coupling, and the appearance of ligand vibrations activated by complex formation [13,14]. In order to identify the metal-ligand vibrations several techniques may be applied, as discussed below.

3.1 Comparison between the spectra of the free ligand and the complex

This "empirical" method involves, *inter alia*, a visual comparison between the spectra of the free ligand and the complex. Since metal-ligand vibrations are absent from the free ligands, a comparison of the spectra yields assignments for the metal-ligand modes. This method often fails to give unambiguous assignments as some ligand vibrations activated by complex formation may appear in the same region as the metal-ligand vibrations. A further difficulty may arise when the localized complexed ligand symmetry is different from the free ligand molecular symmetry [13].

3.2 Comparison between spectra of isostructural complexes

On the basis of symmetry considerations, isostructural complexes should give rise to similar vibrational spectra. Thus, in an isostructural series of complexes, the difference between the infrared spectra may be related to the differences in the nature of the bonding in the series of complexes. For instance, in isostructural complexes containing coordinated halides, the large change in the masses of the halide ligand yields dramatic shifts of the metal-halide frequencies. This allows for their easy identification.

3.3 Isotopic labelling

The replacement of an atom by its isotope results in a change in frequency of any vibration involving that particular isotopic species. The expected isotopic shifts can be calculated, to a reasonable approximation, by assuming the labelled atom to be part of a simple harmonic diatomic oscillator [15]. The vibrational frequency of such a system can be represented by the equation:

$$\nu = 1/2\pi c\,(f/\mu)^{½}$$

while the vibrational frequency of the corresponding isotopically labelled system can be given by:

$$\nu^{i} = 1/2\pi c\,(f/\mu^{i})^{½}$$

where ν = vibrational frequency,

f = harmonic force constant,

μ = reduced mass of the molecule,

c = velocity of light,

and the superscript i refers to the labelled system.

If one then assumes that the force constants are unaltered by isotopic substitution, which to a good approximation is the case [10], the expected isotopic shifts may be calculated from:

$$(\nu^{i}/\nu) = (\mu/\mu^{i})^{½}$$

The ν^{i}/ν ratio is therefore useful in determining the expected frequency shifts on isotopic labelling. However, it should be noted that the observed frequency shifts which result from labelling are subject to certain other factors. These include factors such as the extent to which the labelled atoms participate in the particular

vibration, that is, vibrational coupling, the number and nature of the atoms in the molecule that have been labelled, and the extent of hydrogen bonding. Thus the observed shift will be greatest if the molecule is simple with no vibrational coupling occurring, that is, with each bond being as vibrationally pure as possible.

Both ligand isotopic labelling and metal isotopic labelling can be applied to a complex. However, since the magnitude of the isotopic shift is dependent on the mass difference between the isotopes, the metal isotopic labelling is not as effective as ligand isotopic labelling. Nevertheless, metal isotopic labelling has been successfully employed to aid vibrational assignments [16,17]. Another advantage of ligand labelling is the availability of many isotopic pairs yielding large mass difference ratios.

It has been extensively shown that the isotopic labelling method is by far the most unambiguous and simple method of assigning bands in the infrared spectrum [18]. The major limitation appears to be the availability and cost of the isotopes.

3.4 The ν^D/ν^H ratio

Since deuteration results in the largest isotopic shifts and is generally the most accessible type of labelling, most labelling studies have employed this isotope [15]. The ratio ν^D/ν^H between the frequencies of corresponding bands in the infrared spectra of deuterated and normal molecules serves as an effective distinction between the C-H stretching (or bending) modes and the ring stretching (or bending) modes in aromatic and heterocyclic compounds [15].

Thornton and co-workers [19,20] have studied the ν^D/ν^H ratio for a number of complexes of heterocyclic bases and the results of their findings may be summarized as follows:

- The ratio ν^D/ν^H varies from 0.68 to 0.85 for the C-H modes.
- The ratio ν^D/ν^H varies from 0.85 to 1.00 for the ring modes.

Thus distinction between the above modes and metal-ligand modes, or any other vibration of other functional groups within a complex is possible since the latter generally yield ν^D/ν^H ratios very close to unity.

3.5 Normal Coordinate Analysis

The calculation of normal vibrations has two aspects. Firstly, it provides force constants, and secondly, it supports the assignments of the observed vibrational bands with use of calculated frequencies.

The theory regarding vibrational analysis will not be discussed here since it can be found in many fine references [9,10,21-23]. A brief account of the utilization of vibrational analysis is presented in Chapter 6, and it suffices to say that a normal coordinate analysis tests a set of chosen vibrational assignments. While a good fit between the calculated and experimental frequencies may well be considered to be conclusive proof of a vibrational assignment, there is often difficulty in interpreting the force constants used in the modelling of the molecule.

In conclusion, it should be emphasized that of the several techniques available to aid the choice of correct assignment of the vibrational modes, each has its own merits and limitations. Hence the techniques should be used in a complementary rather than a competitive manner. The more techniques used, the more

information becomes available, thus, the more accurate the final assignment should be.

4. Dynamic Nuclear Magnetic Resonance (DNMR)

Nuclear magnetic resonance spectroscopy, in addition to providing valuable data in the form of chemical shifts and coupling constants, has been extensively used in the study of certain types of rapid equilibria. This has contributed much to the insight into the dynamic nature of molecular systems. The line-widths and spectral shapes may change for various reasons, quite profoundly with temperature, and for this reason considerable effort [24-29] has been channelled into the determination of exchange rates from spectral shapes, so that activation parameters can be obtained from Arrhenius-type temperature-rate plots. Although it is sometimes possible to extract dynamic information from band shapes using simple formulae, the band shape formulae are generally too inexact for algebraic analysis and one must resort to numerical methods. Hence, it is quite normal to compute band shapes using a digital computer and to find a best fit to the experimental band shapes.

There are two basic types of computer programmes for calculating nmr spectra, non-iterative and iterative programmes, the latter being an expansion of the former. Both programmes require as their input a set of molecular parameters (number of nuclei, chemical shift, coupling constants, etc.) and from these the computer calculates a trial spectrum - this is the non-iterative step. When the predicted spectrum bears an adequate resemblance to that observed experimentally, the programme may then be used in the iterative mode. Additional data about the experimental system is fed into the programme, from which the computer obtains optimum values of these parameters by a least squares fit.

Once satisfactory parameters (relaxation times and exchange rate constants) have been determined by the computing process as a function of temperature, we are now in a position to calculate the activation parameters for the chemical system investigated.

Nuclear exchange processes usually lend themselves to clear-cut chemical interpretation and it is therefore standard practice to convert the corresponding rates to activation parameters. The free energy of activation can be calculated from a single rate constant, (K), at a single temperature by means of the Eyring equation,

$$K = (k\,T/h)\,(\exp(-\Delta G^{\ddagger}/R\,T))$$

where k, h, R = Boltzmann, Planck and gas constant, respectively

T = temperature in Kelvin

$\Delta G^{\ddagger}$ = free energy of activation difference between the initial and the transition state.

Rate constants measured over a range of temperatures may be converted into Arrhenius activation energies and frequency factors, or to enthalpies and entropies of activation by using the following two equations:

$$K = A \exp(-E^{a}/R\,T)$$

$$K = (k\,T/h)\,[\exp(-\Delta H^{\ddagger}/R\,T)\exp(\Delta S^{\ddagger}/R)]$$

where A = Arrhenius pre-exponential factor

E^{a} = activation energy

$\Delta H^{\ddagger}$ = enthalpy of activation difference between the initial and the transition state

$\Delta S^{\ddagger}$ = entropy of activation difference between the initial and the transition state.

The generally used method for obtaining activation parameters is therefore to carry out a complete band shape analysis over as wide a temperature range as possible, and then to obtain the Arrhenius activation parameters from a plot of ln$K$ against $1/T$. The enthalpy and entropy of activation are given by the slope and intercept, respectively. However, it is essential that error analysis be performed in order to test the validity of the calculated parameters, as explained below.

Various workers [29-31] have shown by statistical principles that dynamic parameters extracted from NMR band shapes are subject to systematic as well as statistical errors. From their findings it can be stated that $\Delta G^{\ddagger}$ is insensitive to errors in K and T, while E^{a} is very sensitive to errors in K and T. This is because although $\Delta H^{\ddagger}$ and $\Delta S^{\ddagger}$ are error-sensitive, the errors tend to cancel each other with the result that $\Delta G^{\ddagger}$ is insensitive to errors ($\Delta G^{\ddagger} = \Delta H^{\ddagger} - \Delta S^{\ddagger}$). It can further be shown that the most precise results are obtained in the region of coalescence, where the band shape is most sensitive to the rate constant, K. As one diverges from the coalescence region the precision deteriorates, and it is for this reason that a least squares fit with error propagation is preferable to the normal graphical methods.

REFERENCES

1 W.H.WOLLASTON,
Philos. Trans. R. Soc., (London), **94** (1804) 419

2 A.WERNER,
Chem. Ber., **2** (1912) 1228

3 W.P.GRIFFITH,
"The Chemistry of the Rarer Platinum Metals", Interscience Publishers, London, (1967)

4 F.H.JARDINE, J.A.OSBORN, G.WILKINSON AND J.F.YOUNG,
Chem. Ind., (London), (1965) 560

5 J.A.OSBORN, F.H.JARDINE, J.F.YOUNG AND G.WILKINSON,
J.Chem. Soc., **A** (1966) 1711

6 *"Platinum 1987"*, Johnson Matthey Publication, London, (1987)

7 B.N.FIGGIS,
"Introduction to Ligand Fields", Wiley, New York, (1966)

8 F.A.COTTON,
"Chemical Applications of Group Theory",
2nd ed., Wiley-Interscience, New York, (1971)

9 K.NAKAMOTO,
"Infrared and Raman Spectra of Inorganic and Coordination Compounds",
4th ed., Wiley-Interscience, New York, (1986)

10 E.B.WILSON, J.C.DECIUS AND P.C.CROSS,
"Molecular Vibrations", McGraw-Hill, New York, (1955)

11 R.S.HALFORD,
J.Chem. Phys., **14** (1946) 8

12 D.M.ADAMS AND D.C.NEWTON,
"Tables for Factor Group and Point Group Analysis", Beckman - RIIC LH, Croydon, (1970)

13 J.R.FERRARO,
"Low-Frequency Vibrations of Inorganic and Coordination Compounds",
Plenum Press, New York, (1971)

14 D.M.ADAMS,
J. Chem. Soc., (1964) 1771

15 S.PINCHAS AND I.LAULICHT,
"Infrared Spectra of Labelled Compounds", Academic Press, London, (1971)

16 K.NAKAMOTO
Angew. Chem. Int. Ed. Engl., **11** (1972) 666

17 M.L.NIVEN AND D. A.THORNTON,
Spectrosc. Lett., **13** (1980) 419

18 G.C.PERCY AND H.S.STENTON,
J. Chem. Soc. (Dalton Trans.), (1976) 1466, 2429

19 A.T.HUTTON AND D. A.THORNTON,
Spectrochim. Acta, **34A** (1978) 645

20 G.A.FOULDS, J.B.HODGSON, A.T.HUTTON, M.L.NIVEN, G.C.PERCY, P.E.RUTHERFORD AND D. A.THORNTON,
Spectrosc. Lett., **12** (1979) 25

21 P. GANS,
"Vibrating Molecules", Chapman and Hall, London, (1971)

22 N.B.COLTHUP, L.H.DALY AND S.E.WIBERLEY,
"Introduction to Infrared and Raman Spectroscopy", Academic Press, New York & London, (1964)

23 D.F.MCINTOSH AND K.H.MICHAELIAN,
Can. J. Spectrosc., **24** (1979) 1, 35, 65

24 A.ALLERHAND, H.S.GUTOWSKY, J.JONAS AND R. A.MEINZER,
J. Am. Chem. Soc., **88** (1966) 3185

25 D.S.STEPHENSON AND G.BINSCH,
J. Magn. Reson., **32** (1978) 145

26 D.A.KLEIER AND G.BINSCH,
J. Magn. Reson., **3** (1970) 146

27 C.W.HAIGH,
Annu. Rep. NMR Spectrosc., **4** (1971) 311

28 L.M.JACKMAN AND F.A.COTTON (EDS.),
"Dynamic Nuclear Magnetic Resonance Spectroscopy", Academic Press, New York, (1975)

29 J.SANDSTRÖM,
"Dynamic NMR Spectroscopy", Academic Press, London, (1982)

30 R.R.SHOUP, E.D.BECKER AND M.L.MCNEEL,
J. Phys. Chem., **76** (1972) 71

31 A.ALLERHAND AND E.THIELE,
J. Chem. Phys., **45** (1966) 902

CHAPTER 2

EXPERIMENTAL

(1) PHYSICAL METHODS

Infrared Spectra

The mid-infrared spectra (4000–300 cm^{-1}) were recorded on a Perkin-Elmer 983 spectrophotometer using Nujol mulls and hexachlorobutadiene (HCBD) between potassium bromide plates. The far-infrared spectra were determined as Nujol mulls (500–50 cm^{-1}) between polyethylene plates on a Digilab FTS-16B/D interferometer. Solution spectra (2200–1550 cm^{-1}) were determined using potassium bromide solution cells using nitrogen saturated spectroscopic grade dichloromethane.

The quoted wavenumber accuracy of the spectrophotometer is ±2 cm^{-1} for the 4000–2000 cm^{-1} region and ±1 cm^{-1} for the 2000–180 cm^{-1} region. The repeatability is better than 0.1 cm^{-1}. A resolution of 0.5 cm^{-1} can be obtained using the highest scan mode. The model 983 is based on a double-beam, ratio-recording technique with pre-sample chopping principle and has integral data handling as well as digital display facilities. The optics involved are a purgable F4.2 monochromator with 4 gratings and 9 filters [1]. The FTS-16B/D is an automatic ratio recording far-infrared vacuum interferometer with a resolution to 0.5 cm^{-1} throughout the spectral range of 500 to 50 cm^{-1}. The instrument consists of a model 296A Michelson interferometer, 4 interchangeable Mylar beamsplitters, a high pressure mercury arc source, a triglycine sulfate detector, an analog-to-digital converter, a data system with 8K of core memory, a 1.2 million word moving head disk, a digitally controlled plotter, and related software [2].

Raman Spectra

The Raman spectra were recorded on a Spex instrument, model 1403, using a Spectra Physics Model 164 Ar^+-laser for excitation and the 488.0 nm (or 514.5 nm) line with interference filters to remove plasma lines. Laser powers ranged between 100 to 300 mW at the sample. Different slit widths were used to optimize the signal-to-noise ratio and resolution. Samples were recorded either as solutions, powders, or discs. The best results were obtained when the sample was a pure disc mounted in a pellet holder which was rotated to minimize decomposition of the intensely coloured complex in the laser beam. It should be pointed out that in Raman, the relative intensities of combination and overtones bands are much weaker than in infrared. Consequently all the vibrational bands observed are due to fundamental transitions, unless they are part of Fermi-resonance systems.

Electronic Spectra

The electronic spectra were recorded on a Varian Superscan 3 ultraviolet and visible spectrophotometer in the absorbance mode using nitrogen saturated spectroscopic grade dichloromethane in 10 mm cells.

Nuclear Magnetic Resonance Spectra

The ^1H, ^{13}C and ^{15}N nmr spectra were recorded on a Varian VXR-200 Fourier transform spectrometer operating at 200.0, 50.3 and 20.3 MHz, respectively. Various deuterated solvents were used depending on the solubility of the complexes.

The ^1H and ^{13}C chemical shifts (δ values) were measured relative to the internal solvent resonances and are reported in parts per million downfield from tetramethylsilane (TMS) using the following conversion factors.

^{1}H spectra	δ (TMS)	= δ (acetone-d_6)	- 2.05
	δ (TMS)	= δ ($CDCl_3$)	- 7.27
	δ (TMS)	= δ (DMF-d_7)	- 8.01
^{13}C spectra	δ (TMS)	= δ (acetone-d_6)	- 29.80
	δ (TMS)	= δ ($CDCl_3$)	- 77.00
	δ (TMS)	= δ (DMF-d_7)	- 167.70

The ^{15}N chemical shifts are given relative to that of pure nitromethane ($CH_3{}^{15}NO_2$) as an external standard, with negative signs for low frequency and positive signs for high frequency shifts. Generally less than 100 scans were required in order to achieve a signal-to-noise ratio greater than 20:1 for the ^{15}N-enriched complexes in the ^{15}N nmr spectra.

Unless otherwise specified, the nmr spectra were recorded at room temperature (ambient=298K). In the variable temperature nmr runs the sample temperature accuracy was verified by measuring the known peak separations in methanol [3]. Temperature accuracy was within 0.5° over the entire range.

Mass Spectra

Mass spectra were measured on a VG Micromass 16F instrument operating in the electron impact mode, with electron beam energy 70 eV and ion accelerating voltage 3KV, and with ion source temperatures in the range 350–470 K.

Melting Point

Melting points were determined on a Reichert Thermovar hot-stage microscope, and are uncorrected.

Microanalyses

Microanalyses were performed by Mr. W.R.T. Hemsted, of this University, on a Heraeus Universal combustion analyzer model CHN-MIKRO.

Computation

All computations were performed at the computer centre of the University of Cape Town on a Sperry-Univac series 1100 computer.

The normal coordinate analysis programmes were originally written by Dr. B. Van der Veken, Laboratorium voor anorganische chemie RUCA, Antwerpen (Belgium), and were updated to the level 10R1 in FORTRAN(ASCII) by Dr. P.F.M. Verhoeven. The programme package consists of the following routines.

name of routine	function
CART	calculation of molecular geometry from internal coordinates
GMATRIX	calculation of the kinetic energy matrix coefficients
BECMAT	calculation of a force field set from a set of vibrational frequencies
GFMATRIX	calculation of vibrational frequencies from G and F matrices

A listing of the above routines is given in Appendix 1.

The dynamic nuclear magnetic resonance programme was developed by Stephenson and Binsch [4] and is briefly described. DNMR5 [5] is an iterative programme capable of simultaneously optimizing up to 16 parameters (chemical shifts, coupling constants, populations, effective transverse relaxation times, exchange rate constants, two baseline parameters and the spectral origin) by a least-squares fitting of a theoretical band shape to experimentally digitized nmr signal intensities. The optimization is constrained by the total experimental band shape integral corrected for baseline increment and baseline tilt. The programme outputs information regarding the final parameters of the iteration, an error analysis of the final parameters and an agreement factor based on a calculated spectrum. It also, optionally, produces various forms of the original and computed spectra for comparison. An input/output information listing of the program DNMR5 is listed in Appendix 2.

(2) PREPARATION OF COMPLEXES

Prior to the formation of all complexes, the required solvents were dried and distilled under a nitrogen atmosphere. Unless otherwise specified, preparations were performed at room temperature under nitrogen. All yields were practically quantitative (>85%) unless otherwise indicated. The products were stored over silica gel in a vacuum desiccator, the composition and purity being confirmed by microanalyses.

2.1. a) Preparation of $[Rh(CO)_2Cl]_2$

This was prepared according to the method of Deeming and Sharratt [6]. $RhCl_3.3H_2O$ (3.80 mmoles) was dissolved in absolute ethanol (20 ml) and carbon

monoxide was bubbled through the refluxing solution. After 4 hours the colour of the solution changed from an initial deep red to a final pale yellow. Following evaporation to dryness, sublimation (80°C, 0.1 mm Hg) gave dark red crystals of the product (yield 75-90%), M.P. 126-127°C.

2.1. b) Preparation of $[Rh(CO)_2Br]_2$

An excess of LiBr (5 molar in acetone) was added to a solution of $[Rh(CO)_2Cl]_2$ in dry acetone. After stirring for 20 min., the solution was evaporated to dryness using a rotary evaporator, dry dichloromethane added and the yellow solution filtered. The filtrate was evaporated to dryness and the product recrystallized from boiling hexane.

2.1. c) Preparation of the complexes *cis*-$[Rh(CO)_2(Cl)(L)]$

Analytical data and M.P. of the complexes are presented in Table 2.1

L = ammonia

The complex was prepared according to the method of Vallarino and Sheargold [7], that is by the slow addition of a solution of gaseous ammonia in dry hexane to a stirred hexane solution of $[Rh(CO)_2Cl]_2$ (0.257 mmoles in 10 ml). The red-purple gelatinous product precipitated immediately. The addition of the ammonia-hexane solution was continued until the mother liquor assumed a very pale yellow colour. After stirring for an additional 5 min., the product was isolated by vacuum filtration, washed with hexane and dried over silica gel under reduced pressure.

L = pyridine

The complex was prepared by the slow addition of a petroleum ether (B.P. 40-60°C) solution of pyridine (0.50 mmoles in 10 ml) to a stirred petroleum ether solution of $[Rh(CO)_2Cl]_2$ (0.257 mmoles in 10 ml). The orange product precipitated immediately and was isolated and dried as described above.

L = aniline

The complex was prepared by the slow addition of a benzene solution of aniline (0.50 mmoles in 10 ml) to a stirred benzene solution of $[Rh(CO)_2Cl]_2$ (0.257 mmoles in 10 ml). Petroleum ether (B.P. 40-60°C) was added to precipitate the green-purple gelatinous product which was isolated and dried as described above.

L = imidazole and pyridine N-*oxide*

The complexes were prepared by the slow addition of a warm benzene solution of L (0.50 mmoles in 10 ml) to a stirred benzene solution of $[Rh(CO)_2Cl]_2$ (0.257 mmoles in 10 ml). The orange products were further precipitated by the addition of hexane (10 ml) and after stirring for 5 min., the products were isolated and dried as described above.

The labelled complexes were similarly prepared using the following labelled ligands supplied by Merck, Sharp and Dohme (Canada) Ltd (isotopic purity in parentheses); ^{13}CO gas (99%), aniline-ND_2 (99%), aniline-d_7, (99%), aniline-d_5 (99%), imidazole-d_4 (98%), pyridine-d_5 *N*-oxide (98%) and the following labelled ligands supplied by Prochem B.O.C. Ltd: pyridine-d_5 (99%), imidazole-$^{15}N_2$(95%), aniline-^{15}N (99%) and $^{15}NH_3$ gas (99%). The ND_3 complex was prepared from its undeuterated analogue, *cis*-$[Rh(CO)_2(Cl)(NH_3)]$, by exchange in CD_3OD.

2.1. d) Preparation of the complexes *cis*-$[Rh(CO)_2(Br)(L)]$

The bromo complexes were prepared in a similar fashion to their chloro-counterparts, using $[Rh(CO)_2Br]_2$ instead of $[Rh(CO)_2Cl]_2$. Yields were practically quantitative , the M.P. and microanalytical data (C, H, N) are listed in Table 2.2

2.2. a) Preparation of $[Rh(Cl)(COD)]_2$

The method of Giordano and Crabtree [8] was followed for the preparation of $[Rh(Cl)(COD)]_2$. Under nitrogen, $RhCl_3.3H_2O$ (7.6 mmoles) was dissolved in deoxygenated ethanol-water (5:1, 20 ml) and 1,5-cyclooctadiene (3 ml) was added. The mixture was refluxed with continuous stirring for 12 hours, during which time the product precipitated as a yellow-orange solid. The mixture was cooled, filtered, and the product washed with pentane (30 ml) and then with methanol-water (1:5, 100 ml) and dried as described above.

2.2. b) Preparation of $[Rh(Br)(COD)]_2$

An excess of LiBr (5 molar in acetone) was added to a solution of $[Rh(Cl)(COD)]_2$ in dry acetone. After stirring for 20 min., the solution was evaporated to dryness, dry dichloromethane was added and the orange solution was filtered. The filtrate was evaporated to dryness and the solid residue recrystallised from acetone/water to give the pure product.

2.2. c) Preparation of the complexes [Rh(COD)(X)(L)]

Analytical data and M.P. of the complexes are presented in Table 2.3 and 2.4.

L = pyridine, imidazole, aniline, pyridine N-*oxide*

The complexes were prepared by the slow addition of a dichloromethane solution of L (0.42 mmoles in 10 ml) to a stirred solution of $[Rh(COD)(X)]_2$ (0.20 mmoles in 10 ml). After stirring for 20 min., the solvent was partially evaporated in a stream of nitrogen and a precipitate developed. Further product was precipitated by the addition of diethyl ether (20 ml), and after stirring for an additional 5 min., the products were isolated by vacuum filtration, washed with diethyl ether and dried over silica gel under reduced pressure.

L = ammonia

Repeated attempts to prepare the complex $[Rh(COD)(Cl)(NH_3)]$ by the above method or by the reported procedure [9] failed, the elemental analysis always indicating only a trace (<1%) amount of N present in the complex. The complex was successfully prepared by placing two beakers in a vacuum desiccator, one containing solid $[Rh(COD)(Cl)]_2$ (0.1 gram) the other containing aqueous ammonia (26% w/w, 3 ml). The desiccator was partially evacuated and allowed to stand overnight. The solid $[Rh(COD)(Cl)]_2$ had changed colour to a paler yellow, microanalytical data indicating the product as $[Rh(COD)(Cl)(NH_3)]$.

Repeated attempts to prepare the bromide analogue in a similar fashion always failed and gave poor analytical results.

The labelled complexes were similarly prepared using the following labelled ligands supplied by Merck, Sharp and Dohme (Canada) Ltd. (isotopic purity in parentheses): aniline-ND_2 (99%), aniline-d_7, (99%), aniline-d_5 (99%), imidazole-d_4 (98%), pyridine-d_5 *N*-oxide (98%), ammonium-d_4 hydroxide-*d* (26% w/w in D_2O, 99%), and the following labelled ligands supplied by Prochem B.O.C. Ltd: pyridine-d_5 (99%), imidazole-$^{15}N_2$ (95%), and aniline-^{15}N (99%).

2.3. Preparation of $[Rh(COD)(L)_2]ClO_4$ complexes

Analytical data and melting points of the complexes are presented in Table 2.5.

L = pyridine, imidazole, aniline, pyridine N-*oxide*

A solution of $[Rh(COD)(Me_2CO)_x]ClO_4$ was prepared by treating $[RhCl(COD)]_2$ (0.1 mmol) with $AgClO_4$ (0.2 mmol) in 10 ml of dry acetone and removing the precipitated AgCl. The respective ligands, L (0.4 mmol in 5 ml acetone) were added dropwise to the above solution of $[Rh(COD)(Me_2CO)_x]ClO_4$ with continual stirring. After stirring for an additional 20 min., the yellow solution was partially evaporated in a stream of nitrogen, after which dry diethyl ether (10 ml) was slowly added, resulting in a fine precipitate. The products were isolated by vacuum filtration, washed with diethyl ether and dried over silica gel under reduced pressure. The composition and purity of the products were determined by microanalyses.

The labelled complexes were prepared in a similar fashion.

2.4. Preparation of $[Rh(CO)_2(L)_2]ClO_4$ complexes.

Analytical data and melting points of the complexes are presented in Table 2.6

L = pyridine, imidazole, aniline, pyridine N-*oxide*

The carbonyl complexes were all prepared from their corresponding cyclooctadiene analogues. The $[Rh(COD)(L)_2]$ ClO_4 complex was suspended in dry *n*-pentane and carbon monoxide was bubbled through the solution. After several minutes (10-90, depending on the ligand), the suspension changed to a paler yellow colour. The suspension was filtered, washed with *n*-pentane and dried over silica gel under reduced pressure.

The labelled complexes were prepared in a similar manner.

TABLE 2.1 Analytical data and M.P. for the complexes *cis*-$[Rh(CO)_2(Cl)(L)]$.

	*M.P. °C	Analysis, calc. (found) %C	%H	%N
cis-$[Rh(CO)_2(Cl)(NH_3)]$	145	11.36 (11.4)	1.43 (1.4)	6.63 (6.6)
cis-$[Rh(CO)_2(Cl)(ND_3)]$		11.20 (11.2)	1.41 (1.4)	6.53 (6.5)
cis-$[Rh(CO)_2(Cl)(^{15}NH_3)]$		11.31 (11.3)	1.42 (1.4)	6.59 (6.6)
cis-$[Rh(^{13}CO)_2(Cl)(NH_3)]$		11.26 (11.3)	1.42 (1.4)	6.56 (6.6)
cis-$[Rh(CO)_2(Cl)(py)]$	62-64	30.74 (30.7)	1.84 (1.9)	5.12 (5.1)
cis-$[Rh(CO)_2(Cl)(py\text{-}d_5)]$		30.19 (30.1)	1.81 (1.9)	5.03 (4.9)
cis-$[Rh(^{13}CO)_2(Cl)(py)]$		30.52 (30.5)	1.83 (1.8)	5.08 (5.1)
cis-$[Rh(CO)_2(Cl)(pyO)]$	118	29.04 (29.1)	1.74 (1.8)	4.84 (4.8)
cis-$[Rh(CO)_2(Cl)(pyO\text{-}d_5)]$		28.55 (28.5)	1.71 (1.8)	4.76 (4.8)
cis-$[Rh(^{13}CO)_2(Cl)(pyO)]$		28.84 (28.8)	1.73 (1.7)	4.81 (4.8)
cis-$[Rh(CO)_2(Cl)(imid)]$	94-95	22.88 (22.9)	1.54 (1.6)	10.67 (10.7)
cis-$[Rh(CO)_2(Cl)(imid\text{-}d_4)]$		22.54 (22.8)	1.51 (1.5)	10.51 (10.5)
cis-$[Rh(CO)_2(Cl)(imid\text{-}^{15}N)]$		22.79 (22.8)	1.53 (1.5)	10.63 (10.6)
cis-$[Rh(^{13}CO)_2(Cl)(imid)]$		22.71 (22.8)	1.52 (1.5)	10.59 (10.6)
cis-$[Rh(CO)_2(Cl)(an)]$	134-137	33.42 (33.5)	2.45 (2.5)	4.87 (4.9)
cis-$[Rh(CO)_2(Cl)(an\text{-}d_5)]$		32.85 (32.8)	2.41 (2.4)	4.79 (4.8)
cis-$[Rh(CO)_2(Cl)(an\text{-}d_7)]$		32.63 (32.6)	2.40 (2.4)	4.76 (4.8)
cis-$[Rh(CO)_2(Cl)(an\text{-}ND_2)]$		33.19 (33.2)	2.44 (2.4)	4.84 (4.8)
cis-$[Rh(CO)_2(Cl)(an\text{-}^{15}NH_2)]$		33.30 (33.4)	2.45 (2.5)	4.85 (4.9)
cis-$[Rh(^{13}CO)_2(Cl)(an)]$		33.19 (33.2)	2.44 (2.5)	4.84 (4.8)

*Melting or decomposition point.

TABLE 2.2 Analytical data and M.P. for the complexes *cis*-$[Rh(CO)_2(Br)(L)]$.

	*M.P. °C	Analysis, calc. (found) %C	%H	%N
cis-$[Rh(CO)_2(Br)(NH_3)]$	127-129	9.39 (9.4)	1.18 (1.2)	5.47 (5.5)
cis-$[Rh(CO)_2(Br)(ND_3)]$		9.28 (9.3)	1.17 (1.2)	5.41 (5.5)
cis-$[Rh(CO)_2(Br)(^{15}NH_3)]$		9.35 (9.4)	1.18 (1.2)	5.45 (5.5)
cis-$[Rh(^{13}CO)_2(Br)(NH_3)]$		9.32 (9.3)	1.17 (1.1)	5.43 (5.4)
cis-$[Rh(CO)_2(Br)(py)]$	52-53	26.44 (26.3)	1.59 (1.7)	4.41 (4.4)
cis-$[Rh(CO)_2(Br)(py\text{-}d_5)]$		26.04 (26.0)	1.56 (1.6)	4.34 (4.4)
cis-$[Rh(^{13}CO)_2(Br)(py)]$		26.28 (26.2)	1.58 (1.6)	4.38 (4.4)
cis-$[Rh(CO)_2(Br)(pyO)]$	126	25.18 (25.0)	1.51 (1.5)	4.19 (4.2)
cis-$[Rh(CO)_2(Br)(pyO\text{-}d_5)]$		24.81 (24.9)	1.49 (1.5)	4.13 (4.2)
cis-$[Rh(^{13}CO)_2(Br)(pyO)]$		25.03 (24.9)	1.50 (1.5)	4.17 (4.2)
cis-$[Rh(CO)_2(Br)(imid)]$	71-74	19.57 (19.4)	1.31 (1.3)	9.13 (9.1)
cis-$[Rh(CO)_2(Br)(imid\text{-}d_4)]$		19.32 (19.3)	1.30 (1.3)	9.01 (9.0)
cis-$[Rh(CO)_2(Br)(imid\text{-}^{15}N)]$		19.44 (19.3)	1.31 (1.3)	9.07 (9.0)
cis-$[Rh(^{13}CO)_2(Br)(imid)]$		19.44 (19.4)	1.31 (1.3)	9.07 (9.0)
cis-$[Rh(CO)_2(Br)(an)]$	134-135	28.95 (29.1)	2.13 (2.2)	4.22 (4.3)
cis-$[Rh(CO)_2(Br)(an\text{-}d_5)]$		28.52 (28.4)	2.09 (2.1)	4.16 (4.2)
cis-$[Rh(CO)_2(Br)(an\text{-}d_7)]$		28.35 (28.4)	2.08 (2.1)	4.13 (4.2)
cis-$[Rh(CO)_2(Br)(an\text{-}ND_2)]$		28.77 (28.8)	2.11 (2.1)	4.19 (4.2)
cis-$[Rh(CO)_2(Br)(an\text{-}^{15}NH_2)]$		28.86 (28.8)	2.12 (2.1)	4.21 (4.2)
cis-$[Rh(^{13}CO)_2(Br)(an)]$		28.77 (28.8)	2.11 (2.1)	4.19 (4.2)

*Melting or decomposition point.

TABLE 2.3 Analytical data and M.P. for the complexes [Rh(COD)(Cl)(L)].

	*M.P. °C	Analysis, calc. (found) %C	%H	%N
[Rh(COD)(Cl)(NH_3)]	233-235	36.46 (36.4)	5.74 (5.5)	5.31 (5.2)
[Rh(COD)(Cl)(ND_3)]		36.05 (36.1)	5.67 (5.5)	5.25 (5.2)
[Rh(COD)(Cl)(py)]	229-232	47.95 (47.7)	5.26 (5.1)	4.30 (4.5)
[Rh(COD)(Cl)(py-d_5)]		47.22 (47.2)	5.18 (5.2)	4.24 (4.2)
[Rh(COD)(Cl)(pyO)]	235	45.70 (45.3)	5.02 (5.0)	4.10 (4.0)
[Rh(COD)(Cl)(pyO-d_5)]		45.04 (44.7)	4.94 (4.9)	4.04 (3.9)
[Rh(COD)(Cl)(imid)]	168-173	41.99 (41.2)	5.13 (5.0)	8.90 (8.8)
[Rh(COD)(Cl)(imid-d_4)]		41.46 (41.5)	5.06 (5.0)	8.79 (8.8)
[Rh(COD)(Cl)(imid-^{15}N)]		41.73 (41.7)	5.09 (5.1)	8.85 (8.9)
[Rh(COD)(Cl)(an)]	229-230	49.50 (49.2)	5.64 (5.5)	4.12 (4.1)
[Rh(COD)(Cl)(an-d_5)]		48.78 (48.4)	5.56 (5.4)	4.06 (3.9)
[Rh(COD)(Cl)(an-d_7)]		48.50 (48.3)	5.52 (5.5)	4.04 (4.0)
[Rh(COD)(Cl)(an-ND_2)]		49.21 (49.2)	5.60 (5.5)	4.10 (4.1)
[Rh(COD)(Cl)(an-$^{15}NH_2$)]		49.36 (49.3)	5.62 (5.5)	4.11 (4.2)

*Melting or decomposition point.

TABLE 2.4 Analytical data and M.P. for the complexes [Rh(COD)(Br)(L)].

	*M.P.	Analysis, calc. (found)		
	°C	%C	%H	%N
[Rh(COD)(Br)(py)]	215-217	42.19 (42.0)	4.63 (4.5)	3.78 (3.7)
[Rh(COD)(Br)(py-d_5)]		41.63 (41.6)	4.57 (4.6)	3.73 (3.7)
[Rh(COD)(Br)(pyO)]	213-215	40.44 (40.3)	4.44 (4.4)	3.63 (3.6)
[Rh(COD)(Br)(pyO-d_5)]		39.92 (39.8)	4.38 (4.2)	3.58 (3.4)
[Rh(COD)(Br)(imid)]	224-226	36.79 (36.9)	4.49 (4.5)	7.80 (7.8)
[Rh(COD)(Br)(imid-d_4)]		36.39 (36.3)	4.44 (4.4)	7.72 (7.7)
[Rh(COD)(Br)(imid-^{15}N)]		36.59 (36.5)	4.47 (4.5)	7.76 (7.8)
[Rh(COD)(Br)(an)]	215-217	43.78 (43.5)	4.99 (4.9)	3.65 (3.6)
[Rh(COD)(Br)(an-d_5)]		43.21 (43.2)	4.92 (4.9)	3.60 (3.6)
[Rh(COD)(Br)(an-d_7)]		42.99 (42.8)	4.90 (4.8)	3.58 (3.5)
[Rh(COD)(Br)(an-ND_2)]		43.55 (43.4)	4.96 (4.8)	3.63 (3.6)
[Rh(COD)(Br)(an-$^{15}NH_2$)]		43.66 (43.5)	4.97 (4.8)	3.64 (3.5)

*Melting or decomposition point.

TABLE 2.5 Analytical data and M.P. for the complexes $[Rh(COD)(L)_2]ClO_4$.

	*M.P. °C	Analysis, calc. (found) %C	%H	%N
$[Rh(COD)(py)_2]ClO_4$	191-195	46.12 (46.1)	4.73 (4.6)	5.98 (5.8)
$[Rh(COD)(py\text{-}d_5)_2]ClO_4$		45.15 (45.0)	4.63 (4.7)	5.85 (5.9)
$[Rh(COD)(pyO)_2]ClO_4$	174-176	43.18 (43.1)	4.43 (4.5)	5.59 (5.6)
$[Rh(COD)(pyO\text{-}d_5)_2]ClO_4$		42.33 (42.3)	4.34 (4.4)	5.48 (5.5)
$[Rh(COD)(imid)_2]ClO_4$	132-135	37.64 (37.6)	4.51 (4.6)	12.54 (12.5)
$[Rh(COD)(imid\text{-}d_4)_2]ClO_4$		36.98 (37.0)	4.43 (4.1)	12.32 (12.4)
$[Rh(COD)(imid\text{-}^{15}N)_2]ClO_4$		37.31 (37.2)	4.47 (4.2)	12.43 (12.3)
$[Rh(COD)(an)_2]ClO_4$	146-151	48.35 (48.9)	5.27 (5.4)	5.64 (5.8)
$[Rh(COD)(an\text{-}d_5)_2]ClO_4$		47.87 (47.7)	5.22 (5.2)	5.58 (5.6)
$[Rh(COD)(an\text{-}d_7)_2]ClO_4$		47.03 (46.9)	5.13 (5.2)	5.48 (5.2)
$[Rh(COD)(an\text{-}ND_2)_2]ClO_4$		47.97 (47.1)	5.23 (5.2)	5.59 (5.2)
$[Rh(COD)(an\text{-}^{15}NH_2)_2]ClO_4$		48.16 (47.6)	5.25 (5.4)	5.62 (5.4)

*Melting or decomposition point.

TABLE 2.6 Analytical data and M.P. for the complexes $[Rh(CO)_2(L)_2]ClO_4$.

	*M.P. °C	Analysis, calc. (found) %C	%H	%N
$[Rh(CO)_2(py)_2]ClO_4$	119-195	34.60 (34.7)	2.42 (2.5)	6.72 (6.5)
$[Rh(CO)_2(py\text{-}d_5)_2]ClO_4$		33.79 (33.8)	2.36 (2.5)	6.57 (6.5)
$[Rh(CO)_2(pyO)_2]ClO_4$	101-102	32.13 (32.5)	2.25 (2.5)	6.24 (6.2)
$[Rh(CO)_2(pyO\text{-}d_5)_2]ClO_4$		31.43 (30.9)	2.20 (2.3)	6.11 (5.9)
$[Rh(CO)_2(imid)_2]ClO_4$	189-191	24.35 (24.3)	2.04 (2.1)	14.20 (13.9)
$[Rh(CO)_2(imid\text{-}d_4)_2]ClO_4$		23.87 (24.0)	2.00 (2.1)	13.92 (13.8)
$[Rh(CO)_2(imid\text{-}^{15}N)_2]ClO_4$		24.11 (24.2)	2.02 (2.0)	14.06 (13.9)
$[Rh(CO)_2(an)_2]ClO_4$	119-125	37.82 (37.7)	3.17 (3.3)	6.30 (6.2)
$[Rh(CO)_2(an\text{-}d_5)_2]ClO_4$		36.99 (36.6)	3.10 (3.2)	6.16 (6.1)
$[Rh(CO)_2(an\text{-}d_7)_2]ClO_4$		36.66 (36.7)	3.07 (3.1)	6.11 (6.0)
$[Rh(CO)_2(an\text{-}ND_2)_2]ClO_4$		37.48 (37.5)	3.15 (3.2)	6.24 (6.1)
$[Rh(CO)_2(an\text{-}^{15}NH_2)_2]ClO_4$		37.65 (37.7)	3.16 (3.2)	6.27 (6.1)

*Melting or decomposition point.

REFERENCES

1 *"Model 983 Infrared Spectrophotometer Operator's manual"*, Perkin-Elmer, England, (1981)

2 *"Spectrometer Technical Manual M091-0033"*, Digilab Inc., U.S.A., (1975)

3 *"VXR-Series Variable Temperature Accessory"*, Pub. No. 87-178230-00, Varian Associates, Inc., U.S.A.

4 D.S.STEPHENSON AND G.BINSCH, *J. Mag. Res.*, **32** (1978) 145

5 D.S.STEPHENSON AND G.BINSCH, *DNMR5*, **QCPE, 11** (1978) 365

6 A.J.DEEMING AND P.J.SHARRATT, *J. Organomet. Chem.*, **99** (1975) 447

7 L.M.VALLARINO AND S.W.SHEARGOLD, *Inorg. Chim. Acta*, **36** (1979) 243

8 G.GIORDANO AND R.H.CRABTREE, *Inorg. Synth.*, **19** (1979) 218

9 G.ZASSINOVICH, G.MESTRONI AND A.CAMUS *J. Organomet. Chem.*, **91** (1975) 379

CHAPTER 3

INTRODUCTION

In 1871 Schutzenberger [1] first recognized carbon monoxide as a ligand in his preparation and characterization of $[Pt(CO)_2(Cl)_2]$. A few decades followed before Manchot and König [2] in 1925 synthesized the first compound containing a rhodium-carbon bond, incorrectly formulating it as a carbon monoxide adduct of rhodium oxychloride, "$[Rh_2Cl_2O.3CO]$". It was not until 1943 that Hieber and Lagally [3] correctly formulated this compound as the halogen bridged dimer, $[Rh(CO)_2Cl]_2$.

The carbonyl dimer, obtained by reduction of $RhCl_3.xH_2O$ with CO, is perhaps the most important and convenient starting material for Rh(I) chemistry. The red crystals of the air stable complex $[Rh(CO)_2Cl]_2$, are known to undergo reactions of various types with donor ligands depending on the nature of the ligand (L), on the Rh/L molar ratio used, and on the solvent [4-13]. The carbonyl dimer is an excellent source of rhodium(I) species, and the bridge-splitting reactions of $[Rh(CO)_2X]_2$ (X is Cl or Br) with a wide variety of amines was first reported by Vallarino in 1959 [14].

Today, one of the most active areas of research is transition metal complexes wherein carbon monoxide groups are ligands. Interest in the reactions of $[Rh(CO)_2Cl]_2$ has stemmed mainly from the realization that the metal carbonyl forms numerous derivatives, some of which have applications as catalysts in the hydroformylation and hydrogenation reactions [15-21], others exhibiting interesting biological activity [22]. The amenability of many of the complexes to study by physical methods has resulted in much industrial and academic research.

The ability of the CO group to stabilize the metal in low-positive, zero or low-negative oxidation states is believed to be due to a so called "synergic" bonding effect. The accepted view [23,24] of bonding in metal carbonyl complexes is one in which charge is donated from the ligand to the metal by a σ-bond and withdrawn from the metal atom into the π^*-orbital (antibonding) of the ligand by π-bonding. This is diagrammatically represented in Figure 3.1. The electron density in the π^*-orbitals is dependent, amongst other things, on the charge donation from ligand to metal and hence the σ- and π-bonding is synergic.

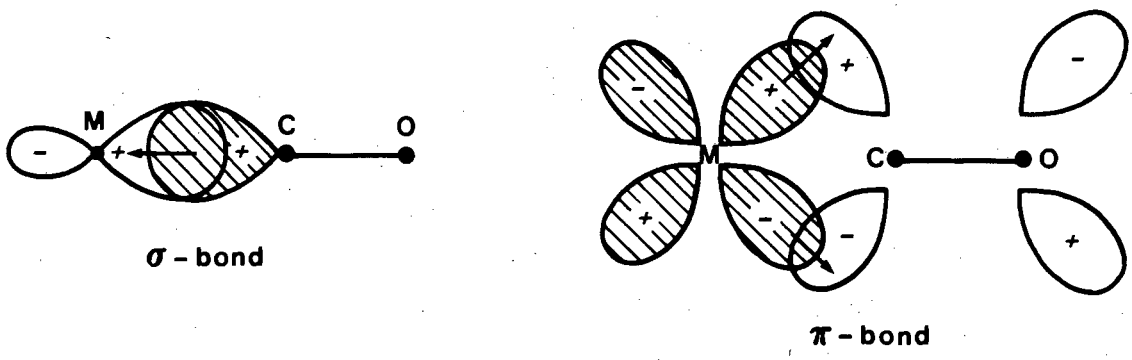

Figure 3.1 Diagrammatic representation of the bonding in metal carbonyls.

According to the preceding description of the bonding, as the extent of back donation from metal to the ligand increases, the M-C bond becomes stronger and the C≡O bond becomes weaker. The infrared spectra of these systems provide a most convenient and useful estimate of these phenomena. Thus the characteristic stretching frequency of the C≡O bond in carbon monoxide itself, is at 2155 cm^{-1}, but in metal carbonyls it is around 2000 cm^{-1}. The lowered frequency shows that the bonding between carbon and oxygen is weakened. Furthermore, the synergic effect could lead to the prediction that as negative charge is added to the metal the ν(CO) frequency would decrease, as it does in the following isoelectronic series [25]:

$Ni(CO)_4$	$Co(CO)_4^-$	$Fe(CO)_4^{2-}$
2060	1890	1790 cm^{-1}

Hence for metal carbonyl complexes, weakening of the C≡O bond insofar as electronic factors are concerned, is due entirely to back-donation from metal *d* π-orbitals to CO π^*-orbitals, with the σ-donation slightly cancelling some of this effect. The vibrational spectra, particularly the infrared spectra, of metal carbonyls have proved to be a rich and convenient source of information regarding molecular structure and bonding.

Although there is much in the literature concerning the infrared-active vibrations of transition metal carbonyl complexes, nearly all of it is directed towards the assignment of absorption bands due to the ν(CO) vibration. These ν(CO) bands are easily identified since they give rise to intense absorption and fall within a restricted frequency range.

Before the 1960s lack of suitable instrumentation restricted the study of two further types of vibrations which are associated with a carbonyl group coordinated to a metal, namely the M-C bond stretching, ν(M-CO), and the M-C-O angle bending, δ(M-CO). Similarly, in substituted metal carbonyls, other groups bound to the metal atom also give rise to additional low frequency modes of vibration. All of these modes should be at least as sensitive to structural changes in the molecule as ν(CO), and are therefore of considerable interest. Unfortunately, when suitable instrumentation became available little effort was devoted to the low infrared frequency region and although absorption bands due to ν(MC), ν(MX), ν(ML) and δ(MCO) vibrations have occasionally been identified [26,27], there have been few attempts to assign them. Furthermore, there have been even fewer studies

employing isotopic labelling, which has been shown to be the most reliable technique [28], to confirm the proposed assignments. Hence, the results of earlier studies have often been difficult to interpret with confidence owing to ambiguities in assignments or the lack of complete vibrational spectra.

Raman data can, in principle, provide the additional information needed for a complete vibrational assignment, but limitations of the Raman technique have restricted its application.

The complete vibrational data of a complex allow one to determine the force constants of the system. The main use for force constants is in seeking a quantitative understanding of bonding relationships.

Numerous reports [29-31] have revealed the versatility of ^{13}C nmr in bonding and structural investigations of transition metal carbonyl complexes. However, these complexes are often fluxional in solution and because of long relaxation times their ^{13}C spectra are difficult to measure. Nevertheless, the potential of ^{13}C nmr spectroscopy for the study of transition metal carbonyl complexes has grown, partially through the advent of Fourier transform pulsed nmr techniques, and partially through the use of ^{13}C-enriched carbon monoxide. Not only are the ^{13}C nmr spectra more informative than the ^{1}H nmr spectra, but relatively faster exchange processes can be observed with ^{13}C nmr than with ^{1}H nmr spectroscopy. This is a consequence of the wider range of the chemical shifts in the ^{13}C nmr spectrum The ^{13}C chemical shifts and carbonyl ^{13}C-M coupling constants are sensitive to changes in the stereochemistry of the complexes and the electronic environment of the CO ligand. An increased transition metal to carbonyl group π-

back donation (and/or decreased carbonyl to metal σ-donation) is associated with decreased shielding of carbonyl carbon resonances.

Undoubtedly, nitrogen is one of the most important atoms in coordination and bio-chemistry. Nitrogen is a constituent of many ligands and is often bound directly to the metal ion. Hence ^{15}N nmr spectroscopy can serve as a sensitive probe of the structural environment at the centre of many reactions. However, the low natural abundance, long relaxation times, and relative insensitivity of the ^{15}N nucleus has hampered its detection in nmr spectroscopy. Recently [32], the advent of new techniques, high-field magnets, large sample probe heads, and ^{15}N-enriched samples has resulted in a dramatic increase in the use of ^{15}N nmr spectroscopy. Hence, it is no surprise that the ^{15}N nucleus has become the third most important nucleus (after ^{1}H and ^{13}C) for structural investigations of molecules by nmr spectroscopy [33].

As expected [33,34] from the similarity of nitrogen and carbon in electronic structure and bonding, the ^{15}N nmr shifts parallel the ^{13}C nmr shifts in many aspects. The ^{15}N nucleus, like ^{13}C, has $S=½$ and so its resonances should be sharp and should reveal spin-spin coupling when present. The major difference is that ^{15}N shifts cover approximately three times the range of ^{13}C shifts. The largest coupling in ^{15}N nmr spectroscopy is observed for N-H bonds, and they depend linearly on the *s*-character of the hybrid orbital involved in the N-H bond. Further, when ^{15}N is bonded to a metal that has a high natural abundance and couples to ^{15}N (for instance ^{103}Rh, $S=½$, 100% natural abundance) one can obtain useful coupling constant data.

In square planar complexes of d^8 electronic configuration, metal to ligand charge transfer transitions have been identified [35-37] in the electronic spectra of

numerous complexes containing π-acceptor ligands (CO for instance) which possess suitable low-energy empty *d*-orbitals. Further, numerous rhodium(I) carbonyl complexes having the same general formula, $[Rh(CO)_2(X)(amine)]$, exhibit a wide variety of colours ranging from yellow to purple. It has been suggested [38,39] that the colours of the complexes could indicate which complexes possess some kind of metal-metal interaction. To further an understanding of metal-metal interactions and the metal to ligand charge transfer transition in low-valent organometallic complexes, uv/visible spectrophotometers have proved to be an invaluable tool.

Based on the above considerations, we have set out to investigate the bridge-splitting reactions of $[Rh(CO)_2X]_2$ (see Figure 3.2) to give the square planar mononuclear species *cis*-$[Rh(CO)_2(X)(L)]$, in which the halogen (X is Cl or Br) as well as the ligand (L is ammonia, pyridine, pyridine *N*-oxide, imidazole, and aniline) have been varied.

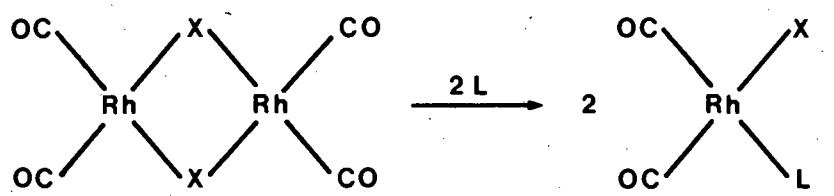

Figure 3.2 Bridge-splitting reaction of $[RhX(CO)_2]_2$ to give *cis*-$[Rh(CO)_2(X)(L)]$

A complete vibrational study (4000-50 cm^{-1}) employing multiple isotopic labelling (^{13}C, ^{2}H, ^{15}N) was undertaken to confirm the proposed band assignments. In the ^{1}H, ^{13}C, and ^{15}N nmr studies, at room and low temperatures, the ^{13}C and ^{15}N atoms were isotopically enriched thus ensuring easily obtainable good quality spectra with the added advantage of detecting the $^{2}J(^{13}C–^{13}C)$ and $^{2}J(^{13}C–^{15}N)$ coupling constants, which are useful for structural information on the complexes.

The complexes were further investigated by uv/visible analyses and characterized by mass spectrometry, microanalyses, and melting points.

ASSIGNMENTS AND RESULTS

RAMAN SPECTRA

Our attempts to obtain Raman (laser) spectra of the complexes were rather unsuccessful since the samples rapidly decomposed in the laser beam. Samples were recorded either as solutions, powders, or discs. The best results were obtained when the sample was a pure disc mounted in a pellet holder which was rotated to minimize decomposition of the intensely coloured complex in the laser beam. Representative spectra are shown in Figures 3.4 and 3.5.

INFRARED SPECTRA

The infrared spectra of the complexes *cis*-[$Rh(CO)_2(X)(L)$] where X is Cl or Br and L is ammonia, pyridine, pyridine *N*-oxide, aniline, and imidazole have been recorded over the range 4000-50 cm^{-1} Representative spectra are shown in Figures 3.6-3.9.

The *cis*-complexes have a square planar geometry of point group C_s. To aid in the assignment of the various modes, use is made of group theory. This allows one to theoretically determine the number of infrared and Raman active modes in a complex. From a consideration of group theory, it is evident that the infrared spectra of our complexes (see Chapter 1) can be divided into three parts: (1) the 2200-1800 cm^{-1} region where the terminal CO stretching modes occur, (2) the 4000-600 cm^{-1} region where most of the internal ligand vibrations occur, and (3) the 625-50 cm^{-1} region where all the skeletal vibrations occur.

In the following discussion each of the above-mentioned regions will be considered separately. Within each region the justification for the chosen assignments will be given followed by the more specific assignments in each complex. The assignments for the complexes *cis*-[$Rh(CO)_2(X)(L)$] in the range 4000-50 cm^{-1} are presented in Tables 3.1-3.5 (for X is Cl) and Tables 3.6-3.10 (for X is Br).

(1) The 2200-1800 cm^{-1} region

This is the region where terminal ν(CO) modes are expected to occur [40]. All the complexes have only two almost equally intense bands in their solution spectra, whereas in the solid-state, that is as Nujol mulls, the bands are substantially split, probably due to solid-state lattice interactions. These two bands are assigned to the "antisymmetric" and "symmetric" ν(CO) modes. There was no indication of any bridging carbonyl groups being present in any of the complexes.

The observation of two almost equally intense bands in the ν(CO) region of the infrared spectrum, confirms the *cis*- geometry of [$Rh(CO)_2(X)(L)$] in all cases. This is in accord with x-ray crystallographic results on the related square planar complexes *cis*-[$Rh(CO)_2(Cl)$(pyrazole)] [41] and *cis*-[$Ir(CO)_2(Cl)$(pyridine)] [42].

A compound with the *trans* geometry would also have two infrared active carbonyl bands, but the "symmetric" stretch would be expected to have a greatly reduced intensity relative to the "antisymmetric" stretch.

The assignments of the ν(CO) bands were confirmed by the labelling studies. Substitution of ^{12}CO groups by ^{13}CO groups resulted in the expected shift to lower frequency (~46 cm^{-1}) by ν(CO) bands for the ^{13}CO relative to the ^{12}CO species.

(2) The 4000-600 cm^{-1} region

(a) Ammonia complexes

The assignment of the internal stretching and deformation modes of the coordinated ammonia ligand are straightforwardly made by comparison with other metal-ammonia complexes [43,44]. The internal vibrations of complexed ammonia ligand usually occur as follows; ν(NH) in the range 3300-3000 cm^{-1}, $\delta_{as}(NH_3)$ between 1630-1600 cm^{-1}, $\delta_s(NH_3)$ between 1350-1200 cm^{-1}, and $\rho(NH_3)$ between 900-700 cm^{-1}.

The assignments are supported by the labelling studies undertaken (ND_3 and $^{15}NH_3$) and are in agreement with data by Vallarino and Sheargold [45].

(b) Pyridine complexes

The assignment of the internal vibrations of the free ligand pyridine is now rather firmly established [46-51]. Our assignments have been based on the excellent spectroscopic studies by Stidham and DiLella [50,51]. Apart from minor shifts and splittings, the pyridine ligand in *cis*-[$Rh(CO)_2(X)(L)$] exhibits a band-for-band correspondence with the free ligand spectrum, thus facilitating an easy assignment.

These assignments were confirmed by isotopic labelling (py-d_5) as the internal vibrations of pyridine shift significantly on deuteration. Their more specific assignments were made from their ν^D/ν^H ratio [52-54]. This ratio, obtained by a comparison of pyridine with that of pyridine-d_5, shows that the ratio between the frequencies of corresponding bands (deuterated : undeuterated) falls between one of two ranges, 0.73 to 0.79 or 0.90 to 0.98. The (essentially) ring vibrations yield the higher ratio, while, as expected, vibrations involving the C-H stretching and bending

motions being more sensitive to deuterium substitution, yield the lower ratio. Since precisely similar ratios are observed for the deuterated and undeuterated complexes, this feature has been used to distinguish between ring and other vibration in the spectrum of the complexes.

(c) Aniline complexes

The band shifts induced by ^{15}N-labelling, ring (d_5) deuteration, amino group (d_2) deuteration, and perdeuteration (d_7) were utilized for the assignment of the internal ligand vibrations. The expected effects of the various types of labelling on vibrations involving the C-C, C-H, N-H, C-N, Rh-N, Rh-X and C≡O bonds are qualitatively depicted in Figure 3.3.

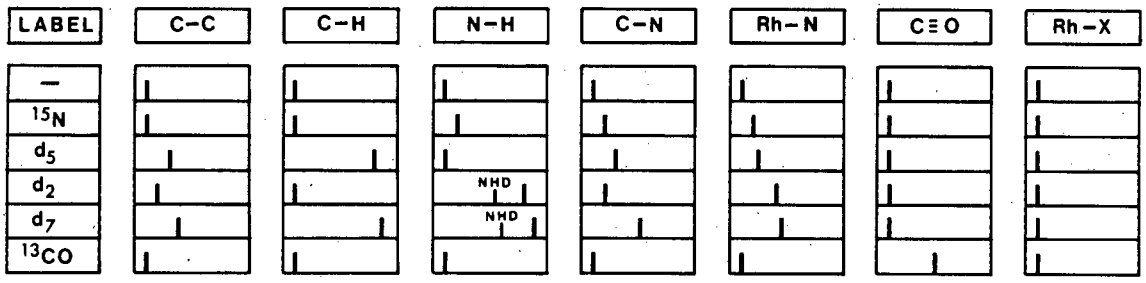

Figure 3.3. Qualitative depiction of expected effects of the various types of labelling on vibrations involving the C-C, C-H, N-H, C-N, Rh-N, Rh-X and C≡O bonds.

An unusual feature of the infrared spectra of the aniline complexes is the effect of ND_2 deuteration on the γ(C-H) modes occurring at approximately 755 cm^{-1} (intense band) and 745 cm^{-1} (weak band). On ND_2 deuteration the intensities of these two peaks swop, suggesting some strong interaction between these similar energy modes [54-56]. The assignments are consistent with previous results made on the free ligand [57,58] and those with similar metal complexes [52,59,60].

(d) Imidazole complexes

Although there have been a few major studies of the vibrational spectra of imidazole [61-68], agreement between the assignments in the earlier work is poor. Our assignments are based on the more recent publications, especially that by Hodgson *et al.* [67], and are supported by the band shifts induced by ^{15}N-labelling and ring (d_4) deuteration. Their more specific assignments were made from their ν^D/ν^H ratio. The results are consistent with previous assignments made on other metal complexes [67,69].

(e) Pyridine *N*-oxide complexes

The internal vibrations of the free ligand pyridine *N*-oxide have been extensively studied [70-78]. We have based our assignments on the more recent work of Gambi and Ghersetti [78]. The assignments are confirmed by the band shifts induced by ring (d_5) deuteration, and the results are consistent with previous assignments made on other related metal complexes [79].

(3) The 625-50 cm^{-1} region

The skeletal vibrations of the complexes *cis*-[$Rh(CO)_2(X)(L)$] occur in this region. Among the many vibrations of the complexes, the skeletal vibrations are the most important since they provide direct information regarding the structure of the complex and the nature of the metal related bonds. Unfortunately, the skeletal vibrations are often difficult to assign because the infrared spectrum is complicated by intermolecular interactions, lattice modes, lowering of symmetry, vibrational coupling, and the appearance of ligand vibrations activated by complex formation [80,81].

To aid in the assignment of the skeletal modes, use is made of group theory. From a consideration of group theory of our complexes (see Chapter 1), the following infrared active modes are expected to occur in the 625-50 cm^{-1} region.

In-plane modes	Out-of-plane modes
ν(RhX) and δ(RhX)	γ(RhX)
ν(RhL) and δ(RhL)	γ(RhL)
δ(RhCO) "in- and out-of phase"	γ(RhCO) "in- and out-of-phase"
ν(RhC) symmetric and antisymmetric	
δ(CRhC)	

Thus in each spectrum the above 13 skeletal modes, in addition to any internal ligand modes which might occur in this region, are possible.

Fortunately, the internal ligand bands can be easily identified by the isotopic labelling studies undertaken and by comparison of the spectra of the complexes with the spectra of either the free ligand or other related complexes.

However, the specific assignments of the 13 skeletal modes require more attention. The skeletal modes can be further sub-divided into three different types, namely the Rh-X, Rh-L, and the Rh-C(O) modes. Their differentiation and specific assignments have been based on band shifts induced by multiple isotopic labelling, which is the most reliable method [28,54], and band movements on substitution of the halogen or the ligand.

(i) The Rh-X modes

The bands which are unshifted by either the ligand labelling (^{2}H or ^{15}N) or by carbonyl labelling (^{13}CO) are assigned to Rh-X modes. The fact that only these bands move significantly upon halogen substitution support the assignments. The ratio ν(Rh-Br)/ν(Rh-Cl) is typically ~0.73, which is normal for terminal metal halogen bonds [82]. Their more specific assignments are made from the usual infrared frequency position of $\nu > \delta > \gamma$.

(ii) The Rh-L modes

The bands which shift most upon ligand labelling are ascribed to Rh-L modes. Support for the assignment is found in the substantial shift that these bands undergo when the ligand is substituted by another ligand. Their more specific assignments are made from the usual infrared frequency position of $\nu > \delta > \gamma$.

(iii) The Rh-C(O) modes

The bands which exhibit the greatest shift upon carbonyl labelling (^{13}CO) are ascribed to Rh-C(O) modes. As in previous studies [83-85], the low frequency bands (< 150 cm^{-1}) are assigned to δ(CRhC) modes whereas the higher frequency bands are due to either RhC stretching or RhCO deformation modes. The assignment of the latter two modes have caused much confusion since they can interact with each other, resulting in modes which may contain contributions from both. Nevertheless, it is still important in studies to decide which mode derives predominantly from which kind of distortion. We have used isotopic labelling and normal coordinate analysis (see Chapter 6) in order to assign the vibrations occurring in our complexes.

To differentiate between the RhC stretch and RhCO deformation modes, the following information is used:

(1) We read in Stammerich *et al.* [86], "Furthermore, a comparative study of all available Raman data on metal carbonyl compounds leads to the purely qualitative conclusion that the shifts corresponding to M-C stretching motions appear with higher intensities and at lower frequencies than those of M-C-O bending modes". This statement is supported by many subsequent investigators [84,85,87-89], the only exception to the above is in the platinum complexes where the order is said to be reversed [90].

(2) The MC stretching modes are generally expected to have lower band intensities than the MCO deformation modes in their infrared spectra [83,91,92].

(3) The MC stretching bands are expected to have smaller frequency shifts relative to the MCO deformation modes on ^{13}CO labelling, whereas $C^{18}O$ labelling causes a greater shift for the MC than the MCO modes [40,93].

(4) The MC stretching modes are generally more sensitive than the MCO deformation modes to substitution of the ligand by another ligand [40].

Consequently, in order to be consistent with all the above statements, the MCO deformation mode, δ(RhCO), has been assigned to the more intense higher frequency band, and the MC stretching mode, ν(Rh-C), to the less intense lower frequency band, in the infrared spectrum of all our complexes.

Within the δ(RhCO) modes there is the choice of in-plane or out-of-plane modes. There appears to be much confusion in the early literature regarding the relative positions of these modes, most assignments being arbitrarily chosen or based upon comparative intensities of the δ(RhCO) bands [26,40,88-91]. In a more recent publication, Adams and Trumble [94] have provided a *direct physical method* for

differentiation between the modes in question. They report: "The absorption spectrum of single crystals of [$Rh(CO)_2(acac)$] in polarized infrared light has enabled direct and unambiguous differentiation of the in-plane and out-of-plane modes". Their observation unequivocally places the δ(RhCO) in-plane mode at higher frequency in relation to the δ(RhCO) out-of-plane mode. Hence our assignments have been based on the excellent spectroscopic studies of Adams and Trumbles [94].

Using the above information we are now in a position to assign all the skeletal vibrations for the complexes. However, it should be mentioned that assignments for the bands occurring at <100 cm^{-1} are tentative due to their broad nature and relative insensitivity towards isotopic labelling.

In cases where fewer bands have been observed than the theoretical number expected, we have considered some bands to be coincidental. For instance, we have not differentiated between the "in-phase" (symmetric) and "out-of-phase" (antisymmetric) RhCO modes. Similar observations have been reported elsewhere [88].

(a) Ammonia complexes

There are no internal vibrations of ammonia in the 625-50 cm^{-1} region, thus the skeletal vibrations are easily identified. The assignments differ from those of Vallarino and Sheargold [45] in two respects. Firstly, the authors regard the band at 609 cm^{-1} as an out-of plane δ(RhCO) mode, and secondly, the band at 497 cm^{-1} as ν(RhC). In the light of the present work this assignment seems improbable for the following reasons: (i) The authors did not study the region beyond 250 cm^{-1} and consequently they did not observe all the skeletal vibrations. Furthermore, in the

region which they studied (4000-250 cm^{-1}) they have not given assignments for all the bands which were observed. (ii) Their assignments are based on empirical methods whereas our assignments are based on multiple isotopic labelling studies. (iii) Our normal coordinate analyses (see Chapter 6) give convergent values when using our assignments whereas non-convergent results are obtained for their assignments. Hence, we have assigned the band at 609 cm^{-1} as an in-plane δ(RhCO) mode, and the band at 497 cm^{-1} as ν(Rh-N).

An unusual feature of the infrared results in the ammonia-complexes is that the δ(RhCO) in-plane mode moves to higher frequency (>12 cm^{-1}) on ND_3 deuteration. This suggests [54-56] that either the normal-mode description in the deuterated and undeuterated complex is somewhat different or that configuration interaction (Fermi resonance) causes the shift. Furthermore, the δ(RhCO) mode gains considerable intensity on deuteration whereas the $\rho(ND_3)$ mode is almost half as intense as the $\rho(NH_3)$ mode. Such observations are indicative of configuration interaction which causes modes of the same symmetry and similar energies to diverge and share intensity. Similar phenomena have been observed for other deuterated/undeuterated metal carbonyl complexes [56,95,96].

(b) Pyridine complexes

The two ligand vibrations, that is the 16a and 16b γ(ring) modes, occurring in the 625-50 cm^{-1} region, are easily identified since they shift substantially (>30 cm^{-1}) on py-d_5 deuteration. As a result the skeletal vibration assignments become simple.

(c) Aniline complexes

The two internal vibrations, namely $\rho(NH_2)$ and γ(ring), occurring in the far-infrared spectrum are very characteristic of aniline. The $\rho(NH_2)$ band is often observed as a doublet while the weak γ(ring) band always occurs at ~210 cm^{-1}. Both bands are easily identified by the shifts induced by isotopic labelling (an-ND_2, an-d_5, an-d_7, and an-$^{15}NH_2$), hence rendering the assignment of the skeletal modes straightforward. Partial substitution of the amino group (NHD) aids in the differentiation between the RhN modes and the other modes.

(d) Imidazole complexes

A single intense vibration of imidazole occurs at ~174 cm^{-1}, hence the skeletal vibrations are straightforwardly made.

(e) Pyridine *N*-oxide complexes

The ligand has several vibrations in the 625-50 cm^{-1} region. However, they can be identified by comparison with either the spectrum of uncoordinated pyridine *N*-oxide [78], or to the spectrum of related metal complexes [79], and are confirmed by our labelling studies. Once again the skeletal modes are readily assigned.

In all of the above complexes the δ(RhCO) mode shifts to lower frequency upon substituting Cl by Br. This corresponds to an increase in the π-acceptor power of the *trans* halide ligand [88].

^{1}H, ^{13}C and ^{15}N NMR

The ^{1}H, ^{13}C and ^{15}N nmr data for the complexes *cis*-[$Rh(CO)_2(X)(L)$] (X is Cl or Br and L is aniline (an), pyridine (py), pyridine *N*-oxide (pyO), ammonia (NH_3), and imidazole (imid)) are presented in Tables 3.11-3.15. Representative spectra are shown in Figures 3.10-3.17.

(1) ^{1}H nmr

Although the ^{103}Rh isotope is present in 100% natural abundance and does undergo coupling with protons, no *J*(Rh-H) coupling could be observed in the spectra of the complexes. However, complexation between the respective ligands (L), and rhodium is confirmed by the upfield shift of the resonances of the complex relative to that of free ligand in the ^{1}H nmr spectra (see Tables 3.11-3.15). The chemical shift of the ligand moves insignificantly with varying X (Cl or Br). The spectra were recorded both in a polar (acetone-d_6) and a less polar solvent ($CDCl_3$).

cis-[$Rh(CO)_2(X)(L)$] (X is Cl or Br and L is NH_3, an, py and pyO).

The ^{1}H nmr spectra of the above complexes reveal the usual spectral pattern associated with the coordinated ligands. In instances where the N-atom in the ligand was enriched to ^{15}N, additional $^{1}J(^{15}N\text{-}H)$ coupling constant information could be obtained (see Tables 3.11-3.15). These values depend linearly on the *s*-character of the hybrid orbital involved in the N-H bond [32-34].

cis-[$Rh(CO)_2(X)(L)$] (X is Cl or Br and L is imidazole)

The ^{1}H nmr spectra of the imidazole complexes are worthy of additional comment. The data (Table 3.13) reveal that at room-temperature, in acetone solutions, there

are only two signals for the H_a, H_b and H_c protons of imidazole instead of the three resonances expected for a complex of the structure shown (see Table 3.13). The lower field signal is assigned to H_a (integrating for one proton), while the other signal is assigned to H_b and H_c (integrating for two protons), which are equivalent if exchange is occurring. On cooling solutions of the complexes, changes in the ^1H nmr spectra occur. That is, the single resonance of H_b and H_c splits into two separate resonances showing the expected resonances consistent with the "instantaneous" structure (see Table 3.13 and Figure 3.11).

Explanation of the fluxional process occurring within these complexes may involve an *inter*molecular (dissociative/associative) mechanism, or an *intra*molecular exchange process. Similar phenomena have been reported [97,98] for some related Rh and Ru complexes. Based on our previous work on the fluxional behavior occurring in Pt complexes [99], we predict that an *inter*molecular exchange process is occurring. Further evidence for an *inter*molecular exchange process is the observation that the ^1H nmr spectra of the complexes are solvent dependent. At room temperature, in acetone, the imidazole complexes undergo fast exchange while in $CDCL_3$ the complexes undergo slow exchange, that is three resonances are seen for the imidazole ligand (H_a, H_b and H_c).

The inclusion of ^{15}N-enriched imidazole in the complexes causes the broad ^{15}N-H peak to become a relatively sharp doublet, while the ^{15}N-H_a peak becomes a triplet. Thus the $^1J(^{15}N\text{-}H)$ and $^2J(^{15}N\text{-}H_a)$ coupling can easily be observed.

(2) ^{13}C nmr

In the past, several problems in the measurement of metal-carbonyl ^{13}C nmr spectra have been encountered [29,100,101]. To overcome the problem of not detecting

signals for metal-carbonyls using natural abundance ^{13}C [45,102,103], we have incorporated enriched ^{13}CO in our complexes, with the advantageous reduction in acquisition time for recording the spectra, and in addition, useful coupling constants can be observed. Enriched ^{13}CO is essential since most of the complexes decompose slowly in solution at temperatures above 0°C.

According to the preceding ^{1}H nmr spectral results it would appear that only the imidazole complexes undergo some exchange process. However, the ^{13}C nmr spectra (because of the relatively faster nmr time scale of ^{13}C) reveal that all the complexes are undergoing some exchange process in solution.

With reference to the square planar structure of the *cis*-$[Rh(CO)_2(X)(L)]$ complexes, the ^{13}C nmr spectra should show resonances due to the coordinated ligand (L), and a doublet of doublets for the carbonyl groups. The ^{103}Rh-^{13}C coupling gives rise to the doublet and the difference in chemical shift between the set of doublets is due to the nonequivalent CO groups in the complex. Only the metal-carbonyl carbon atoms show $J(^{103}Rh$-$^{13}C)$ coupling, and their chemical shifts and coupling constants values are found to be within the range established for related rhodium(I) carbonyl complexes [29,104-106]. Further splitting of the carbonyl resonances is due to the $^{2}J(^{13}C$-Rh-$^{13}C)$ coupling and the values are in argreement with *cis*-coordinated carbonyl groups [107,108].

The assignment of resonances in the ^{13}C nmr spectra arising from the coordinated ligand have been based on direct comparison with the free ligand [109-110] and with the aid of coupling constants wherever possible. However, the assignment of the signals to specific CO groups has been highly controversial [104,111-114]. Previous assignments have either relied on comparisons with other complexes, or,

alternatively no specific assignment have been given [103,108]. We now provide a direct physical demonstration of differentiation between the CO groups. This has been achieved by recording the ^{13}C nmr spectra of the doubly enriched complexes, that is of the complexes *cis*-[Rh($^{13}CO)_2$(X)(^{15}N-ligand)]. The low-temperature spectra (see Figure 3.14c) clearly show that only one of the ^{13}CO groups couples (detectable) to the ^{15}N-ligand. Bearing in mind that it is well documented [100,115-117] that *trans* coupling is much greater than *cis* coupling, we have assigned the resonance which couples to the ^{15}N-ligand as the CO group *trans* to the ^{15}N-ligand. Further support for this assignment comes from the ^{13}C nmr spectra of the complexes *cis*-[Rh($^{13}CO)_2$(X)($^{15}ND_3$)]. Substitution of hydrogen by deuterium has a marked effect on the ^{13}C nmr spectra [118], for now not only do we observe $^2J(^{13}C–^{15}N)$ coupling, but the resonances have additional unresolved fine structure due to $^3J(^{13}C–Rh–^{15}N–D)$ coupling (see Figure 3.14d). Hence these resonances can be unambiguously assigned to the CO groups *trans* to the ^{15}N-ligand. This is the first time [119] $^2J(^{13}C–Rh–^{15}N)$ has been recorded.*

The ^{13}C nmr spectra of the *cis*-[Rh$(CO)_2$(X)(L)] complexes can be basically divided into two groups. The first group all reveal a broad poorly resolved doublet of doublet peaks at room temperature in the carbonyl region of their ^{13}C nmr spectra, while the second group reveal only a single broad doublet at room temperature and require extensive cooling before the doublet of doublets can be resolved. The ammonia, pyridine and imidazole complexes fall into the former group while the pyridine *N*-oxide and aniline complexes fall into the latter group.

* The only reference to $^2J(^{13}C-M-^{15}N)$ has been made by Butler *at al.* who measured $^2J(^{13}C-Fe-^{15}N)$ in the complex $[Fe(CN)_5NO]^{2-}$.

A.R.BUTLER, C.GLIDEWELL, A.R.HYDE AND J.MCGINNIS, *Inorg. Chem.*, **24** (1985) 2931

cis-**[Rh(CO)$_2$(X)(L)] (X is Cl or Br and L is NH$_3$, py, imid)**

The above complexes reveal the expected peak pattern of the carbonyl groups at room temperature. Low temperature (-30°C) ^{13}C nmr spectra of the complexes exhibit resolution of the broad doublet of doublet while warming the solution has the tendency to collapse the doublet of doublets. In all instances the bromo complexes require a lower temperature than their chloro counterparts in order to observe the resolved doublet of doublets.

cis-**[Rh(CO)$_2$(X)(L)] (X is Cl or Br and L is pyO and aniline)**

The carbonyl region of the ^{13}C nmr spectra of the above complexes at low temperatures (-60°C) reveal a sharp doublet of doublets. As the temperature of the solution is raised the doublet of doublets collapses into a broad hump, until finally at room-temperature only one doublet occurs (see Figure 3.13). This phenomenon suggests some exchange process is occurring.

The retention of $^1J(^{103}\text{Rh}\text{-}^{13}\text{CO})$ coupling indicates that the exchange process is almost certainly the exchange of ligand (L):

$$[\text{Rh(CO)}_2\text{(X)(L)}] \quad + \quad \text{L}^* \rightleftharpoons [\text{Rh(CO)}_2\text{(X)(L}^*\text{)}] \quad + \quad \text{L}$$

rather than a process involving CO exchange. Although this has previously been suggested as probable [103], our ^{13}C and ^{15}N nmr spectral results now conclusively demonstrate this to be the case. The ^{13}C nmr spectra of the doubly enriched complexes *cis*-[Rh(^{13}CO)$_2$(X)(^{15}N-ligand)] reveal the expected spectral pattern (as described above) at low temperatures. However, on warming the solution, the $^2J(^{13}\text{C}\text{–}^{15}\text{N})$ coupling starts to collapse until finally only a broad doublet of doublets is observed indicating that the ^{15}N-ligand exchange is too fast for ^{15}N coupling to be

observed. Furthermore, in instances where the $^{2}J(^{13}C–^{13}C)$ coupling could be observed at low temperatures, the coupling is still maintained at higher temperatures which indicates that the carbonyl groups are not undergoing exchange within the temperature range studied. The ^{15}N nmr results (see ^{15}N nmr section) conclusively show that an *inter*molecular exchange process involving ligand (L), is occurring.

We have studied the fluxional processes occurring within the complexes between 20°C and –55°C by a complete band shape analysis using a simulation computer programme (see Chapter 6).

Although numerous reports have been published [25,29-31,120-123] regarding the correlation between the ^{13}C nmr shifts and infrared stretching frequencies, there appears to be much conflict in the interpretation of the results as several factors determine each of these values. Nevertheless, it has been shown [122,124] that only in a closely related series of complexes, for instance *trans*-$[Pt(Cl)_2(CO)(R\text{-}py)]$ (R-py is a *para*-substituted pyridine) where only electronic effects alter the bonding, that the complex having the higher $\nu(CO)$ value shows, (i) the lower ^{13}C chemical shift for the carbonyl group, and (ii) the larger $^{1}J(Pt–^{13}CO)$ coupling constant.

Hence it is not surprising that in our complexes correlations of ^{13}CO data (^{13}CO chemical shift or $^{1}J(^{13}CO\text{-}Rh)$ coupling) versus infrared data ($\nu(CO)$, $\nu(Rh\text{-}C)$ or force constants) results in a large scatter of points. This is a consequence of the different modes of bonding between the various ligands and the rhodium metal. However, the $^{1}J(Rh\text{-}CO_b)$ coupling constants of the chloro- complexes are always smaller than their bromo- counterparts, while the $^{13}CO_b$ chemical shifts of the chloro- complexes are always higher than their bromo- counterparts. On the other

hand there are no such trends for the CO_a group. This is because, in the complexes, the halogen is *trans* to the CO_b group and the *trans*-influence affects the ligand *trans* to itself most. The smaller ^1J(Rh-CO_a) coupling constant relative to ^1J(Rh-CO_b) infers that the ligand is a better charge donor than the halogen [25,122,123].

(3) ^{15}N nmr

Representative coupled and decoupled ^{15}N nmr spectra are shown in Figures 3.15-3.17. The ^{15}N nmr spectra are particularly useful as they describe the interaction between ligand (L), and the metal centre. In the complexes *cis*-[Rh(CO)$_2$(X)(^{15}N-ligand)], the ^{15}N-ligand couples to ^{103}Rh, thus one expects to observe a doublet for each resonance in the ^{15}N nmr spectra. Any loss of ^1J(^{15}N-^{103}Rh) coupling correlates to bond-scissions, and is extremely sensitive and the most definitive nmr test of an *inter*molecular exchange process [125].

The ^{15}N nmr spectra of the *cis*-[Rh(CO)$_2$(X)(^{15}N-imid)] complexes reveal the expected spectral pattern at room temperature. However, the $^{15}NH_3$ and ^{15}N-aniline complexes show only a single resonance in their ^{15}N nmr spectra at room temperature. At low temperatures this singlet splits into the expected doublet, indicating that the ^{15}N-ligand is dissociating from the Rh centre for a sufficiently long time on the nmr time scale. Hence we conclude that an *inter*molecular exchange process involving ligand (L), is occurring. As previously mentioned, the bromo- complexes require a lower temperature than their chloro- counterparts in order to observe the resolved doublet.

The ^1J(^{15}N-^{103}Rh) coupling constants are easily rationalized [32-34,126,127] in terms of the metal-nitrogen bonding, and correlate simply with the *s*-character of the bonding electron on nitrogen, the aromatic nitrogens (sp^2) having the larger ^1J(^{15}N-

^{103}Rh) coupling values than the saturated nitrogens (sp^3). The coupled ^{15}N nmr spectra allow observation of $^1J(^{15}N\text{-}H)$ coupling constants and these values depend linearly on the *s*-character of the hybrid orbital involved in the N-H bond [32-34].

ELECTRONIC SPECTRA

The electronic spectral data of the complexes *cis*-[Rh(CO)$_2$(X)(L)] (X is Cl or Br and L is aniline, pyridine, pyridine *N*-oxide, imidazole, or ammonia) are presented in Table 3.16.

Although the complexes have different colours in the solid state, their dichloromethane solutions are all yellow. The solution spectra in the uv/vis region show a rather simple pattern quite similar to that usually observed for four-coordinate square planar d^8 systems [128,129].

By analogy with similar complexes previously studied [130-133] we expect to observe the $\pi \rightarrow \pi^*$(CO), the d(Rh)$\rightarrow\pi^*$(CO), and the $X^- \rightarrow Rh^{+1}$ transitions. In addition, in complexes where L is an amine that possess π-electrons which may interact with Rh, there is the possibility of the d(Rh)$\rightarrow\pi^*$(amine) charge transfer transition. However, since some of the transitions overlap with each other, resulting in very broad bands, specific assignments are tentative. Nevertheless, the absorptions occurring in the range 326-342 nm with extinction coefficients between 295-455 m^2mole^{-1}, are assigned to the $d\rightarrow\pi^*$ metal-to-ligand charge transfer bands that are characteristic of a number of rhodium(I) complexes containing π-acceptor ligands [36,133,134].

Absorption in the 380-600 nm region is indicative [39,134-137] of metal-metal interaction resulting from the close proximity of two rhodium centers, possibly in a stacked arrangement, see Figure 3.18. Solid state (diffuse reflectance and

transmission) electronic spectra obtained by many authors [39,45,137,138] have confirmed these metal-metal interaction. Vallarino and Sheargold [45] propose that steric hindrance (by bulky ligands) of the N-donor atom is the determining factor in the choice of "stacked" or "normal" structures in the solid state. The solution spectra of our complexes exhibit no bands in the 380-600 nm region. This can be ascribed to the existence of discrete monomeric rhodium units in solution. However, the fact that the ligands in our complexes do not offer substantial steric hindrance would indicate that our complexes should also possess metal-metal interactions in the solid state. The absence of solid state spectroscopy facilities terminated further study in this field.

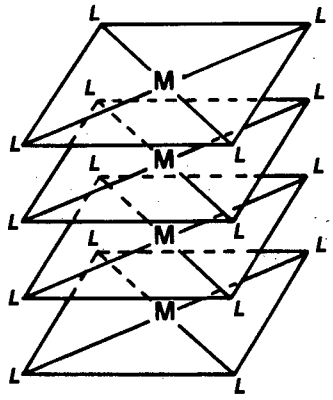

Figure 3.18 "Stacked" arrangement of the planar complexes.

MASS SPECTRA

The mass spectra of the complexes *cis*-$[Rh(CO)_2(X)(L)]$ do not show the expected molecular ion peak or high mass fragements thereof. However, all the spectra reveal peaks due to (i) the ligand (L), associated with the respective complexes, and (ii) the $[Rh(CO)_2X]_2$ dimer molecular ion peak and its fragementation pathway. This may be due to the low volatility of the complexes and the peaks observed in the

spectra may be thermal decomposition products of the *cis*-[$Rh(CO)_2(X)(L)$] complexes.

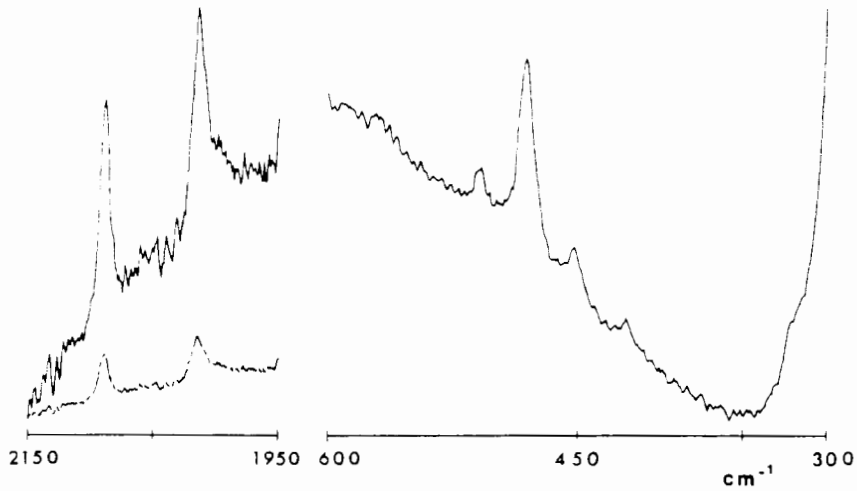

Figure 3.4 Raman spectrum of *cis*-$[Rh(CO)_2(Cl)(py)]$ (rotating KCl pellet).

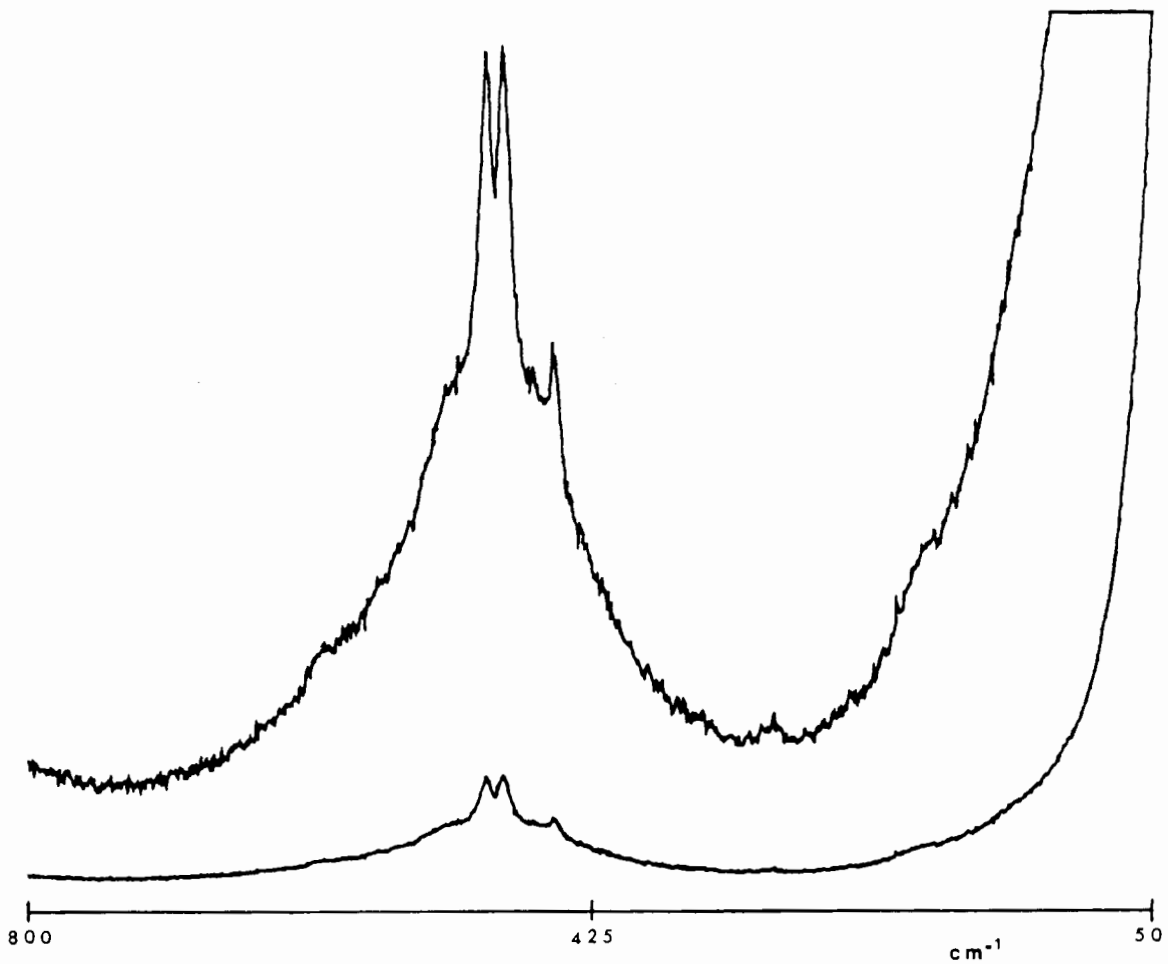

Figure 3.5 Raman spectrum of *cis*-$[Rh(CO)_2(Cl)(NH_3)]$ (rotating KCl pellet).

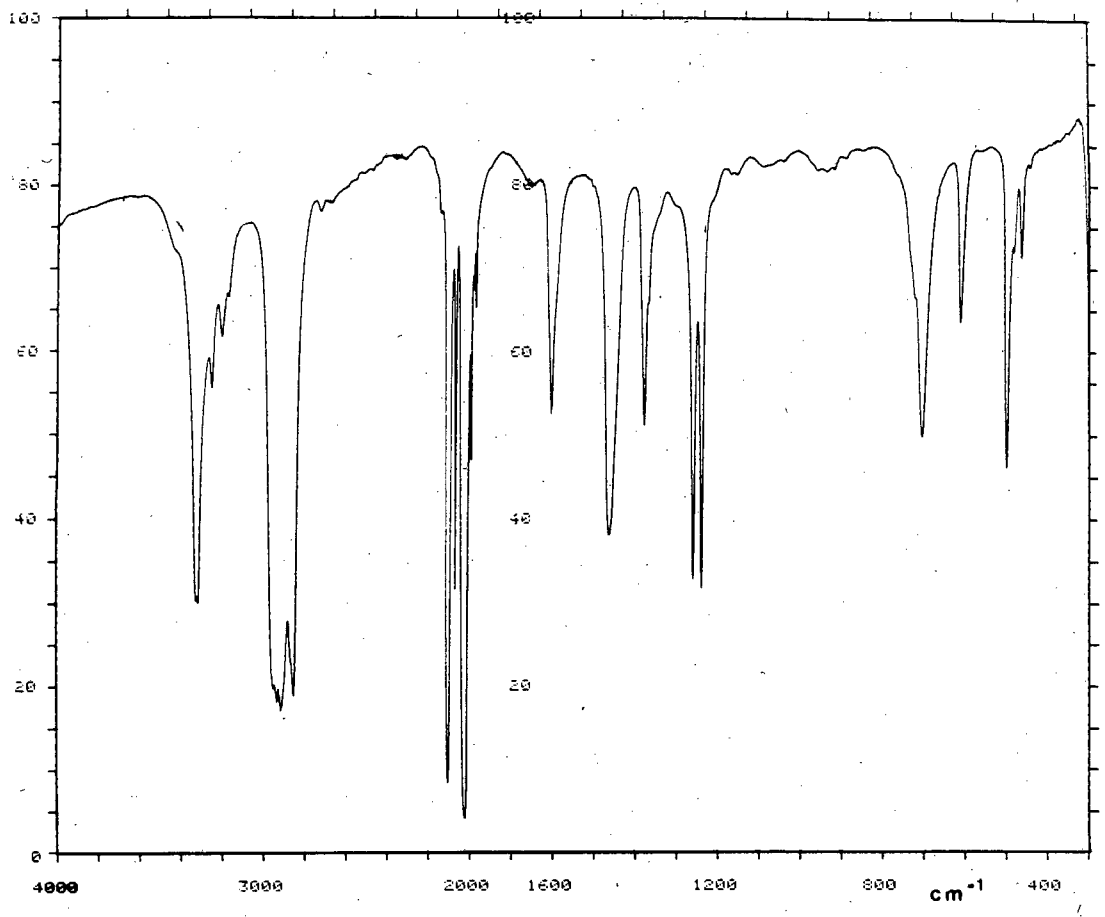

Figure 3.6 Infrared spectrum of *cis*-$[Rh(CO)_2(Cl)(NH_3)]$ (Nujol mull).

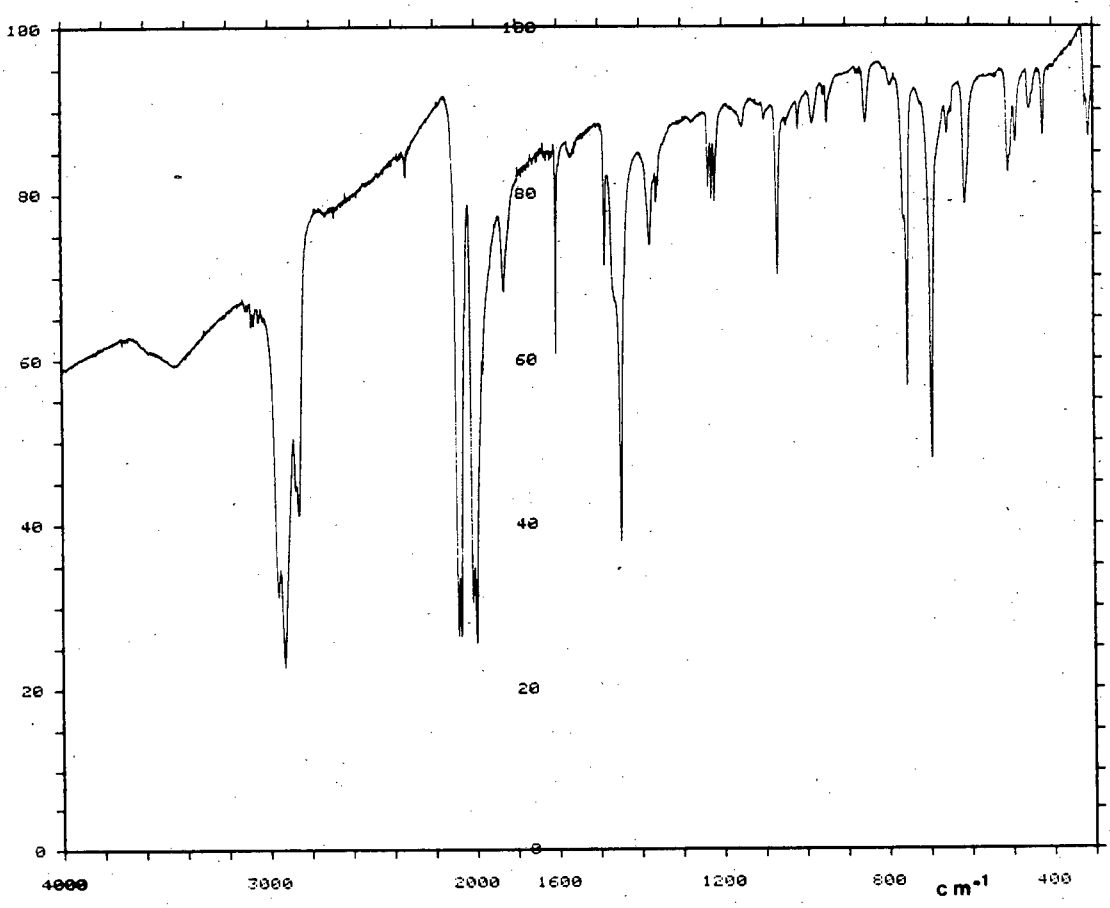

Figure 3.7 Infrared spectrum of *cis*-$[Rh(CO)_2(Cl)(py)]$ (Nujol mull).

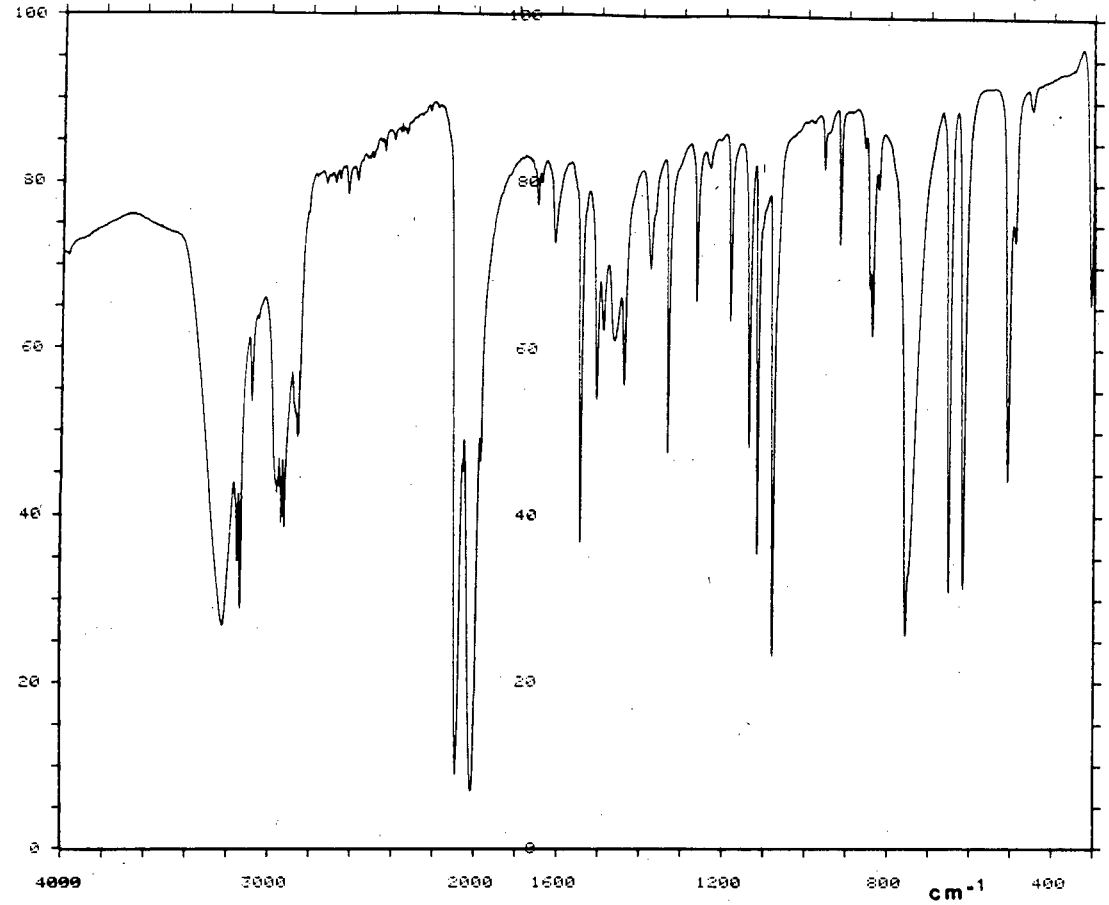

Figure 3.8 Infrared spectrum of *cis*-$[Rh(CO)_2(Cl)(imid)]$ (Nujol mull).

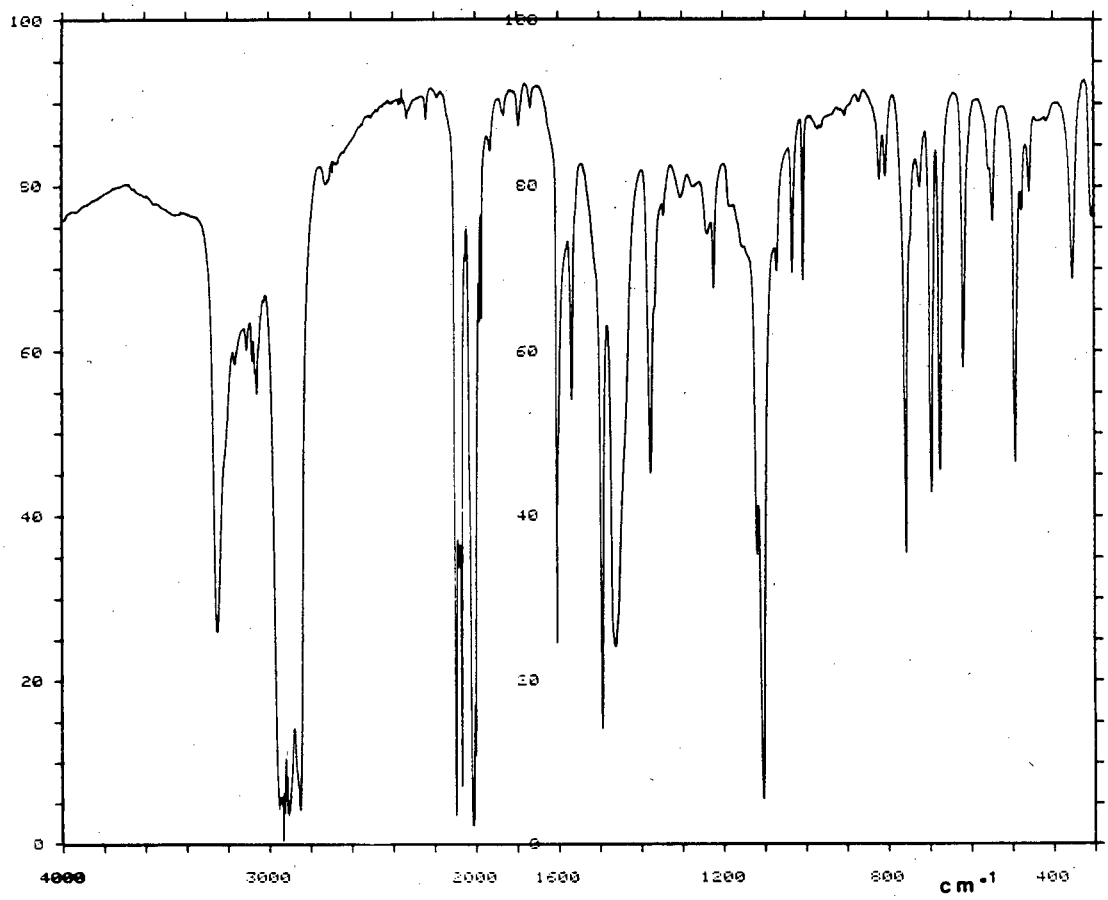

Figure 3.9 Infrared spectrum of *cis*-$[Rh(CO)_2(Cl)(an)]$ (Nujol mull).

TABLE 3.1 Infrared assignments of *cis*-$[Rh(CO)_2(Cl)(NH_3)]$ (cm^{-1}).

NH_3	ND_3	$^{15}NH_3$	^{13}CO	Assignment
3325	} 2483	3319	3328	ν(N-H)
3313		3308	3315	
3248	2365	3244	3248	
3199	2331	3196	3201	
3181	-----	3162	3168	
(2088)	(2088)	(2089)	(2039)	ν(C≡O)
(2012)	(2012)	(2012)	(1967)	
2102	2079	2097	{ 2075, 2047	
2066	2066	2066	{ 2019, 2013	
2020	2018	2021	1975	
1989	1989	1990	1947	
1976	-----	1976	1932	
1967	1967	1967	1923	
1602	1168	1599	1602	$\delta_{as}(NH_3)$
1258	968	1250	1257	$\delta_s(NH_3)$
1237	956	1230	1236	
702	552	698	700	$\rho(NH_3)$
609	623	608	571	δ(Rh-C-O) in-plane
497	463	495	490	ν(Rh-N)
481	478	481	473	δ(Rh-C-O) out-of-plane
463	463	463	453	ν(Rh-C)
446	445	446	440	ν(Rh-C)
300	300	300	{ 301, 298	ν(Rh-Cl)
197	184	193	196	δ(Rh-N)
158	148	155	158	γ(Rh-N)
120	120	120	120	δ(C-Rh-C)
103	103	103	103	δ(Rh-Cl)
69	70	68	68	γ(Rh-Cl)

Values in parentheses are those recorded in CH_2Cl_2 solution.

TABLE 3.2 Infrared assignments of *cis*-$[Rh(CO)_2(Cl)(py)]$ (cm^{-1}).

py	py-d_5	^{13}CO	Assignment	*Wilson Band No.
3106	2354	3108	ν(C-H)	20b
3080	-----	3081		2
3071	2302	3071		7a
3048	2291	3047		20a/7b
(2089)	(2088)	(2039)	ν(C≡O)	
(2013)	(2012)	(1968)		
2067	2066	2018		
2007	2007	1961		
1971	1971	1923		
1658	1652	1660	combination	1+6b
1640	1593	1640		1+6a
1605	1562	1607	ν(ring)	8a
1568	1532	1570		8b
1484	1342	1484		19a
1444	1318	1444		19b
1403	1370	1402	combination	
1356	1334	1356	ν(ring)	14
1235	978	1234	δ(C-H)	3
1220	898	1218		9a
1156	}841	1153		}15
1146		1145		
1099	820	1099		18b
1070	}832	1069		}18a
1064		1063		
1045	1043	1044	ν(ring)	12
1016	1013	1014		1
991	817	-----	γ(C-H)	17a
954	722	953		5
866	674	866		10a/10b
760	602	760	γ(ring)	4
721	{582 564	720	combination	

py	py-d_5	^{13}CO	Assignment	*Wilson Band No.
698	537	697	γ(C-H)	11
651	642	650	δ(ring)	6b
643	{624, 619}	641	δ(ring)	6a
614	611	593	δ(Rh-C≡O) in-plane	
502	501	492	ν(Rh-C)/δ(Rh-C≡O) out-of-plane	
454	452	444	ν(Rh-C)	
424	390	421	γ(ring)	16b
393	340	394	γ(ring)	16a
310	310	309	ν(Rh-Cl)	
206	197	205	ν(Rh-N)	
171	165	170	δ(Rh-N)	
139	137	138	δ(C-Rh-C)	
110	110	109	δ(Rh-Cl)	
90	90	90	γ(Rh-Cl)	
57	52	57	γ(Rh-N)	

Values in parentheses are those recorded in CH_2Cl_2 solution.

* E.B.Wilson, *Phys. Rev.*, **45** (1934) 706

TABLE 3.3 Infrared assignments of *cis*-[$Rh(CO)_2(Cl)$(imid)] (cm^{-1}).

imid	imid-d_4	imid-^{15}N	^{13}CO	Assignment
3218	2392	3176	3189	ν(N-H)
3146	2350	-----	3147	ν(C-H)
3131	2344	3131	3132	ν(C-H)
3076	2344	3062	3077	ν(C-H)
2969	-----	2948	-----	ν(C-H)
(2083)	(2083)	(2083)	(2035)	ν(C≡O)
(2009)	(2009)	(2009)	(1963)	ν(C≡O)
2091	2072, 2063	2074, 2065	2063, 2052	ν(C≡O)
2057	2048	2050	2023	ν(C≡O)
2015	2001	2003	2002, 1978	ν(C≡O)
1971	1965	1975	1968, 1956	ν(C≡O)
1544	1470, 1454	1538	1544	ν(ring)
1506	1412	1504	1509	ν(ring)
1489	1412	1494	1489	ν(ring)
1439	1346	1431	1444	ν(ring)
1332	1307, 1271	1315	1325	ν(ring)
1265	948	1261, 1251	1267	δ(C-H)
1233	917	1214	1231	δ(N-H)
1182	1182, 1168	1173	1183	combination/overtone
1135	1131, 1122	1125	1138	ν(ring)
1115	893	1110	1100	δ(C-H)
1078	873	1067	1074	δ(C-H)
957	575	939	951	γ(N-H)
	981, 972			δ(ring)
	779, 770			γ(C-H)
918	829	905	919	δ(ring)
858	----	860	860	combination/overtone
848	664	839	840	γ(C-H)
838	650	839	840	γ(C-H)
756	590	764	764	γ(C-H)
748	575	747	747	γ(C-H)

imid	imid-d_4	imid-^{15}N	^{13}CO	Assignment
651	557	644	651	} γ(ring)
616	{521	607	615	} γ(ring)
	{616	616	598	δ(Rh-C≡O)in-plane
509	506	507	496	δ(Rh-C≡O)out-of-plane
490	486	487	480	ν(Rh-C)
451	448	448	440	ν(Rh-C)
308	307	307	306	ν(Rh-Cl)
256	253	249	255	ν(Rh-N)
224	218	223	223	δ(Rh-N)
175	175	178	180	δ(Rh-N-C)
150	149	150	150	δ(Rh-Cl)
~111	~110	~110	~110	δ(C-Rh-C)/γ(Rh-N)
~70	~67	~67	~68	γ(Rh-Cl)

Values in parentheses are those recorded in CH_2Cl_2 solution.

Table 3.4 Infrared assignments of *cis*-$[Rh(CO)_2(Cl)(pyO)]$ (cm^{-1}).

pyO	pyO-d_5	^{13}CO	Assignment	*Band Number Wilson	Gambi & Ghersetti
3106	2312	3107		20b/2	1/12
3075	2299	3076		20a	2
3033	2292	3034	ν(C-H)	7b	13
2938	2212	2939		7a	3
(2081)	(2080)	(2032)			
(2006)	(2006)	(1961)			
2076	2077	2055, 2047			
2061	2060	2022	ν(C≡O)		
2047	2047	1998, 1993			
1991	1992	1967			
1963	1964, 1959	1951			
1614	1569	1615		8a	4
1571	1539	1572	ν(ring)	8b	14
1476	1355, 1349	1475		19a/19b	5/15
1421	1409	1421	combination/overtone		
1246	1236	1245	ν(ring)	14	16
1199	1196	1198		3	17
1183	1154	1182	ν(N-O)	}13	6
1179	1148	1178			
1157	883	1156		9a	7
1147	870	1147	δ(C-H)	15	18
1071	820	1070		18b	19
1025	986	1024	ν(ring)	12	9
1010	841	1009	combination/overtone		
953	792	952	γ(C-H)	5/17a	22/25
829	764	827	ν(ring)	1	10
787	563	786	γ(C-H)	}11	27
775	546	773			
680	656	679	γ(ring)	}4	28
676	649	674			
639	613	638	δ(ring)	6b	20

pyO	pyO-d_5	^{13}CO	Assignment	*Band Number Wilson	Gambi & Ghersetti
629	627	610	δ(Rh-C≡O) in-plane		
572	563	571	δ(ring)	6a	11
547	518	545	γ(ring)	16b	29
501	508	491	δ(Rh-C≡O) out-of-plane		
493 486	}478	486	ν(Rh-C)/ν(Rh-O)		
461	432	458	β(N-O)	9b	21
448	448	439	ν(Rh-C)		
384	370	383	γ(ring)	16a	24
310	309	310	ν(Rh-Cl)		
299	298	298	δ(Rh-O)		
217	207	216	γ(N-O)	17b	30
139	137	138	δ(Rh-Cl)		
111	111	111	δ(C-Rh-C)		
66	64	66	γ(Rh-Cl)/γ(Rh-O)		

Values in parentheses are those recorded in CH_2Cl_2 solution.

* E.B.Wilson, *Phys. Rev.*, 45 (1934) 706
A.Gambi & S.Ghersetti, *Spectrosc. Lett.*, 10 (1977) 627

Table 3.5 Infrared assignments of *cis*-$[Rh(CO)_2(Cl)(aniline)]$ (cm^{-1}).

an	an-d_5	an-ND_2	an-d_7	an-$^{15}NH_2$	^{13}CO	Assignment
3254	3254	2443	2435	3243	3255	ν(N-H)
3164	3149	-----	-----	3161	3164	
3107	3104	2335	2346	3102	3108	ν(N-H).....Cl
3080	2295	3070	2301, 2290	3081	3081	ν(C-H)
3068	2286	3061	2274	3069	3069	
3057	2273	3048		3059	3058	
(2088)	(2088)	(2088)	(2088)	(2087)	(2040)	ν(C≡O)
(2014)	(2014)	(2014)	(2014)	(2015)	(1969)	
2098	2096	2091	2097	2096	2070	
2081	-----	-----	-----	------	2060	
2068	2068	2068	2068	2069	2047	
2050	2050	2053	2050	2050	2021	
2029	-----	2039	-----	-----	1994	
2013	2014	2014	2014	2014	1971	
2001	2000	2001	2001	2001	1956	
1981	1981	1992	1981	1982	1935	
1970	1970	1969	1970	1971	1925	
1606	1571	1605	1563	1606	1606	ν(ring)
1567	1563	1244(NHD), 1106, 1094	1205(NHD), 1115, 1105	1563	1567	NH_2 scissor
1495	1386	1494	1383	1495	1495	ν(ring)
1470	1373	1459	1341	1470	1470	
1433	1422	1408	1417	1434	1428	
1344	-----	1340	-----	1344	1344	
1304	1305	1305	1304	-----	------	
1239	1166	1236	-----	1236	1238	ν(C-N)
1222				1218	1221	
1185	879	1181	882	1185	1185	δ(C-H)
1119	1118	-----	-----	1110	1117	NH_2 twist
1104	1103	921(NHD), 866	917(NHD), 841	1096	1103	
1069	847	1030	834	1068	1069	δ(C-H)
1031	765	1003	757	1030	1030	

an	an-d_5	an-ND_2	an-d_7	an-$^{15}NH_2$	^{13}CO	Assignment
1005	756	987	732	1003	1003	δ(C-H)
968	963	959	961	968	968	ν(ring)
904	645	890	649	903	903	γ(C-H)
820	818	817	{817 810	815	818	ν(ring)
805	593	789	585	801	803	γ(C-H)
756	557	738	553	754	754	
745	542	747	567	744	744	
695	507	692	498	693	693	
673	673	{544(NHD) 522	528	665	671	NH_2 wag
616	613	614	611	614	{616 597	δ(ring) δ(Rh-C≡O) in-plane
556	557	463	}444	548	555	NH_2 rock
546	542	447		540	544	
492	482	491	479	491	484	δ(Rh-C≡O) out-of-plane
476	469	469	463	476	466	ν(Rh-C)
457	457	449	444	457	443	ν(Rh-C)
413	388	355	{381(NHD) 340	407	412	ν(Rh-N)
352	340	{322(NHD) 304	293	350	352	δ(Rh-N)
308	307	304	303	307	307	ν(Rh-Cl)
207	196	210	195	206	206	γ(ring)
147	145	144	144	146	147	δ(Rh-Cl)
105	105	105	105	105	105	δ(C-Rh-C)
75	~71	~75	71	71	73	γ(Rh-Cl)/γ(Rh-N)

Values in parentheses are those recorded in CH_2Cl_2 solution.

TABLE 3.6 Infrared assignments of *cis*-$[Rh(CO)_2(Br)(NH_3)]$ (cm^{-1}).

NH_3	ND_3	$^{15}NH_3$	^{13}CO	Assignment
3310	2483	3302	3310	
3240	2385	3236	3240	
3191	2359	3183	3190	ν(N-H)
3156	2334	-----	3157	
(2087)	(2087)	(2087)	(2040)	
(2012)	(2012)	(2012)	(1967)	
2097	2097	2101	2072	
2067	2067	2066	2040	
2051	-----	-----	2013	ν(C≡O)
2022	2021	2018	1983	
1993	1991	1991	1932	
1980	-----	-----	1924	
1971	1970	1970	1913	
1596	1163	1594	1596	$\delta_{as}(NH_3)$
1251	963	1245	1251	$\delta_s(NH_3)$
1236	954	1230	1236	
698	552	694	696	$\rho(NH_3)$
606	616	604	586	δ(Rh-C-O) in-plane
493	}470	489	483	ν(Rh-N)
468		468	457	ν(Rh-C)
451	445	450	437	ν(Rh-C)
214	214	214	214	ν(Rh-Br)
192	}168	188	192	δ(Rh-N)
182		178	182	
161	147	159	161	γ(Rh-N)
105	104	104	104	δ(C-Rh-C)
84	84	84	84	δ(Rh-Br)
54	54	---	55	γ(Rh-Br)

Values in parentheses are those recorded in CH_2Cl_2 solution.

Table 3.7 Infrared assignments of *cis*-$[Rh(CO)_2(Br)(py)]$ (cm^{-1}).

py	py-d_5	^{13}CO	Assignment	*Wilson Band No.
3112	2349	3115	ν(C-H)	20b
3095	2336	3098		2
3073	2310	3077		7a
3045	2296	3050		20a
3027	2284	3028		7b
(2086)	(2086)	(2037)	ν(C≡O)	
(2014)	(2014)	(1968)		
2084	2086	2057		
-----	2078	2028		
2069	2067	2019		
-----	2022	2006		
2016	2012	1979		
1996	1995	1966, 1950		
1965	1971	1924		
1661	1648	1663	combination	1 + 6b
1630	1598	1630		1 + 6a
1607	1566	1607	ν(ring)	8a
1571	1535, 1532	1572		8b
1484	1342	1485		19a
1446	1320	1448		19b
1400	1375	1400	combination	
1358	1334	1359	ν(ring)	14
1231	979	1234	δ(C-H)	3
1224	896	1220		9a
1217		1218		
1151	841	1156		15
1098	833	1095		18b
1065	837	1070, 1066		18a
1045	1044	1046	ν(ring)	12
1015	1012	1016		1
981	809	983	γ(C-H)	17a
947	776	948		5

py	py-d_5	^{13}CO	Assignment	*Wilson Band No.
874	680	871	γ(C-H)	10a/10b
761 752	}602	755	γ(ring)	4
692	533	693	γ(C-H)	11
649	638	649	δ(ring)	6b
643	618	643	δ(ring)	6a
604	603	584	δ(Rh-C≡O) in-plane	
500	500	492	δ(Rh-C≡O) out-of-plane	
487	487	475	ν(Rh-C)	
446	444	434	ν(Rh-C)	
421	387	417	γ(ring)	16b
397	340	394	γ(ring)	16a
235	233	235	ν(Rh-Br)	
214	208	213	ν(Rh-N)	
191	182	189	δ(Rh-N)	
159	156	159	δ(C-Rh-C)	
93	92	93	δ(Rh-Br)	
72	71	70	γ(Rh-Br)	
61	57	61	γ(Rh-N)	

Values in parentheses are those recorded in CH_2Cl_2 solution.

* E.B.Wilson, *Phys. Rev.*, **45** (1934) 706

TABLE 3.8 Infrared assignments of *cis*-$[Rh(CO)_2(Br)(imid)]$ (cm^{-1}).

imid	imid-d_4	imid-^{15}N	^{13}CO	Assignment
3227	2371	3216	3181	ν(N-H)
3157	2360	3155	3158	ν(C-H)
3133	2332	3133	3134	ν(C-H)
3079	2332	3064	3080	ν(C-H)
2970	2294	2951	-----	ν(C-H)
(2082)	(2082)	(2082)	(2034)	ν(C≡O)
(2009)	(2009)	(2008)	(1963)	ν(C≡O)
2086	2086	2087	2026	ν(C≡O)
2012	2014	2012	2001	ν(C≡O)
1995	1994	-----	1973, 1962	ν(C≡O)
1966	-----	1970	1951	ν(C≡O)
1545	1462, 1446	1538	1543	ν(ring)
1503	1405	1493	1505	ν(ring)
1485	1405	1476	1486	ν(ring)
1436	1360	1422	1439	ν(ring)
1329	1315, 1288	1322	1328	ν(ring)
1262	945	1247	1261	δ(C-H)
1231	901	1214	1232	δ(N-H)
1178	1198, 1187	1164	1180	combination/overtone
1132	1136, 1117	1121	1132, 1142	ν(ring)
1112	891	1111	1092	δ(C-H)
1075	881	1069	1069	δ(C-H)
	573			γ(N-H)
954	980, 973	940	950	δ(ring)
	783, 719			γ(C-H)
915	820	901	913	δ(ring)
857	838	857	----	combination/overtone
835	667, 651	834	833	γ(C-H)
756	595	756	748	γ(C-H)
734	573	734	748	γ(C-H)
650	552	641	653	γ(ring)

imid	imid-d_4	imid-^{15}N	^{13}CO	Assignment
612	{526	606	611	γ(ring)
	{611	----	591	δ(Rh-C≡O)in-plane
503	502	502	490	δ(Rh-C≡O)out-of-plane
490	488	490	479	ν(Rh-C)
443	442	442	434	ν(Rh-C)
259	255	257	258	ν(Rh-N)
238	233	238	236	ν(Rh-Br)
197	191	196	196	δ(Rh-N)
173	166	170	176	δ(Rh-N-C)
107	106	108	107	δ(C-Rh-C)
~100	~98	~100	~99	δ(Rh-Br)
~71	~69	~69	~70	γ(Rh-Br)/γ(Rh-N)

Values in parentheses are those recorded in CH_2Cl_2 solution.

Table 3.9 Infrared assignments of *cis*-$[Rh(CO)_2(Br)(pyO)]$ (cm^{-1}).

pyO	pyO-d_5	^{13}CO	Assignment	*Band Number Wilson	Gambi & Ghersetti
3107	2312	3106		20b/2	1/12
3076	2299	3075		20a	2
3033	2293	3032	ν(C-H)	7b	13
2938	2211	2938		7a	3
(2080)	(2080)	(2031)			
(2007)	(2007)	(1961)			
2077	2076	2055, 2049			
2062	2062	2027			
2047	2047	2000, 1996	ν(C≡O)		
-----	2001	1949			
1996	1996	1924			
1970	1970	1921			
1966	1966	1915			
1960	1960	1906			
1615	1569	1615		8a	4
1571	1539	1571	ν(ring)	8b	14
1474	1355, 1347	1473		19a/19b	5/15
1419	1409	1418	combination/overtone		
1244	1235	1244	ν(ring)	14	16
1219	1210	-----	combination/overtone		
1196	1190	1196	ν(ring)	3	17
1180	1154	1180	ν(N-O)	13	6
1176	1143	1176			
1155	867	1155		9a	7
1147	839	1147	δ(C-H)	15	18
1071	819	1071		18b	19
1052	1042	1051	combination/overtone		
1023	982	1023	ν(ring)	12	9
1007	----	1007	combination/overtone		
949	789	949	γ(C-H)	5/17a	22/25
827	761	827	ν(ring)	1	10

pyO	pyO-d_5	^{13}CO	Assignment	*Band Number Wilson	Gambi & Ghersetti
783	563	783	γ(C-H)	11	27
771	545	771			
678	653	678	γ(ring)	4	28
674	646	674			
638	613	638	δ(ring)	6b	20
620	618	604	δ(Rh-C≡O) in-plane		
570	561	570	δ(ring)	6a	11
546	515	544	γ(ring)	16b	29
505	505	496	δ(Rh-C≡O) out-of-plane		
484	472	483	ν(Rh-C)/ν(Rh-O)		
479		468			
458	432	454	β(N-O)	9b	21
449	445	439	ν(Rh-C)		
376	362	375	γ(ring)	16a	24
219	222	219	γ(N-O)	17b	30
213	213	212	ν(Rh-Br)		
156	153	----	δ(Rh-O)		
121	121	121	δ(Rh-Br)		
112	110	112	δ(C-Rh-C)		
95	88	95	γ(Rh-O)		
65	65	65	γ(Rh-Br)		

Values in parentheses are those recorded in CH_2Cl_2 solution.

* E.B.Wilson, *Phys. Rev.*, **45** (1934) 706

A.Gambi & S.Ghersetti, *Spectrosc. Lett.*, **10** (1977) 627

Table 3.10 Infrared assignments of *cis*-[Rh(CO)$_2$(Br)(aniline)] (cm^{-1}).

an	an-d_5	an-ND$_2$	an-d_7	an-^{15}NH$_2$	^{13}CO	Assignment
3245	3245	2433	2433	3237	3245	ν(N-H)
3163	-----	2395	2391	3158	3163	
3106	3103	2332	2343	3099	3105	ν(N-H).....Br
3082	2294	3072	-----	3082	3081	ν(C-H)
3066	2286	3055	2287	3066	3066	
3058				3058	3057	
3025	2273	3017	2272	3024		
(2087)	(2087)	(2087)	(2087)	(2087)	(2038)	ν(C≡O)
(2015)	(2015)	(2015)	(2014)	(2014)	(1969)	
2095	2094	2089	2094	2095	2078	
2068	2068	2068	2068	2068	2058	
2051	2051	2051	2034	2050	2043	
2013	2013	2013	2013	2013	2015	
2002	2002	2002	2001	2002	1991, 1968	
1983	1981	1981	1981	1981	1942	
1974	1972	1972	1971	1972	1934, 1925	
1605	1570	1606	1562	1605	1606	ν(ring)
1565	1559	1242(NHD), 1101, 1094	1202(NHD), 1111, 1100	1560	1565	NH_2 scissor
1495	1386	1494	1384	1494	1494	ν(ring)
1470	1372	1459	1339	1470	1470	
1431	1423	1406	1419	1429	-----	
1344	-----	1335	1290	1343	1343	
1294	1291	-----	-----	1293	-----	
1237	1163	1233	1158	1235	1237	ν(C-N)
1219				1216	1219	
1184	876	1181	881	1184	1184	δ(C-H)
1111	1109	917(NHD)	896	1104	1111	NH_2 twist
1101	1098	864	841	1094	1101	
1068	834	1028	833	1068	1068	δ(C-H)
1029	762	1003	756	1029	1029	
1003	752	986	740	1003	1003	
969	961	----	961	969	968	ν(ring)

an	an-d_5	an-ND_2	an-d_7	an-$^{15}NH_2$	^{13}CO	Assignment
901	642	889	643	901	901	γ(C-H)
817	817	814	{817, 810}	814	817	ν(ring)
803	593	790	589	799	803	γ(C-H)
754	556	737	553	754	754	γ(C-H)
744	541	753	526	744	744	
692	502	691	494	692	692	
665	665	{557(NHD), 519}	{583(NHD), 526}	657	664	NH_2 wag
615	615	}606	606	615	616	δ(ring)
608	607			606	592	δ(Rh-C≡O) in-plane
554	555	474	}445	547	554	NH_2 rock
544	541	445		538	543	
485	}467	485	460	485	477	δ(Rh-C≡O) out-of-plane
461		----		460	448	ν(Rh-C)
450	450	445	445	449	435	ν(Rh-C)
409	386	{380(NHD), 355}	{378(NHD), 341}	----	408	ν(Rh-N)
351	339	{322(NHD), 308}	290	349	351	δ(Rh-N)
218	218	218	218	219	218	ν(Rh-Br)
208	195	207	194	207	207	γ(ring)
122	120	121	119	121	122	δ(Rh-Br)
104	102	104	102	103	104	δ(C-Rh-C)
83	~83	~83	83	83	83	γ(Rh-Br)/γ(Rh-N)

Values in parentheses are those recorded in CH_2Cl_2 solution.

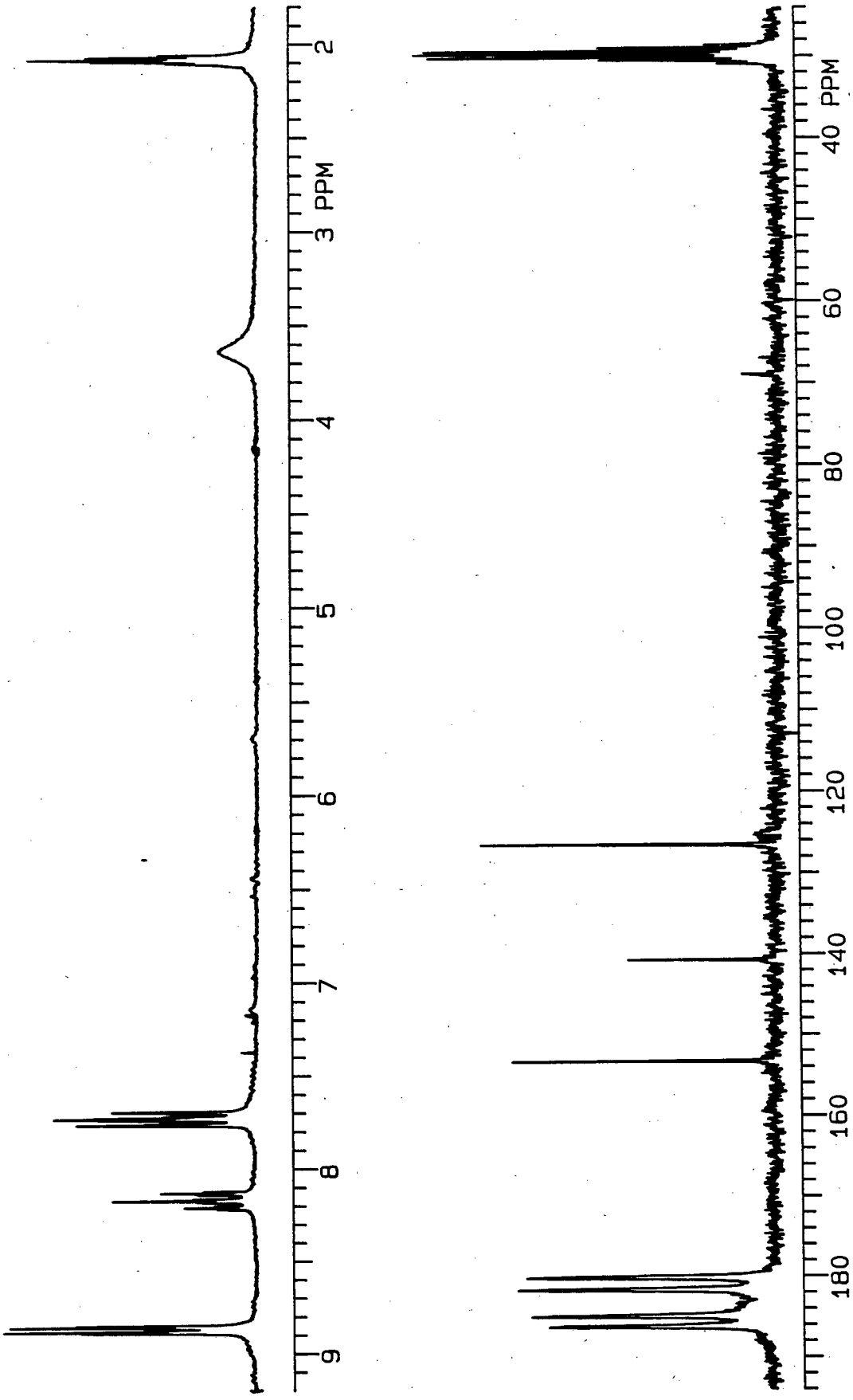

FIGURE 3.10 ^{1}H and ^{13}C nmr spectra of *cis*-[$Rh(CO)_2(Br)(py)$] (acetone-d_6, Temp. = –30°C).

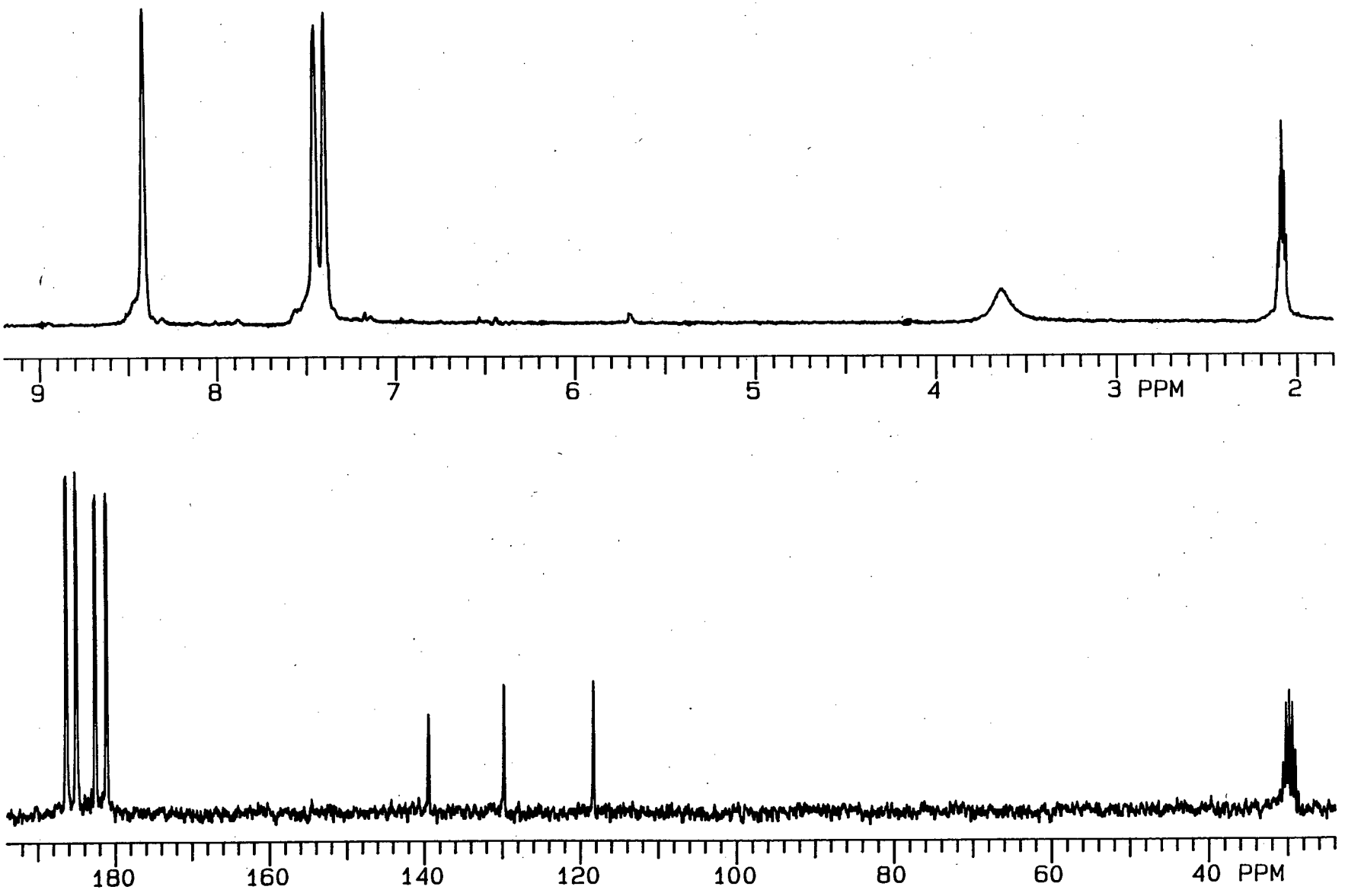

FIGURE 3.11 ^{1}H and ^{13}C nmr spectra of *cis*-$[Rh(CO)_2(Cl)(imid)]$ (acetone-d_6, Temp. = −20°C).

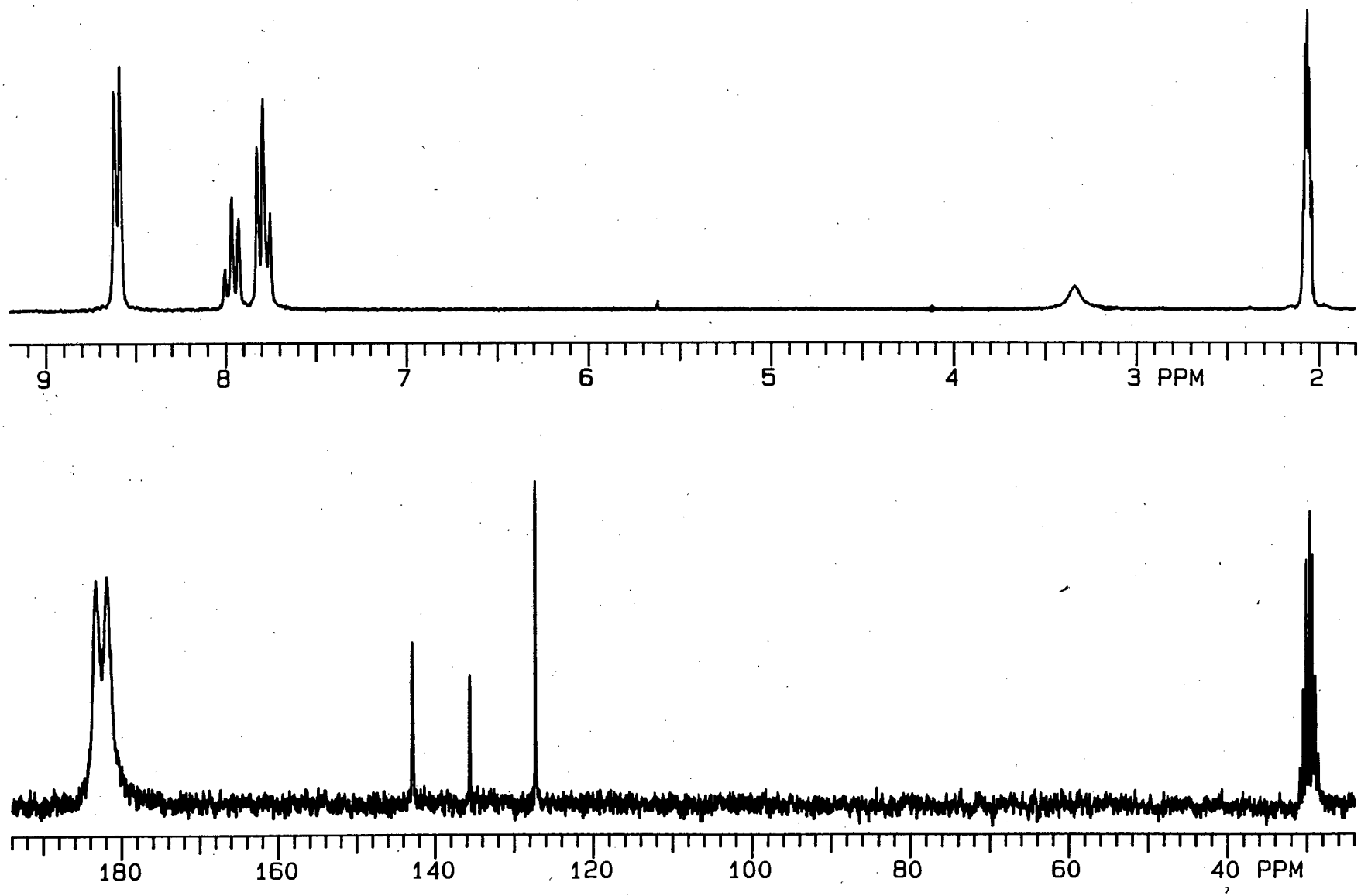

FIGURE 3.12 ^{1}H and ^{13}C nmr spectra of *cis*-$[Rh(CO)_2(Br)(pyO)]$ (acetone-d_6, Temp. = 25°C).

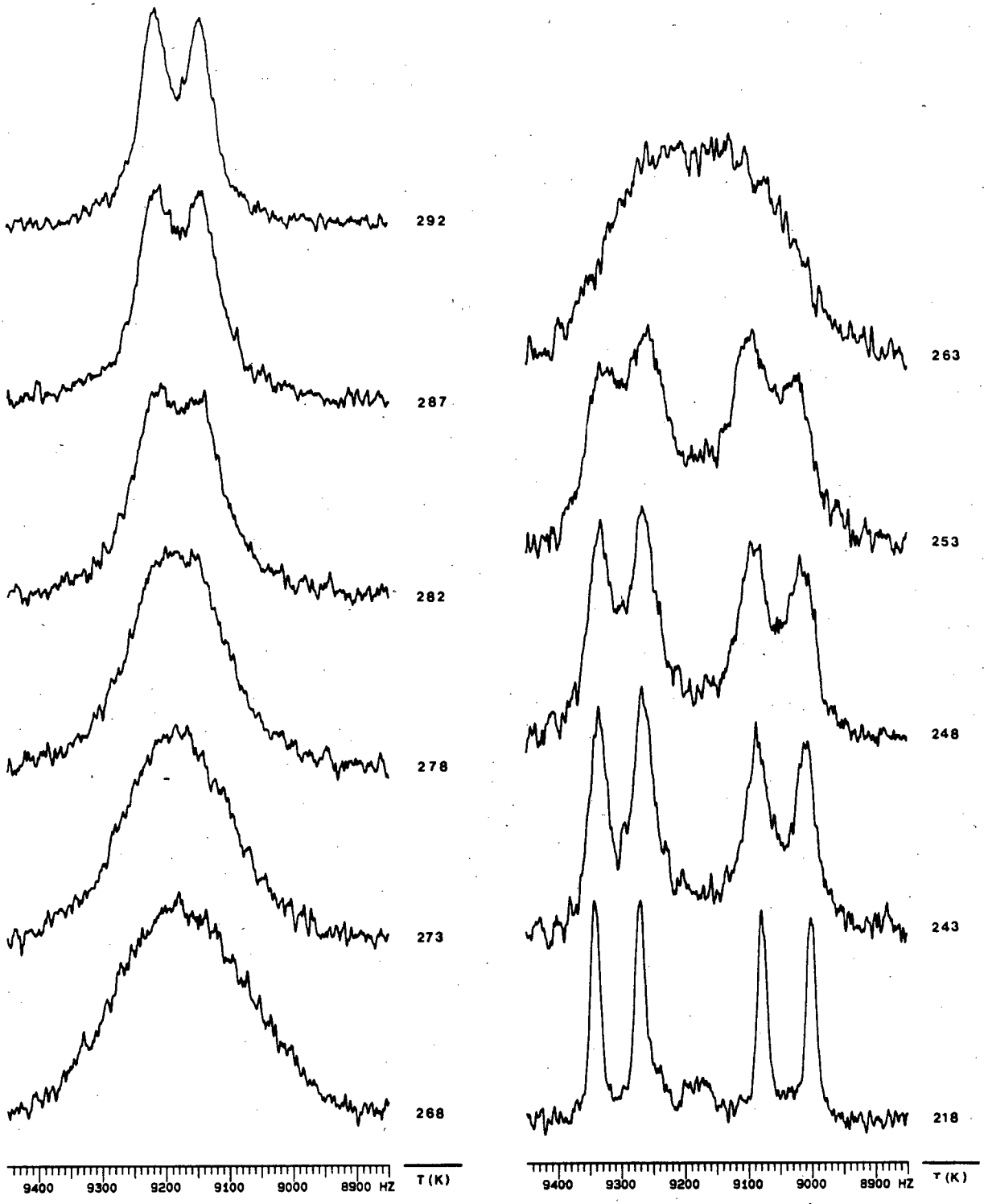

FIGURE 3.13 The ^{13}C nmr spectra at various temperatures of the carbonyl groups of *cis*-$[Rh(CO)_2(Br)(pyO)]$.

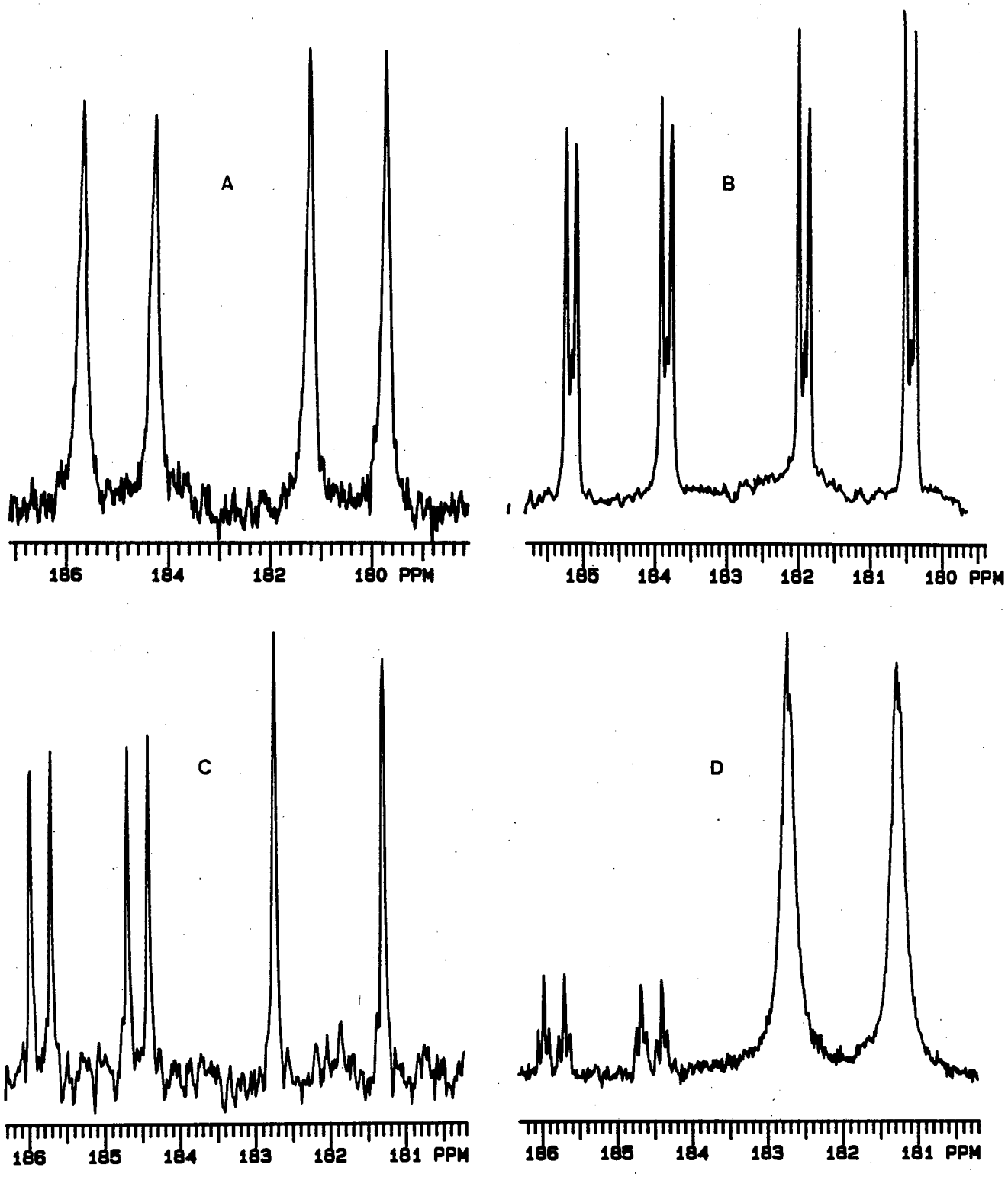

FIGURE 3.14 **^{13}C nmr spectra of *cis*-[Rh(CO)$_2$(Cl)(L)] complexes at various degrees of isotopic enrichment (in acetone-d_6).**

A *cis*-[Rh(^{13}CO)$_2$(Cl)(pyO)]
^{13}C ~ 30%, Temp. = −50°C

B *cis*-[Rh(^{13}CO)$_2$(Cl)(an)]
^{13}C ~ 80%, Temp. = −40°C

C *cis*-[Rh(^{13}CO)$_2$(Cl)(^{15}NH$_3$)]
^{13}C ~ 30%, ^{15}N ~ 95%, Temp. = −30°C

D *cis*-[Rh(^{13}CO)$_2$(Cl)(^{15}ND$_3$)]
^{13}C ~ 30%, ^{15}N and D ~ 95%, Temp. = −30°C

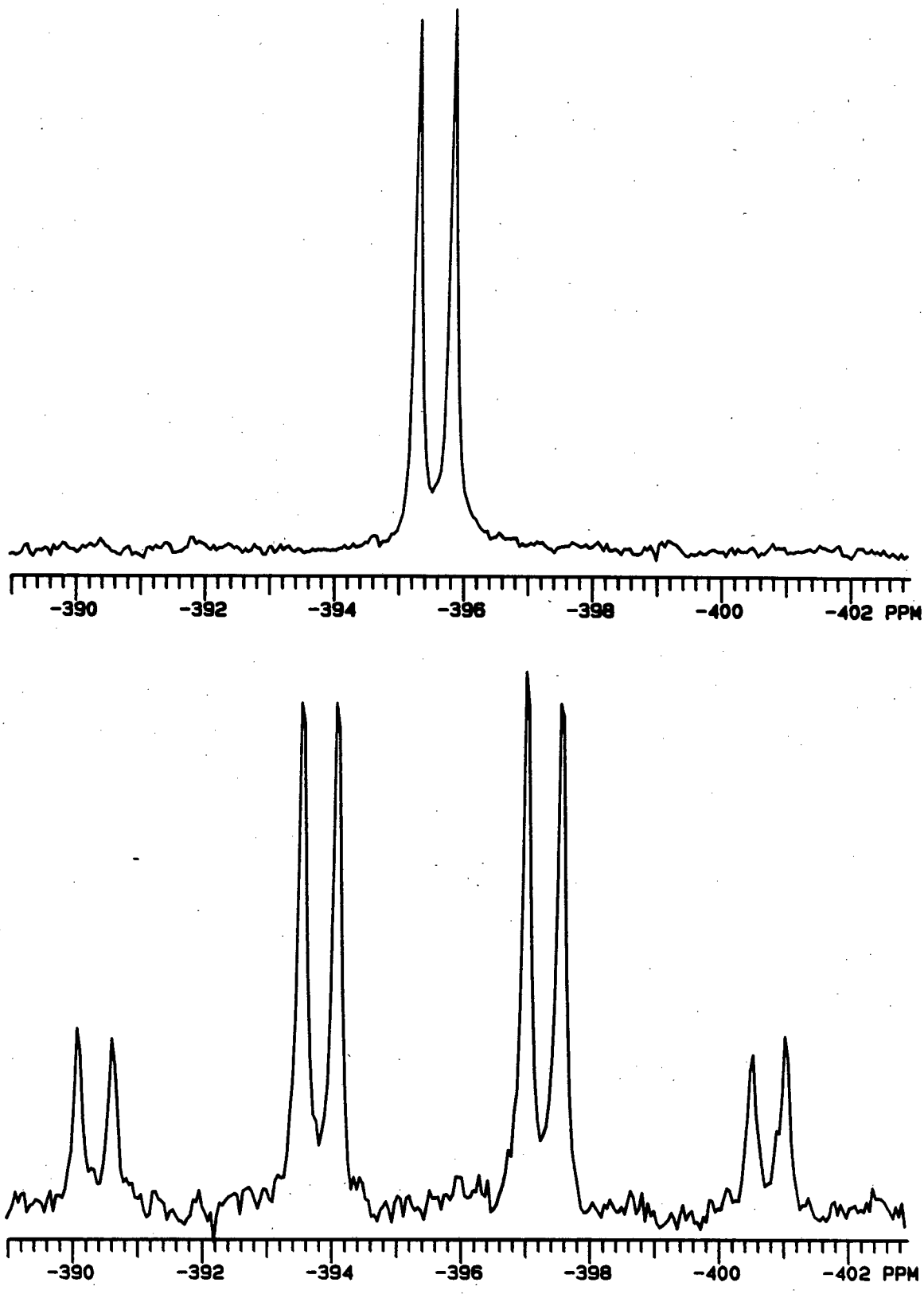

FIGURE 3.15 **^{1}H Decoupled and coupled ^{15}N nmr spectra of *cis*-$[Rh(CO)_2(Cl)(^{15}NH_3)]$.** (Temp. = −20°C, acetone-d_6, external reference $CH_3{}^{15}NO_2$)

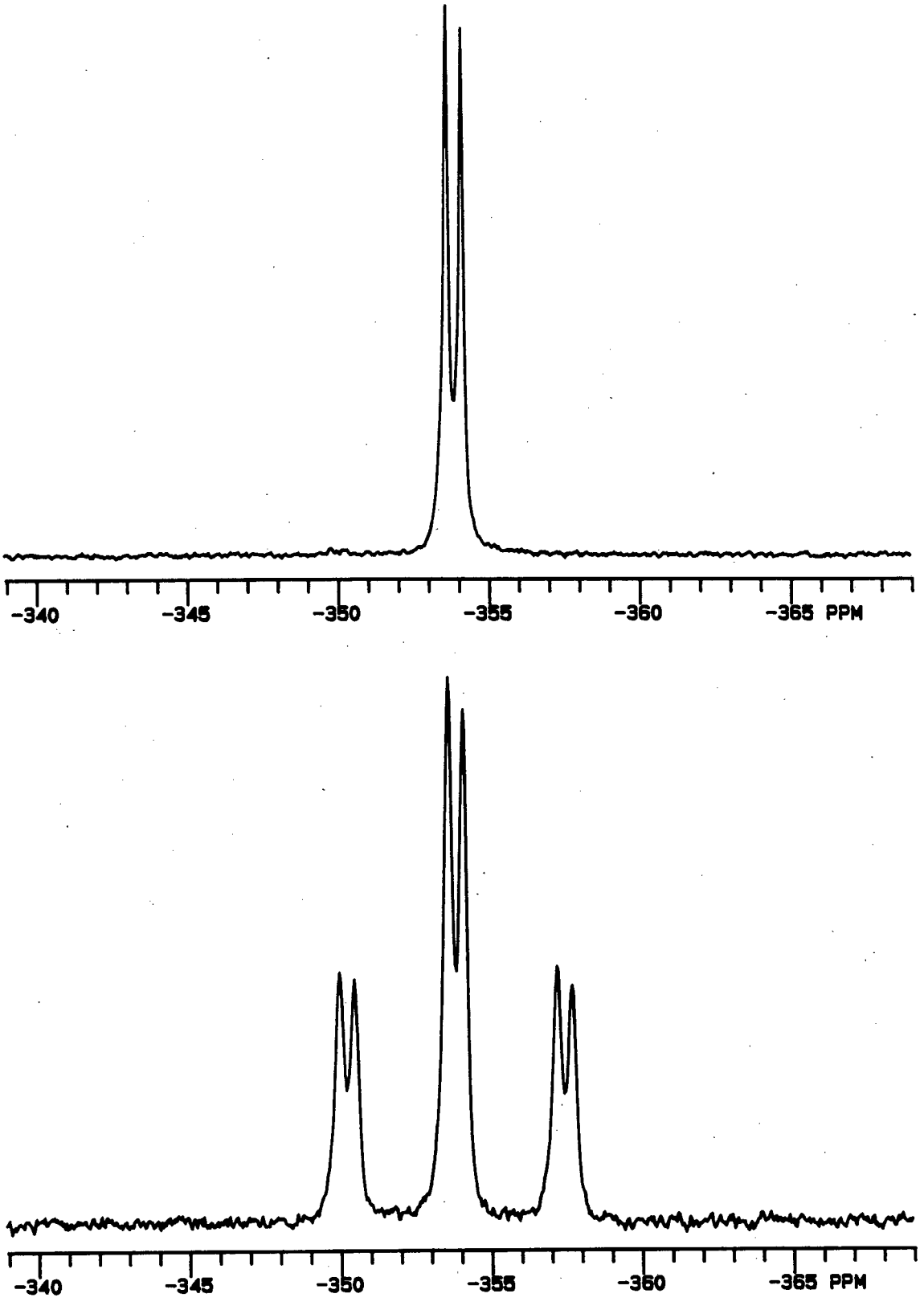

FIGURE 3.16 ^{1}H **Decoupled and coupled** ^{15}N **nmr spectra of** *cis*-$[Rh(CO)_2(Cl)(an\text{-}^{15}N)]$. (Temp. = −70°C, acetone-d_6, external reference $CH_3{}^{15}NO_2$)

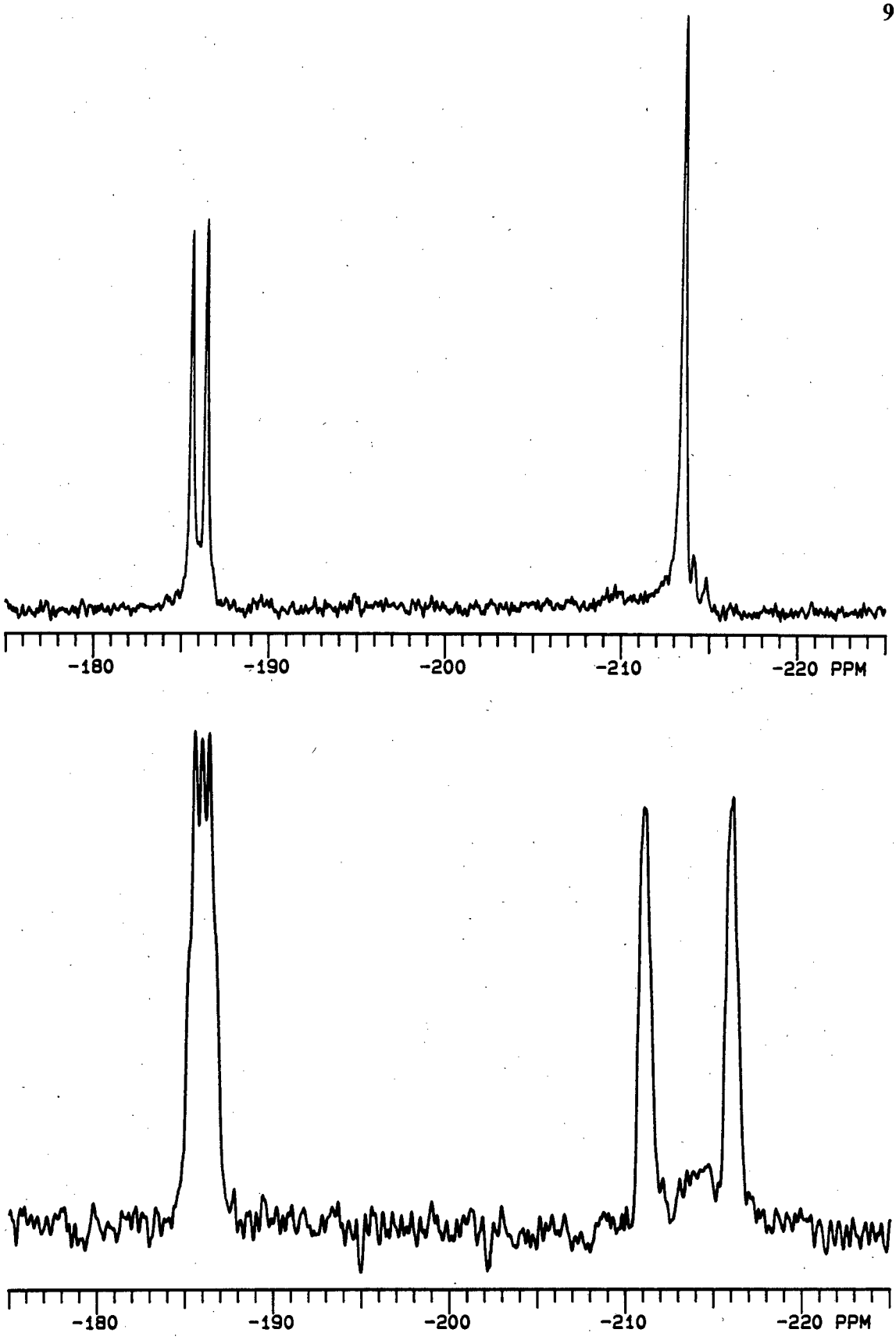

FIGURE 3.17 **^{1}H Decoupled and coupled ^{15}N nmr spectra of *cis*-[Rh(CO)$_2$(Cl)(imid-^{15}N)]**
(Temp. = 25°C, acetone-d_6, external reference $CH_3{}^{15}NO_2$)

TABLE 3.11 ^{1}H, ^{13}C and ^{15}N nmr data of *cis*-$[Rh(CO)_2(X)(NH_3)]$ (X is Cl or Br).

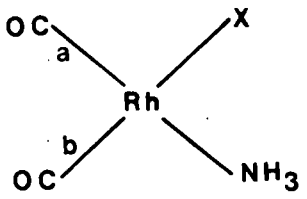

X	T (°C)	Chemical Shifts (ppm)		Coupling Constants (Hz)	
^{1}H nmr		N-H		$^{1}J(^{15}N\text{-}H)$	
Cl	25	3.51		70.61	
Cl($CDCl_3$)	25	2.40			
Br	25	3.51		70.56	
^{13}C nmr		CO_a	CO_b	$^{1}J(Rh\text{-}CO_a)$	$^{1}J(Rh\text{-}CO_b)$
Cl	-30	185.18	181.99	65.21	72.66
				$^{2}J(^{13}C\text{–}^{13}C) = 6.84$	
				$^{2}J(^{13}C\text{–}^{15}N) = 13.82$	
Br	-30	185.02	181.83	65.30	73.28
				$^{2}J(^{13}C\text{–}^{13}C) = 6.78$	
				$^{2}J(^{13}C\text{–}^{15}N) = 13.85$	
^{15}N nmr		^{15}N-H		$^{1}J(^{15}N\text{-}Rh)$	$^{1}J(^{15}N\text{-}H)$
Cl	-20	-395.60		10.97	70.57
Br	-20	-399.09		10.89	70.42

All spectra recorded in acetone-d_6 unless otherwise specified.
Chemical shifts of ^{1}H and ^{13}C relative to TMS.
Chemical shift of ^{15}N relative to external $CH_3{}^{15}NO_2$.

TABLE 3.12 ^{1}H and ^{13}C nmr data of *cis*-$[Rh(CO)_2(X)(py)]$ (X is Cl or Br).

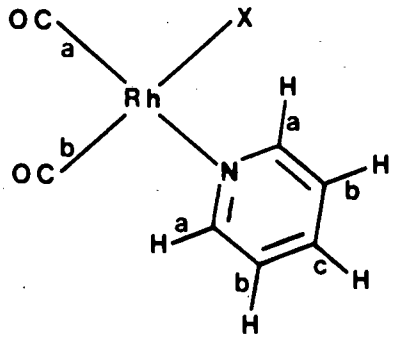

X	T (°C)	Chemical Shifts (ppm)			Coupling Constants (Hz)			
^{1}H nmr		H_a	H_b	H_c				
Cl	25	8.86	7.73	8.16				
$Cl(CDCl_3)$	25	8.72	7.48	7.91				
Br	25	8.86	7.73	8.17				
^{13}C nmr		C_a	C_b	C_c	CO_a	CO_b	$^{1}J(Rh\text{-}CO_a)$	$^{1}J(Rh\text{-}CO_b)$
Cl	−10	153.24	126.64	140.85	185.17	181.60	64.30	71.64
							$^{2}J(^{13}C\text{–}^{13}C) \approx 7.0$	
Br	−30	153.47	126.59	140.71	185.54	180.86	63.48	76.03
							$^{2}J(^{13}C\text{–}^{13}C) \approx 7.0$	

All spectra recorded in acetone-d_6 unless otherwise specified.
Chemical shifts of ^{1}H and ^{13}C relative to TMS.

TABLE 3.13 ^{1}H, ^{13}C and ^{15}N nmr data of *cis*-[$Rh(CO)_2(X)(imid)$] (X is Cl or Br).

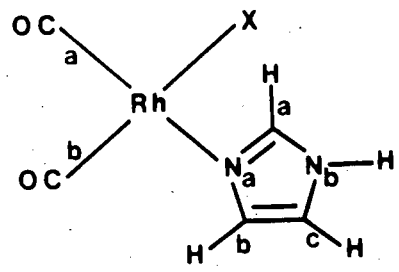

X	T (°C)	Chemical Shifts (ppm)				Coupling Constants (Hz)	
^{1}H nmr		H_a	H_b	H_c	N-H	$^{1}J(^{15}N\text{-}H)$	$^{2}J(^{15}N\text{-}H_a)$
Cl	−20	8.42	7.46	7.38	12.41	99.86	7.48
Cl($CDCl_3$)	25	8.10	7.20	7.08	10.30		
Br	−30	8.46	7.47	7.42	12.50	99.94	7.54

^{13}C nmr		C_a	C_b	C_c	CO_a	CO_b	$^{1}J(Rh\text{-}CO_a)$	$^{1}J(Rh\text{-}CO_b)$
Cl	−30	139.80	130.18	118.67	185.74	181.89	64.80	73.30
							$^{2}J(^{13}C\text{–}^{13}C) = 6.52$	
							$^{2}J(^{13}C\text{–}^{15}N) = 16.85$	
Br	−30	140.14	130.26	118.36	186.57	181.33	63.44	75.31
							$^{2}J(^{13}C\text{–}^{13}C) = 6.90$	
							$^{2}J(^{13}C\text{–}^{15}N) = 16.49$	

^{15}N nmr		N_a	N_b	$^{1}J(^{15}N_a\text{-}Rh)$	$^{1}J(^{15}N_b\text{-}H)$
Cl	−30	−186.01	−213.53	16.47	100.10
Br	−30	−187.99	−212.18	16.46	99.75

All spectra recorded in acetone-d_6 unless otherwise specified.
Chemical shifts of ^{1}H and ^{13}C relative to TMS.
Chemical shift of ^{15}N relative to external $CH_3{}^{15}NO_2$.

TABLE 3.14 ^{1}H and ^{13}C nmr data of *cis*-$[Rh(CO)_2(X)(pyO)]$ (X is Cl or Br).

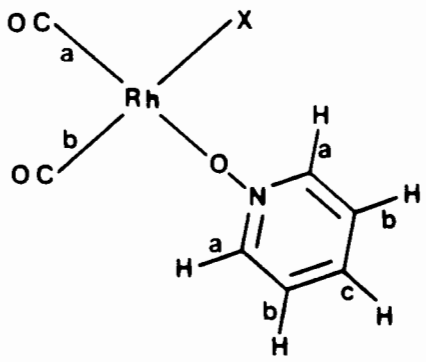

X	T (°C)	Chemical Shifts (ppm)			Coupling Constants (Hz)	
^{1}H nmr		H_a	H_b	H_c		
Cl	25	8.61	7.78	8.00		
$Cl(CDCl_3)$	25	8.45	7.38	7.70		
Br	25	8.58	7.77	7.95		
^{13}C nmr		C_a	C_b	C_c	CO_a CO_b	$^{1}J(Rh\text{-}CO_a)$ $^{1}J(Rh\text{-}CO_b)$
Cl	−50	142.92	127.31	136.29	184.95 180.45	71.59 75.06
						$^{2}J(^{13}C\text{–}^{13}C) \approx 6.9$
Br	−55	142.86	127.31	135.61	184.97 179.68	73.70 77.63
						$^{2}J(^{13}C\text{–}^{13}C) \approx 7.0$

All spectra recorded in acetone-d_6 unless otherwise specified.

Chemical shifts of ^{1}H and ^{13}C relative to TMS.

TABLE 3.15 ^{1}H, ^{13}C and ^{15}N nmr data of *cis*-$[Rh(CO)_2(X)(an)]$ (X is Cl or Br).

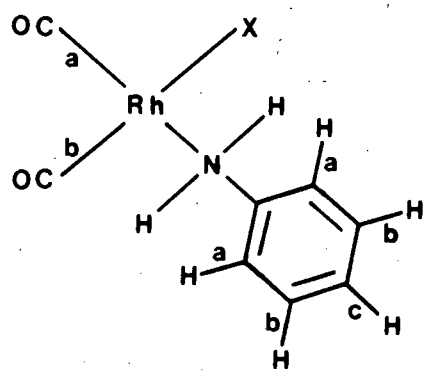

X	T (°C)	Chemical Shifts (ppm)				Coupling Constants (Hz)			
^{1}H nmr		H_a	H_b	H_c	N-H			^{1}J(N-H)	
Cl	25	--7.35--			6.35				
Cl($CDCl_3$)	25	--7.22--			5.12			66.6	
Br	25	--7.35--			6.35				
^{13}C nmr		C_a	C_b	C_c	C	CO_a	CO_b	^{1}J(Rh-CO_a)	^{1}J(Rh-CO_b)
Cl	-60	121.59	130.09	125.29	142.70	184.46	181.20	67.28	74.38
								$^{2}J(^{13}C\text{-}^{13}C)$ = 7.27	
								$^{2}J(^{13}C\text{-}^{15}N)$ = 12.58	
Br	-70	121.78	129.95	125.36	143.16	184.82	180.72	66.07	76.47
								$^{2}J(^{13}C\text{-}^{13}C)$ = 7.75	
								$^{2}J(^{13}C\text{-}^{15}N)$ = 12.77	
^{15}N nmr				N				$^{1}J(^{15}N\text{-Rh})$	$^{1}J(^{15}N\text{-H})$
Cl	-70			-353.93				10.16	73.26
Br	-80			-357.05				9.88	72.93

All spectra recorded in acetone-d_6 unless otherwise specified.
Chemical shifts of ^{1}H and ^{13}C relative to TMS.
Chemical shift of ^{15}N relative to external $CH_3{}^{15}NO_2$.

TABLE 3.16 UV data for the complexes *cis*-$[Rh(CO)_2(X)(L)]$.

	X = Cl		X = Br	
L	λ_{max} (nm)	ε (m^2mole^{-1})	λ_{max} (nm)	ε (m^2mole^{-1})
ammonia	262	530	268	595
	335	405	335	405
imidazole	261	610	266	685
	340	355	340	360
pyridine	260	1010	260	995
	341	295	342	305
pyridine *N*-oxide	271	1850	272	1795
	327	455	326	390
aniline	242	1005	240	990
	263	840	269	805
	332	390	335	380

REFERENCES

1 P.SCHUTZENBERGER,
J. Chem. Soc., (1871) 1008

2 W.MANCHOT AND J.KÖNIG,
Chem. Ber., **58B** (1925) 2173

3 W.HIEBER AND H.LAGALLY,
Z. Anorg. Allg. Chem., **251** (1943) 96

4 W.HIEBER, H.HEUSINGER AND O.VOHLER,
Chem. Ber., **90** (1957) 2425

5 J.ALTMAN AND G.WILKINSON,
J. Chem. Soc., (1964) 5654

6 D.N. LAWSON AND G.WILKINSON,
J. Chem. Soc., (1965) 1900

7 F. BONATI AND R.UGO,
J. Organomet. Chem., **7** (1967) 167

8 J.T. MAGUE AND J.P.MITCHENER,
Inorg. Chem., **8** (1969) 119

9 D.P.MADDEN, A.J. CARTY AND T. BIRCHALL,
Inorg. Chem., **11** (1972) 1453

10 F. BONATI AND G.MINGHETTI,
J. Organomet. Chem., **60** (1973) C43

11 P. UGUAGLIATI, G. DEGANELLO AND U. BELLUCO,
Inorg. Chim. Acta, **9** (1974) 203

12 K.G. ALLUM, R.D.HANCOCK, I.V HOWELL, S. MCKENZIE, R.C. PITKETHLY AND P.J. ROBINSON,
J. Organomet. Chem., **87** (1975) 203

13 G.WILKINSON, F.G.A.STONE AND E.W.ABEL (EDS.),
"Comprehensive Organometallic Chemistry", Pergamon Press, Oxford, **5** (1982) 277

14 L.VALLARINO,
Gazz. Chim. Ital., **89** (1959) 1632

15 D.EVANS, J.A.OSBORN AND G.WILKINSON,
J. Chem. Soc., **A** (1968) 3133

16 L.CASSAR AND J.HALPERN,
J. Chem. Soc. (Chem. Commun.), (1970) 1082

17 A.SPENCER,
J. Organomet. Chem., **194** (1980) 113

18 G.VILLAIN AND A.GASSET,
J. Mol. Catal., **7** (1980) 355

19 T.SAKAKURA AND M.TANAKA,
J. Chem. Soc. (Chem. Commun.), (1987) 758

20 R.B.KING, A.D.KING AND M.Z.IQBAL,
J. Am. Chem. Soc., **101** (1979) 4893

21 W.M.BOWSER AND W.H.WEINBERG,
J. Am. Chem. Soc., **103** (1981) 1453

22 R.D.GILLARD, K.HARRISON AND I.H.MATHER,
J. Chem. Soc. (Dalton Trans.), (1975) 133

23 E.W.ABEL,
Chem. Soc. Quart.Rev., **17** (1963) 133

24 E.W.ABEL AND F.G.A.STONE,
Chem. Soc. Quart. Rev., **23** (1969) 325

25 J.E.HUHEEY,
"Inorganic Chemistry", Harper & Row, New York, 2nd ed., (1978) p. 404

26 D.M.ADAMS,
J. Chem. Soc., (1964) 1771

27 M.A.BENNETT AND R.J.H.CLARK,
J. Chem. Soc., (1964) 5560

28 G.C.PERCY AND H.S.STENTON,
J. Chem. Soc. (Dalton Trans.), (1976) 1466, 2429

29 L.J.TODD AND J.R.WILKINSON,
J. Organomet. Chem., **77** (1974) 1

30 G.M.BODNER,
Inorg. Chem., **14** (1975) 1932

31 P.S.BRATERMAN, D.W.MILNE ,E.W.RANDALL AND E.ROSENBERG,
J. Chem. Soc. (Dalton Trans.), (1973) 1027

32 J.MASON (ED.)
"Multinuclear NMR", Plenum Press, New York, (1987) Ch.12

33 W.VON PHILIPSBORN AND R.MÜLLER
Angew. Chem. Int. Ed. Engl., **25** (1986) 383

34 M.WITANOWSKI AND G.A.WEBB (EDS.),
"Nitrogen NMR", Plenum Press, London, (1973)

35 W.R.MASON AND H.B.GRAY,
J. Am. Chem. Soc., **90** (1968) 5721

36 H.ISCI AND W.R.MASON,
Inorg. Chem., **14** (1975) 905, 913

37 G.L.GEOFFROY, H.ISCI, J.LITRENTI AND W.R.MASON,
Inorg. Chem., **16** (1977) 1950

38 L.M.VALLARINO,
Int. Conf. on Coord. Chem., Special Pub., The Chemical Society, London, **13** (1959) 123

39 F.PRUCHNIK AND K.WAJDA,
J. Organomet. Chem., **164** (1979) 71

40 P.S.BRATERMAN,
"Metal Carbonyl Spectra", Academic Press, London, (1975)

41 M.J.DECKER, D.O.K.FJELDSTED, S.R.STOBART AND M.J.ZAWOROTKO,
J. Chem. Soc. (Chem.Commun.), (1983) 1525

42 D.Y.JETER AND E.B.FLEISCHER,
J. Coord. Chem., **4** (1973) 107

43 K.H.SCHMIDT AND A.MÜLLER,
Coord. Chem. Rev., **19** (1976) 41

44 A.V.BABAEVA AND O.N.EVSTAF'EVA,
Russ. J. Inorg. Chem. (Engl. Transl.), **6** (1961) 29

45 L.M.VALLARINO AND S.W.SHEARGOLD,
Inorg. Chim. Acta, **36** (1979) 243

46 C.H.KLINE AND J.TURKEVICH,
J. Chem. Phys.,**12** (1944) 300

47 L.CORRSIN, B.J.FAX AND R.C.LORD,
J. Chem. Phys., **21** (1953) 1170

48 D.A.LONG AND E.L.THOMAS,
Trans. Faraday Soc., **59** (1963) 783

49 L.HARSÁNYI AND F.KILÁR,
J. Mol. Struct., **65** (1980) 141

50 H.D.STIDHAM AND D.P.DILELLA,
J. Raman Spectrosc., **8** (1979) 180, **9** (1980) 90, 247

51 D.P.DILELLA,
J. Raman Spectrosc., **9** (1980) 239

52 A.T.HUTTON AND D.A.THORNTON,
Spectrochim. Acta, **34A** (1978) 645

53 G.A.FOULDS, J.B.HODGSON, A.T.HUTTON, M.L.NIVEN, G.C.PERCY,P.E.RUTHERFORD AND D.A.THORNTON, *Spectrosc. Lett.*, **12** (1979) 25

54 S.PINCHAS AND I.LAULICHT, *"Infrared Spectra of Labelled Compounds"*, Academic Press, New York, (1971)

55 E.B.WILSON, J.C.DECIUS AND P.C. CROSS, *"Molecular Vibrations"*, McGraw-Hill, New York, (1955)

56 A.M.ENGLISH, K.R.PLOWMAN AND I.S.BUTLER, *Inorg. Chem.*, **21** (1982) 338

57 J.C.EVANS, *Spectrochim. Acta*, **16** (1960) 428

58 G.N.R.TRIPATHI, *J. Chem. Phys.*, **73** (1980) 5521

59 T.P.E. AUF DER HEYDE, G.A.FOULDS, D.A.THORNTON AND G.M.WATKINS, *J. Mol. Struct.*, **77** (1981) 19

60 J.A.LEE-THORP, J.E.RÜEDE AND D.A.THORNTON, *J. Mol. Struct.*, **50** (1978) 65

61 A.M.BELLOCQ, C.PERCHARD, A.NOVAK AND M.L.JOSIEN, *J. Chim. Phys.*, **62** (1965) 1334

62 C.PERCHARD, A.M.BELLOCQ AND A.NOVAK, *J. Chim. Phys.*, **62** (1965) 1344

63 C.PERCHARD AND A.NOVAK, *J. Chem. Phys.*, **48** (1968) 3079

64 M.CORDES AND J.L.WALTER, *Spectrochim. Acta*, **24A** (1968) 237

65 L.COLOMBO, *J. Chem. Phys.*, **49** (1968) 4688

66 L.COLOMBO, P.BLECKMANN, B.SCHRADER, R.SCHNEIDER AND T.PLESSER, *J. Chem. Phys.*, **61** (1974) 3270

67 J.B.HODGSON, G.C.PERCY AND D.A.THORNTON, *J. Mol. Struct.*, **66** (1980) 75, 81

68 M.MAJOUBE AND G.VERGOTEN, *J. Chem. Phys.*, **76** (1982) 2838

69 S.J.ARCHER, T.P.E.AUF DER HEYDE, G.A.FOULDS AND D.A.THORNTON,
Transition Met. Chem., **7** (1982) 59

70 M.ITO AND N.HATA,
Bull. Chem. Soc. Japan, **28** (1955) 353

71 Y.KAKIUTI, S.KIDA AND J.V.QUAGLIANO,
Spectrochim. Acta, **19** (1963) 201

72 V.I.BEREZIN,
Optika i Spektr., **18** (1965) 212

73 S.SZÓKE, A.GELLÉRI AND E.BAITZ,
Acta Chim. Acad. Sci. Hung., **48** (1966) 343

74 G.VARSÁNYI, S.SZÓKE, G.KERESZTURY AND A.GELLÉRI,
Acta Chim. Acad. Sci. Hung., **65** (1970) 73

75 Y.KAKIUTI, H.SAITO AND M.AKIYAMA,
J. Mol. Spectrosc., **35** (1970) 66

76 H.D.BIST AND J.S.PARIHAR,
Chem. Phys. Lett., **32** (1975) 244

77 H.D.BIST, J.S.PARIHAR AND J.C.D.BRAND,
J. Mol. Spectrosc., **59** (1976) 435

78 A.GAMBI AND S.GHERSETTI,
Spectrosc. Lett., **10** (1977) 627

79 G.M.WATKINS,
Ph.D. Thesis, University of Cape Town (1988)

80 J.R.FERRARO,
"Low-Frequency Vibrations of Inorganic and Coordination Compounds", Plenum Press, New York, (1971)

81 K.NAKAMOTO,
"Infrared and Raman Spectra of Inorganic and Coordination Compounds", 4th ed., Wiley-Interscience, (1986)

82 R.J.H.CLARK AND C.S.WILLIAMS,
Inorg. Chem., **4** (1965) 350

83 R.S.MCDOWELL AND L.H.JONES,
J. Chem. Phys., **36** (1962) 3321

84 R.CATALIOTTI, A.POLETTI AND A.SANTUCCI,
J. Mol. Struct., **5** (1970) 215

85 D.M.ADAMS,
"Metal-Ligand and Related Vibrations", Arnold, London, (1967)

86 H.STAMMREICH, K.KAWAI, Y.TAVARES, P.KRUMHOLZ, J.BEHMOIRAS AND S.BRIL,
J. Chem. Phys., **32** (1960) 1482

87 L.M.HAINES AND M.H.B.STIDDARD,
Adv. Inorg. Chem. Radiochem., **12** (1969) 53

88 Y.S.VARSHAVSKII, M.M.SINGH AND N.A.BUZINA,
Russ. J. Inorg. Chem. (Engl. Transl.), **16** (1971) 725

89 M.F.GUNS, E.G.CLAEYS AND G.P. VAN DER KELEN,
J. Mol. Struct., **65** (1980) 3

90 R.G.DENNING AND M.J.WARE,
Spectrochim. Acta, **24A** (1968) 1785

91 A.R.MANNING,
J. Chem. Soc., **A** (1968) 1670

92 J.BROWNING, P.GOGGIN, R.GOODFELLOW, M.NORTON, A.RATTRAY, B.F.TAYLOR AND J.MINK,
J. Chem. Soc. (Dalton Trans.), (1977) 2061

93 M.BIGORGNE AND G.BOUQUET,
Compt. Rend., **C264** (1967) 1485

94 D.M.ADAMS AND W.R.TRUMBLE,
J. Chem. Soc. (Dalton Trans.), (1974) 690

95 D.M.ADAMS, R.E.CHRISTOPHER AND D.C.STEVENS,
Inorg. Chem., **14** (1975) 1562

96 D.J.PARKER,
J. Chem. Soc. (Dalton Trans.), (1974) 155

97 M.TSUTSUI, D.OSTFELD AND L.M.HOFFMAN,
J. Am. Chem. Soc., **93** (1971) 1820

98 N.F.BORKETT AND M.I.BRUCE,
J. Organomet. Chem., **65** (1974) C51

99 G.A.FOULDS, P.S.HALL AND D.A.THORNTON,
J. Mol. Struct., **161** (1987) 237

100 P.W.JOLLY AND R.MYNOTT,
Adv. Organomet. Chem., **19** (1981) 257

101 B.E.MANN,
Adv. Organomet. Chem., **12** (1974) 135

102 G.BANDITELLI, A.L.BANDINI, F.BONATI AND G.MINGHETTI,
J. Organomet. Chem., **218** (1981) 229

103 A.J.PRIBULA AND R.S.DRAGO,
J. Am. Chem. Soc., **98** (1976) 2784

104 H.VAN DER POEL, G.VAN KOTEN AND K.VRIEZE,
Inorg. Chim. Acta, **51** (1981) 241, 253

105 C.BROWN, B.T.HEATON, L.LONGHETTI, W.T.POVEY AND D.O.SMITH,
J. Organomet. Chem., **192** (1980) 93

106 E.W.ABEL AND S.J.SKITTRALL,
J. Organomet. Chem., **193** (1980) 389

107 Y.S.VARSHAVSKII, N.V.KISELEVA, T.G.CHERKASOVA, L.S.BRESLER, A.S.KHACHATUROV AND N.A.BUZINA,
Koord. Khim., **8** (1982) 1386, **Chem. Abstr., 98** (1983) 45632x

108 J.T.MAGUE AND A.R.SANGER,
Inorg. Chem., **18** (1979) 2060

109 J.B.STOTHERS,
"^{13}C nmr Spectroscopy", Academic Press, New York, (1972)

110 J.ELGUERO,
J. Chem. Soc. (Chem. Commun.), (1981) 1207

111 A.MAISONNAT, P.KALCK AND R.POILBLANC,
Inorg. Chem., **13** (1974) 661, 2996

112 A.MAISONNAT AND R.POILBLANC,
Inorg. Chim. Acta, **29** (1978) 203

113 E.W.ABEL AND S.A.MUCKLEJOHN,
Inorg. Chim. Acta, **37** (1979) 107

114 J.F. VAN BAAR, K.VRIEZE AND D.J.STUFKENS,
J. Organomet. Chem., **97** (1975) 461

115 B.E.MANN AND B.F.TAYLOR,
"^{13}C nmr Data for Organometallic Compounds",
Academic Press, London, (1981)

116 E.G.FINER AND R.K.HARRIS,
Prog. Nucl. Magn. Reson. Spectrosc., **6** (1971) 61

117 S.AIME,
Inorg. Chim. Acta, **62** (1982) 51

118 P.E.HANSEN,
Prog. Nucl. Magn. Reson. Spectrosc., **14** (1981) 175

119 *Nucl. Magn. Reson. (Specialist Periodical Report)*,
The Chemical Society, London, **1–18** (1972–1988)

120 B.E.MANN,
J. Chem. Soc. (Dalton Trans.), (1973) 2012

121 W.J.CHERWINSKI, B.F.G.JOHNSON, J.LEWIS AND J.R.NORTON,
J. Chem. Soc. (Dalton Trans.), (1975) 1156

122 D.G.COOPER AND J.POWELL,
Inorg. Chem., **16** (1977) 142

123 L.S.BRESLER, N.A.BUZINA, Y.S.VARSHAVSKY,
N.V.KISELEVA AND T.G.CHERKASOVA,
J. Organomet. Chem., **171** (1979) 229

124 A.R.BRAUSE, M.RYCHECK AND M.ORCHIN,
J. Am. Chem. Soc., **89** (1967) 6500

125 L.M.JACKMAN AND F.A.COTTON (EDS.),
"Dynamic Nuclear Magnetic Resonance Spectroscopy",
Academic Press, New York, (1975)

126 K.S.BOSE AND E.H.ABBOTT,
Inorg. Chem., **16** (1977) 3190

127 T.G.APPELTON, J.R.HALL AND S.F.RALPH,
Inorg. Chem., **27** (1988) 4435

128 D.SUTTON,
"Electronic Spectra of Transition Metal Complexes",
McGraw-Hill, London, (1968)

129 R.L.CARLIN (ED.),
"Transition Metal Chemistry", Marcel Dekker Inc., New York, **1** (1965)

130 G.A.FOULDS AND D.A.THORNTON,
J. Mol. Struct., **98** (1983) 309

131 G.A.FOULDS, P.S.HALL AND D.A.THORNTON,
J. Mol. Struct., **117** (1984) 95

132 P.S.HALL, D.A.THORNTON AND G.A.FOULDS,
Polyhedron, **6** (1987) 85

133 G.L.GEOFFROY, M.S.WRIGHTON, G.S.HAMMOND AND H.B.GRAY,
J. Am. Chem. Soc., **96** (1974) 3105

134 A.L.BALCH AND R.D.COOPER,
J. Organomet. Chem., **169** (1979) 97

135 K.R.MANN, J.G.GORDON AND H.B.GRAY,
J. Am. Chem. Soc., **97** (1975) 3553

136 A.L.BALCH AND B.TULYATHAN,
Inorg. Chem., **16** (1977) 2840

137 A.L.BALCH,
J. Am. Chem. Soc., **98** (1976) 8049

138 L.F.DAHL, C.MARTELL AND D.L.WAMPLER,
J. Am. Chem. Soc., **83** (1961) 1761

CHAPTER 4

INTRODUCTION

In continuation of our studies on square planar systems, we have investigated the spectroscopic properties of some Rh(I) complexes of formula [Rh(COD)(X)(L)] where COD is the neutral bidendate ligand, 1,5-cyclooctadiene, X an anion, and L represents various neutral monodendate ligands.

The chemistry of cyclooctadiene complexes of rhodium has continuously developed since the isolation of the complex $[Rh(COD)Cl]_2$ in 1956 by Chatt and Venanzi [1,2]. The product is obtained when an ethanolic solution of $RhCl_3.3H_2O$ is heated under reflux with an excess of the diene.

$$RhCl_3.3H_2O \xrightarrow[\Delta]{COD} [Rh(COD)Cl]_2$$

The molecular structure of $[Rh(COD)Cl]_2$ has been determined by x-ray diffraction techniques [3,4]. The structure involves two intersecting square planes, as expected, but is unusual in that the Rh_2Cl_2 bridge is planar and not folded as in the $[Rh(CO)_2Cl]_2$ complex [5]. Thus the close parallelism of bonding often considered to hold between "isostructural" olefin and carbonyl complexes, does not exist in this case.

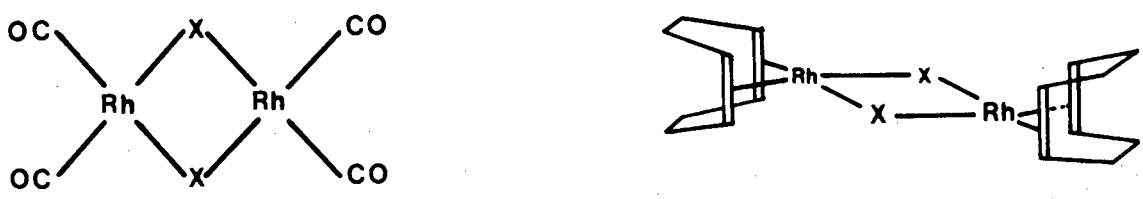

Figure 4.1 **Diagrammatic representation of the structures of $[Rh(CO)_2X]_2$ and $[Rh(COD)X]_2$.**

It is well known [2,6-9] that reaction of the dimeric diene complex of rhodium(I) with uncharged monodendate ligands, leads to bridge splitting and the formation of monomeric species of the type [Rh(diene)(X)(L)].

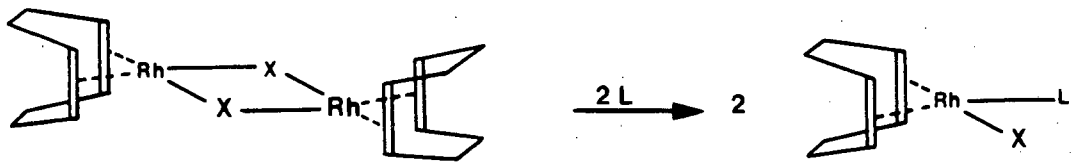

Figure 4.2 **Reaction of $[RhX(COD)]_2$ with uncharged monodendate ligand (L).**

Because of their significant activity as homogeneous catalysts, the organometallic rhodium(I) complexes have been extensively studied in the catalytic sector [10-15]. Several publications have appeared [16,17], mainly preparative in nature, incorporating various phosphine ligands. In addition, numerous authors [18-26] have studied in detail the kinetics and possible mechanism of reaction of the 1,5-cyclooctadiene metal(I) complexes by dynamic nmr and spectrophotometry.

However, detailed spectroscopic studies of the Rh(I) complexes are lacking. The infrared (and Raman) studies of 1,5-cyclooctadiene and its complexes have mainly been limited to either the free ligand or the dimeric complexes $[M(COD)Cl]_2$ where M is a variety of transition metals [27-32]. Furthermore, in most cases the authors merely list the frequencies and intensities of the bands [27,29-31,33,34]. In instances where infrared assignments have been proposed, the assignments are incomplete or ambiguous.

Hence, we have synthesized a series of complexes [Rh(COD)(X)(L)] where X is Cl or Br and L is aniline, pyridine, pyridine *N*-oxide, ammonia and imidazole and

studied them by infrared, uv, nmr and mass spectral techniques. In addition, we have isotopically enriched (^{2}H and ^{15}N) the ligands (L) in order to verify our infrared assignments. The ^{1}H, ^{13}C, and ^{15}N nmr studies were performed at room and low temperatures. The ^{15}N atoms were isotopically enriched, thus ensuring easily obtainable, good quality ^{15}N nmr spectra. The complexes were further investigated by uv/visible analyses and characterized by mass spectrometry, microanalyses and melting points.

ASSIGNMENTS AND RESULTS

INFRARED SPECTRA

The infrared spectra of the complexes [Rh(COD)(X)(L)] where COD is 1,5-cyclooctadiene, X is Cl or Br and L is ammonia, pyridine, pyridine *N*-oxide, aniline and imidazole have been recorded over the range 4000–50 cm^{-1}. Representative spectra are shown in Figures 4.5–4.8. The assignments for the complexes are presented in Tables 4.1–4.5 (for X is Cl) and Tables 4.6–4.9 (for X is Br).

Like the *cis*-[$Rh(CO)_2(X)(L)$] complexes, the [Rh(COD)(X)(L)] complexes adopt a square planar geometry [35] of point group C_s (see Chapter 1). Thus on the basis of symmetry consideration and Group Theory, the "isostructural" complexes should give rise to similar vibrational modes whenever the vibrations do not involve the cyclooctadiene or CO moiety. Hence the assignment of modes in [Rh(COD)(X)(L)] complexes, other than modes belonging to the COD moiety, are simplified by direct comparison to the analogous *cis*-[$Rh(CO)_2(X)(L)$] complexes.

However, the internal vibrations of the ligands COD and L occur in the same region, thus rendering the assignments a difficult task. We have used ligand (L) isotopic labelling (^2H and ^{15}N) to support our assignments. This labelling allows easy differentiation between the cyclooctadiene modes and the ligand (L) modes as the former are unshifted by ligand labelling. The assignment of the internal vibrations of the ligands (L) are based upon direct comparison to the free ligands or related metal complexes. The more specific assignments were made from their ν^D/ν^H ratios and the results are consistent with previous assignments made on other complexes. (See Chapters 1 and 3 for a detailed explanation of the reasons for the chosen ligand assignments).

The assignments of the internal vibrations of COD are based upon comparison with the uncomplexed 1,5-cyclooctadiene or other related metal complexes [27,29-32,36]. Fortunately, like the vibrations of the ligands L, most of the COD vibrations occur above 500 cm^{-1} and consequently do not couple significantly with the skeletal vibration modes. However, it should be noted that due to the commercial unavailability of COD-d_8, (because of its lengthy and expensive preparation [10]), there is no mention in the literature of any vibrational studies on COD-d_8 or its complexes. Consequently, not all the internal vibrations belonging to the COD moiety could be unambiguously assigned.

The infrared spectra of the complexes do not show any strong bands between 1650 and 1675 cm^{-1} which would be characteristic of the ν(C=C) vibration of uncoordinated 1,5-cyclooctadiene [29-32]. This suggests that both double bonds of the diene (olefin) are coordinated to the Rh(I) ion, and therefore, the two bands having ν(C=C) character are shifted to lower frequency upon coordination. It has been shown [29] that of the d^8 metal ions, Rh(I), Pt(II) and Pd(II), the Rh(I) complexes produce the greatest frequency shift for the ν(C=C) vibration. This is a consequence of the degree of overlap between the metal and the π-bonds of the olefinic unit [29,31]. This lowering of frequency is dependent on the metal involved and on the proportion of ν(C=C) character in each vibration.

The assignment of Bands I and II, that is the ν(C=C) mode of the COD moiety, in the complexes as well as their percentage shifts relative to uncomplexed 1,5-cyclooctadiene are shown below.

Compound	Frequency (cm^{-1})		% Lowering	
	Band I	Band II	Band I	Band II
1,5-cyclooctadiene	1658	1266	----	----
[Rh(COD)(Cl)(L)]				
L = pyridine	1493	1212	9.9	4.3
pyridine *N*-oxide	1465	1224	11.6	3.3
imidazole	1496	1259	9.8	0.5
aniline	1494	1224	9.9	3.3
ammonia	1487	1226	10.3	3.2
[Rh(COD)(Br)(L)]				
L = pyridine	1494	1210	9.9	4.4
pyridine *N*-oxide	1465	1224	11.6	3.3
imidazole	1495	1258	9.8	0.6
aniline	1493	1226	9.9	3.2

The fractional ν(C=C) character appears to be greater in Band I indicating that this is more perturbed upon coordination. These assignments are in agreement with those of Wertz and Moseley [32].

The strong band in the range 250–285 cm^{-1}, which is absent from the spectra of the corresponding bromide complexes, has been assigned to the metal-chlorine stretching frequency. In the bromide complexes the strong bond occurring between 175–195 cm^{-1} has been assigned to the metal-bromine stretching frequency. The ratio ν(Rh-Br)/ν(Rh-Cl) is typically ~0.69, which is normal for terminal metal

halogen bonds [37]. The ν(Rh-X) mode in the complexes [Rh(COD)(X)(L)] is approximately 20 cm^{-1} higher than in the $[Rh(COD)X]_2$ dimer. This difference between terminal and bridging ν(M-X) agrees well with the difference observed in other square planar complexes [28,38].

It is of interest to compare the ν(Rh-X) frequencies of the 1,5-cyclooctadiene complexes to those observed for the analogous carbonyl complexes (obtained from Chapter 3). The frequencies (cm^{-1}) of the ν(Rh-X) mode in carbonyl and 1,5-cyclooctadiene complexes of the type $[Rh(X)(Y)_2(L)]$ (X is Cl or Br, $(Y)_2$ is COD or $(CO)_2$ and L are various ligands) are shown below.

		ν(Rh–Cl) X = Cl		ν(Rh–Br) X = Br	
		$(CO)_2$	COD	$(CO)_2$	COD
L =	(pyridine)	310	255	235	175
	(pyridine *N*-oxide)	310	276	213	191
	(imidazole)	308	253	238	175
	(aniline)	308	282	218	195
	(ammonia)	308	277	214	----

The results reveal that the bond formed between the metal and the olefin (COD) is accompanied by a weakening of the bond between the metal and the halide. These results are consistent with the idea of increased σ donation and decreased π acceptance by olefin relative to the carbonyl ligand [23].

The bands which shift most upon ligand labelling in the 200–600 cm^{-1} region are ascribed to metal-ligand modes. Support for the assignment is found in the substantial shift that these bands undergo when ligand substitution occurs. Furthermore, the bands assigned to the ν(Rh-L) modes occur in the expected infrared region.

The remaining bands in the 600–250 cm^{-1} region (that is, bands other than the Rh-X, Rh-L and internal ligand (L), bands) have been assigned to COD related vibrations. Whether these bands arise from internal COD vibrations or ν(Rh-COD) vibrations cannot be determined since both sets of vibrations occur in the same region. However, from a comparison of free 1,5-cyclooctadiene and the dimer $[Rh(COD)X]_2$, four bands have been assigned to ν(Rh-COD) in the 600–250 cm^{-1} region [29,31,32]. They are the two stretching vibrations and the two tilt vibrations, shown below.

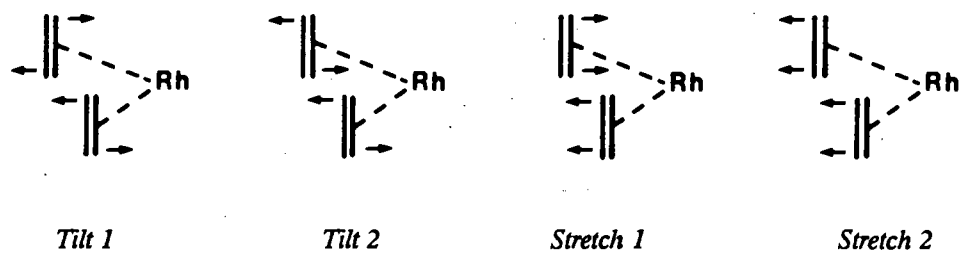

Figure 4.3 Rhodium-olefinic bond tilting and stretching vibrations.

In the complexes [Rh(COD)(X)(L)], where the symmetry is altered, the "stretch 2" band gives rise to two bands instead of one band. Consequently, like Brodzski and Pannetier [36], we assign 5 bands to ν(Rh-COD) in our complexes.

^{1}H, ^{13}C and ^{15}N NMR

The ^{1}H, ^{13}C and ^{15}N nmr data for the complexes [Rh(COD)(X)(L)] (X is Cl or Br and L is aniline (an), pyridine (py), pyridine *N*-oxide (pyO), ammonia (NH_3), and imidazole (imid) and COD is 1,5-cyclooctadiene) are presented in Tables 4.10 – 4.14. Representative spectra are shown in Figures 4.9–4.11.

(1) ^{1}H nmr

Compared to their carbonyl analogues (see Chapter 3), the [Rh(COD(X)(L)] complexes have a relatively complex ^{1}H nmr spectrum (see Figures 4.9 and 4.10). However, like their carbonyl analogues, the resonances in the ^{1}H nmr spectra move insignificantly with varying X (Cl or Br). Complexation of the ligands (L) and COD to rhodium is confirmed by the upfield shift of the resonances of the complex relative to that of free ligand in the ^{1}H nmr spectra. The spectra were recorded in various deuterated solvents depending on the solubility of the complexes.

The ^{1}H nmr spectra of the complexes can be considered in two parts, (i) the ligand (L) resonances and, (ii) the COD resonances.

(I) THE LIGAND (L) RESONANCES

[Rh(COD)(X)(L)] (X is Cl or Br and L is py, pyO, an and NH_3)

The ^{1}H nmr spectra of the above complexes reveal the usual spectral pattern (coupling constant values and integration) associated with the coordinated ligands.

In the ammonia and aniline complexes the resonances of the H atom attached to the N atom could not be detected. These proton resonances are notoriously difficult to

observe due to broadening effects of the ^{14}N quadropole moment [39]. However, in the aniline complexes, where the N atom in the ligand was isotopically enriched to ^{15}N, the ^{1}J (^{15}N-H) coupling constant could easily be obtained.

[Rh(COD)(X)(L)] (X is Cl or Br and L is imid)

At room-temperature (in $CDCl_3$ or DMF-d_7) the above complexes reveal only two signals for the H_a, H_b and H_c protons of imidazole instead of the three resonances expected for a complex of the structure shown (see Table 4.12). This phenomenon was previously observed in the carbonyl analogues (see Chapter 3) and consequently the same reasoning is followed for the assignments of the protons. Thus, the lower field signal is assigned to H_a, while the other signal is assigned to H_b and H_c, which are equivalent if exchange is occurring. Once again, parallel to the behaviour of the carbonyl counterparts, the single resonances of H_b and H_c split into two separate resonances on cooling, showing the expected resonances consistent with the instantaneous structure (see Table 4.12 and Figure 4.10). Previous authors [11] have recorded the ^{1}H nmr spectrum of [Rh(COD)(Cl)(imid)] in CD_2Cl_2, and failed to resolve the H_b and H_c resonances, even after cooling to -80°C. The different behaviour of the H_b and H_c resonances on cooling in varying solvents is an indication of solvent participation in the species in solution. We thus favour explaining the fluxional process occurring within these complexes by an *inter*molecular mechanism. Similar fluxional behaviour has been reported [18,36,40] for some related complexes and has been ascribed to a facile dissociation/association of L. Confirmation of this *inter*molecular (dissociation/association) mechanism is provided by the ^{15}N nmr results (see ^{15}N nmr section).

The inclusion of ^{15}N-enriched imidazole in the complexes causes the broad ^{15}N-H peak in the ^{1}H nmr spectra to become a relatively sharp doublet, while the ^{15}N-H_a peak becomes a triplet (see Figure 4.10). Thus the $^{1}J(^{15}N\text{-}H)$ and $^{2}J(^{15}N\text{-}H_a)$ coupling can easily be observed.

(II) THE COD RESONANCES

All the complexes have in their ^{1}H spectrum (see Figures 4.9 and 4.10) at room temperature in $CDCl_3$:

(i) a relatively broad peak at ~4 ppm (integrating for 4 protons),

(ii) a broad ill-defined multiplet centred at ~2.5 ppm (integrating for 4 protons),

(iii) a multiplet centred at ~1.8 ppm (integrating for 4 protons).

Based on numerous nmr studies on related complexes [11,36,40-42] we assign the broad peak at ~4 ppm to the four olefinic protons (=CH), which cannot be differentiated because of rapid ligand exchange, that is,

$$[Rh(COD)(L)(X)] + L^* \longleftrightarrow \text{intermediate} \longleftrightarrow [Rh(COD)(L^*)(X)] + L$$

Similar processes have been found in related systems and the mechanism is reported to proceed *via* a 5-coordinate intermediate [18,36].

The ^{1}H nmr spectra of the complexes were also recorded at low temperatures. However, only in the imidazole and aniline complexes were any appreciable changes noted. In the low temperature ^{1}H nmr spectra, the broad resonance at ~4 ppm splits into two peaks. In accordance with previous assignments [11,40] the higher field peak is assigned to the protons *trans* to the halogen (H_c), and the lower field peak is assigned to the protons *trans* to the ligand (H_d).

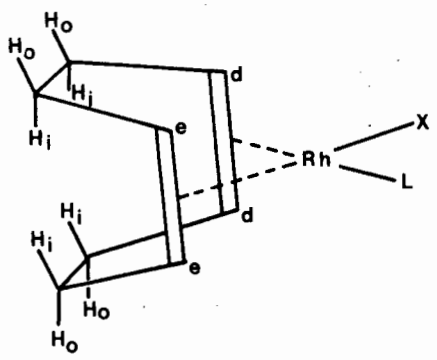

FIGURE 4.4 Diagrammatic representation of the structure of [Rh(COD)(X)(L)].
H_o (H_i) = methylenic protons of COD directed "outwards" ("inwards").

Similarly, based on comprehensive nmr studies [43,44], we assign the unresolved multiplet at ~2.5 ppm to protons of the COD ligand directed "outwards", and the multiplet at ~1.8 ppm to the protons of the COD ligand directed "inwards" (see Figure 4.4). The large chemical shift differences between these "outside" and "inside" orientations have been ascribed to steric crowding and magnetic anisotropy [44].

(2) ^{13}C nmr

Although numerous 1,5-cyclooctadiene complexes have been studied by ^{1}H nmr, few ^{13}C nmr studies have been reported mainly because the complexes have a low solubility in many solvents and thus require long acquisition times for recording their ^{13}C nmr spectra. According to the preceding ^{1}H nmr spectral results, it would appear that only the imidazole complexes undergo an exchange process. However, the ^{13}C nmr spectra (because of the relatively faster nmr time scale of ^{13}C) reveal that all the complexes are undergoing some exchange process in solution.

At room-temperature the spectra of each of the complexes reveal the usual spectral pattern associated with the coordinated ligands (L). On the other hand, the COD

ligand shows only two signals for the eight carbon atoms, one sharp signal at ~30 ppm corresponding to the four methylenic carbons, and a broadish signal at ~80 ppm corresponding to the four olefinic carbons. This assignment is in agreement with numerous other studies of COD complexes [40,43-46]. At room temperature the peak centered at ~80 ppm varies from being a broad hump to a sharp doublet in the ^{13}C nmr spectra of the various complexes, the doublet arising from the ^{1}J (^{103}Rh-C) coupling. In the variable-temperature (+ 55° to -30°C) ^{13}C nmr spectra, various changes, depending on the ligand, occur in the spectra. However, in all instances the ligand (L) resonances alter insignificantly while the COD resonances change substantially. Hence, the following discussion explains the changes occurring in the COD resonances only.

[Rh(COD)(X)(imid)] (X is Cl or Br)

The first change observed upon cooling the solutions of these complexes is that the single broad peak assigned to the four olefinic carbons (at ~ 80 ppm) splits into two separate resonances, each in turn split by $^{1}J(^{103}Rh$-C) coupling (see Figure 4.10 and Table 4.12). The spin-spin coupling constant values are in agreement with similar systems previously reported [25,43,47]. The higher field doublet is assigned to the olefinic carbons *trans* to the halogen (C_e) and the lower field doublet to the two olefinic carbons *trans* to the ligand (C_d). This is the order of assignment made on related cyclooctadiene complexes [42].

Although we are able to differentiate between the two sets of olefinic carbons, that is *trans* to halogen (C_e) or *trans* to ligand (C_d), we are unable to distinguish between the carbons in each set. Similarly, in the iridium analogue, [Ir(COD)(Cl)(py)] the carbons in each set could not be distinguished [40]. Recently, it has been shown [43, 44] that it is possible to distinguish between the carbons in each olefinic set if the

ligand *trans* to each olefinic set differs substantially, hence causing each of the four olefinic carbon atoms to resonate over a relatively wide chemical shift range.

The second change observed upon cooling the solutions is that the peak assigned to the four methylenic carbons splits into two resonances on cooling. This corresponds to the two different sets of methylenic carbons. However, we are once again unable to distinguish between the carbons in each methylenic set.

The ^{13}C nmr results show that in solution the COD moiety in the complexes undergo a fluxional process. The fact that the high-temperature spectra show only one peak with no $^{1}J(^{103}Rh\text{-}C)$ coupling present, indicates that the exchange process is *via* an *inter*molecular exchange, involving the COD moiety rather than by an *intra*molecular exchange process.

[Rh(COD)(X)(L)] (X is Cl or Br and L is py, pyO, an and NH_3)

The variable temperature ^{13}C nmr spectra of the above complexes all behave in a similar fashion. That is, the signal assigned to the four olefinic carbons (at ~80ppm) has a tendency to form a single broad peak, with no $^{1}J(^{103}Rh\text{-}C)$ coupling present at high-temperatures, while at low-temperatures the peak sharpens and is split by the $^{1}J(^{103}Rh\text{-}C)$ coupling (see Figure 4.9). The only difference between the spectra of the various complexes is the coalescence temperature of of the olefinic carbon resonance. The peak assigned to the four methylenic carbons (at ~30 ppm) is unchanged over the temperature range studied.

Thus like the imidazole complexes,these compounds also undergo an *inter*molecular exchange process involving the COD moiety. However, their exchange process is much faster since our low-temperature ^{13}C nmr spectra could not differentiate

between the two different sets of olefinic (or methylenic) carbons. It has been suggested [48,49] that the exchange process proceeds *via* a five-coordinate intermediate which subsequently undergoes one or more polytopal rearrangements. This tends to cause the four carbon atoms (either olefinic or methylenic) to become equivalent.

(3) ^{15}N nmr spectra

Representative coupled and decoupled ^{15}N nmr spectra are shown in Figure 4.11. The inclusion of ^{15}N-enriched ligand (aniline or imidazole) in the complexes allows ready determination of the ^{15}N nmr spectra. With regard to the square planar structure of the complexes [Rh(COD)(X)(^{15}N-ligand)] (see Tables 4.12 and 4.14), the ^{15}N-ligand couples to the ^{103}Rh; thus one expects to observe a doublet for this resonance in the ^{15}N nmr spectra. The absence of $^{1}J(^{15}N–^{103}Rh)$ coupling correlates to bond-scissions, and is extremely sensitive and the most definitive nmr test of an *inter*molecular exchange process [50].

The room temperature ^{15}N nmr spectra of the [Rh(COD)(X)(^{15}N-imid)] (X is Cl or Br) complexes do not show any $^{1}J(^{15}N–^{103}Rh)$ coupling. Upon cooling the solutions (to –40°C), the resonance in the ^{15}N nmr spectra assigned to $^{15}N_a$–Rh splits into the expected doublet, thus indicating that at room temperature the ^{15}N-imidazole ligand is dissociating from the Rh centre with a rate greater than $1/J$ (see Figure 4.11). Hence we conclude that an *inter*molecular exchange process involving an Rh–N bond rupture is occurring. The observed $^{1}J(^{15}N_a–^{103}Rh)$ coupling constant values correlate well with data obtained from similar complexes elsewhere [Chapter 3, 51].

Like the imidazole complexes, the room-temperature ^{15}N nmr spectra of the ^{15}N-aniline complexes have a single sharp resonance with no $^{1}J(^{15}N–^{103}Rh)$ coupling

present. Upon cooling the solution (to -30°C) the sharp resonance broadens considerably and eventually (at -65°C) is on the point of forming a doublet when the freezing point of the solvent (DMF-d_7) is reached. Regrettably, the complexes were not sufficiently soluble in solvents with a lower freezing point than DMF-d_7,thus the ^1J (^{15}N–^{103}Rh) values could not be measured. Nevertheless, it may be assumed that, like the imidazole complexes, an *inter*molecular exchange process occurs in these complexes also.

In summing up the combined results of the ^{1}H, ^{13}C and ^{15}N nmr it can be stated that more than one type of fluxional process is occurring in solution, and that the fluxional processes involve both the ligand (L) and the COD moieties.

ELECTRONIC SPECTRA

The electronic spectral data of the complexes [Rh(COD)(X)(L)] (X is Cl or Br and L is aniline, pyridine, pyridine *N*-oxide, imidazole or ammonia) are presented in Table 4.15

The solution spectra in the uv/vis region show a rather simple pattern similar to that usually observed for four-coordinate square planar d^8 systems [52,53]. By analogy with systems previously studied (see Chapter 3) we expect to observe the $\pi\rightarrow\pi^*$(COD), the d(Rh)$\rightarrow\pi^*$(COD), and the $X^-\rightarrow Rh^+$ transitions. In addition, for complexes where L is an amine which possesses π-electrons which may interact with Rh, there is the possibility of the d(Rh)$\rightarrow\pi^*$(amine) charge transfer transition. Like the carbonyl analogues (see Chapter 3), the electronic spectra yield very broad bands, so that specific assignments are tentative. Nevertheless, the absorptions occurring in the range 270–240 nm with extinction coefficients between 400–800 m^2

$mole^{-1}$, are assigned to the $d \rightarrow \pi^*$ metal-to-ligand charge transfer bands which are characteristic of a number of rhodium(I) complexes containing π-acceptor ligands [53,54].

By analogy with the carbonyl complexes, the COD complexes are also monomeric in solution and consequently do not have metal-metal interactions. However, it has previously been shown [55,56] that in the solid-state similar complexes possess metal-metal interactions.

MASS SPECTRA

The mass spectra of the complexes are not very informative. However, in the various complexes peaks, at *m/e* 493 and 582 were detected which can be assigned to $[Rh(COD)Cl]_2$ and $[Rh(COD)Br]_2$, respectively. In addition, all the spectra reveal peaks due to the ligand (L) associated with the respective complex and the $[Rh(COD)X]_2$ dimer fragmentation pathway. Molecular ions were not seen.

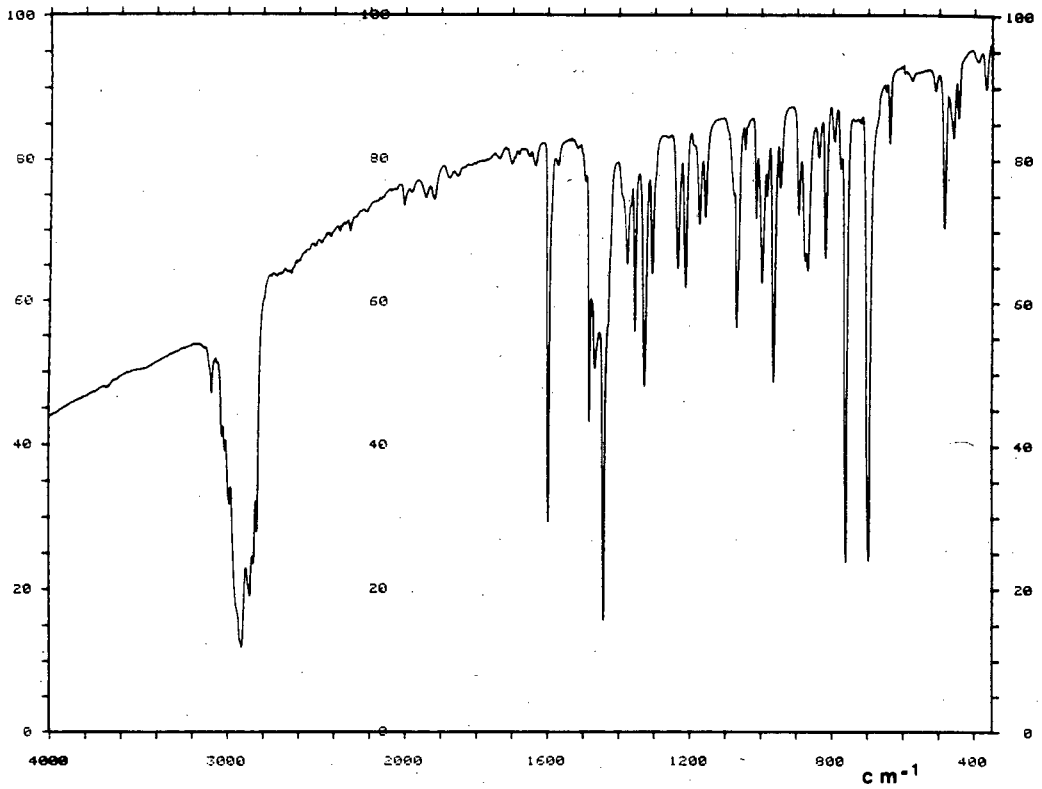

Figure 4.5 Infrared spectrum of [Rh(COD)(Cl)(py)] (Nujol mull).

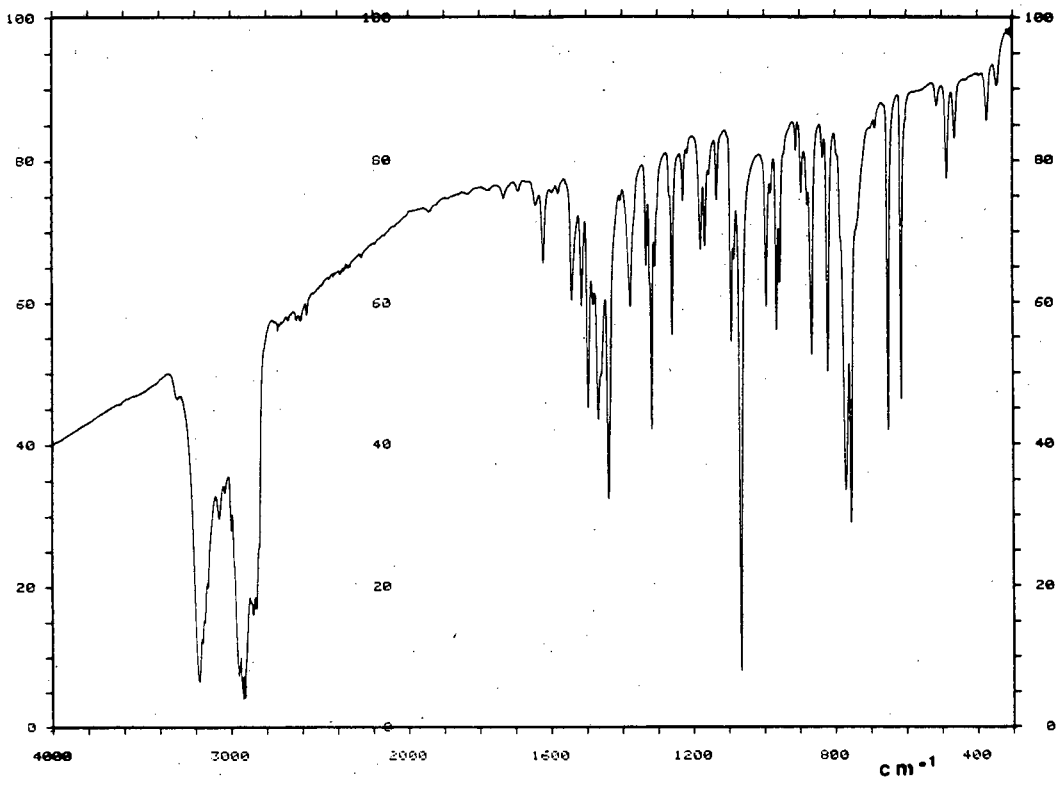

Figure 4.6 Infrared spectrum of [Rh(COD)(Cl)(imid)] (Nujol mull).

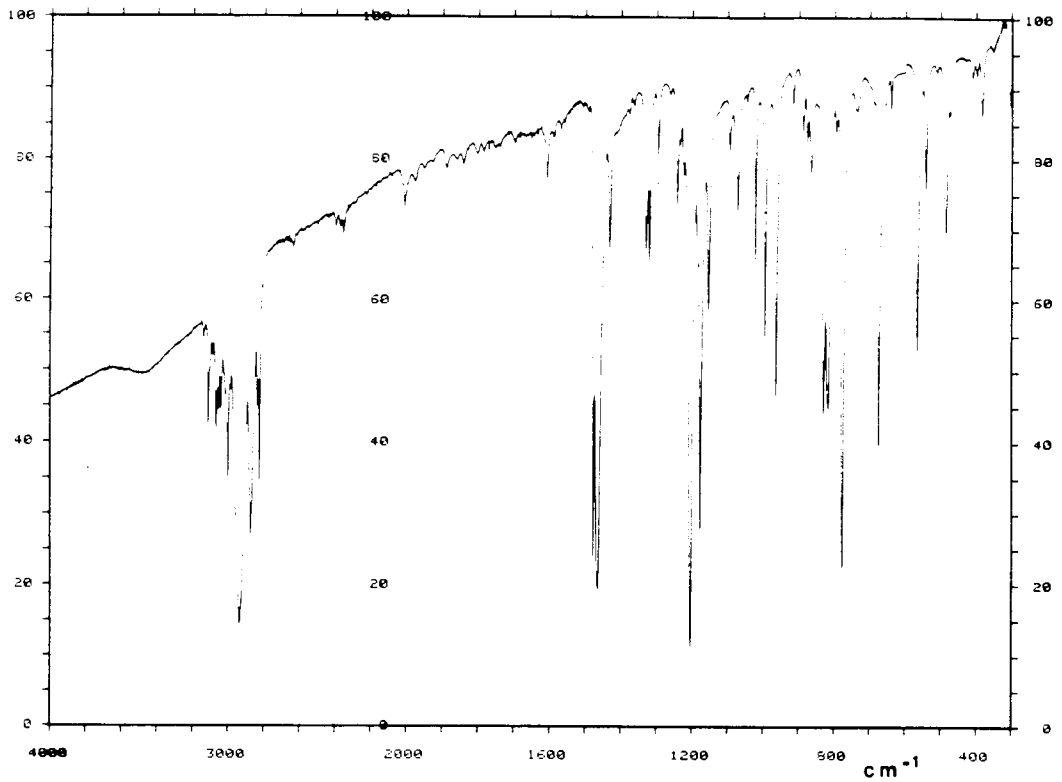

Figure 4.7 Infrared spectrum of [Rh(COD)(Cl)(pyO)] (Nujol mull).

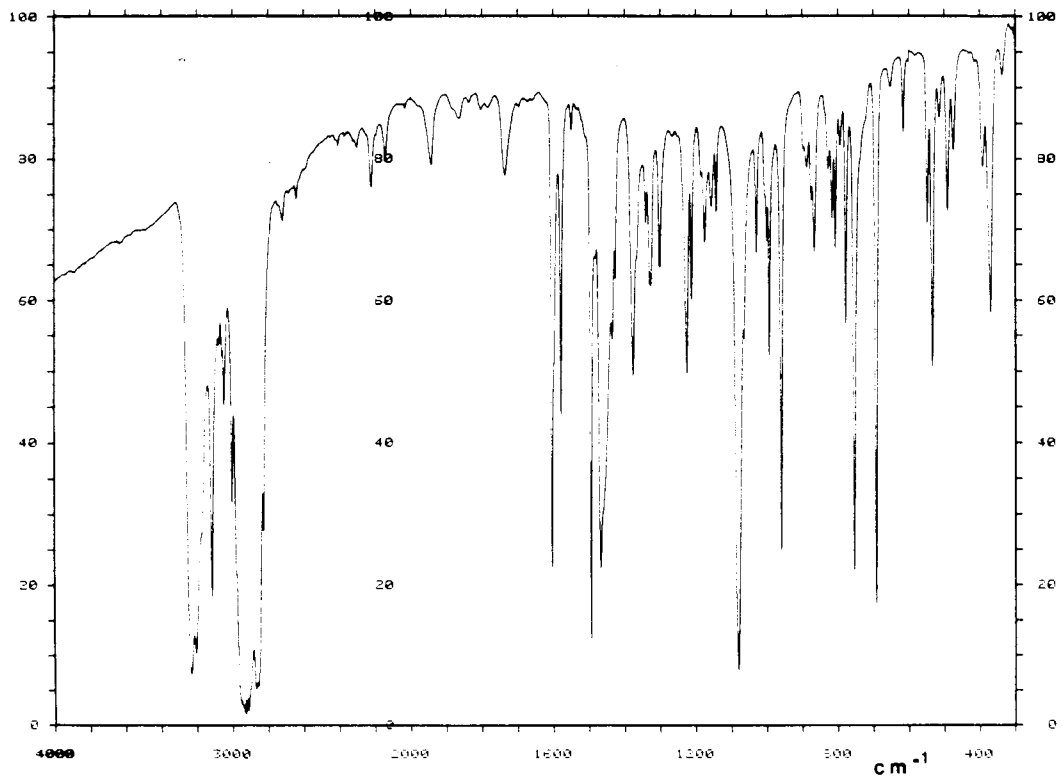

Figure 4.8 Infrared spectrum of [Rh(COD)(Cl)(an)] (Nujol mull).

TABLE 4.1 Infrared assignments of [Rh(COD)(Cl)(NH_3)] (cm^{-1}).

NH_3	ND_3	Assignment
3301	2466	ν(N-H)
3281	2447	
3221	2351	
3195		
3155	2302	
3004	3003	ν(C-H) COD
2984	2983	
2932	2930	
2908	2907	
2870	2869	
2829	2827	
1601	1172	$\delta_{as}(NH_3)$
1487	1486	ν(C=C) COD BAND I
1473	1473	ν(C=C)
1465	1464	COD
1449	1448	COD
1429	1428	$\delta(CH_2)$ COD
1375	1375	COD
1328	1326	ρ_w(C-H) COD
1297	1297	
1249	961	$\delta_s(NH_3)$
1235		
1226	1225	ν(C=C) COD BAND II
1212	1212	COD
1173	1172	ρ_w(C-H) COD
1154	1154	COD
1074	1075	
996	995	
963	961	
888	888	
875	875	ρ(C-C-C) COD
865	863	ρ_w(C-H) COD
831	831	COD
816	816	COD
798	795	ρ_r(C-H) COD

NH_3	ND_3	Assignment
774	773	ρ_r(C-H) COD
720	721	COD
685	690	COD
665	510	$\rho(NH_3)$
487	485	ν(Rh-COD)
470	466	ν(Rh-COD)
426	}398	ν(Rh-N)
394		ν(Rh-COD)
373	372	ν(Rh-COD)
334	331	ν(Rh-COD)
277	277	ν(Rh-Cl)
261	258	COD
233	210	δ(Rh-N)
174	173	
153	146	γ(Rh-N)
100	99	δ(Rh-Cl)
62	60	γ(Rh-Cl)

TABLE 4.2 Infrared assignments of [Rh(COD)(Cl)(py)] (cm^{-1}).

py	py-d_5	Assignment	*Wilson Band No.
3333	2461	ν(C-H)	20b
3087	2338, 2302	ν(C-H)	2
3030	2273	ν(C-H)	7a
3013	2266	ν(C-H)	20a/7b
2989	2989	ν(C-H) COD	
2933	2932	ν(C-H) COD	
2917	2917	ν(C-H) COD	
2875	2874	ν(C-H) COD	
2832	2832	ν(C-H) COD	
1650	1643	combination	1 + 6b
1635	1589	combination	1 + 6a
1597	1557	ν(ring)	8a
1568	1531	ν(ring)	8b
1493	1493	ν(C=C) COD BAND I	
1483	1328	ν(ring)	19a
1470	1469	ν(C=C) COD	
1442	1313	ν(ring)	19b
1429	1429	$\delta(CH_2)$ COD	
1354	1339	ν(ring)	14
1327	1328	ρ_w(C-H) COD	
1306	1307	ρ_w(C-H) COD	
1234	976	δ(C-H)	3
1212	1214	ν(C=C) COD BAND II	
	899	δ(C-H)	9a
1173	1173	ρ_w(C-H) COD	
	838	δ(C-H)	15
1156	1156	COD	
1075	1075	COD	
	819	δ(C-H)	18b
1068	826	δ(C-H)	18a
1046	1041	ν(ring)	12
1014	1012	ν(ring)	1
997	996	COD	
982	809	γ(C-H)	17a
963	964	COD	

py	py-d_5	Assignment	*Wilson Band No.
946	720	γ(C-H)	5
894	689	γ(C-H)	10a/10b
876	876	ρ(C-C-C) COD	
868	868	ρ_w(C-H) COD	
838	838	COD	
819	819	COD	
795	795	ρ_r(C-H) COD	
777	777	ρ_r(C-H) COD	
761	613	γ(ring)	4
698	536	γ(C-H)	11
649	641	δ(ring)	6b
639	----	δ(ring)	6a
578	576	ν(Rh-COD)	
511	510	COD	
485	484	ν(Rh-COD)	
460	460	ν(Rh-COD)	
446	409 395	} γ(ring)	16b
388	340	γ(ring)	16a
368	367	ν(Rh-COD)	
341	340	ν(Rh-COD)	
285	282	ν(Rh-N)	
255	254	ν(Rh-Cl)	
210 200	205 194	} δ(Rh-N)	
152	151	δ(Rh-Cl)	
96	93	γ(Rh-N)	
73	71	γ(Rh-Cl)	

* E.B.Wilson, *Phys. Rev.*, **45** (1934) 706

TABLE 4.3 Infrared assignments of [Rh(COD)(Cl)(imid)] (cm^{-1}).

imid	imid-^{15}N	imid-d_4	Assignment
3179	3166	3176	ν(N-H)
3128	3105	-----	
3066	3049	2338	ν(C-H)
3035			
3000	2998	2339	
2984	2983	2983	ν(C-H) COD
2956	-----	-----	
2938	2937	2937	
2923	2922	2922	
2883	2882	2878	
2837	2836	2836	
1542	1532	1478	ν(ring)
1514	1512	1451	ν(ring)
1496	1494	1495	ν(C=C) COD BAND I
1468	1467	1464	ν(C=C) COD
1439	1431	1440	$\delta(CH_2)$ COD
	1360	1432	ν(ring)
1405	1395	1406	COD
1376	1374	1375	COD
1332	1331	1331	COD
1322	1321	1321	ν(ring)
1317	1307	1307	ρ_w(C-H) COD
1307			
1259	1252	946	ν(C=C) COD BAND II
	1246		δ(C-H)
1228	1212	919	δ(N-H)
1166	1175	1178	ρ_w(C-H) COD
	1160		ν(ring)
1156	1156	1154	COD
1134	1119	1116	ν(ring)
1092	1091	1095	COD
		886	δ(C-H)
1083	1083	878	δ(C-H)
1066	1060	868	δ(C-H)
994	994	994	COD
981	981	982	

imid	imid-^{15}N	imid-d_4	Assignment
965	964	964	COD
	929	576	γ(N-H)
956	955	982	δ(ring)
	----	775	γ(C-H)
910		720	δ(ring)
895	}895	{895	ρ(C-C-C) COD
		{664	γ(C-H)
878	878	878	ρ_w(C-H) COD
865	865	868	ρ_w(C-H) COD
835	835	{830	COD
		{642	γ(C-H)
821	820	822	COD
770	769	}540	} γ(C-H)
755	754		
687	688	575	γ(ring)
650	642	551	γ(ring)
614	610	519	γ(ring)
515	515	----	COD
486	486	487	ν(Rh-COD)
465	464	465	ν(Rh-COD)
374	373	374	ν(Rh-COD)
344	345	345	ν(Rh-COD)
282	282	281	COD
265	264	264	ν(Rh-COD)
253	253	253	ν(Rh-Cl)
236	232	230	ν(Rh-N)
219	217	211	} δ(Rh-N)
184	182	178	
171	172	172	δ(Rh-N-C)
163	163	162	δ(Rh-Cl)
125	123	122	γ(Rh-N)
96	96	93	
65	64	65	
51	---	51	

Table 4.4 Infrared assignments of [Rh(COD)(Cl)(pyO)] (cm^{-1}).

pyO	pyO-d_5	Assignment	*Band Number Wilson	Gambi & Ghersetti
3137 3110	} 2318	ν(C-H)	}20b/2	1/12
3087	2305		20a	2
3066	2282		7b	13
3053 3040	} 2262		}7a	3
2999	2999	ν(C-H) COD		
2937	2936			
2872	2872			
2834	2833			
2823	2823			
1608	1565	ν(ring)	8a	4
1569	1538		8b	14
1476	{ 1353 1341		19a/19b	5/15
1465	1468	ν(C=C) COD BAND I		
1433	1433	$\delta(CH_2)$ COD		
1330	-----	ρ_w(C-H) COD		
1321	1321			
1297	1296			
1263	1263	COD		
1243	1231	ν(ring)	14	16
1224	1223	ν(C=C) COD BAND II		
1204	}1164	ν(ring)	3	17
1177		ν(N-O)	13	6
1154	861	δ(C-H)	9a/15	7/18
1072	{ 1076 811	COD δ(C-H)	18b	19
1046	1041	COD		
1022	982	ν(ring)	12	9
994	995	COD		
963	{ 963 796	COD γ(C-H)	5/17a	22/25
888	890	ρ(C-C-C) COD		

pyO	pyO-d_5	Assignment	*Band Number Wilson	Gambi & Ghersetti
876	873	ρ(C-C-C) COD		
865	852	ρ_w(C-H) COD		
829	827	COD		
	767	ν(ring)	1	10
815	761			
795	796	ρ_r(C-H) COD		
776	775	ρ_r(C-H) COD		
	541	γ(C-H)	11	27
737	737	COD		
673	642	γ(ring)	4	28
641	615	δ(ring)	6b	20
566	552	δ(ring)	6a	11
543	515	γ(ring)	16b	29
511		COD		
487	490	ν(Rh-COD)		
	475	ν(Rh-pyO)		
478	444	β(N-O)	9b	21
411	409	ν(Rh-COD)		
399	----	ν(Rh-COD)		
384	384	ν(Rh-COD) + γ(ring)	16a	24
354	357	ν(Rh-COD)		
304	292	δ(Rh-pyO)		
276	276	ν(Rh-Cl)		
251	251	COD		
204	194	γ(N-O)	17b	30
175	175			
156	156	δ(Rh-Cl)		
133	121			
112				
102	103			
71	---			
60	61			

* E.B.Wilson, *Phys. Rev.*, **45** (1934) 706
A.Gambi & S.Ghersetti, *Spectrosc. Lett.*, **10** (1977) 627

Table 4.5 Infrared assignments of [Rh(COD)(Cl)(aniline)] (cm^{-1}).

an	an-d_5	an-ND_2	an-d_7	an-$^{15}NH_2$	Assignment
3232	3230	2421	2421	3222	ν(N-H)
3205	3202	2381	2380	3196	
-----	3152	2328	2337	3165	ν(N-H).....Cl
3116	3115	-----	2310	3109	
3077	2290	-----	2279	-----	ν(C-H)
3060	2278	-----		3059	
3048	2267	3046	2266	3048	
3004	3003	3001	3001	3003	ν(C-H) COD
2980	2979	2978	2978	2980	
2944	2943	2941	2941	2943	
2913	2911	2911	2908	2910	
2870	2869	2870	2867	2869	
2847	2847	-----	2844	2847	
2825	2825	2824	2823	2824	
1578	1573	1246(NHD)	1211(NHD)	1573	NH_2 scissor
1550	1568	1080	1115	1543	
1494	1492	1493	1480	1493	ν(C=C) COD BAND I
	1387		1385		ν(ring)
1468	1471	1469	1469	1467	ν(C=C) COD
1450	1451	1448	-----	1450	COD
1434	1434	1431	1432	1433	COD
	1425		1426		ν(ring)
1426	1426	1426	1426	1426	$\delta(CH_2)$ COD
1368	1370	1367	1370	1368	
1341	1328	1328	1347	1344	ν(ring)
1325			1328	1324	
1302	1302	-----	1300	1302	ρ_w(C-H) COD
1224	1228	1227	-----	1228	ν(C=C) COD BAND II
	1161			1220	ν(C-N)
1213	1212	1212	1212	1212	COD
1176	1175	1175	1174	1174	ρ_w(C-H) COD
1156	-----	1157	1157	-----	COD
1143	-----	843	835	1139	NH_2 twist
			841		
1081	1079	1080	1078	1075	COD
	867	1058	855		δ(C-H)
1064	844	1030	752	-----	δ(C-H)
1030	760			1030	

an	an-d_5	an-ND_2	an-d_7	an-$^{15}NH_2$	Assignment
1006	1006	-----	1006	1006	COD
1001	750	}995	721	1000	δ(C-H)
993	993		993	993	COD
959	960	959	959	959	COD
887	888	887	888	887	ρ(C-C-C) COD
876	876	875	}871	875	
866	867	866		866	ρ_w(C-H) COD
827	824	827	828	828	ν(ring) + COD
817	813	816	812	816	ν(ring) + COD
807	795	}790	808	806	ρ_r(C-H) COD
795	592		593	794	γ(C-H)
778	778	778	778	778	ρ_r(C-H) COD
754	{750	753	752	753	COD
	{556	734	553		γ(C-H)
692	492	691	492	691	γ(C-H)
653	{658	541	521	----	NH_2 wag
	{643				
616	----	617	----	616	δ(ring)
548	----	----	459	542	NH_2 rock
533	534	533	534	531	ν(Rh-COD)
492	492	491	492	492	ν(Rh-COD)
475	469	474	----	475	ν(Rh-COD)
392	372	369	358	388	ν(Rh-N)
369	358	340	332	366	
339	333	316	307	337	δ(Rh-N)
282	282	281	282	282	ν(Rh-Cl)
260	261	259	260	261	ν(Rh-COD)
250	249	248	248	248	ν(Rh-COD)
204	194	204	193	204	γ(ring)
170	}170	166	168	168	
162					
140	138	139	137	139	δ(Rh-Cl)
109	{117	117	106	119	
	{94	100		100	
76	70	71	---	75	

TABLE 4.6 Infrared assignments of [Rh(COD)(Br)(py)] (cm^{-1}).

py	py-d_5	Assignment	*Wilson Band No.
3091	2333	ν(C-H)	20b/2
3034	2281		7a
3014	2268		20a/7b
2996	2998	ν(C-H) COD	
2932	2932		
2917	2920		
2875	2876		
2832	2832		
1652	1642	combination	1 + 6b
1634	1589		1 + 6a
1599	1559	ν(ring)	8a
1571	1532		8b
1494	1495	ν(C=C) COD BAND I	
1482	1328	ν(ring)	19a
1467	1467	ν(C=C) COD	
1442	1316	ν(ring)	19b
1428	1429	$\delta(CH_2)$ COD	
1353	1340	ν(ring)	14
1327	1328	ρ_w(C-H) COD	
1304	1303		
1232	975	δ(C-H)	3
1210	1214	ν(C=C) COD BAND II	
	887	δ(C-H)	9a
1172	1173	ρ_w(C-H) COD	
	835	δ(C-H)	15
1154	1157	COD	
1075	1075	COD	
	816	δ(C-H)	18b
1067	825	δ(C-H)	18a
1044	1040	ν(ring)	12
1011	-----	ν(ring)	1
996	994	COD	
979	806	γ(C-H)	17a

py	py-d_5	Assignment	*Wilson Band No.
962	964	COD	
943	734	γ(C-H)	5
891	691	γ(C-H)	10a/10b
873	874	ρ(C-C-C) COD	
837	835	COD	
817	816	COD	
793	792	ρ_r(C-H) COD	
774	776	ρ_r(C-H) COD	
758	612	γ(ring)	4
696	535	γ(C-H)	11
648	638	δ(ring)	6b
637	612	δ(ring)	6a
575	575	ν(Rh-COD)	
509	510	COD	
482	482	ν(Rh-COD)	
455	455	ν(Rh-COD)	
445	407 402	γ(ring)	16b
391	335	γ(ring)	16a
364	363	ν(Rh-COD)	
336	335	ν(Rh-COD)	
259	255	ν(Rh-N)	
218	212	δ(Rh-N)	
200	196		
175	173	ν(Rh-Br)	
126	123	γ(Rh-N)	
87	85	δ(Rh-Br)	
67	66	γ(Rh-Br)	

* E.B.Wilson, *Phys. Rev.*, **45** (1934) 706

TABLE 4.7 Infrared assignments of [Rh(COD)(Br)(imid)] (cm^{-1}).

imid	imid-^{15}N	imid-d_4	Assignment
3210	3197	3206	ν(N-H)
3180	-----	2378	ν(C-H)
3159	3156		
3145	3143	2333	
3129	3126		
3067	3053	2280	
3031	-----	3030	ν(C-H) COD
3004	3004	3004	
2983	2983	2983	
2961	-----	2960	
2936	2934	2936	
2921	2919	2921	
2879	2879	2879	
2833	2831	2833	
1539	1531	1480	ν(ring)
1511	1508	1449	ν(ring)
1495	1493	1494	ν(C=C) COD BAND I
1467	1467	1467	ν(C=C) COD
1435	1431	1439	$\delta(CH_2)$ COD
	1375		ν(ring)
-----	1419	1417	COD
1332	1331	1331	ν(ring) + COD
1316	1322	1322	ρ_w(C-H) COD
1307	1306	1307	
1265	1251	946	δ(C-H)
1258	1244	894	ν(C=C) COD BAND II
	1238		δ(N-H)
1177	1175	1172	ρ_w(C-H) COD
1165	1158	1160	COD
1130	1115	1113	ν(ring)
1092	1091	1090	COD
		884	δ(C-H)
1065	1058	875	δ(C-H)
993	993	993	COD
979	979	979	
965	964	964	

imid	imid-^{15}N	imid-d_4	Assignment
	927	575	γ(N-H)
955	954	979	δ(ring)
	----	779	γ(C-H)
910		718	δ(ring)
894	}894	{894	ρ(C-C-C) COD
		{687	γ(C-H)
864	863	867	ρ_w(C-H) COD
834	834	{832	COD
		{641	γ(C-H)
818	817	823	COD
754	754	555	γ(C-H)
687	686	575	γ(ring)
650	{649	555	} γ(ring)
	{642		
612	604	520	γ(ring)
513	513	----	COD
483	483	484	ν(Rh-COD)
460	459	460	ν(Rh-COD)
431	432	----	ν(Rh-COD)
370	370	370	ν(Rh-COD)
337	{343	340	} ν(Rh-COD)
	{338		
245	245	{249	COD
		{229	ν(Rh-N)
220	218	214	δ(Rh-N)
175	174	173	ν(Rh-Br) + δ(Rh-N-C)
138	137	138	δ(Rh-Br)
120	118	117	γ(Rh-N)
99	}82	99	
76		77	
55	55	55	

Table 4.8 Infrared assignments of [Rh(COD)(Br)(pyO)] (cm^{-1}).

pyO	pyO-d_5	Assignment	*Band Number Wilson	Gambi & Ghersetti
3136 3108	} 2319		}20b/2	1/12
3084	2305		20a	2
3063	2281	ν(C-H)	7b	13
3052 3038	} 2261		}7a	3
3006	3006			
2998	2997			
2936	2936			
2871	2871	ν(C-H) COD		
2833	2832			
2823	2823			
1607	1563		8a	4
1558	1538	ν(ring)	8b	14
1475	{ 1352 1341		19a/19b	5/15
1465	1469	ν(C=C) COD BAND I		
1432	1429	$\delta(CH_2)$ COD		
1331	1331			
1321	1321	ρ_w(C-H) COD		
1296	1296			
1262	1265	COD		
1245	1232	ν(ring)	14	16
1224	1222	ν(C=C) COD BAND II		
1202	}1164	ν(ring)	3	17
1184		ν(N-O)	13	6
1175	}870	δ(C-H)	9a	7
1153			15	18
1071	{ 1076 812	COD δ(C-H)	18b	19
1046	-----	COD		
1022	982	ν(ring)	12	9
993	993	COD		
961	{ 962 794	COD γ(C-H)	5/17a	22/25

pyO	pyO-d_5	Assignment	*Band Number Wilson	Gambi & Ghersetti
887	890	ρ(C-C-C) COD		
874	870	ρ(C-C-C) COD		
865	852	ρ_w(C-H) COD		
828	827	COD		
815	766	ν(ring)	1	10
793	794	ρ_r(C-H) COD		
773	775	ρ_r(C-H) COD		
	541	γ(C-H)	11	27
739	737	COD		
673	641	γ(ring)	4	28
640	615	δ(ring)	6b	20
566	551	δ(ring)	6a	11
542	515	γ(ring)	16b	29
486	489	ν(Rh-COD)		
472	473	ν(Rh-pyO) + ν(Rh-COD)		
	443	β(N-O)	9b	21
411	----	ν(Rh-COD)		
397	397	ν(Rh-COD)		
380	380	ν(Rh-COD) + γ(ring)	16a	24
304	293	δ(Rh-pyO)		
258	258	COD		
200	191	γ(N-O)	17b	30
191		ν(Rh-Br)		
170	170			
143	139	δ(Rh-pyO)		
124	124	δ(Rh-Br)		
112	110			
74	72			
60	56			

* E.B.Wilson, *Phys. Rev.*, **45** (1934) 706
A.Gambi & S.Ghersetti, *Spectrosc. Lett.*, **10** (1977) 627

Table 4.9 Infrared assignments of [Rh(COD)(Br)(aniline)] (cm^{-1}).

an	an-d_5	an-ND_2	an-d_7	an-$^{15}NH_2$	Assignment
3225	3224	2416	2417	3215	ν(N-H)
3200	3197	2375	2377	3193	
3165	3151	2326	2335	3160	ν(N-H).....Br
3116	3116	-----		3107	
3044	2288	3037	2309	3042	ν(C-H)
3021	2263	3019		3020	
2995	2994	2993	2998	2995	ν(C-H) COD
2980	2981	2980	2981	2980	
2943	2942	2939	2940	2941	
2912	2913	2915	2911	2911	
2873	2873	2872	2868	2871	
2827	2827	2826	2830	2825	
1576	1570	1252(NHD)	1205(NHD)	1571	NH_2 scissor
1546	1538	1071	1116	1540	
1493	1489	1492	1482	1492	ν(C=C) COD BAND I
	1386		1383		ν(ring)
1467	1469	1464	1469	1466	ν(C=C) COD
1427	1427	1427	1424	1426	$\delta(CH_2)$ COD
1329	1330	1328	1325	1329	ν(ring
1305	1304	1303	1303	1303	ρ_w(c-H) COD
1226	1225	1221	1227	1221	ν(C=C) COD BAND II
	1167				ν(C-N)
1214	1214	1214	1213	1214	COD
1174	1174	1172	1173	1174	ρ_w(C-H) COD
1153	1154	1153	1163	1153	COD
1143	-----	838	840	1140	NH_2 twist
			827		
1071	1069	1071	1082	1065	COD
		1053	855		δ(C-H)
1027	761	1026	752	1027	δ(C-H)
1006	1005	1006	1005	1005	COD
999	752	995	721	999	δ(C-H)
994	995		992	993	COD
957	959	957	958	958	COD
891	891	889	882	890	ρ(C-C-C) COD
871	871	869	875	866	
816	817	815	814	816	ν(ring) + COD

an	an-d_5	an-ND_2	an-d_7	an-$^{15}NH_2$	Assignment
806	795	790	799	802	ρ_r(C-H) COD
792	592		592	792	γ(C-H)
775	775	775	776	776	ρ_r(C-H) COD
759	761	752	752	754	COD
	558	732	556		γ(C-H)
694	474	692	474	692	γ(C-H)
658	643	538	520	655	NH_2 wag
615	----	617	----	615	δ(ring)
546	532	483	462	540	NH_2 rock
533				528	
485	483		486	485	ν(Rh-COD)
465	464	465	462	467	ν(Rh-COD)
398	378	380	352	386	ν(Rh-N)
374	352	338	330	371	
364	331	362	354	360	ν(Rh-COD)
332		313	303	332	(Rh-N)
272	271	----	272	273	ν(Rh-COD)
254	253	252	254	255	ν(Rh-COD)
204	193	202	193	202	γ(ring)
195		194		195	ν(Rh-Br)
151	148	149	148	150	
118	114	112	112	114	
111					
82	80	82	83	83	
72	73	72	66	72	
56	57	57		55	

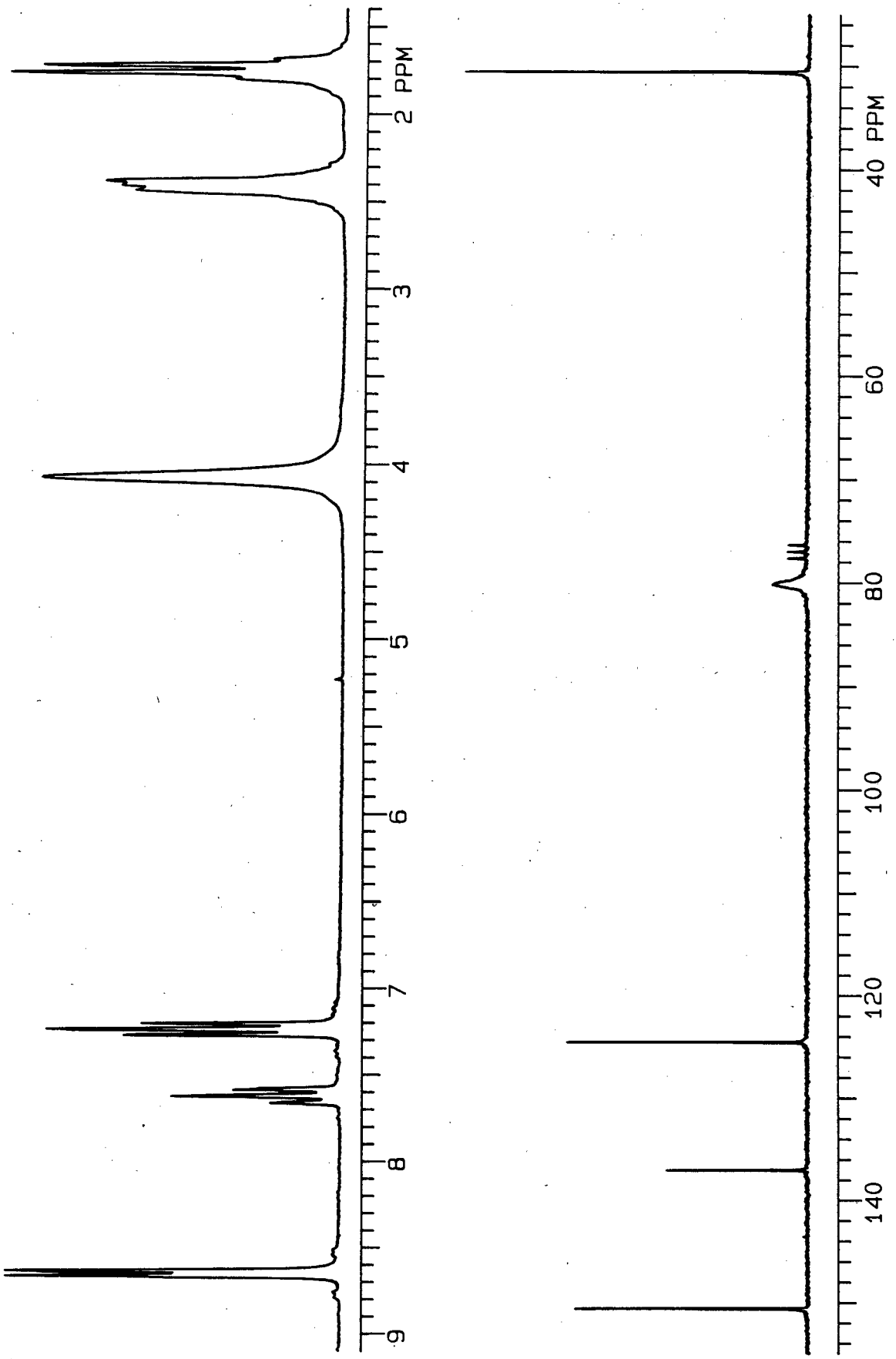

FIGURE 4.9 ^{1}H and ^{13}C nmr spectra of [Rh(COD)(Cl)(py)] ($CDCl_3$, Temp.=25°C).

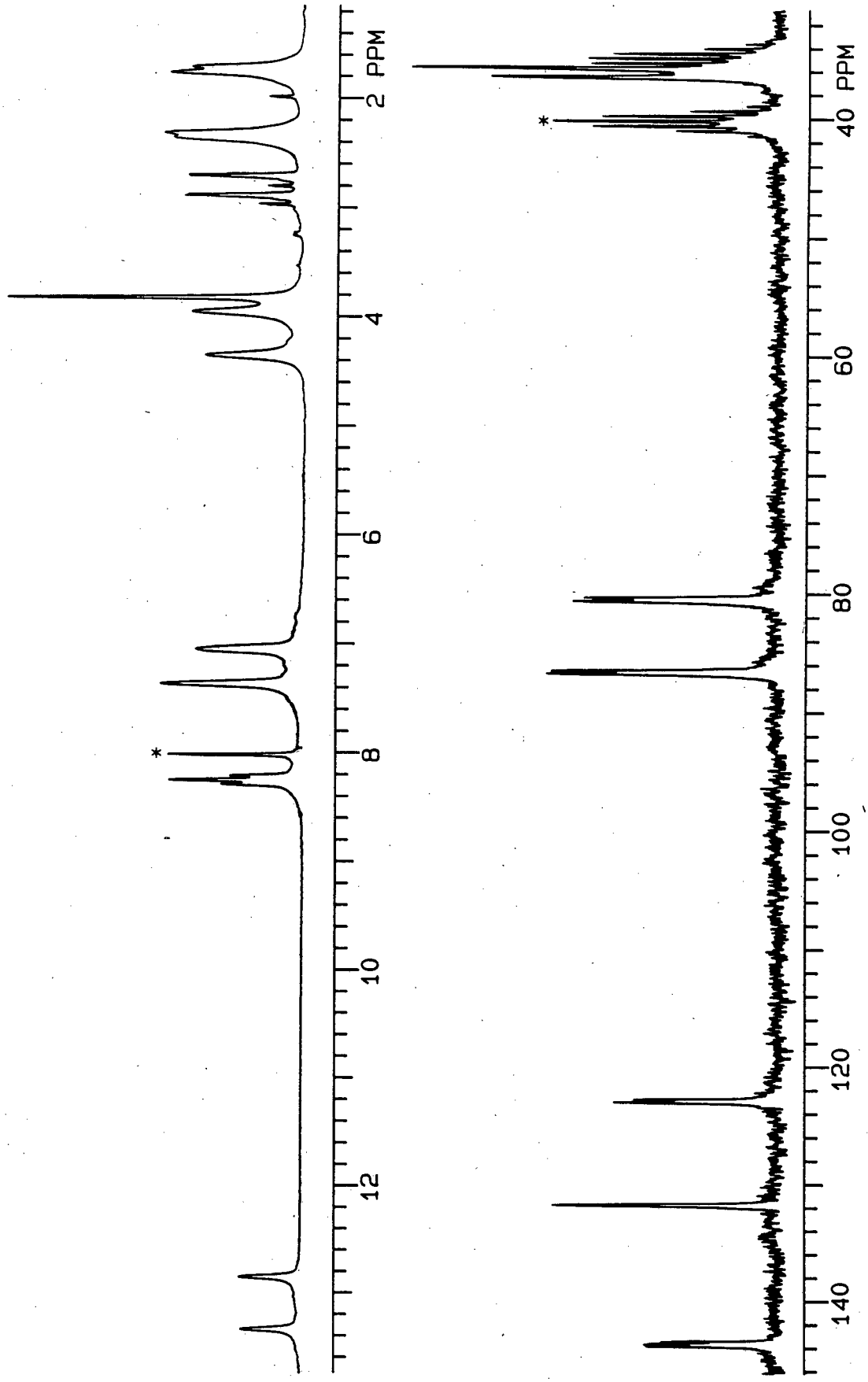

FIGURE 4.10 ^{1}H and ^{13}C nmr spectra of [Rh(COD)(Cl)(imid-^{15}N)] (* = DMF-d_7, Temp.=-30°C).

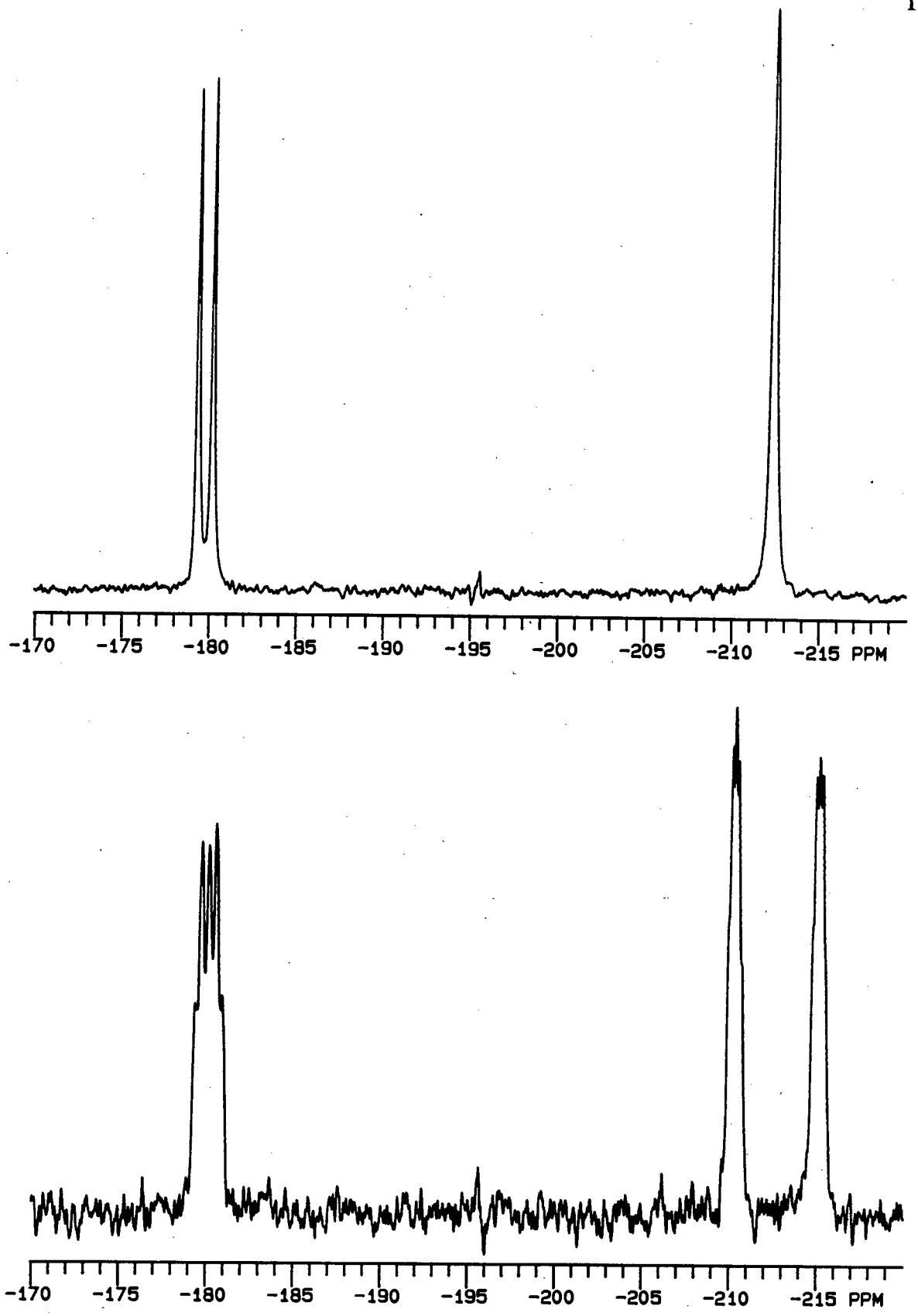

FIGURE 4.11 **^{1}H decoupled and coupled ^{15}N nmr spectra of [Rh(COD)(Cl)(imid-^{15}N)].** (Temp. = -30°C, DMF-d_7, external reference $CH_3{}^{15}NO_2$)

TABLE 4.10 ^{1}H and ^{13}C nmr data of [Rh(COD)(X)(NH_3)] (X is Cl or Br).

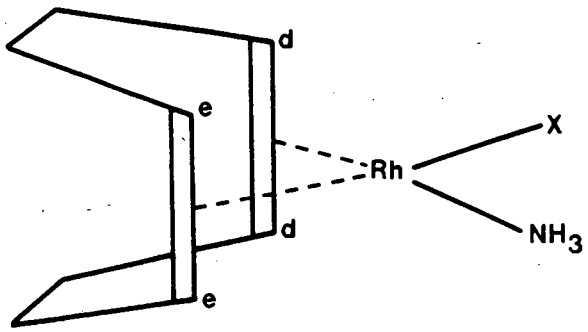

	T (°C)	Chemical Shifts (ppm) NH_3	COD		
^{1}H nmr		N-H	$H_{d,e}$	$^{*}H_o$	$^{*}H_i$
Cl	25	not observed	4.12	2.42	1.75
^{13}C nmr			$C_{d,e}$	C	
Cl	−20		†78.5	30.82	
			$^{1}J(^{103}Rh–C)$ = not observed		

All spectra recorded in $CDCl_3$ unless otherwise specified.
Chemical shifts of ^{1}H and ^{13}C relative to TMS.
$H_{d,e}$ ($C_{d,e}$) = Olefinic protons (carbons) of COD.
$^{*}H_o$ (H_i) = Methylenic protons of COD directed "outwards" ("inwards").
† Peak remains broad from +55° to −20°C.

TABLE 4.11 ^{1}H and ^{13}C nmr data of [Rh(COD)(X)(py)] (X is Cl or Br).

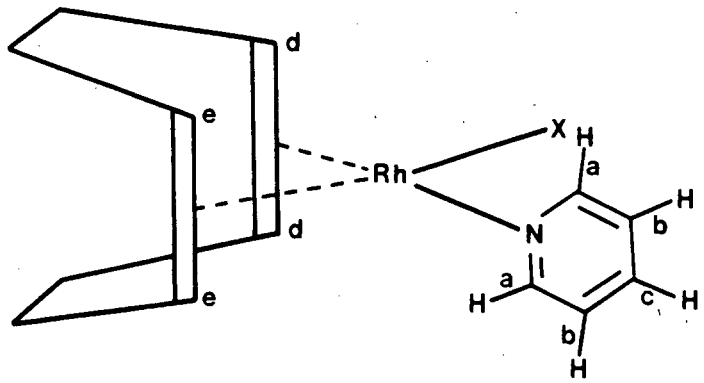

X	T (°C)	Chemical Shifts (ppm) pyridine			COD		
^{1}H nmr		H_a	H_b	H_c	$H_{d,e}$	$^{*}H_o$	$^{*}H_i$
Cl	25	8.75	7.33	7.71	4.16	2.51	1.83
Br	25	8.79	7.32	7.70	4.29	2.48	1.79
^{13}C nmr		C_a	C_b	C_c	$C_{d,e}$	C	
Cl	-20	150.58	124.54	137.01	78.51	30.61	
					$^{1}J(^{103}Rh\text{-}C)$ = 13.96 Hz		
Br	-20	151.11	124.64	136.99	79.6	30.94	
					$^{1}J(^{103}Rh\text{-}C)$ = 13.84 Hz		

All spectra recorded in $CDCl_3$ unless otherwise specified.
Chemical shifts of ^{1}H and ^{13}C relative to TMS.
$H_{d,e}$ ($C_{d,e}$) = Olefinic protons (carbons) of COD.
$^{*}H_o$ (H_i) = Methylenic protons of COD directed "outwards" ("inwards").

TABLE 4.12 ^{1}H, ^{13}C and ^{15}N nmr data of [Rh(COD)(X)(imid)] (X is Cl or Br).

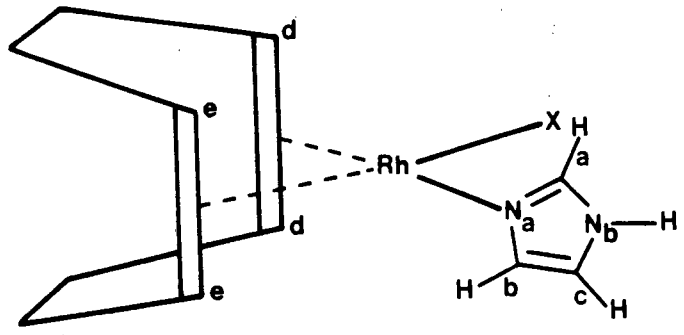

X	T (°C)	Chemical Shifts (ppm)							
		imidazole				COD			
^{1}H nmr		H_a	H_b	H_c	N-H	H_d	H_e	$^{*}H_o$	$^{*}H_i$
Cl(DMF-d_7)	−20	8.25	7.36	7.04	13.09	4.35	3.89	2.34	1.74
		$^{2}J(^{15}N\text{-}H_a)$ = 7.78 Hz				$^{1}J(^{15}N\text{-}H)$ = 97.84 Hz			
Br(DMF-d_7)	−20	8.29	7.36	7.11	13.08	4.47	3.88	2.30	1.70
		$^{2}J(^{15}N\text{-}H_a)$ = 7.81 Hz				$^{1}J(^{15}N\text{-}H)$ = 98.02 Hz			
^{13}C nmr		C_a		C_b	C_c	C_d		C_e	C
Cl(DMF-d_7)	−20	143.62		131.71	122.87	86.57		80.49	36.13
		$^{1}J(^{103}Rh\text{–}C_d)$ = 11.89 Hz				$^{1}J(^{103}Rh\text{–}C_e)$ = 13.35 Hz			
Br(DMF-d_7)	−20	144.38		132.59	122.89	85.99		81.80	36.18
		$^{1}J(^{103}Rh\text{–}C_d)$ = 11.86 Hz				$^{1}J(^{103}Rh\text{–}C_e)$ = 13.75 Hz			
^{15}N nmr		N_a		N_b		$^{1}J(^{15}N_a\text{-Rh})$		$^{1}J(^{15}N_b\text{-H})$	
Cl(DMF-d_7)	−30	−180.15		−212.73		17.16		97.91	
Br(DMF-d_7)	−30	−185.48		−217.35		17.08		97.75	

All spectra recorded in $CDCl_3$ unless otherwise specified.
Chemical shifts of ^{1}H and ^{13}C relative to TMS.
Chemical shift of ^{15}N relative to external $CH_3{}^{15}NO_2$.
$H_{d,e}$ ($C_{d,e}$) = Olefinic protons (carbons) of COD.
$^{*}H_o$ (H_i) = Methylenic protons of COD directed "outwards" ("inwards").

TABLE 4.13 ^{1}H and ^{13}C nmr data of [Rh(COD)(X)(pyO)] (X is Cl or Br).

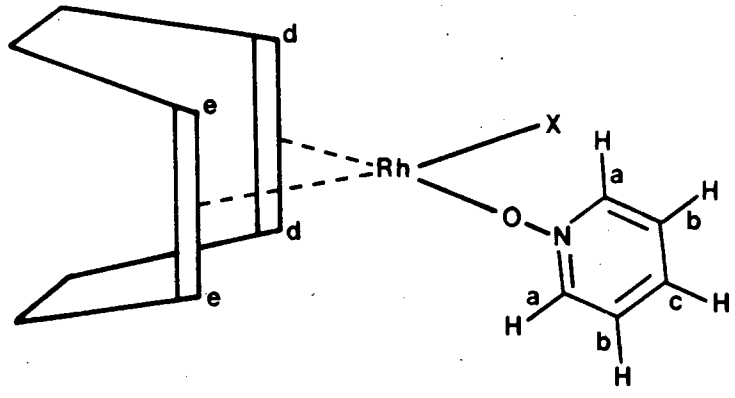

X	T (°C)	Chemical Shifts (ppm) pyridine *N*-oxide			COD		
^{1}H nmr		H_a	H_b	H_c	$H_{d,e}$	$^{*}H_o$	$^{*}H_i$
Cl	25	8.16	7.27	7.37	4.10	2.37	1.64
Br	25	8.26	7.25	7.37	4.41	2.45	1.74
^{13}C nmr		C_a	C_b	C_c	$C_{d,e}$	C	
Cl	−30	139.47	125.88	126.77	78.53	30.55	
					$^{1}J(^{103}Rh–C)$ = 13.96 Hz		
Br	−30	139.50	125.95	126.55	78.75	30.85	
					$^{1}J(^{103}Rh–C)$ = 13.56 Hz		

All spectra recorded in $CDCl_3$ unless otherwise specified.
Chemical shifts of ^{1}H and ^{13}C relative to TMS.
$H_{d,e}$ ($C_{d,e}$) = Olefinic protons (carbons) of COD.
$^{*}H_o$ (H_i) = Methylenic protons of COD directed "outwards" ("inwards").

TABLE 4.14 ^{1}H, ^{13}C and ^{15}N nmr data of [Rh(COD)(X)(an)] (X is Cl or Br).

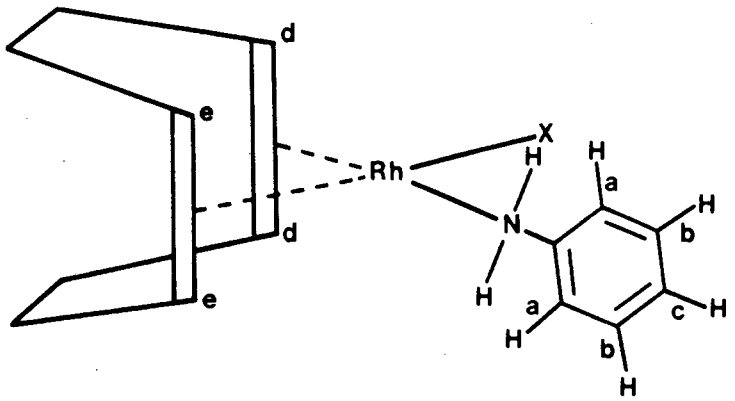

X	T (°C)	Chemical Shifts (ppm) aniline				COD			
^{1}H nmr		H_a	H_b	H_c	N-H	H_d	H_e	$^{*}H_o$	$^{*}H_i$
Cl	-30	----7.26 & 6.95----			3.80	4.43	3.98	2.48	1.68
Br	-30	----7.24 & 6.79----			3.91	4.36	4.12	2.37	1.66
^{13}C nmr		C_a	C_b	C_c	C	$C_{d,e}$		C	
Cl	25	116.20	129.31	119.98	145.15	78.83		30.81	
					$^{1}J(^{103}Rh–C)$ = 13.76 Hz				
Br	25	116.33	129.31	120.17	143.74	78.93		30.95	
					$^{1}J(^{103}Rh–C)$ = 13.53 Hz				
^{15}N nmr		N							
Cl	-60	-349.55							
Br	-65	-354.73							

All spectra recorded in $CDCl_3$ unless otherwise specified.
Chemical shifts of ^{1}H and ^{13}C relative to TMS.
Chemical shift of ^{15}N relative to external $CH_3{}^{15}NO_2$.
$H_{d,e}$ ($C_{d,e}$) = Olefinic protons (carbons) of COD.
$^{*}H_o$ (H_i) = Methylenic protons of COD directed "outwards" ("inwards").

TABLE 4.15 UV data for the complexes [Rh(COD)(X)(L)].

	X = Cl		X = Br	
L	λ_{max} (nm)	ε (m^2mole^{-1})	λ_{max} (nm)	ε (m^2mole^{-1})
ammonia	232	1170	----	----
	266	435	----	----
	356	170	----	----
imidazole	230	1225	233	2425
	266	580	268	780
	374	240	371	290
pyridine	234	1500	242	1760
	350	225	350	140
pyridine *N*-oxide	238	1520	246	1690
	274	1830	274	1845
	350	265	353	155
aniline	235	2300	242	2325
	282	460	285	640
	348	207	356	200

REFERENCES

1 J.CHATT AND L.M.VENANZI,
Nature, **177** (1956) 852

2 J.CHATT AND L.M.VENANZI,
J. Chem. Soc., (1957) 4735

3 J.A.IBERS AND R.G.SNYDER,
J. Am. Chem. Soc., **84** (1962) 495

4 J.A.IBERS AND R.G.SNYDER,
Acta Cryst., **15** (1962) 923

5 L.F.DAHL, C.MARTELL AND D.L.WAMPLER,
J. Am. Chem. Soc., **83** (1961) 1761

6 F.BONATI AND G.WILKINSON,
J. Chem. Soc., (1964) 3156

7 J.C.TREBELLAS, J.R.OLECHOWSKI, H.B.JONASSEN AND D.W.MOORE,
J. Organomet. Chem., **9** (1967) 153

8 L.M.HAINES,
Inorg. Chem., **9** (1970) 1517

9 M.J.DOYLE, M.F.LAPPERT, P.L.PYE AND P.TERREROS,
J. Chem. Soc.(Dalton Trans.), (1984) 2355

10 R.G.SALOMON AND N.E.SANADI,
J. Am. Chem. Soc., **97** (1975) 6214

11 R.H.CRABTREE, A.GAUTIER, G.GIORDANO AND T.KHAN,
J. Organomet. Chem., **141** (1977) 113

12 A.J.NAAKTGEBOREN, R.J.M.NOLTE AND W.DRENTH,
J. Am. Chem. Soc., **102** (1980) 3350

13 K.FELFÖLDI, I.KAPOCSI AND M.BARTÓK,
J. Organomet. Chem., **277** (1984) 439

14 M.IGLESIAS, C.DEL PINO, A.CORNA, S.GARCÍA-BLANCO AND S.MARTÍNEZ-CARRERA,
Inorg. Chim. Acta, **127** (1987) 215

15 G.WILKINSON, F.G.A.STONE AND E.W.ABEL (EDS.),
"Comprehensive Organometallic Chemistry", Pergamon Press, Oxford, **5** (1982) 277

16 H.A.TAYIM AND F.T.MAHMOUD,
J. Organomet. Chem., **92**, (1975) 107

17 B.DENISE AND G.PANNETIER,
J. Organomet. Chem., **148** (1978) 155

18 K.VRIEZE, H.C.VOLGER AND A.P.PRAAT,
J. Organomet. Chem., **14** (1968) 185, 429,
and **15** (1968) 195, 447 plus references therein.

19 L.CATTALINI, R.UGO AND A.ORIO,
J. Am. Chem. Soc., **90** (1968) 4800

20 H.C.VOLGER, M.M.P.GAASBEEK, H.HOGEVEEN AND K.VRIEZE,
Inorg. Chim. Acta, **3** (1969) 145

21 W.ROBB AND C.G.NICHOLSON,
Inorg. Chim. Acta, **7** (1973) 645

22 B.DENISE AND G.PANNETIER,
J. Organomet. Chem., **99** (1975) 455

23 M.P.LI AND R.S.DRAGO,
J. Am. Chem. Soc., **98** (1976) 5129

24 W.ROBB AND C.G.NICHOLSON,
S. Afr. J. Chem., **30** (1977) 213, 221

25 R.BONNAIRE, J.M.MANOLI, C.POTVIN, N.PLATZER,
N.GOASDOUE AND D.DAVOUST,
Inorg. Chem., **21** (1982) 2032

26 I.RENCKEN AND S.W.ORCHARD,
Inorg. Chem., **25** (1986) 1972

27 P.J.HENDRA AND D.B.POWELL,
Spectrochim. Acta, **17** (1961) 913

28 D.M.ADAMS AND P.J.CHANDLER,
J. Chem. Soc., **A** (1969) 588

29 D.B.POWELL AND T.J.LEEDHAM,
Spectrochim. Acta, **28A** (1972) 337

30 T.J.LEEDHAM, D.B.POWELL AND J.G.V.SCOTT,
Spectrochim. Acta, **29A** (1973) 559

31 G.G.BARNA AND I.S.BUTLER,
J. Raman Spect., **7** (1978) 168

32 D.W.WERTZ AND M.A.MOSELEY,
Inorg. Chem., **19** (1980) 705

33 A.L.ONDERDELINDEN AND A.VAN DER ENT,
Inorg.Chim. Acta, **6** (1972) 420

34 G.PANNETIER, R.BONNAIRE, P.FOUGEROUX AND P.ALÉPÉE, *J. Less-Common Metals*, **21** (1970) 103

35 M.J.DECKER, D.O.K.FJELDSTED, S.R.STOBART AND M.J.ZAWOROTKO, *J. Chem. Soc. (Chem. Commun.)*, (1983) 1525

36 D.BRODZKI AND G.PANNETIER, *J. Organomet. Chem.*, **63** (1973) 431

37 R.J.H.CLARK AND C.S.WILLIAMS, *Inorg. Chem.*, **4** (1965) 350

38 K.NAKAMOTO, *"Infrared and Raman Spectra of Inorganic and Coordination Compounds"*, 4th ed., Wiley-Interscience, New York (1986) p.329

39 J.A.POPLE, W.G.SCHNEIDER AND H.J.BERNSTEIN, *"High-resolution Nuclear Magnetic Resonance"*, McGraw-Hill, (1959), p.226

40 R.H.CRABTREE AND G.E.MORRIS, *J. Organomet. Chem.*, **135** (1977) 395

41 P.FOUGEROUX, B.BENISE, R.BONNAIRE AND G.PANNETIER, *J. Organomet. Chem.*, **60** (1973) 375

42 R.N.HASZELDINE, R.J.LUNT AND R.V.PARISH, *J. Chem. Soc.*, **A** (1971) 3711

43 H.BRUNNER, P.BEIER, G.RIEPL, I.BERNAL, G.M.REISNER, R.BENN AND A.RUFIŃSKA, *Organomet.*, **4** (1985) 1732

44 G.S.RODMAN AND K.R.MANN, *Inorg. Chem.*, **27** (1988) 3338

45 R.BONNAIRE AND N.PLATZER, *J. Organomet. Chem.*, **104** (1976) 107

46 R.J.COZENS, K.S.MURRAY AND B.O.WEST, *J. Organomet. Chem.*, **27** (1971) 399

47 L.A.ORO, M.ESTEBAN, R.M.CLARAMUNT, J.ELGUERO, C.FOCES-FOCES AND F.H.CANO, *J. Organomet. Chem.*, **276** (1984) 79

48 M.I.HEITNER AND S.J.LIPPARD, *J. Am. Chem. Soc.*, **92** (1970) 3486

49 M.I.HEITNER AND S.J.LIPPARD, *Inorg.Chem.*, 11 (1972) 1447

50 L.M.JACKMAN AND F.A.Cotton (ED.),
"Dynamic Nuclear Magnetic Resonance Spectroscopy",
Academic Press, New York, (1975)

51 T.G.APPELTON, J.R.HALL AND S.F.RALPH,
Inorg. Chem., **27** (1988) 4435

52 D.SUTTON,
"Electronic Spectra of Transition Metal Complexes",
McGraw-Hill, London, (1968)

53 R.A.EPSTEIN, G.L.GEOFFROY, M.E.KEENEY AND W.R.MASON
Inorg. Chem., **18** (1979) 478

54 H.ISCI AND W.R.MASON,
Inorg. Chem., **14** (1975) 905, 913

55 N.A.BAILEY, E.COATES, G.B.ROBERTON, F.BONATI AND R.UGO,
J. Chem. Soc. (Chem. Commun.), (1967) 1041

56 A.L.BALCH,
J. Am. Chem. Soc., **98** (1976) 8049

CHAPTER 5

INTRODUCTION

In continuation of our studies on square planar systems, we have now extended our work to cationic complexes of rhodium(I). In recent years numerous cationic complexes of rhodium(I) containing diolefin ligands have been described [1-6]. Several cationic complexes of the general formula $[Rh(diolefin)(L)_2]A$, where L is a neutral donor ligand, A an anion and the diolefin is a neutral bidentate ligand, are active catalysts [7-9]. In addition, some of the complexes are believed to have some biological importance [10]. Hence we have investigated the spectroscopic properties of rhodium(I) complexes of formula $[Rh(COD)(L)_2]A$ and $[Rh(CO)_2(L)_2]A$ where COD is the neutral bidentate ligand, 1,5-cyclooctadiene, A is an anion, and L represents various neutral monodentate ligands.

A relatively recent review [11] describes the various synthetic routes available for the preparation of the numerous cationic complexes of rhodium(I) known to date. The synthetic route for the preparation of our complexes involved the addition of $AgClO_4$ to an acetone solution of $[Rh(COD)Cl]_2$, which leads to the formation of non-isolable complexes [12] of general formula $[Rh(COD)(Me_2CO)_x]ClO_4$.

$$\tfrac{1}{2}[Rh(COD)Cl]_2 + x(Me_2CO) + AgClO_4 \longrightarrow [Rh(COD)(Me_2CO)_x]ClO_4 + AgCl$$

The acetone may be readily displaced by addition of the ligands (L), and the resulting complexes can be precipitated from the solution by the addition of ether.

$$[Rh(COD)(Me_2CO)_x]ClO_4 + 2L \longrightarrow [Rh(COD)(L)_2]ClO_4 + x(Me_2CO)$$

The cationic complexes may react further by the bubbling of carbon monoxide, at ordinary pressures and temperatures, through solutions or suspensions of the $[Rh(COD)(L)_2]ClO_4$ complexes. This leads to the displacement of the cyclooctadiene and to the formation of the corresponding *cis*-dicarbonyl derivative.

$$[Rh(COD)(L)_2]ClO_4 + 2CO \longrightarrow \textit{cis}\text{-}[Rh(CO)_2(L)_2]ClO_4 + COD$$

The cationic complexes, $[Rh(YY)(L)_2]A$ (YY is COD or $(CO)_2$), have a square planar structure similar to the rhodium(I) complexes previously studied (see Chapters 3 and 4). However, the cationic complexes have a higher symmetry, their point group being C_{2v}. Thus the infrared and Raman spectra have a slightly different pattern compared with the neutral complexes [Rh(COD)(X)(L)] or $[Rh(CO)_2(X)(L)]$ which have a symmetry point group of C_s.

In the complexes $[Rh(YY)(L)_2]A$, the ligands (L) have similar environments, and thus, in the nmr spectra, we expect to observe one set of resonances for both of the ligands (L). Similarly, the two carbonyl (or COD) moieties have identical environments and we expect to observe simplified nmr spectra in comparison with the [Rh(COD)(X)(L)] or $[Rh(CO)_2(X)(L)]$ complexes where the carbonyl (or COD) groups occur in non-equivalent environments.

For the infrared studies, the application of Group Theory (see Chapter 1) is required in order to predict the number of infrared (and Raman) active modes in the square planar (point group C_{2v}) complexes $[Rh(YY)(L)_2]A$ where (YY) is COD or $(CO)_2$. By regarding the ligands (L) and (YY) as point masses, one can obtain all the skeletal vibrations of the complex. Thus, all of the possible molecular motions (Γ_{total}) for $[Rh(YY)(L)_2]A$ are given by

$$\Gamma_{total} = 5A_1 + 2A_2 + 3B_1 + 5B_2$$

From Γ_{total}, one can obtain the number and types of stretches and bends.

$$\Gamma_{stretch} = 2A_1 + 2B_2$$

$$\Gamma_{bend} = 2A_1 + A_2 + B_1 + B_2$$

All the above modes are infrared and Raman active, excepting the A_2 mode which is only Raman active. Consequently, in the infrared spectra of the cationic complexes we expect to observe the following eight normal vibrational modes.

ν(Rh-L) symmetric and antisymmetric

ν(Rh-YY) symmetric and antisymmetric

δ(Rh-L) and δ(Rh-YY) in-plane

γ(Rh-L) and γ(Rh-YY) out-of-plane.

In addition to the above eight skeletal modes, there are, in the carbonyl complexes, normal modes principally associated with coordinated carbon monoxide. These are the symmetric and antisymmetric carbonyl stretch, ν(C≡O), and the in-plane and out-of-plane metal to carbonyl deformation, δ(Rh–CO) and γ(Rh–CO), respectively. Furthermore, the infrared spectra of the complexes should reveal bands due to the uncoordinated anion ClO_4^-, as well as the bands related to the internal vibrations of the various ligands (L) and the coordinated COD molecule.

We have synthesized a series of complexes $[Rh(COD)(L)_2]ClO_4$ and $[Rh(CO)_2(L)_2]ClO_4$ where L represents aniline, pyridine, pyridine *N*-oxide and imidazole and studied them by infrared, nmr and mass spectral techniques. In addition, we have isotopically enriched (^2H and ^{15}N) the ligands (L) in order to

verify our infrared assignments. The nmr studies (^{1}H, ^{13}C and ^{15}N) were performed at both ambient and low-temperatures. The complexes were characterized by mass spectrometry, microanalyses and melting points.

ASSIGNMENTS AND RESULTS

INFRARED SPECTRA

The infrared spectra of the complexes $[Rh(COD)(L)_2]ClO_4$ and $[Rh(CO)_2(L)_2]ClO_4$ where COD is 1,5-cyclooctadiene and L represents pyridine, pyridine *N*-oxide, aniline and imidazole, have been recorded over the range 4000–50 cm^{-1}. The assignments for the complexes $[Rh(COD)(L)_2]ClO_4$ and $[Rh(CO)_2(L)_2]ClO_4$ are presented in Tables 5.1–5.4 and Tables 5.5–5.8, respectively. Representative spectra are shown in Figures 5.1 and 5.2.

The assignments of the internal vibrations of the ligands (L) are based upon direct comparison with the free ligand or with related metal complexes. In addition, we have used isotopic labelling (^2H and ^{15}N) of L to support our assignments. The more specific assignments were made from the ν^D/ν^H ratios and the results are consistent with previous assignments made on other related complexes. (Chapters 1 and 3 provide a detailed explanation of the ligand assignments chosen).

All the cationic complexes show a broad, poorly resolved band at ~1100 cm^{-1}. This is characteristic of the uncoordinated anion ClO_4^- of symmetry T_d [13].

The assignments of the internal vibrations of COD are based upon comparison with the uncomplexed 1,5-cyclooctadiene or with other related metal complexes [14-20]. The cationic COD complexes do not show any strong bands between 1650 and 1675 cm^{-1} which would be characteristic of the ν(C=C) vibration of uncoordinated 1,5-cyclooctadiene [15-18]. This suggests that both double bonds of the diene (COD) are coordinated to the Rh(I) ion, and therefore the bands having ν(C=C) character

are shifted to lower frequency upon coordination. Further support for the assignment, is that these bands are not present in the analogous cationic carbonyl complexes. Similarly, the bands assigned to the other modes of COD, are not present in the analogous carbonyl complexes.

All the carbonyl complexes show two almost equally intense bands in their solution spectra in the 2200-1800 cm^{-1} region, whereas in the solid-state, (*i.e.* as Nujol mulls) the bands are substantially split, probably because of solid-state lattice interactions. The observation of two almost equally intense bands in the $\nu(C{\equiv}O)$ region of the infrared spectrum, confirms the *cis*- geometry in all cases. There was no indication of the presence of any bridging carbonyl groups in any of the carbonyl complexes, although it had previously been reported [19] that the complex $[Rh(CO)_2(py)_2]PF_6$ exhibited bands in the 1800 cm^{-1} region. This was attributed to the formation of dimeric cations of the type,

$$[(py)_2(CO)Rh\langle^{CO}_{CO}\rangle Rh(CO)(py)_2]^{2+}$$

It is of interest to compare the wavenumbers of the $\nu(C{\equiv}O)$ mode of the cationic $[Rh(CO)_2(L)_2]ClO_4$ complexes to those of the *cis*-$[Rh(CO)_2(X)(L)]$ complexes (see below).

		Wavenumbers (cm^{-1}) of the $\nu(C{\equiv}O)$ mode					
		$[Rh(CO)_2(L)_2]^+$		$[Rh(CO)_2(Cl)(L)]$		$[Rh(CO)_2(Br)(L)]$	
L =	pyridine	2103	2042	2089	2013	2086	2014
	pyridine *N*-oxide	2088	2017	2081	2006	2080	2007
	imidazole	2092	2028	2083	2009	2082	2009
	aniline	2099	2033	2088	2014	2087	2015

In all instances the $\nu(C\equiv O)$ occurs at a higher wavenumber in the cationic complexes relative to the neutral complexes. This is in agreement with the "synergic" bonding of metal carbonyl complexes (see Introduction to Chapter 3) since an increased positive charge on the metal centre results in a higher $\nu(C\equiv O)$ wavenumber.

^{1}H, ^{13}C and ^{15}N NMR

The ^{1}H, ^{13}C and ^{15}N nmr data for the complexes $[Rh(COD)(L)_2]ClO_4$ and $[Rh(CO)_2(L)_2]ClO_4$ (L represents aniline (an), pyridine (py), pyridine *N*-oxide (pyO) and imidazole (imid) and COD is 1,5-cyclooctadiene) are presented in Tables 5.9–5.12. Representative spectra are shown in Figures 5.3 and 5.4.

(1) ^{1}H nmr

The ^{1}H nmr spectra of the cationic carbonyl and cyclooctadiene complexes are relatively easy to interpret. Apart from the imidazole complex, $[Rh(CO)_2(imid)_2]ClO_4$, all the complexes show the expected spectral pattern, coupling and integration associated with the various coordinated ligands (L). Parallel to the behaviour of the *cis*-$[Rh(CO)_2(X)(imid)]$ (X is Cl or Br) complexes previously studied (see Chapter 3, ^{1}H nmr section), the $[Rh(CO)_2(imid)_2]ClO_4$ complex also reveals an exchange process involving the imidazole ligand. Once again, only upon cooling solutions of the above cationic complex does the single resonance of H_b and H_c split into two separate resonances showing the resonances consistent with the "instantaneous" structure (see Table 5.10).

The cationic cyclooctadiene complexes have additional resonances in their ^{1}H nmr spectra relative to their carbonyl counterparts, due to the twelve protons of the COD moiety. The assignments of the COD resonances are straightforwardly made in comparison with our previous studies (see Chapter 4) and ^{1}H nmr data on related complexes [19,21]. The peak occurring at ~4 ppm (integrating for four protons) is assigned to the four olefinic protons of COD, whilst the two multiplets occurring between 1.5 and 3.0 ppm are assigned to the "inwardly" and "outwardly" directed methylenic protons of COD (see Chapter 4, 1H nmr section, for the explanation of the "inwardly" and "outwardly" directed protons of COD).

(2) ^{13}C nmr

Like the ^{1}H nmr spectra, the ^{13}C resonances of the ligands (L) in the complexes reveal the usual spectral pattern associated with the coordinated ligands. All the complexes reveal $^{1}J(^{103}Rh–C)$ coupling. As can be expected, the lower percentage *s*-character in the Rh–COD bond compared with the Rh–CO bond results in the substantially lower $^{1}J(Rh–C_{COD})$ (~12 Hz) relative to $^{1}J(Rh–C_{CO})$ (~70 Hz).

(3) ^{15}N nmr

Only the cationic cyclooctadiene complex, $[Rh(COD)(imid)_2]^+$, was sufficiently soluble for recording an ^{15}N nmr spectrum. The cationic complex reveals $^{1}J(^{15}N–Rh)$ at room temperature, whereas, in its neutral "analogue" [Rh(COD)(X)(imid)], the $^{1}J(^{15}N–Rh)$ was only observed at low temperature (see Chapter 4). This indicates that the exchange process, if present, is slower in the cationic complexes compared with the neutral complex.

MASS SPECTRA

The mass spectra of the complexes are not very informative. Besides revealing peaks due to the ligand (L) associated with the respective complexes, numerous other peaks, some higher than the molecular ion peak were observed. The molecular ion peaks were not observed.

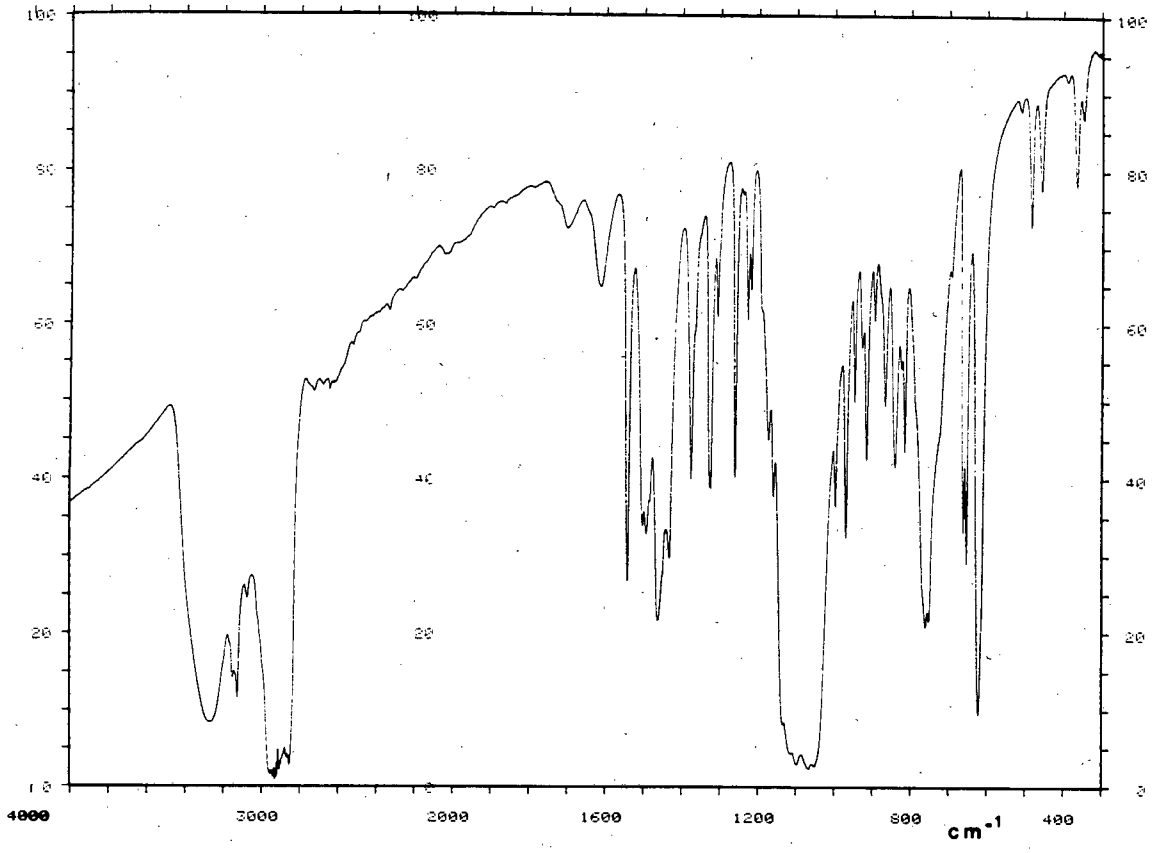

Figure 5.1 Infrared spectrum of $[Rh(COD)(imid)_2]ClO_4$ (Nujol mull).

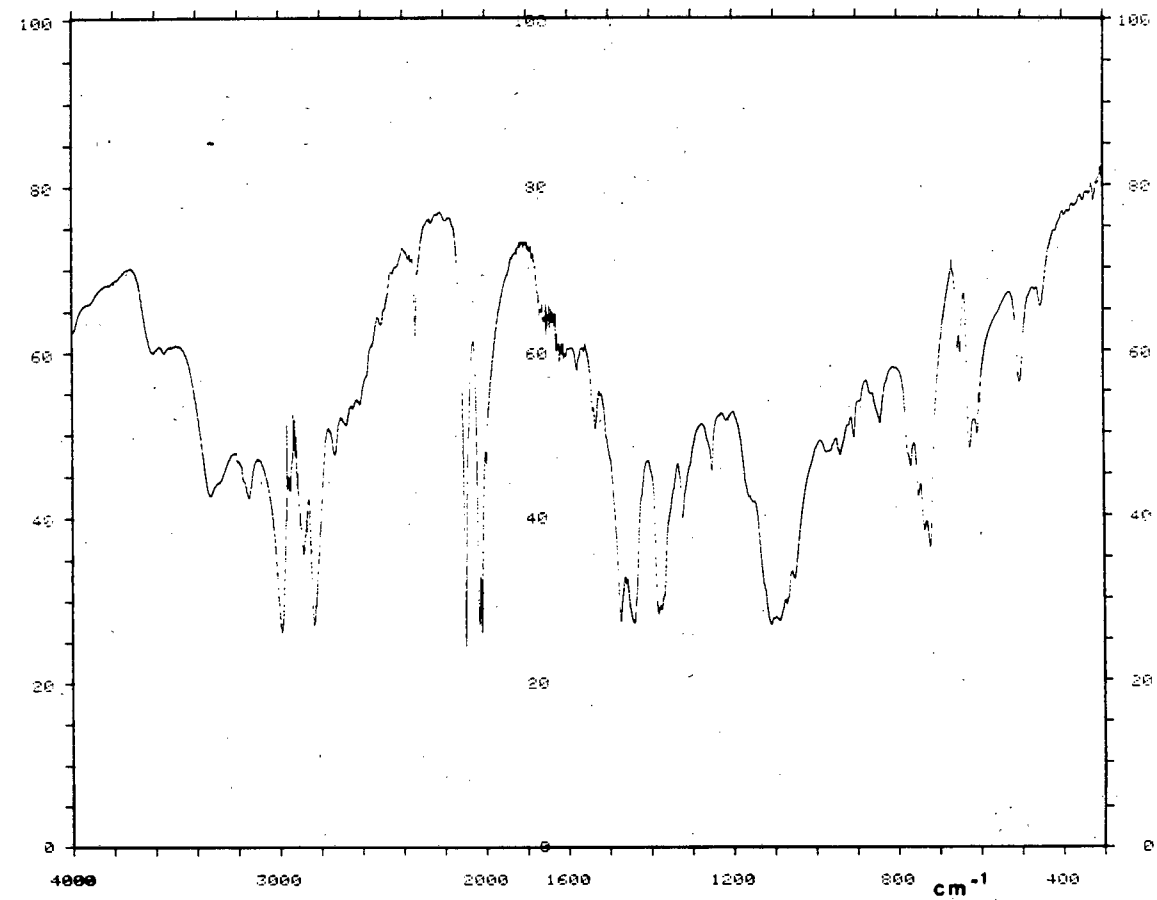

Figure 5.2 Infrared spectrum of $[Rh(CO)_2(imid)_2]ClO_4$ (Nujol mull).

TABLE 5.1 Infrared assignments of $[Rh(COD)(py)_2]ClO_4$ (cm^{-1}).

py	py-d_5	Assignment	*Wilson Band No.
3089	2296	ν(C-H)	20b/2
3038	2278		2/7a
3020	2260		20a/7b
3004	3004	ν(C-H) COD	
2977	2978		
2952	2956		
2928	2927		
2901	2903		
2887	2889		
2838	2838		
1651	1653	combination	1 + 6b/6a
1600	1558	ν(ring)	8a
1543	1531		8b
1482	1479	ν(C=C) COD	
	1334	ν(ring)	19a
1443	1447	ν(C=C) COD	
	1313	ν(ring)	19b
1428	1429	$\delta(CH_2)$ COD	
1359	1334	ν(ring)	14
1334		ρ_w(C-H) COD	
1305	1304	ρ_w(C-H) COD	
1234	974	δ(C-H)	3
1225	1225	ν(C=C) COD	
1214	1215	ν(C=C) COD	
	894	δ(C-H)	9a
1172	1172	ρ_w(C-H) COD	
	832	δ(C-H)	15
1086	1085	COD + ClO_4^-	
	823	δ(C-H) + ClO_4^-	18b
1042	1041	ν(ring)	12
1012	1011		1
995	995	COD	
988	810	γ(C-H)	17a
974	974	COD	
946	720	γ(C-H)	5
928	928	COD	
894	690	γ(C-H)	10a/10b

py	py-d_5	Assignment	*Wilson Band No.
869	868	ρ(C-C-C) COD	
815	815	COD	
788	787	ρ_r(C-H) COD	
766	622	γ(ring)	4
701	539	γ(C-H)	11
649	647	δ(ring)	6b
552	{562, 538}	ν(Rh-COD)	
478	477	ν(Rh-COD)	
459	452	γ(ring)	16b
440	{408, 403}	γ(ring)	16a
349	{352, 342}	δ(Rh-COD)	
298	297	δ(Rh-COD)	
262	258	ν(Rh-N)	
221	219	ν(Rh-N)	
173	168	δ(Rh-N)	

All bands below 150 cm^{-1} were very broad and unresolved.

* E.B.Wilson, *Phys. Rev.*, 45 (1934) 706

TABLE 5.2 Infrared assignments of $[Rh(COD)(imid)_2]ClO_4$ (cm^{-1}).

imid	imid-^{15}N	imid-d_4	Assignment
3277	3259	3284	ν(N-H)
3152	3141	-----	
3127	-----	2368	ν(C-H)
3075	-----	2338	
2997	-----	2998	ν(C-H) COD
2946	2940	2945	
2884	2880	2884	
2835	-----	2835	
1541	1532	1483	ν(ring)
1502	1493	1444	ν(ring)
1494			ν(C=C) COD
1431	1424	1432	$\delta(CH_2)$ COD
	1319		ν(ring)
1326	1326	1327	ν(ring) + COD
1307	1306	1307	ρ_w(C-H) COD
1260	1246	1269	ν(C=C) COD
		943	δ(C-H)
1219	1214	927	δ(N-H)
1172	-----	1170	ν(ring)
1158	-----	1158	COD + ClO_4^-
1098	-----	1099	
		886	δ(C-H) + ClO_4^-
1067	1066	866	δ(C-H) + ClO_4^-
996	994	996	COD
968	966	965	
	929	575	γ(N-H)
946	----	946	δ(ring)
	----	770	γ(C-H)
927	927	927	COD
913	903	721	δ(ring)
893		885	ρ(C-C-C) COD
866	866	866	ρ_w(C-H) COD
839	----	650	γ(C-H)
824	826	824	COD
814	----	815	

imid	imid-^{15}N	imid-d_4	Assignment
761 751	}750	527	} γ(C-H)
692	692	575	γ(ring)
661 653	}649	553	} γ(ring)
622	621	527	γ(ring)
511 485	509 483	---- 485	} ν(Rh-COD)
460	460	459	ν(Rh-COD)
391	389	390	δ(Rh-COD)
367 348	369 350	366 347	} δ(Rh-COD)
268	266	252	ν(Rh-N)
233	232	226	ν(Rh-N)
210	208	202	δ(Rh-N)
186 170	}173	}168	} δ(Rh-N)
159	158	----	δ(Rh-N-C)
138	138	136	
87	----	85	

Table 5.3 Infrared assignments of $[Rh(COD)(pyO)_2]ClO_4$ (cm^{-1}).

pyO	pyO-d_5	Assignment	*Band Number Wilson	Gambi & Ghersetti
3137	2310	ν(C-H)	20b/2	1/12
3078	2300		20a/7b/7a	2/13/3
3008	3000	ν(C-H) COD		
2985	2984			
2943	2943			
2917	2917			
2881	2881			
2836	2836			
1612	1569	ν(ring)	8a	4
1566	1536		8b	14
1476	1342		19a/19b	5/15
1462	1465	ν(C=C) COD		
1432	1432	$\delta(CH_2)$ COD		
1326	-----	ρ_w(C-H) COD		
1301	1301			
1198	1160	ν(ring)	3	17
1175		ν(N-O)	13	6
1156	854	δ(C-H)	9a	7
1150	836	δ(C-H)	15	18
1072	1076	COD		
	811	δ(C-H)	18b	19
1090	1090	COD + ClO_4^-		
1042	1041			
1021	980	ν(ring)	12	9
999	998	COD		
980	980			
961	963	COD		
	817	γ(C-H)	5	22
945	775		17a	25
883	883	ρ(C-C-C) COD		
868	870	ρ_w(C-H) COD		
830	836	COD		
822	761	ν(ring)	1	10
790	542	γ(C-H)	11	27
778	775	ρ_r(C-H) COD		

pyO	pyO-d_5	Assignment	*Band Number Wilson	Gambi & Ghersetti
720	721	COD		
683 676	}645	} γ(ring)	4	28
641	611	δ(ring)	6b	20
622	622	COD		
563	559	δ(ring)	6a	11
548	{513 542	γ(ring) COD	16b	29
485	490 }446	ν(Rh-COD) ν(Rh-pyO)		
456		β(N-O)	9b	21
393	{393 362	ν(Rh-COD) γ(ring)	16a	24
399	----	ν(Rh-COD)		
384	384	ν(Rh-COD) + γ(ring)	16a	24
354	357	ν(Rh-COD)		
332	328	ν(Rh-pyO)		
324	310	δ(Rh-pyO)		
261	261	COD		
217	206	δ(Rh-pyO)		
205	194	γ(N-O)	17b	30
112 90 68	110 88 70	} γ(Rh-COD) + γ(Rh-pyO)		

* E.B.Wilson, *Phys. Rev.*, **45** (1934) 706
A.Gambi & S.Ghersetti, *Spectrosc. Lett.*, **10** (1977) 627

Table 5.4 Infrared assignments of $[Rh(COD)(an)_2]ClO_4$ (cm^{-1}).

an	an-d_5	an-ND_2	an-d_7	an-$^{15}NH_2$	Assignment
3291	3291	2453	2454	3271	ν(N-H)
3250	3252	2357	2415	3243	
3146	3146	2320	2338	3140	ν(N-H).....Cl
3082	2290	3082	2327	3084	ν(C-H)
3047	2268	-----	2286	3046	
3010	3010	-----	3016	-----	ν(C-H) COD
2943	2944	2942	2942	2943	
2916	2916	2916	-----	-----	
2882	2882	-----	2879	2879	
2836	2836	2838	2832	2832	
1566	1534	1241(NHD)	1215(NHD)	1558	NH_2 scissor
		1081	1075		
1494	1496	1491	1486	1493	ν(C=C) COD
	1385		1383		ν(ring)
1474	1472	1457	1472	1473	ν(C=C) COD
1447	1447				COD
1429	1429	-----	1425	1430	COD
	1414				ν(ring)
1329	1328	1327	1327	1327	ν(ring)
1301	1301	1300	1301	1303	ρ_w(C-H) COD
1226	1226	1231	1215	1216	ν(C=C) COD
	1166	1216			ν(C-N)
1204	1204	-----	1207	1205	COD
1185	1172	1177	1176	1178	ρ_w(C-H) COD
1172					
1118	1119	-----	1118	-----	COD + ClO_4^-
1081	1079	1081	1075	1084	COD + ClO_4^-
	867				
1057	840	----	779	----	δ(C-H) + ClO_4^-
1027	760	----	750	----	
998	998	998	996	999	COD
	752		720		δ(C-H)
966	966	960	961	966	COD
930	930	928	928	929	
892	893	886	882	888	ρ(C-C-C) COD
867	867	861	866	----	
826	827	817	827	829	COD
	814		812		ν(ring)

an	an-d_5	an-ND_2	an-d_7	an-$^{15}NH_2$	Assignment
808	794	795	----	800	ρ_r(C-H) COD
777	777	----	780	778	
754	758	755	749	----	COD
	557	736	558		γ(C-H)
699	484	696	486	698	γ(C-H)
668	655	542	526	662	NH_2 wag
621	622	621	622	622	δ(ring)
606	588	518	457	----	NH_2 rock
578	575	----	572	579	δ(ring)
485	485	485	486	485	ν(Rh-COD)
471	465	467	457	465	ν(Rh-N)
382	378	370	368	370	ν(Rh-N)
367	355	330	325	357	δ(Rh-N)
331	329	309	301	328	
276	274	274	274	274	δ(Rh-COD)
247	246	252	252	254	δ(Rh-COD)
		237	206	244	δ(Rh-N)
206	195	206	194	206	γ(ring)
175	177	179	176	167	γ(Rh-N)
158	156	160	158		
138	136	133	120	134	γ(Rh-N)
81	80	84	73	83	γ(Rh-COD)
63	64	66		65	

TABLE 5.5 Infrared assignments of $[Rh(CO)_2(py)_2]ClO_4$ (cm^{-1}).

py	py-d_5	Assignment	*Wilson Band No.
3099	2469	ν(C-H)	20b/2
3074	2334		7a
3029	2292		20a/7b
(2103)	(2103)	ν(C≡O)	
(2042)	(2041)		
2100	2101		
2077	2076		
2031	2031		
2011	2011		
1994	1994		
1651	1653	combination	1+6b/6a
1605	1562	ν(ring)	8a
1485	1343		19a
1447	1319		19b
1355	1334		14
1240	976	δ(C-H) + ClO_4^-	3
1208	892		9a
1160	843		15
1089	}832		18b
1064			
1047	1042	ν(ring)	12
1015	1017		1
997	815	γ(C-H)	}17a
986	811		
961	}785		}5
954			
881	686		10a/10b
776	618	γ(ring)	}4
764	605		
706	546	γ(C-H)	}11
699	539		

py	py-d_5	Assignment	*Wilson Band No.
648	651 643	δ(ring)	6a/6b
623	623	δ(Rh-C≡O) in-plane	
607	605		
516	509	δ(Rh-C≡O) out-of-plane	
494	492	ν(Rh-C)	
475	----		
462	459		
445	444	ν(Rh-C)	
	408	γ(ring)	16b
414	384	γ(ring)	16a
400	348		
250	241	ν(Rh-N)	
206	195		
169	162	δ(Rh-N)	
144	138		
80	75	γ(Rh-N) + γ(Rh-C)	
70	67		

Values in parentheses are those recorded in CH_2Cl_2 solution.

* E.B.Wilson, *Phys. Rev.*, 45 (1934) 706

TABLE 5.6 Infrared assignments of $[Rh(CO)_2(imid)_2]ClO_4$ (cm^{-1}).

imid	imid-d_4	imid-^{15}N	Assignment
3360	2363	3333	ν(N-H)
3152		3143	ν(C-H)
2977	2335	2950	
(2092)	(2094)	(2094)	ν(C≡O)
(2028)	(2028)	(2028)	
2092	2093	2091	
2011	2015	2013	
-----	1992	1992	
1546	1487	1531	ν(ring)
1463	1451	1461	
1450		1451	
1435	1397	1428	
1331	1324	1330	
1262	945	-----	δ(C-H)
1244		1215	δ(N-H)
	1160	1160	ν(ring) + ClO_4^-
1097	889	1108	δ(C-H) + ClO_4^-
	874	1050	δ(C-H) + ClO_4^-
	562		γ(N-H)
956	982	937	δ(ring)
	971		
	773		γ(C-H)
915	822	903	δ(ring)
834	624	840	γ(C-H)
746	562	749	γ(C-H)
658		649	γ(ring)
622	624	621	δ(Rh-C≡O) in-plane
502	498	503	δ(Rh-C≡O) out-of plane
456	454	454	ν(Rh-C)
314	315	312	
278	264	276	ν(Rh-N)
----	242	248	

imid	imid-d_4	imid-^{15}N	Assignment
----	219	223	δ(Rh-N)
199	186	190	
160	164	166	γ(Rh-N) + γ(Rh-C)
	156	154	
102	104	104	
84	84	86	

Values in parentheses are those recorded in CH_2Cl_2 solution.

Table 5.7 Infrared assignments of $[Rh(CO)_2(pyO)_2]ClO_4$ (cm^{-1}).

pyO	pyO-d_5	Assignment	*Band Number Wilson	Gambi & Ghersetti
3113	2314	ν(C-H)	20b/2	1/12
3087	2302		20a	2
3060	2290		7b	13
3026	2268		7a	3
(2088)	(2089)	ν(C≡O)		
(2017)	(2016)			
2087	2084			
2009	2007			
1983	1983			
1607	1567	ν(ring)	8a	4
1570	1538		8b	14
1472	1348		19a/19b	5/15
1244	1236	ν(ring)	14	16
1207	-----		}3	17
1198	-----			
1178	1152	ν(N-O)	13	6
1155	858	δ(C-H) + ClO_4^-	9a	7
1086	841		15	18
1043	832		18b	19
1023	980	ν(ring)	12	9
990	821	γ(C-H)	5	22
940	}780		17a	25
930				
835	}769	ν(ring)	1	10
829				
783	562	γ(C-H)	}11	27
765	537			
671	}653	γ(ring)	4	28
623	}623	δ(Rh-C≡O) in-plane		
587	}562	δ(ring)	6a	11
570				

pyO	pyO-d_5	Assignment	*Band Number Wilson	Gambi & Ghersetti
549	537	γ(ring)	16b	29
492	489	δ(Rh-C≡O) / ν(Rh-C)		
	474	β(N-O) / ν(Rh-O)	9b	21
460	458	ν(Rh-C)		
387	369	γ(ring)	16a	24
420	----	ν(Rh-C)		
345	333	ν(Rh-O)		
313	312	δ(Rh-C)		
287	276	δ(Rh-O)		
236	226	δ(Rh-O)		
204	199	γ(N-O)	17b	30
161	158	γ(Rh-O) + γ(Rh-C)		
108	110			
88	82			
70				

Values in parentheses are those recorded in CH_2Cl_2 solution.

* E.B.Wilson, *Phys. Rev.*, **45** (1934) 706
A.Gambi & S.Ghersetti, *Spectrosc. Lett.*, **10** (1977) 627

Table 5.8 Infrared assignments of $[Rh(CO)_2(an)_2]ClO_4$ (cm^{-1}).

an	an-d_5	an-ND_2	an-d_7	an-$^{15}NH_2$	Assignment
3265	3245	2433	2433	3257	ν(N-H)
3230		2411	2411	3224	
3137	3137	2359	2349	3132	ν(N-H).....Cl
3048	2360	-----	2284	-----	ν(C-H)
3021	2273	3018		3019	
(2099)	(2098)	(2098)	(2099)	(2098)	ν(C≡O)
(2033)	(2033)	(2032)	(2033)	(2032)	
2101	2097	2097	2096	-----	
2080	2080	2081	-----	2080	
2062	-----	-----	2064	2063	
2028	2034	2034	2031	2034	
2000	2000	2001	-----	2000	
1600	1563	1598	1561	1598	ν(ring)
1517	1514	-----	-----	1510	NH_2 scissor
1494	1382	1493	1381	1492	ν(ring)
1473		1473	1339	1472	
1432	1421	1430	-----	1428	
1299	1299	1298	1290	1299	
1228	1150	1229	1150	1223	ν(C-N)
1216		1213		1213	
1185	872	1180	-----	1181	δ(C-H)
1140	1150	931(NHD)	912(NHD)	1132	NH_2 twist + ClO_4^-
	1130	886	842		
1073	842			1072	δ(C-H) + ClO_4^-
1026	752	1059	817	1026	
1001			756		
968	958	967	958	968	ν(ring)
931	932	931	931	931	
907	624	886	623	----	γ(C-H)
900					

an	an-d_5	an-ND_2	an-d_7	an-$^{15}NH_2$	Assignment
802	613	802	}533	799	γ(C-H)
758	}555	758	}552	757	
743		----		742	
690	508	689	496	689	
668	----	556	533	665	NH_2 wag
620	624	620	623	621	δ(Rh-C≡O) in-plane
570	}555	461	479	---	NH_2 rock
558				551	
539	----	524	447	533	
488	485	486	486	485	ν(Rh-C)
466	464	461	----	464	
433	402	366	328	426	ν(Rh-N)
356	345	328	294	355	
----	253	224	224	266	δ(Rh-N)
213	200	213	199	212	γ(ring)
134	134	136	{154	136	γ(Rh-N) + γ(Rh-C)
			128		
91	90	90	90	90	

Values in parentheses are those recorded in CH_2Cl_2 solution.

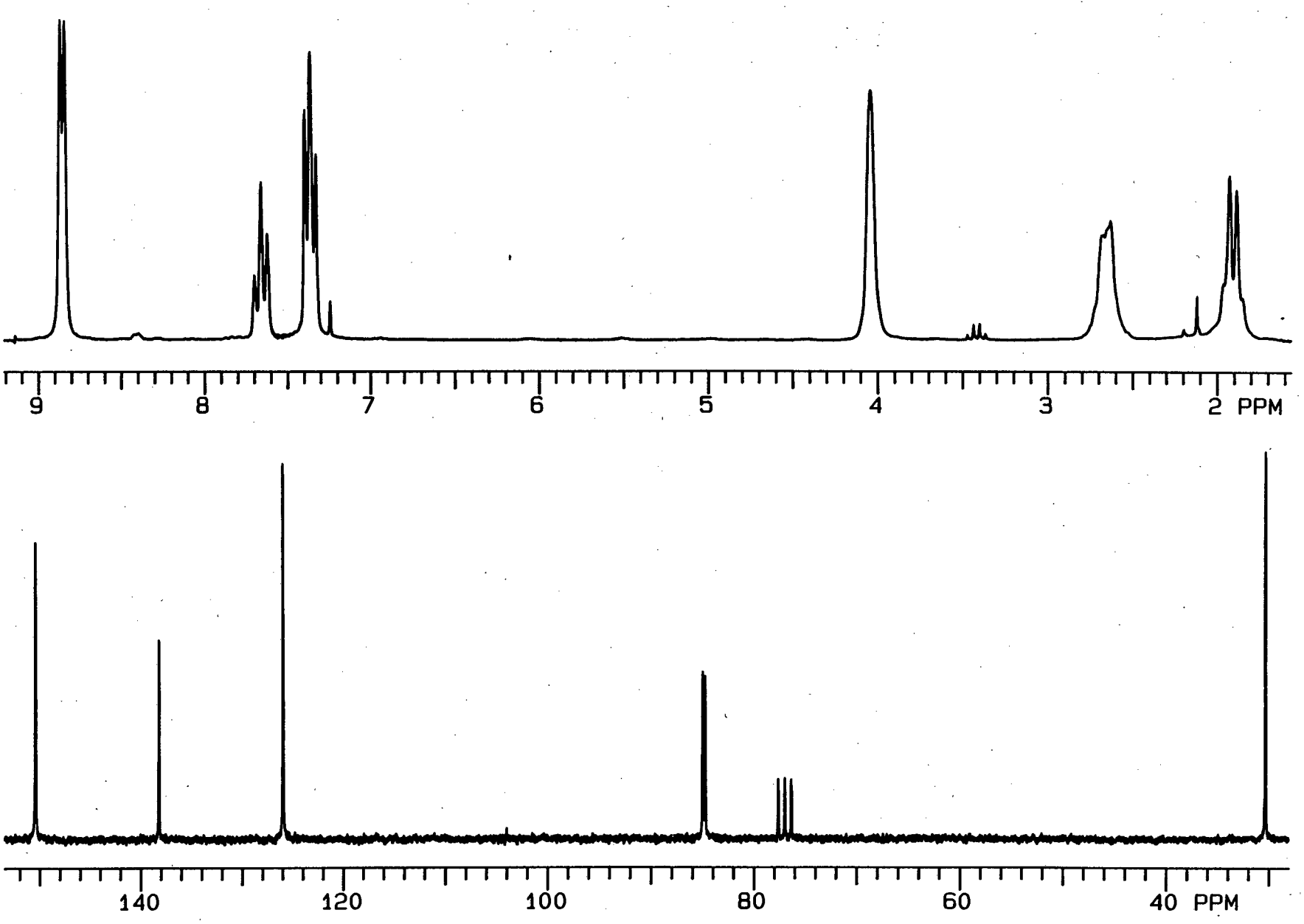

FIGURE 5.3 ^{1}H and ^{13}C nmr spectra of $[Rh(COD)(py)_2]ClO_4$ ($CDCl_3$, Temp. = 25°C).

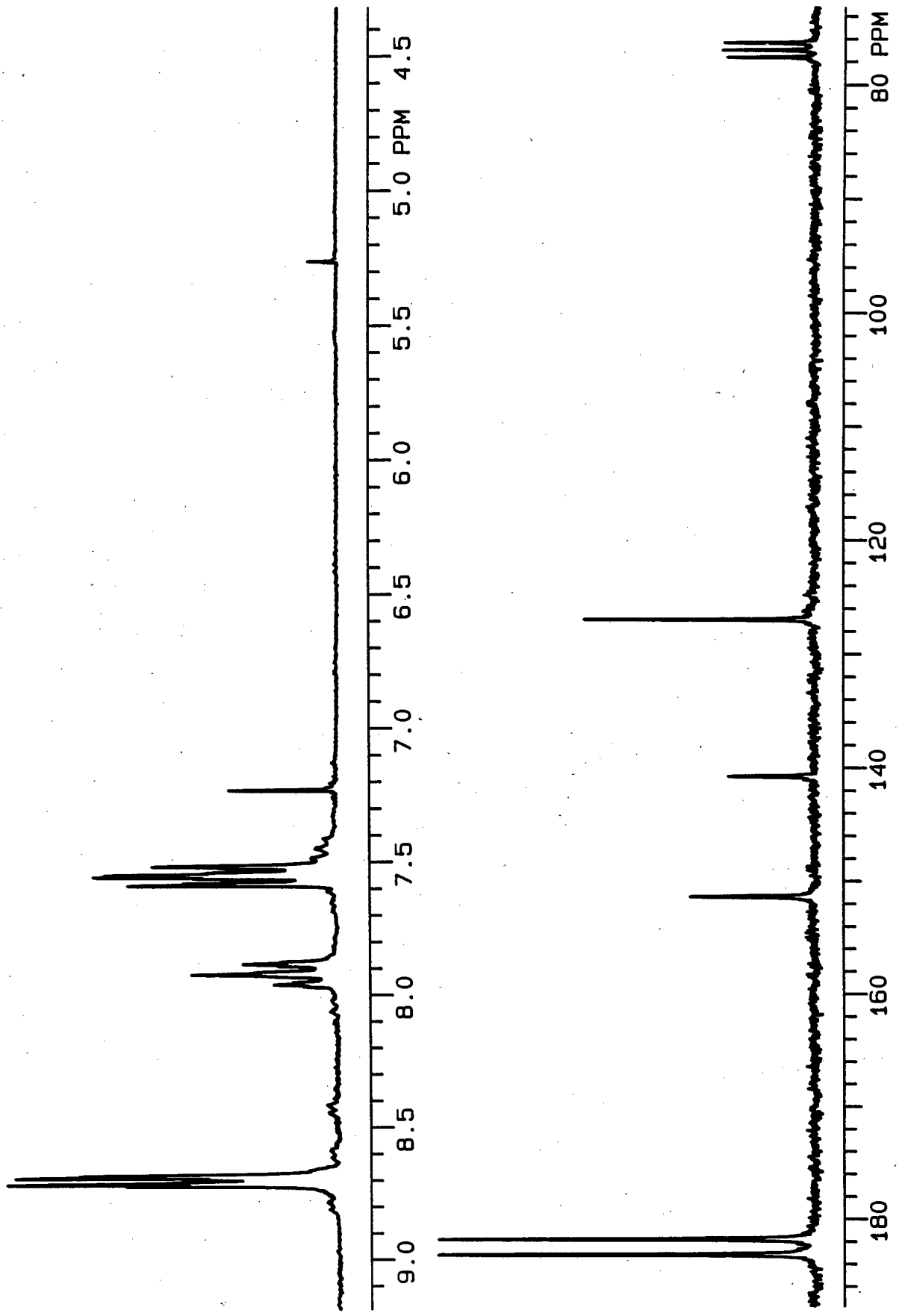

FIGURE 5.4 ^{1}H and ^{13}C nmr spectra of $[Rh(CO)_2(py)_2]ClO_4$ ($CDCl_3$, Temp.=25°C).

TABLE 5.9 ^{1}H and ^{13}C nmr data of $[Rh(YY)(py)_2]ClO_4$ (YY is COD or $(CO)_2$)

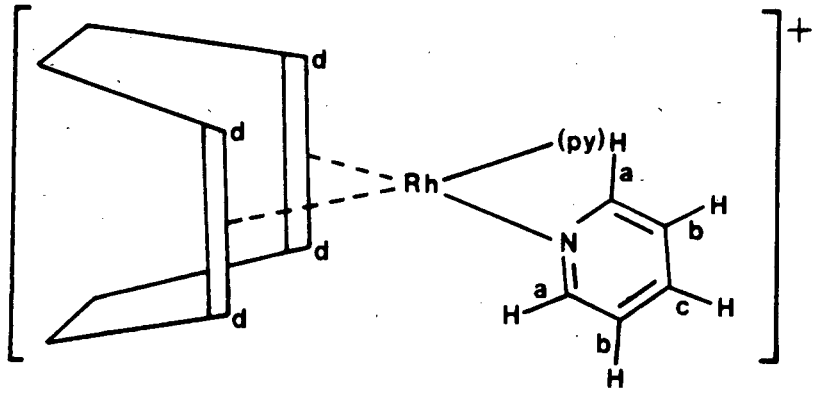

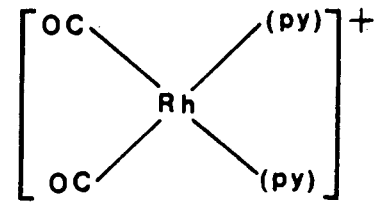

	T (°C)	Chemical Shifts (ppm) pyridine			COD		
$[Rh(COD)(py)_2]ClO_4$							
^{1}H nmr		H_a	H_b	H_c	H_d	$^{*}H_o$	$^{*}H_i$
	25	8.89	7.40	7.70	4.07	2.71	1.94
^{13}C nmr		C_a	C_b	C_c	C_d	C	
	25	150.43	125.91	138.21	84.86	30.38	
					$^{1}J(^{103}Rh–C_d)$ = 12.25 Hz		
$[Rh(CO)_2(py)_2]ClO_4$							
^{1}H nmr		H_a	H_b	H_c			
	25	8.75	7.62	7.99			
^{13}C nmr		C_a	C_b	C_c	CO		
	25	151.38	126.97	140.75	182.47		
					$^{1}J(^{103}Rh–C)$ = 69.20 Hz		

All spectra recorded in $CDCl_3$ unless otherwise specified.
Chemical shifts of ^{1}H and ^{13}C relative to TMS.
H_d (C_d) = Olefinic protons (carbons) of COD.
$^{*}H_o$ (H_i) = Methylenic protons of COD directed "outwards" ("inwards").

TABLE 5.10 ^{1}H, ^{13}C and ^{15}N nmr data of $[Rh(YY)(imid)_2]ClO_4$ (YY is COD or $(CO)_2$).

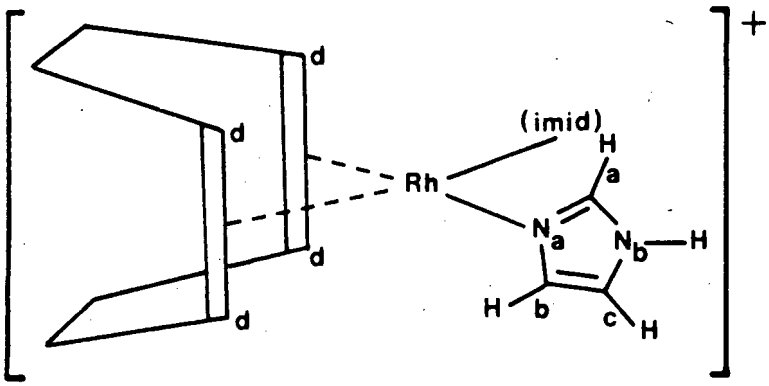

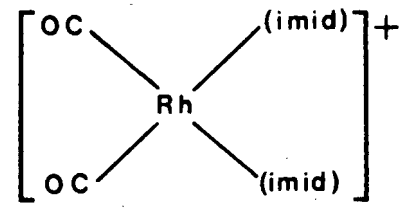

	T (°C)	Chemical Shifts (ppm)						
		imidazole				COD		
[Rh(COD)(imid)$_2$]ClO$_4$								
^{1}H nmr		H_a	H_b	H_c	N-H	H_d	$^{*}H_o$	$^{*}H_i$
	25	7.45	7.06	6.72	11.00	4.10	2.51	1.93
^{13}C nmr		C_a	C_b	C_c		C_d	C	
	25	136.53	126.40	117.95		82.16	30.63	
						$^{1}J(^{103}Rh–C_d)$ = 12.31 Hz		
^{15}N nmr		N_a		N_b		$^{1}J(^{15}N_a$-Rh)	$^{1}J(^{15}N_b$-H)	
	25	-184.60		-220.59		17.75	100.30	
[Rh(CO)$_2$(imid)$_2$]ClO$_4$								
^{1}H nmr		H_a	H_b	H_c	N-H			
	-10	8.39	8.08	7.90	11.34	$^{1}J(^{15}N$-H) = 100.55 Hz		
^{13}C nmr		C_a	C_b	C_c		CO		
	-10	136.97	128.56	118.40		184.02		
						$^{1}J(^{103}Rh–C)$ = 67.33 Hz		

All spectra recorded in $CDCl_3$ unless otherwise specified.
Chemical shifts of ^{1}H and ^{13}C relative to TMS.
Chemical shift of ^{15}N relative to external $CH_3{}^{15}NO_2$.
H_d (C_d) = Olefinic protons (carbons) of COD.
$^{*}H_o$ (H_i) = Methylenic protons of COD directed "outwards" ("inwards").

TABLE 5.11 ^{1}H and ^{13}C nmr data of $[Rh(YY)(pyO)_2]ClO_4$ (YY is COD or $(CO)_2$).

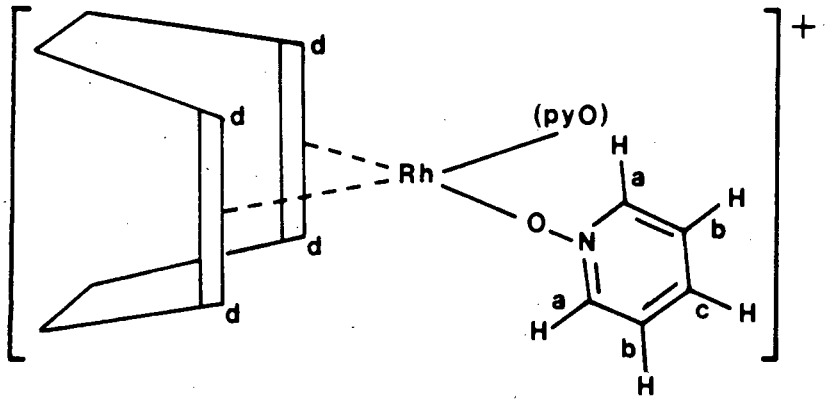

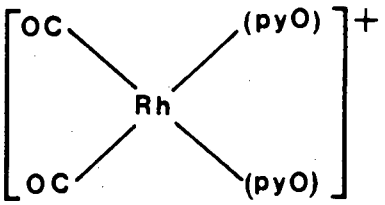

	T (°C)	Chemical Shifts (ppm) pyridine *N*-oxide			COD		
[Rh(COD)(pyO)$_2$]ClO$_4$							
^{1}H nmr		H_a	H_b	H_c	H_d	$^{*}H_o$	$^{*}H_i$
	25	8.56	7.61	7.71	3.68	2.51	1.62
^{13}C nmr		C_a	C_b	C_c	C_d	C	
	25	140.69	127.03	134.04	77.24	30.11	
					$^{1}J(^{103}Rh–C_d)$ = 14.74 Hz		
[Rh(CO)$_2$(pyO)$_2$]ClO$_4$							
^{1}H nmr		H_a	H_b	H_c			
	25	8.77	7.75	7.87			
^{13}C nmr		C_a	C_b	C_c	CO		
	25	140.96	127.62	135.72	181.48		
					$^{1}J(^{103}Rh–C)$ = 75.35 Hz		

All spectra recorded in $CDCl_3$ unless otherwise specified.
Chemical shifts of ^{1}H and ^{13}C relative to TMS.
H_d (C_d) = Olefinic protons (carbons) of COD.
$^{*}H_o$ (H_i) = Methylenic protons of COD directed "outwards" ("inwards").

TABLE 5.12 ^{1}H and ^{13}C nmr data of $[Rh(YY)(an)_2]ClO_4$ (YY is COD or $(CO)_2$).

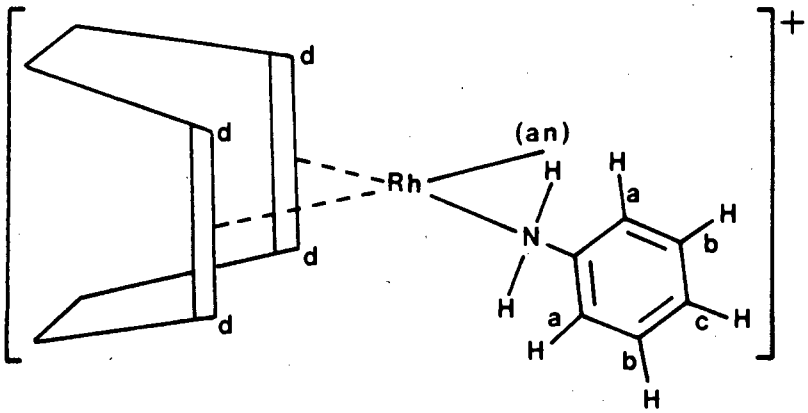

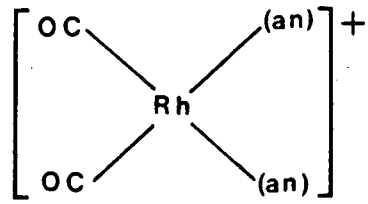

	T (°C)	Chemical Shifts (ppm) aniline				COD		
[Rh(COD)(an)$_2$]ClO$_4$								
^{1}H nmr		H_a	H_b	H_c	N-H	H_d	$^{*}H_o$	$^{*}H_i$
	25	---7.13 & 6.97---			----	3.51	2.25	1.56
^{13}C nmr		C_a	C_b	C_c	C	C_d	C	
	25	120.54	129.19	124.52	140.06	81.60	29.96	
						$^{1}J(^{103}Rh–C_d)$ = 11.99 Hz		
[Rh(CO)$_2$(an)$_2$]ClO$_4$								
^{1}H nmr		H_a	H_b	H_c	N-H			
	25	-----7.20-----			----			
^{13}C nmr		C_a	C_b	C_c	C	CO		
	25	120.13	129.77	125.75	142.83	179.91		
						$^{1}J(^{103}Rh–C)$ = 71.18 Hz		

All spectra recorded in $CDCl_3$ unless otherwise specified.
Chemical shifts of ^{1}H and ^{13}C relative to TMS.
H_d (C_d) = Olefinic protons (carbons) of COD.
$^{*}H_o$ (H_i) = Methylenic protons of COD directed "outwards" ("inwards").

REFERENCES

1 A.CHRISTOFIDES AND A.SYGOLLITOU-KOURAKOU, *Inorg. Chim. Acta*, **141** (1988) 161

2 A.CHRISTOFIDES, *Inorg. Chim. Acta*, **133** (1987) 29

3 A.CHRISTOFIDES, D.DRIGAS AND E.TOURKA, *Inorg. Chim. Acta*, **126** (1987) 95

4 M.IGLESIAS, C.D.PINO, A.CORMA, S.GARCÍA-BLANCO AND S. M.CARREA, *Inorg. Chim. Acta*, **127** (1987) 215

5 G.CLAUTI, G.ZASSINOVICH AND G.MESTRONI, *Inorg. Chim. Acta*, **112** (1986) 103

6 M.A.GARRALDA AND L.IBARLUCEA, *J. Organomet. Chem.*, **311** (1986) 225

7 R.USON, L.A.ORO, M.A.CIRIANO AND F.J.LAHOZ, *J. Organomet. Chem.*, **240** (1982) 429

8 R.USON, L.A.ORO, M.A.GARRALDA, M.C.CLAVER AND P.LAHUERTA, *Transition Met. Chem.*, **4** (1979) 55

9 R.R.SCHROCK AND J.A.OSBORN, *J. Amer. Chem. Soc.*, **98** (1976) 2134, 2143, 4450

10 G.ZASSINOVICH, G.MESTRONI AND A.CAMUS, *J. Organomet. Chem.*, **91** (1975) 379

11 M.A.GARRALDA AND L.A.ORO, *Transition Met. Chem.*, **5** (1980) 65

12 R.R.SCHROCK AND J.A.OSBORN, *J. Amer. Chem. Soc.*, **93** (1971) 3089

13 B.J.HATHAWAY AND A.E.UNDERHILL, *J. Chem. Soc.*, (1961) 3091

14 P.J.HENDRA AND D.B.POWELL, *Spectrochim. Acta*, **17** (1961) 913

15 D.B.POWELL AND T.J.LEEDHAM, *Spectrochim. Acta*, **28A** (1972) 337

16 T.J.LEEDHAM, D.B.POWELL AND J.G.V.SCOTT, *Spectrochim. Acta*, **29A** (1973) 559

17 G.G.BARNA AND I.S.BUTLER,
J. Raman Spect., **7** (1978) 168

18 D.W.WERTZ AND M.A. MOSELEY,
Inorg. Chem., **19** (1980) 705

19 B.DENISE and G.PANNETIER,
J. Organomet. Chem., **63** (1973) 423

20 D.BRODZKI AND G.PANNETIER,
J. Organomet. Chem., **63** (1973) 431

21 R.H.CRABTREE AND G.E.MORRIS,
J. Organomet. Chem., **135** (1977) 395

CHAPTER 6

(1) NORMAL COORDINATE ANALYSIS

INTRODUCTION

The calculation of normal vibrations has two aspects. Firstly, to obtain accurate force constants, and secondly, to justify the assignments of the observed vibrational bands using calculated frequencies.

In diatomic molecules, the vibration of the nuclei occurs along the molecular axis. Through quantum mechanical considerations [1,2] these vibrations can be reduced to the motion of a single particle by introducing a "mass-weighting" factor, μ, the reduced mass. In polyatomic molecules, however, the situation is much more complicated because all the nuclei perform their own harmonic oscillations. Nevertheless, it can be shown that one can still reduce the problem of a multi-body case to a single-body problem by introducing a "geometry-mass-weighting" factor.

The interatomic forces within a molecule are determined by the existing electronic configuration. Such forces are manifested by the vibrational frequencies of the molecule. By means of infrared absorption spectra and Raman spectra one can observe most, if not all, of the fundamental frequencies of the molecule of interest. In order to derive relations between these frequencies and the interatomic forces it is necessary to assume some general potential function. The calculation of normal frequencies and force constants by the least squares method seems to be fairly well established [3,4,5]. However, this method does not always lead to satisfactory results, some of the difficulties encountered are summarized by Aldous and Mills [6]. Therefore, several approximation methods and/or simplified models have been developed which allow the calculation of a complete generalized valence force field

from the vibrational frequencies only [7-12]. The theory which relates the force field of a molecule to its normal vibrations is now well understood [13].

In the Wilson GF matrix method [14,15] for the analysis of polyatomic molecules, the G matrix is the factor which does not only contain information about the constituent atomic masses but must necessarily also hold structural information, that is, bond lengths and bond angles. The Wilson method uses as the basic vectors five internal coordinates, namely: (1) bond stretch, (2) valence angle bend, (3) out-of-plane wag, (4) torsion, and (5) linear bend. Decius [16] has proved that this set of basic vectors is sufficient to completely describe the normal vibrations.

The vibrational eigenvalue problem (or secular equation) in the Wilson GF matrix notation [15] can be stated as:

$$\mathbf{GFL} = \mathbf{L}\Lambda$$

where G is the matrix containing the coefficients of the kinetic energy in terms of the symmetry coordinates, F is the matrix of unknown symmetry force constants, L contains the eigenvectors columnwise, and Λ is a diagonal matrix containing the vibrational eigenvalues. The advantage of the Wilson GF matrix method and hence its popularity lies in the ease of the interpretation of the elements of the F matrix, that is, the force constants in terms of familiar stretches and bends. On the other hand the mathematics involved in the construction of the kinetic energy motions is a far more difficult task than in other methods [5,17].

The theory regarding vibrational analysis will not be discussed here since it can be found in many fine references [15,18-21], and McIntosch and Michallian [17] have published an excellent three-part series of papers "designed to give the beginning

vibrational spectroscopist a more complete introduction to the use of the Wilson GF matrix method in the analysis of the vibrational spectra of polyatomic molecules".

For large molecules it becomes necessary to solve the vibrational eigenvalue problem by means of a high speed computer. A listing of the main body of each programme used in this work is presented in Appendix 1, and a flowchart of the programme BECMAT, which calculates the general valence force field constants, is shown in Figure 6.1. The programme is based on the iterative eigenvector method (EVM) suggested by Becher and Mattes [7,22].

Although Averbukh *et al.* [23] have strongly criticized the method of Becher and Mattes, Alix *et al.* [24,25] have refuted the formers' criticisms. In addition, the correlation between the calculated force constants and the physically true solution, hence its reliability, has been previously demonstrated [26,27]. Furthermore, by considering extensive experimental frequencies of various isotopic species, it has been shown [28,29] that the Becher and Mattes procedure yields a valence force field fulfilling the requirements stated by Averbukh *et al.* [23].

The Becher and Mattes method is very sensitive to the choice of symmetry coordinates and to the assignment of the experimental frequencies. Whenever one of them is incorrect, the method fails, and non-convergent values for the force constants and an illogical potential energy distribution (PED) is obtained. The PED lets us know what percentage each internal coordinate contributes to the total potential energy of a given normal coordinate. That is, the degree of coupling can be determined between each normal coordinate, and thus band assignments are made possible if the appropriate internal coordinate of the PED makes up most of the potential energy of the normal mode in question [17].

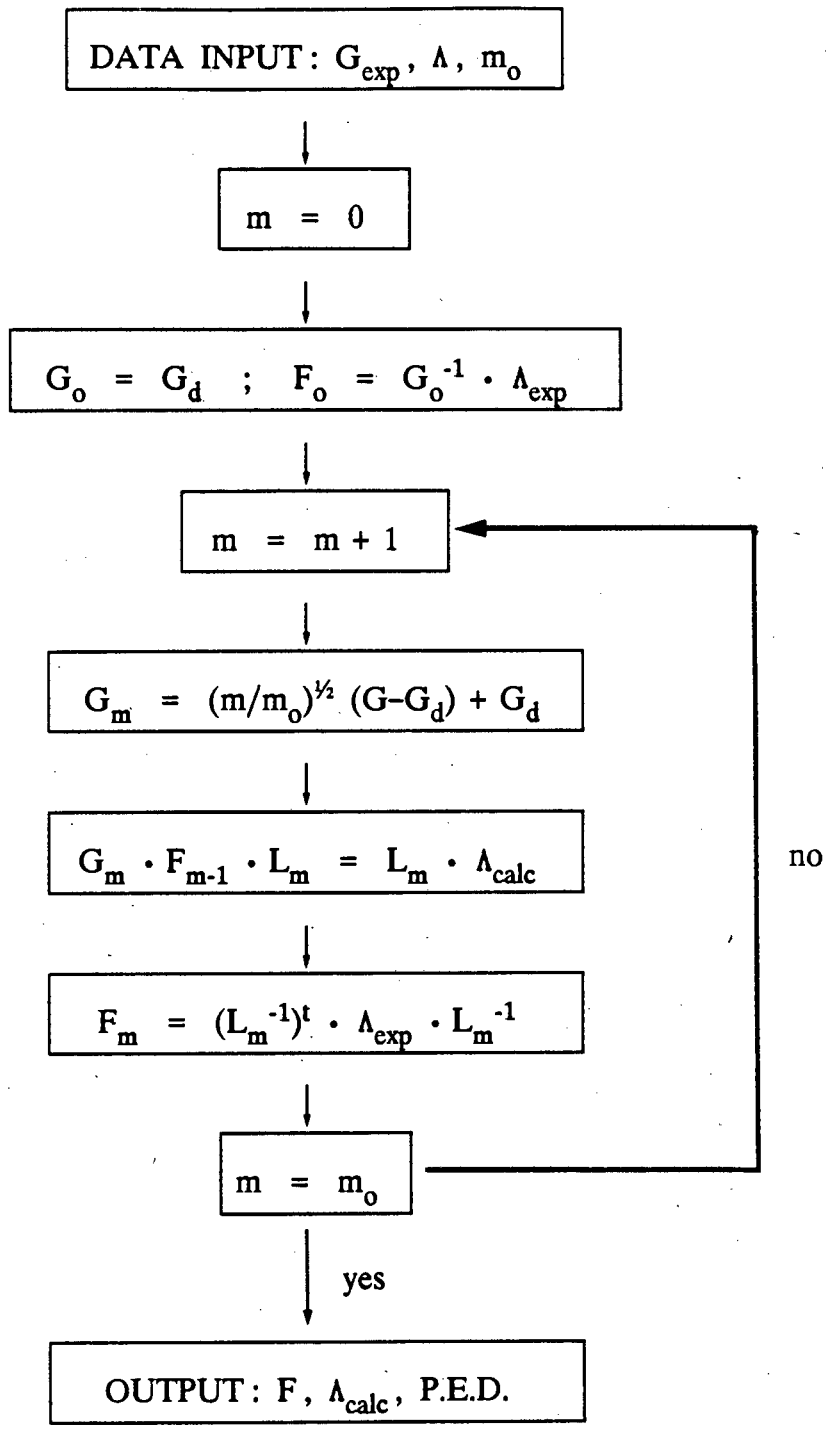

FIGURE 6.1 The eigenvector method flowchart (from ref. 29).

PROCEDURE AND GENERAL REMARKS

The method of calculating the PED within the normal modes, the force constants, and the isotopic frequency shifts using computer programmes [Appendix 1, 7,22], may be summarized as follows:

(a) calculation of atomic coordinates from internal coordinates,

(b) using the geometrical parameters together with coded instructions defining the internal coordinates and symmetry coordinates, to calculate the kinetic energy matrix (the **G** matrix),

(c) using the **G** matrix together with the experimental frequencies, all assigned to their corresponding diagonal **G** matrix, to calculate the symmetric force constants (the **F** matrix) and their associated PED,

(d) refinement of the force constants until the values converge. If non-convergent results occur, then the assignments in steps (b) and (c) need to be altered,

(e) steps (b)–(d) are repeated on each isotopic species of a complex, and an average refined force constant value is obtained,

(f) using the average refined force constant values (**F** matrix) and the kinetic energy matrix (**G** matrix) of an isotopic species to calculate the frequencies of the isotopic species in question,

(g) step (f) is repeated after reducing the average refined force constants values to a simplified form.

In the following sections we have calculated general valence force field by applying the EVM of Becher and Mattes to the complexes *cis*-[$Rh(CO)_2(X)(L)$] where X is Cl or Br and L is ammonia, pyridine, or imidazole.

By considering the ligand (L), to behave as a dynamic unit, one can treat the skeletal vibrations of the complex as those of a seven-body model (see Figure 6.2).

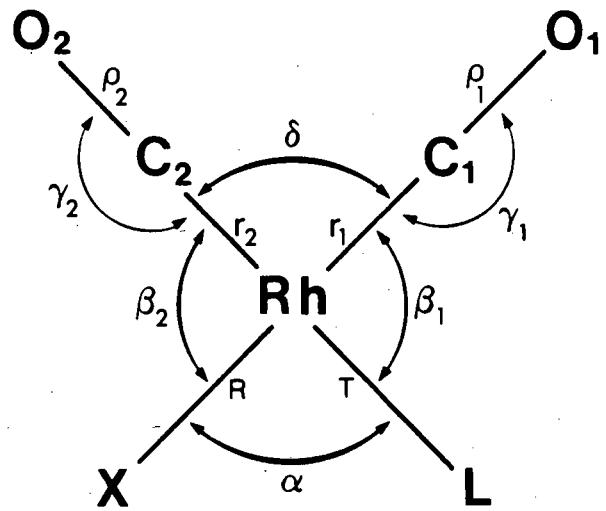

FIGURE 6.2 **The model and internal coordinates of *cis*-[Rh(CO)$_2$(X)(L)], symmetry C_s.**

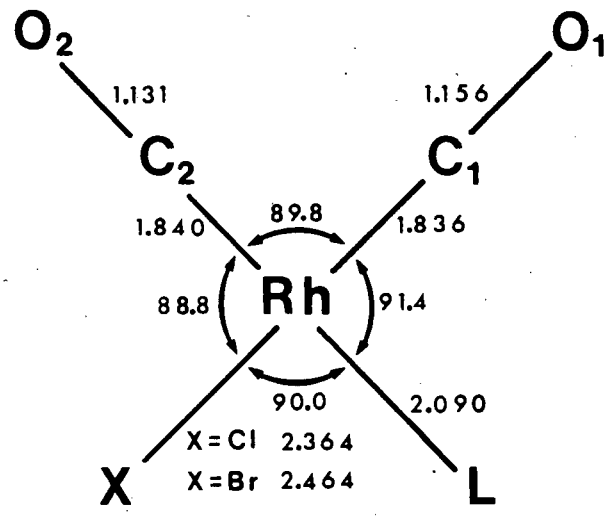

FIGURE 6.3 **The selected bond lengths (Å) and angles (°) of *cis*-[Rh(CO)$_2$(X)(L)].**

The validity of considering the ligand as a point mass has been studied by numerous authors [29-35], and found to be applicable to metal complexes, especially when the skeletal vibrations are only slightly coupled to the ligand vibrations. Some of the authors have demonstrated the usefulness of transferring the force constants from the point-mass-model (PMM) to the whole complex, and the results reveal the reliability and applicability of the PMM.

In our complexes, apart from minor shifts and splittings, each ligand band of the free ligand is faithfully reproduced in the infrared spectrum of the complex. In addition, nearly all the ligand bands appear above 500 cm^{-1}, except one imidazole band at approximately 174 cm^{-1}, and the two γ(ring) bands of pyridine (16b and 16a) at approximately 422 and 395 cm^{-1}, and are therefore well separated from the skeletal vibrations occurring in the region 500-100 cm^{-1}. Further, the ligands do not have bands appearing in the region 2200-1800 cm^{-1}, and thus the ν(CO) bands which occur in this region will not be expected to couple to any of the ligand vibrations.

The *cis*- complexes have a square planar structure of point group C_s. The adopted model, the in-plane internal coordinates, and the numbering of the atoms used are shown in Figure 6.2. Bond lengths and angles were selected from the iso-structurally related complex *cis*-[$Rh(CO)_2(Cl)(L)$] where L is pyrazole [36], and are shown in Figure 6.3. A bond distance lengthening of 0.1Å is allowed for the metal-halogen bond in the bromo-complexes. For the sake of convenience we have adopted identical structural parameters for all our complexes (L is ammonia, pyridine, or imidazole) since this is accounted for by the indifference of the stretching force constants on the bond length values [29].

The normal coordinate analysis is applied to the 11 infrared active *in-plane* vibrations only (see Chapter 1 for all the vibrations). An appropriate set of symmetry coordinates together with the symbols referring to the normalized vibrations which they describe, are given in Table 6.1 . The relationship between the force constants in symmetry coordinate representation and those in internal coordinate terms is shown in Table 6.2.

With regard to the contribution of the symmetry coordinate, only average values greater than 10% (rounded to the nearest 1%) are reported. The symmetry force constants have been calculated using the **F** matrix values obtained from a ninety nine-step calculation. The reported symmetry force fields, which satisfactorily predict the isotopic shifts, were set up from the simplified force field which in turn was obtained from an average force field of all the isotopic derivatives of each complex. The elements in the **F** matrix are rounded off to the nearest 10^{-3} in accordance with their associated uncertainties in the experimental frequencies, taken to be 2 cm^{-1}. The uncertainties in the experimental frequencies are affected by the profile of the corresponding band and the accuracy of the instrument.

The internal force constants were calculated from the symmetry force constants by means of the equation:

$$F^{int} = U^{t} \cdot F^{sym} \cdot U$$

where F^{int} and F^{sym} are the internal and symmetric force constants respectively, and U and U^{t} are the inverse and inverse transpose matrix respectively. The associated uncertainties of the internal force constants were calculated by applying the harmonic oscillator formula, assuming an uncertainty of 2 cm^{-1} on the experimental frequencies. In this approach each normal coordinate is determined by one

frequency. Therefore, that frequency can be correlated to one diagonal force constant, leading to the relation:

$$\Delta F_{ii} = 2F_{ii}(\Delta\nu_i/\Delta\nu)$$

With regard to the comparison of the calculated and observed frequency values the percentage deviation quoted is derived from an average of the individual absolute deviations, calculated as follows:

$$\text{individual deviation (\%)} = \frac{|\nu_{calc} - \nu_{obs}| \times 100}{\nu_{obs}}$$

In the calculation of the **F** matrix we have expressed masses in atomic mass units and bond lengths in Ångström. The resulting force constants will have units of:

mdyne/Å	for the stretching elements
mdyne rad^{-1}	for the stretch-bend interaction elements
mdyne Å rad^{-2}	for the bending elements

The use of non-standardized units for force constants is still common practice in the literature, however, conversion to SI units can simply be performed by:

$$\text{Å} = 100 \text{ pm} \quad \text{and} \quad \text{mdyne} = 10^{-8} \text{ N}.$$

RESULTS AND DISCUSSION

In the following section we report the results of the normal coordinate analysis on the complexes *cis*-$[Rh(CO)_2(X)(L)]$ where X is Cl or Br and L is ammonia, pyridine, or imidazole.

The results which include; (1) the distribution of the potential energy within the normal modes, (2) the calculated frequencies of the parent compound and its

isotopic analogues, (3) the force constants in symmetry coordinates, (4) the force constants in internal coordinates, are presented in tabular form (Tables 6.3-6.15).

The calculation of the PED for each normal vibrational mode confirms all our proposed assignments. It is fortunate that S_6 and S_{11} have only very small contributions from the other skeletal vibrations since the assignments in these two frequency modes are tentative.

The PED show that in all the complexes the ν(CO) modes have no significant coupling to other motions of the molecule. The PED also shows that in all the chloro-complexes there is significant coupling between the ν(Rh-C_1) and ν(Rh-X) mode, whereas this is not the case in any of the bromo-complexes since the higher mass of the halogen causes the ν(Rh-Br) mode to move to a substantially lower frequency relative to the ν(Rh-C_1) mode, and thus reduces the coupling.

It is seen that the agreement between the calculated and observed frequencies are good in all instances, except for the δ(MX) mode in *cis*-[Rh$(CO)_2$(Br)(imid)] and the ν(RhCO) and ν(ML) modes in the ammonia-complexes. This discrepancy can be accounted for by examining the complete vibrational assignment (see Chapter 3) of the above complexes, as discussed below.

In the imidazole complex the broad nature of the low frequency bands (S_6 and S_{11}) renders the assignment tentative. However, since the low frequency bands (S_6 δ(CMC) and S_{11} δ(MX)) are not significantly coupled to the other skeletal vibrations, the assignments of the latter vibrations are still valid.

In the ammonia-complexes the larger deviation than expected occurring for the ν(RhL) and δ(RhCO) modes can be attributed to the following points.

(i) The ν(ML) mode is almost certainly coupled to the δ(RhCO) out-of-plane mode. However, this interaction is not accounted for by the normal coordinate analysis as we only considered the in-plane modes of the complex.

(ii) The unusual behaviour, that is, the increase of frequency of the δ(RhCO) band upon deuteration of the *cis*-[$Rh(CO)_2(X)(NH_3)$] complexes can be ascribed to Fermi resonance [37] between the δ(RhCO) mode and the $\rho(NH_3)$ or ν(RhN) mode.

Due to the different modes of bonding between the various ligands and the rhodium metal no quantitative comparision is entirely justified. However, the *trans* influence is clearly demonstrated by (1) the assigned frequencies and (2) the CO force constants. Any difference between the Rh–C_1 and Rh–C_2 bond lengths falls within the uncertainties of the measurement, but the stretching frequencies are a much more sensitive probe in distinguishing the small differences between bonds, compare below:

bond length (Å)		2.364(1)		1.835(6)		1.156	
	Cl		**Rh**		**C_1**		**O_1**
wavenumber (cm^{-1})		300		463		2012	
force constant (mdyne/Å)		1.69		2.48		16.10	

bond length (Å)		2.090(4)		1.840(7)		1.131	
	NH_3		**Rh**		**C_2**		**O_2**
wavenumber (cm^{-1})		497		446		2088	
force constant (mdyne/Å)		2.19		2.72		17.46	

The fact that the *trans* influence is best observed by the force constants of the C≡O groups is understood, as triple bonds are more sensitive for any change in electron

density than single bonds, like Rh–C. One would expect a slight decrease of the $Rh–C_1$ force constant as coupling with the *trans* Rh–Cl bond will surely effect its value. The coupling which we have calculated can be explained by Pearson's [38] definition of a "softer character" for the Rh–Cl bond and thus would enhance the transmittance of any electronic effects. The force field calculation show a strong $Rh–NH_3$ bond which is thus responsible for the significantly higher force constant of the *trans* $C_2{\equiv}O_2$ group compared to the *cis* $C_1{\equiv}O_1$ group.

The force constant values obtained are in agreement with previous studies [39,40] done on related complexes. From the satisfactory agreement between observed and calculated frequency values, that is the small % deviation values, one may conclude that point-mass-modelling and simplified force field, as assumed in our treatment, describe, to a good approximation, the vibrational properties of the square planar rhodium carbonyl complexes.

TABLE 6.1 Symmetry coordinates for the infrared active in plane vibrations of *cis*-$[Rh(CO)_2(X)(L)]$ belonging to the point group C_s.

			Description
S_1	=	$\Delta\rho_2$	$\nu(C_2\text{-}O_2)$
S_2	=	$1/\sqrt{2}(\Delta\gamma_1 + \Delta\gamma_2)$	δ(Rh-C-O) "in-phase"
S_3	=	Δr_2	$\nu(Rh\text{-}C_2)$
S_4	=	ΔT	ν(Rh-L)
S_5	=	$\frac{1}{2}(\Delta\alpha - \Delta\beta_1 + \Delta\beta_2 - \Delta\delta)$	δ(Rh-L)
S_6	=	$\frac{1}{2}(\Delta\alpha - \Delta\beta_1 - \Delta\beta_2 + \Delta\delta)$	δ(C-Rh-C)
S_7	=	$\Delta\rho_1$	$\nu(C_1\text{-}O_1)$
S_8	=	$1/\sqrt{2}(\Delta\gamma_1 - \Delta\gamma_2)$	δ(Rh-C-O) "out-of-phase"
S_9	=	Δr_1	$\nu(Rh\text{-}C_1)$
S_{10}	=	ΔR	ν(Rh-X)
S_{11}	=	$\frac{1}{2}(\Delta\alpha + \Delta\beta_1 - \Delta\beta_2 - \Delta\delta)$	δ(Rh-X)

TABLE 6.2 Relationship between force constants in symmetry coordinate representation and those in internal coordinate representation.

$$F_{11} = f_{\rho_2} \qquad F_{77} = f_{\rho_1}$$

$$F_{22} = \tfrac{1}{2}(f_{\gamma_1} + f_{\gamma_2}) + f_{\gamma_1\gamma_2} \qquad F_{88} = \tfrac{1}{2}(f_{\gamma_1} + f_{\gamma_2}) - f_{\gamma_1\gamma_2}$$

$$F_{33} = f_{r_2} \qquad F_{99} = f_{r_1}$$

$$F_{44} = f_T \qquad F_{10\,10} = f_R$$

$$F_{55} = \tfrac{1}{4}(f_\alpha + f_{\beta_1} + f_{\beta_2} + f_\delta) - \tfrac{1}{2}(f_{\alpha\beta_1} - f_{\alpha\beta_2} + f_{\alpha\delta}) - \tfrac{1}{2}(f_{\beta_1\beta_2} - f_{\beta_1\delta}) - \tfrac{1}{2}(f_{\beta_2\delta})$$

$$F_{66} = \tfrac{1}{4}(f_\alpha + f_{\beta_1} + f_{\beta_2} + f_\delta) - \tfrac{1}{2}(f_{\alpha\beta_1} + f_{\alpha\beta_2} - f_{\alpha\delta}) + \tfrac{1}{2}(f_{\beta_1\beta_2} - f_{\beta_1\delta}) - \tfrac{1}{2}(f_{\beta_2\delta})$$

$$F_{11\,11} = \tfrac{1}{4}(f_\alpha + f_{\beta_1} + f_{\beta_2} + f_\delta) + \tfrac{1}{2}(f_{\alpha\beta_1} - f_{\alpha\beta_2} - f_{\alpha\delta}) - \tfrac{1}{2}(f_{\beta_1\beta_2} + f_{\beta_1\delta}) + \tfrac{1}{2}(f_{\beta_2\delta})$$

$$F_{13} = f_{\rho_2 r_2} \qquad F_{79} = f_{\rho_1 r_1}$$

$$F_{34} = f_{r_2 T} \qquad F_{9\,10} = f_{r_1 R}$$

TABLE 6.3 Frequencies and the potential energy distribution (P.E.D.) in normal vibrational modes of *cis*-$[Rh(CO)_2(X)(L)]$.

MODE		L = NH_3				L = py				L = imid			
		X = Cl		X = Br		X = Cl		X = Br		X = Cl		X = Br	
		Freq. (cm^{-1})	P.E.D. (%)	Freq. (cm^{-1})	P.E.D. (%)	Freq. (cm^{-1})	P.E.D. (%)	Freq. (cm^{-1})	P.E.D. (%)	Freq. (cm^{-1})	P.E.D. (%)	Freq. (cm^{-1})	P.E.D. (%)
S_1	$\nu(C_2\text{-}O_2)$	2088	$95(S_1)$	2087	$95(S_1)$	2089	$95(S_1)$	2086	$95(S_1)$	2083	$95(S_1)$	2082	$96(S_1)$
S_2	δ(Rh-C-O)	609	$91(S_2)$	606	$92(S_2)$	614	$90(S_2)$	604	$88(S_2)$	616	$84(S_2) + 10(S_5)$	612	$88(S_2)$
S_3	$\nu(Rh\text{-}C_2)$	446	$97(S_3)$	451	$97(S_3)$	454	$93(S_3)$	446	$92(S_3)$	451	$86(S_3) + 11(S_4)$	443	$85(S_3) + 12(S_4)$
S_4	ν(Rh-N)	497	$94(S_4)$	493	$94(S_4)$	206	$89(S_4)$	214	$89(S_4)$	256	$83(S_4) + 11(S_3)$	259	$83(S_4) + 15(S_3)$
S_5	δ(Rh-N)	197	$84(S_5) + 12(S_6)$	182	$85(S_5)$	171	$91(S_5)$	191	$86(S_5)$	224	$93(S_5)$	197	$93(S_5)$
S_6	δ(C-Rh-C)	120	$91(S_6)$	105	$74(S_6) + 20(S_{11})$	139	$93(S_6)$	159	$85(S_6)$	111	$98(S_6)$	107	$57(S_6) + 40(S_{11})$
S_7	$\nu(C_1\text{-}O_1)$	2012	$95(S_7)$	2012	$94(S_7)$	2013	$94(S_7)$	2014	$94(S_7)$	2009	$94(S_7)$	2009	$94(S_7)$
S_8	δ(Rh-C-O)	609	$85(S_8)$	606	$91(S_9)$	614	$81(S_8) + 10(S_6)$	604	$75(S_8) + 13(S_6)$	616	$77(S_8) + 12(S_5)$	612	$80(S_8) + 10(S_5)$
S_9	$\nu(Rh\text{-}C_1)$	463	$80(S_9) + 15(S_{10})$	468	$91(S_9)$	502	$84(S_9) + 11(S_{10})$	487	$88(S_9)$	490	$81(S_9) + 13(S_{10})$	490	$88(S_9)$
S_{10}	ν(Rh-X)	300	$79(S_{10}) + 19(S_9)$	214	$83(S_{10})$	310	$83(S_{10}) + 15(S_9)$	235	$83(S_{10})$	308	$81(S_{10}) + 16(S_9)$	238	$83(S_7)$
S_{11}	δ(Rh-X)	103	$98(S_{11})$	84	$82(S_{11}) + 16(S_6)$	110	$97(S_{11})$	93	$94(S_{11})$	150	$96(S_{11})$	100	$60(S_{11}) + 39(S_6)$

TABLE 6.4 Comparison of the observed frequencies with those calculated from the average force field of *cis*-[$Rh(CO)_2(Cl)(NH_3)$] and its isotopic derivatives.

MODE	NH_3		ND_3		$^{15}NH_3$		^{13}CO	
	obs.	calc.	obs.	calc.	obs.	calc.	obs.	calc.
$\nu(C_2\text{-}O_2)$	2088	2088.0	2088	2088.0	2089	2088.0	2039	2040.1
$\nu(C_1\text{-}O_1)$	2012	2012.4	2012	2012.4	2012	2012.4	1967	1966.1
δ(Rh-C-O)	609	609.6	623	609.6*	608	609.6	591	591.5
δ(Rh-C-O)	609	608.8	623	608.6*	608	608.7	591	590.8
ν(Rh-N)	497	497.8	463	467.7	495	486.4	490	497.4
$\nu(Rh\text{-}C_1)$	463	461.4	463	461.3	463	461.4	453	457.1
$\nu(Rh\text{-}C_2)$	446	446.0	445	442.2	446	445.3	440	440.1
ν(Rh-Cl)	300	300.2	300	300.2	300	300.2	299	299.0
δ(Rh-N)	197	196.3	184	185.9	193	192.5	196	196.0
δ(C-Rh-C)	120	120.4	120	119.4	120	120.0	120	119.8
δ(Rh-Cl)	103	103.0	103	102.7	103	102.9	103	102.7
% deviation	= 0.128		= 0.436		= 0.283		= 0.283	

* denotes frequencies not used in % deviation calculation, see text for explanation.

TABLE 6.5 Comparison of the observed frequencies with those calculated from the average force field of *cis*-$[Rh(CO)_2(Br)(NH_3)]$ and its isotopic derivatives.

MODE	NH_3		ND_3		$^{15}NH_3$		^{13}CO	
	obs.	calc.	obs.	calc.	obs.	calc.	obs.	calc.
$\nu(C_2\text{-}O_2)$	2087	2087.2	2087	2087.2	2087	2087.2	2040	2039.4
$\nu(C_1\text{-}O_1)$	2012	2012.4	2012	2012.4	2012	2012.4	1967	1966.0
δ(Rh-C-O)	606	606.5	616	606.4*	604	606.5	586	588.7
δ(Rh-C-O)	606	604.2	616	604.1*	604	604.1	586	586.0
ν(Rh-N)	493	496.5	470	467.2	489	485.1	483	496.1
$\nu(Rh\text{-}C_1)$	468	466.9	470	466.4	468	466.9	457	461.7
$\nu(Rh\text{-}C_2)$	451	447.4	445	443.4	450	446.7	437	441.5
ν(Rh-Br)	214	214.8	214	214.6	214	214.7	214	214.1
δ(Rh-N)	182	180.9	168	171.4	178	177.5	182	180.8
δ(C-Rh-C)	105	104.9	104	104.1	104	104.6	104	104.2
δ(Rh-Br)	84	84.2	84	83.5	84	83.9	84	83.9
% deviation	= 0.315		= 0.527		= 0.306		= 0.575	

* denotes frequencies not used in % deviation calculation, see text for explanation.

TABLE 6.6 Comparison of the observed frequencies with those calculated from the average force field of *cis*-[$Rh(CO)_2(Cl)(py)$] and its isotopic derivatives.

MODE	py		py-d_5		^{13}CO	
	obs.	calc.	obs.	calc.	obs.	calc.
$\nu(C_2\text{-}O_2)$	2089	2088.0	2088	2088.0	2039	2040.1
$\nu(C_1\text{-}O_1)$	2013	2013.4	2012	2013.4	1968	1966.6
δ(Rh-C-O)	614	614.9	611	614.9	593	596.4
δ(Rh-C-O)	614	611.3	611	611.3	593	592.9
$\nu(Rh\text{-}C_1)$	502	501.1	501	501.0	492	496.0
$\nu(Rh\text{-}C_2)$	454	451.3	452	451.2	444	445.9
ν(Rh-Cl)	310	310.1	310	310.1	309	309.0
ν(Rh-N)	206	205.8	197	202.4	205	205.1
δ(Rh-N)	171	169.2	165	168.3	170	168.5
δ(C-Rh-C)	139	138.5	137	137.2	138	138.0
δ(Rh-Cl)	110	109.8	110	109.2	109	109.4
% deviation	= 0.287		= 0.598		= 0.296	

TABLE 6.7 Comparison of the observed frequencies with those calculated from the average force field of *cis*-[$Rh(CO)_2(Br)(py)$] and its isotopic derivatives.

MODE	py		py-d_5		^{13}CO	
	obs.	calc.	obs.	calc.	obs.	calc.
$\nu(C_2\text{-}O_2)$	2086	2085.8	2086	2085.8	2037	2038.0
$\nu(C_1\text{-}O_1)$	2014	2014.3	2014	2014.3	1968	1967.7
δ(Rh-C-O)	604	610.7	603	610.7	584	591.8
δ(Rh-C-O)	604	603.2	603	603.2	584	584.8
$\nu(Rh\text{-}C_1)$	487	486.2	487	486.2	475	481.0
$\nu(Rh\text{-}C_2)$	446	443.8	444	443.6	434	438.6
ν(Rh-Br)	235	235.1	233	235.0	235	234.3
ν(Rh-N)	214	214.4	208	210.8	213	213.7
δ(Rh-N)	191	189.0	182	188.2	189	188.2
δ(C-Rh-C)	159	158.9	156	157.2	159	158.4
δ(Rh-Br)	93	93.1	92	92.5	93	92.9
% deviation	= 0.306		= 0.474		= 0.490	

TABLE 6.8 Comparison of the observed frequencies with those calculated from the average force field of *cis*-[$Rh(CO)_2(Cl)$(imid)] and its isotopic derivatives.

MODE	imid		imid-d_4		imid-^{15}N		^{13}CO	
	obs.	calc.	obs.	calc.	obs.	calc.	obs.	calc.
$\nu(C_2\text{-}O_2)$	2083	2083.0	2083	2083.0	2083	2083.0	2035	2035.2
$\nu(C_1\text{-}O_1)$	2009	2009.2	2009	2009.2	2009	2009.2	1963	1962.7
δ(Rh-C-O)	616	620.2	616	620.2	616	620.2	598	601.5
δ(Rh-C-O)	616	615.4	616	615.4	616	615.4	598	596.5
$\nu(Rh\text{-}C_1)$	490	490.6	486	490.6	487	490.6	480	485.0
$\nu(Rh\text{-}C_2)$	451	448.5	448	448.1	448	448.4	440	443.8
ν(Rh-Cl)	308	307.5	307	307.5	307	307.5	306	306.4
ν(Rh-N)	256	255.8	253	251.9	249	254.1	255	254.6
δ(Rh-N)	224	222.2	218	220.5	223	221.8	223	221.5
δ(Rh-Cl)	150	149.7	149	149.0	150	149.6	150	149.4
δ(C-Rh-C)	111	110.0	110	109.3	110	109.8	110	109.6
% deviation	= 0.328		= 0.380		= 0.438		= 0.408	

TABLE 6.9 Comparison of the observed frequencies with those calculated from the average force field of *cis*-[$Rh(CO)_2(Br)$(imid)] and its isotopic derivatives.

MODE	imid		imid-d_4		imid-^{15}N		^{13}CO	
	obs.	calc.	obs.	calc.	obs.	calc.	obs.	calc.
$\nu(C_2\text{-}O_2)$	2082	2082.0	2082	2082.0	2082	2082.0	2034	2034.3
$\nu(C_1\text{-}O_1)$	2009	2009.0	2009	2009.0	2008	2009.0	1963	1962.5
δ(Rh-C-O)	612	616.6	611	616.6	masked	616.6*	591	598.1
δ(Rh-C-O)	612	610.7	611	610.7	masked	610.7*	591	591.9
$\nu(Rh\text{-}C_1)$	490	489.7	488	489.7	490	489.7	479	484.5
$\nu(Rh\text{-}C_2)$	443	441.9	442	441.4	442	441.8	434	437.3
ν(Rh-Br)	259	258.7	255	254.4	257	257.6	258	257.6
ν(Rh-N)	238	237.1	233	237.0	238	237.1	236	236.2
δ(Rh-N)	197	195.5	191	194.0	196	195.1	196	194.8
δ(C-Rh-C)	107	106.7	106	106.1	108	106.6	107	106.0
δ(Rh-Br)	~100	93.4*	~98	92.7*	~100	93.2*	~99	93.2*
% deviation	= 0.281		= 0.507		= 0.341		= 0.509	

* denotes frequencies not used in % deviation calculation, see text for explanation.

TABLE 6.10 The symmetry force constants of *cis*-$[Rh(CO)_2(X)(L)]$ (see text for units).

	X = Cl			X = Br		
	NH_3	py	imid	NH_3	py	imid
$F_{1\,1}$	17.460	17.401	17.294	17.448	17.362	17.281
$F_{2\,2}$	.988	1.019	1.046	.979	1.000	1.031
$F_{3\,3}$	2.715	2.552	2.388	2.732	2.440	2.308
$F_{4\,4}$	2.189	1.251	1.855	2.178	1.388	1.960
$F_{5\,5}$	.963	1.347	2.341	.858	1.824	1.908
$F_{6\,6}$	.347	.630	.399	.267	.976	.420
$F_{7\,7}$	16.101	16.091	16.033	16.139	16.143	16.059
$F_{8\,8}$	1.000	1.036	.973	.986	1.057	1.031
$F_{9\,9}$	2.484	3.000	2.803	2.717	2.891	2.935
$F_{10\,10}$	1.692	1.780	1.807	1.472	1.861	1.918
$F_{11\,11}$	.430	.560	1.046	.418	.574	.618
$F_{1\,3}$	.655	.556	.490	.660	.522	.470
$F_{2\,5}$	.094	.173	.312	.084	.235	.247
$F_{2\,11}$	−.047	−.063	−.121	−.052	−.071	−.078
$F_{3\,4}$	.355	−.124	−.175	.359	−.134	−.171
$F_{5\,6}$	−.027	.027	.010	−.020	.056	.012
$F_{5\,8}$	−.108	−.166	−.312	−.094	−.225	−.252
$F_{5\,10}$	−.077	−.148	−.296	−.194	−.460	−.508
$F_{6\,8}$	.084	.149	.078	.061	.240	.089
$F_{7\,9}$	.497	.629	.578	.599	.627	.642
$F_{8\,9}$	.061	.072	.058	.073	.071	.073
$F_{8\,11}$	−.048	−.064	−.120	−.046	−.069	−.059
$F_{9\,10}$	−.181	−.212	−.217	−.139	−.186	−.191

TABLE 6.11 The internal coordinate force constants of *cis*-[$Rh(CO)_2(X)(L)$] (in mdyne/Å).

	X = Cl			X = Br		
	NH_3	py	imid	NH_3	py	imid
$f(C_1\text{-}O_1)$	16.101(.029)	16.091(.029)	16.033(.029)	16.139(.030)	16.143(.031)	16.059(.030)
$f(C_2\text{-}O_2)$	17.460(.033)	17.401(.032)	17.294(.031)	17.448(.033)	17.362(.032)	17.281(.031)
$f(Rh\text{-}C_1)$	2.484(.019)	3.000(.021)	2.803(.020)	2.717(.021)	2.891(.022)	2.935(.022)
$f(Rh\text{-}C_2)$	2.715(.025)	2.552(.021)	2.388(.019)	2.732(.025)	2.440(.020)	2.308(.018)
$f(Rh\text{-}X)$	1.692(.025)	1.780(.025)	1.807(.026)	1.472(.030)	1.861(.035)	1.918(.035)
$f(Rh\text{-}L)$	2.189(.018)	1.251(.028)	1.855(.034)	2.178(.018)	1.388(.029)	1.960(.034)
$f(X\text{-}Rh\text{-}L)$	.095(.004)	.145(.006)	.214(.007)	.083(.004)	.191(.007)	.163(.007)
$f(L\text{-}Rh\text{-}C_1)$	.107(.004)	.165(.007)	.242(.007)	.096(.004)	.222(.008)	.189(.007)
$f(X\text{-}Rh\text{-}C_2)$	.107(.004)	.148(.006)	.224(.007)	.092(.004)	.189(.007)	.170(.007)
$f(C\text{-}Rh\text{-}C)$	.122(.006)	.169(.007)	.256(.008)	.108(.004)	.222(.008)	.199(.007)
$f(Rh\text{-}C_1\text{-}O_1)$	.338(.003)	.346(.003)	.337(.003)	.334(.003)	.345(.004)	.345(.003)
$f(Rh\text{-}C_2\text{-}O_2)$	.329(.003)	.343(.004)	.341(.004)	.325(.003)	.345(.004)	.348(.004)
$f'(C_1\text{-}O_1/Rh\text{-}C_1)$	.497(.008)	.629(.007)	.578(.007)	.599(.008)	.627(.008)	.642(.008)
$f'(Rh\text{-}C_2/Rh\text{-}L)$	.355(.012)	−.124(.024)	−.175(.020)	.359(.008)	−.134(.021)	−.171(.017)
$f'(C_2\text{-}O_2/Rh\text{-}C_2)$	.655(.009)	.556(.008)	.490(.008)	.660(.009)	.522(.008)	.470(.008)
$f'(Rh\text{-}C_1/Rh\text{-}X)$	−.181(.017)	−.212(.016)	−.217(.016)	−.139(.022)	−.186(.020)	−.191(.020)

The values within parenthesis are the uncertainties derived from the average force field by applying the harmonic oscillator approach.

The f' force constants indicate interaction force constants. That is, non-diagonal elements of the F matrix.

(2) DYNAMIC NUCLEAR MAGNETIC RESONANCE (DNMR)

INTRODUCTION

Inorganic, and in particular organometallic chemistry is riven with a large number of stereochemically nonrigid molecules. This situation was not recognized until the 1960s, when nmr studies uncovered for many molecules spectral features explicable only in terms of rapid molecular rearrangements. By the late 1960s, nmr studies of stereochemically nonrigid molecules had become commonplace. Since then, an impressive array of computer programmes for generating theoretical spectra from a set of chemical shifts and coupling constants have been developed [41-43]. Hence, computer-aided nmr studies have been used extensively in the study of rapid equilibria. From these studies, activation parameters for the experimental system may be determined. The method generally used for obtaining activation parameters is therefore implementation of a complete band shape analysis of the nmr spectra over as wide a temperature range as possible, followed by determination of the Arrhenius activation parameters from a plot of $\ln K$ against $1/T$, which provides the parameters of interest from the slope and intercept, see Chapter 1.

This band shape analysis has been applied by various workers [44-48] to rhodium(I) complexes. The rhodium complexes are particularly amenable to nmr studies because ^{103}Rh has a nuclear spin of ½ and the spectra are characterized by the appearance of $^{1}J(^{103}\text{Rh–L})$ coupling. This spin-spin coupling provides an indication of the type of exchange occurring within the complexes. In *intra*molecular exchange processes, nuclear positions in a molecule are permutable without bond-breaking, hence spin-spin coupling will be maintained between the nuclei involved. In *inter*molecular exchange processes, there are bond-breaking and bond-formation

steps. Bond-scission necessarily leads to loss of spin-spin coupling between the nuclei in the two fragments generated in the scission process. This loss of spin-spin coupling is a strong nmr test of an *inter*molecular exchange process and is extremely sensitive [49].

The present work was undertaken to examine the interesting fluxional behaviour occurring in the ^{13}C nmr spectra of the complexes *cis*-[$Rh(CO)_2(X)(L)$] (X is Cl or Br and L is ammonia, pyridine, pyridine *N*-oxide, imidazole or aniline). Chapter 3 (nmr section) gives a detailed explanation of the fluxional process exhibited by the above complexes. The complexes *cis*-[$Rh(CO)_2(X)$(pyridine *N*-oxide)] (X is Cl or Br) were chosen for the DNMR studies in preference to the other complexes (L is ammonia, pyridine, imidazole or aniline) mainly because the coalescence temperature occurs in an accessible temperature range, but also because the pyridine *N*-oxide complexes do not decompose as rapidly in solution.

The combined results obtained from the variable temperature ^{1}H, ^{13}C and ^{15}N nmr (Chapter 3) conclusively show that in the temperature range studied, (i) the fluxional process certainly involves the loss of L rather than the loss of CO, and (ii) the exchange of L occurs *via* an *inter*molecular exchange process.

PROCEDURE, RESULTS AND DISCUSSION

The variable temperature (25°C to -55°C) ^{13}C nmr spectra of the complexes *cis*-[Rh($^{13}CO)_2$(X)(pyO)] (X is Cl or Br) were recorded in acetone-d_6, a low freezing point solvent. The level of enrichment of ^{13}CO was kept below ~30%. This was necessary to avoid broadening or partial splitting of the carbonyl resonances because of the occurrence of $^2J(^{13}CO–Rh–^{13}CO)$ coupling.

After the carbonyl region of the spectra (170–190 ppm) were appropriately expanded, the spectra were visually compared with computer simulated spectra. The computer simulated spectra were obtained by providing the programme DNMR5 [43,50,Appendix 2] with the parameters (coupling constants, peak positions, relaxation times, *etc.*) found for the experimental system at the lowest temperature recorded, that is, in the limiting slow-exchange. Whenever the simulated and experimental spectra bore an adequate resemblance to each other, then the kinetic parameters of the experimental spectra were considered to be equal to those of the simulated spectra. The ^{13}C nmr temperature-dependent spectra (of the carbonyl region) as well as the superimposed computer simulated spectra are presented in Figures 6.5 and 6.6. At room temperature (~25°C), the spectra show a doublet with ^1J(Rh–CO). As the sample temperature is lowered, the doublet collapses into a broad hump (at ~–5°C) and then separates into the two doublets as a result of the two different carbonyl environments, each doublet having a characteristic ^1J(Rh-CO) value. The J value is dependent upon the ligand *trans* to the carbonyl group. The activation parameters and their associated errors are given in Tables 6.13 and 6.14. A weighted least squares analysis of ln$K$ against $1/T$ was performed in order to take into account the variable accuracy of the measurements since measurements near the coalescence temperature are more precise as the band

shape is more sensitive to the rate constant, K, in this region [51]. The plots (see Figures 6.7 and 6.8) result in a straight line, the slopes of which yield $\Delta H^{\ddagger}$, the enthalpy of activation, directly and an intercept, from which $\Delta S^{\ddagger}$, the entropy of activation may be determined, since

$$\ln K = -\Delta H^{\ddagger}/R\,T + ((\Delta S^{\ddagger}/R) + \ln(kT/h))$$

where K = rate constant in s^{-1},

T = temperature in K

k, h, R = Boltzmann, Planck and gas constant, respectively.

The results for the exchange in the *cis*-[$Rh(CO)_2(Cl)(pyO)$] complex are,

$$\Delta H^{\ddagger} = 53.3 \pm 1.0 \text{ kJ mol}^{-1}$$
$$\Delta S^{\ddagger} = 5.5 \pm 0.6 \text{ J mol}^{-1}\text{ K}^{-1}$$

Similarly, the results for the *cis*-[$Rh(CO)_2(Br)(pyO)$] complex are,

$$\Delta H^{\ddagger} = 48.3 \pm 0.8 \text{ kJ mol}^{-1}$$
$$\Delta S^{\ddagger} = -11.0 \pm 0.3 \text{ J mol}^{-1}\text{ K}^{-1}$$

The activation parameters for the ligand exchange are similar to those found in other square planar rhodium complexes [52]. In general, the enthalpy of activation depends on the strengths of the bonds that are being broken and formed in getting to the transition state. Thus the slightly higher value of $\Delta H^{\ddagger}$ obtained for the chloro complex relative to the bromo complex would indicate that the Rh–(pyO) bond in the chloro complex is slightly stronger than the Rh–(pyO) bond in the bromo complex. The infrared studies (see Chapter 3) are in agreement with this, the Rh–

(pyO) band in the chloro complex occurring approximately 8 cm^{-1} higher than in the bromo complex.

With regard to the mechanism of the exchange process, there are two pathways which are consistent with all the nmr data (see Chapter 3 for the nmr data), and these are briefly described below.

1) Attack at the square planar centre by a solvent molecule occurs to give a five-coordinate trigonal bipyramidal intermediate. The trigonal bipyramidal intermediate then undergoes a Berry pseudorotation for interchange of axial and equatorial ligands, followed by loss of the solvent molecule to result in the stereospecific product (see below).

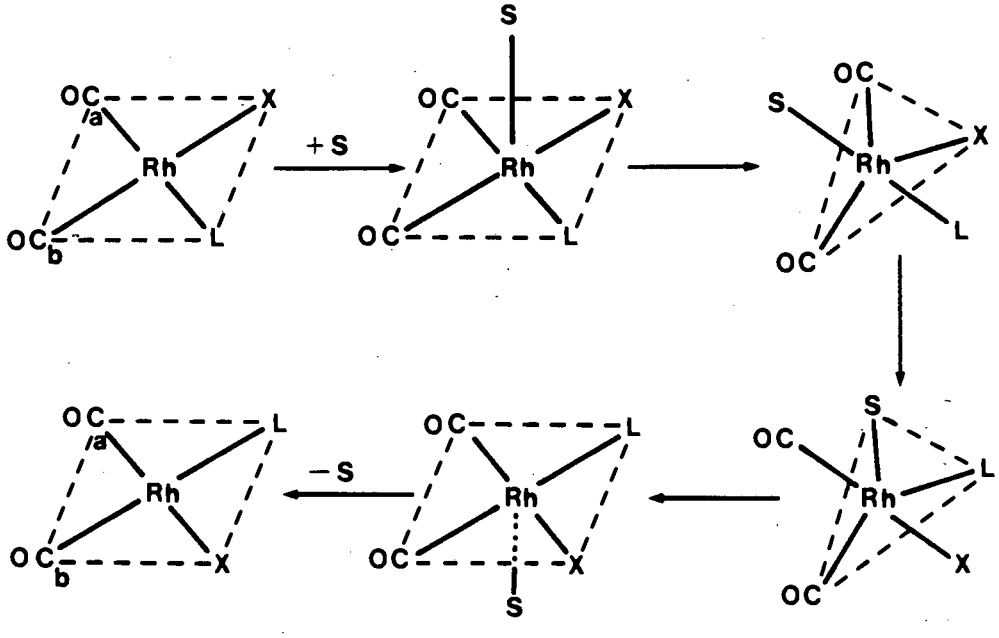

The five-coordinate intermediate pathway.

2) The complexes *cis*-$[Rh(CO)_2(X)(L)]$ can undergo loss of ligand, L, either *via* formation of a solvated five-coordinate intermediate as described above, or by

the formation of a solvated three-coordinate intermediate, which can subsequently undergo attack by free ligand, L (see below).

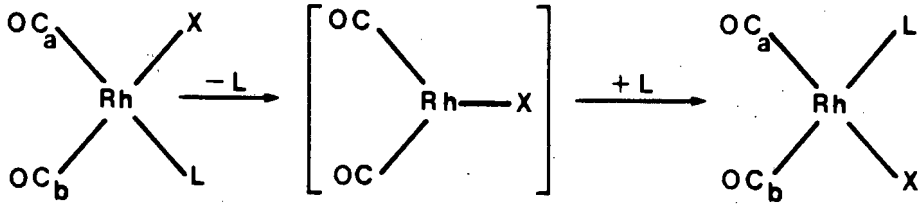

The three-coordinate intermediate pathway.

The loss of CO is not considered as the ^{1}J(Rh–CO) coupling is maintained over the temperature range employed. On the other hand the ^{1}J(Rh–^{15}N) coupling is lost, implying that Rh–N bond scission occurs. This implies that the second mechanism occurrs to some extent.

The first mechanism would account for the solvent dependence of the reaction kinetics of the related complexes *cis*-[Rh(CO)$_2$(X)(imid)] (see Chapter 3) and other similar platinum complexes [53,54]. On the other hand this mechanism does not account for the loss of ^{1}J(Rh–^{15}N) coupling that is observed. One method of determining the relative importance of these two pathways would be to study the kinetics of ligand, L exchange *via* ^{15}N nmr. Unfortunately, the stability of the complexes and the time necesssary to record the ^{15}N spectra precluded this experiment being carried out in detail. Nevertheless, from the preliminary results obtained from the ^{15}N nmr study of the *cis*-[Rh(CO)$_2$(Cl)(an)] complex, we are able to estimate that the rate of exchange of the aniline ligand is ~25 s^{-1} (T_c ~−35°C). At this temperature, the corresponding rate for carbonyl equilibration in the ^{13}C nmr spectra is 20 s^{-1} (see Table 6.13). This suggests that the second pathway is important, if not dominant.

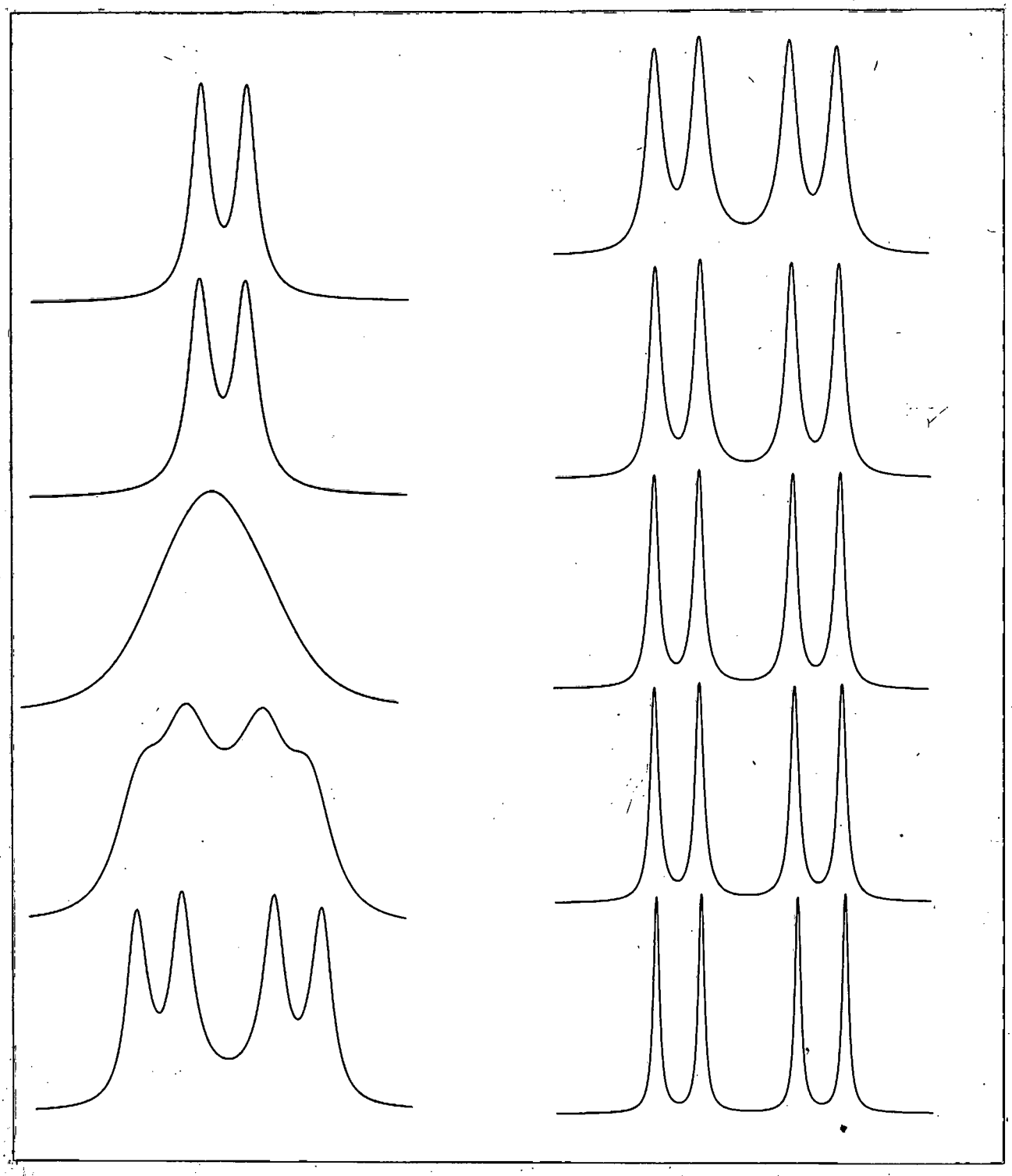

FIGURE 6.5 (a) **The computer simulated spectra of *cis*-[Rh(CO)$_2$(Cl)(pyO)].**

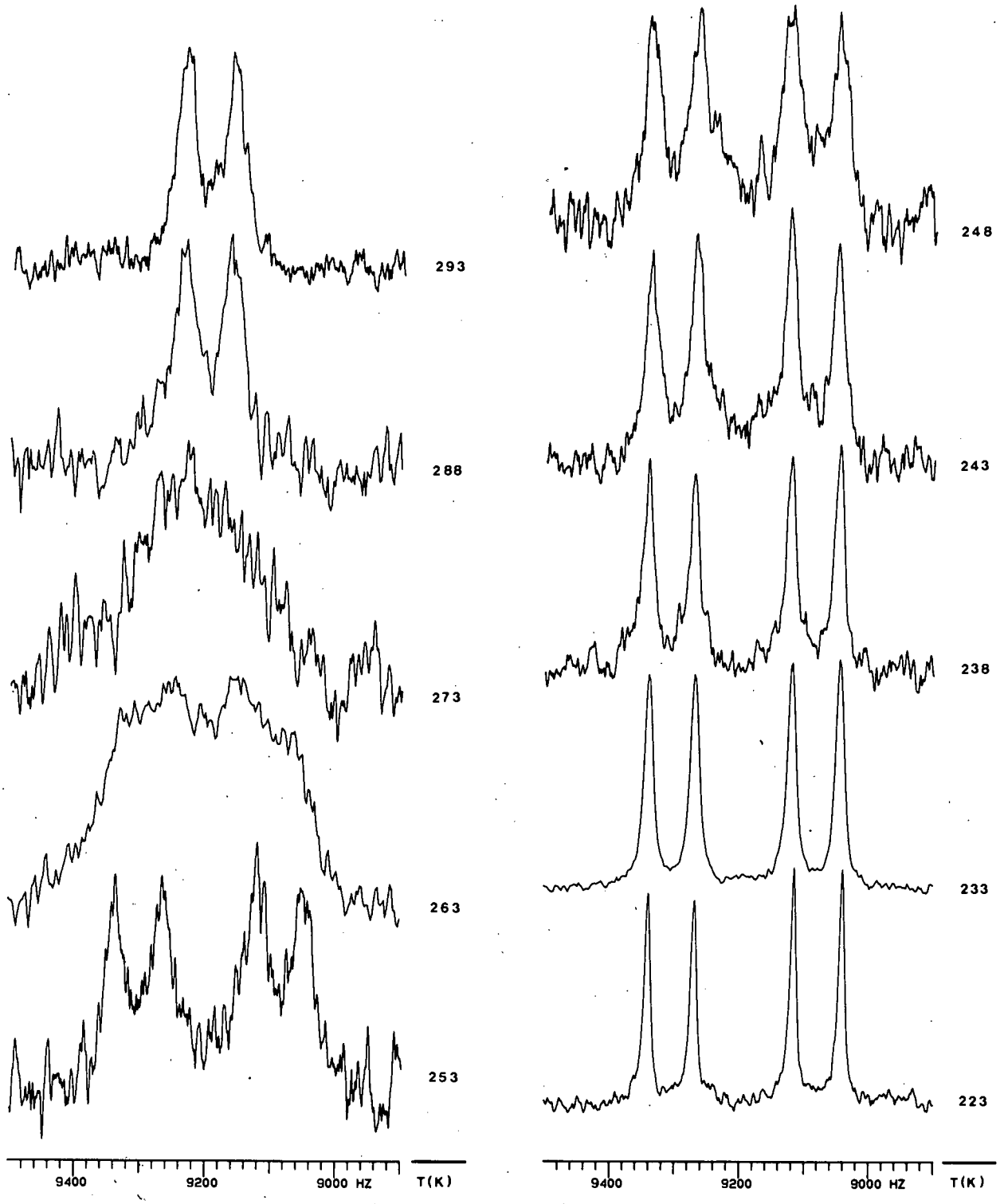

FIGURE 6.5 (b) The ^{13}C nmr (carbonyl region) temperature–dependent spectra of *cis*-$[Rh(CO)_2(Cl)(pyO)]$.

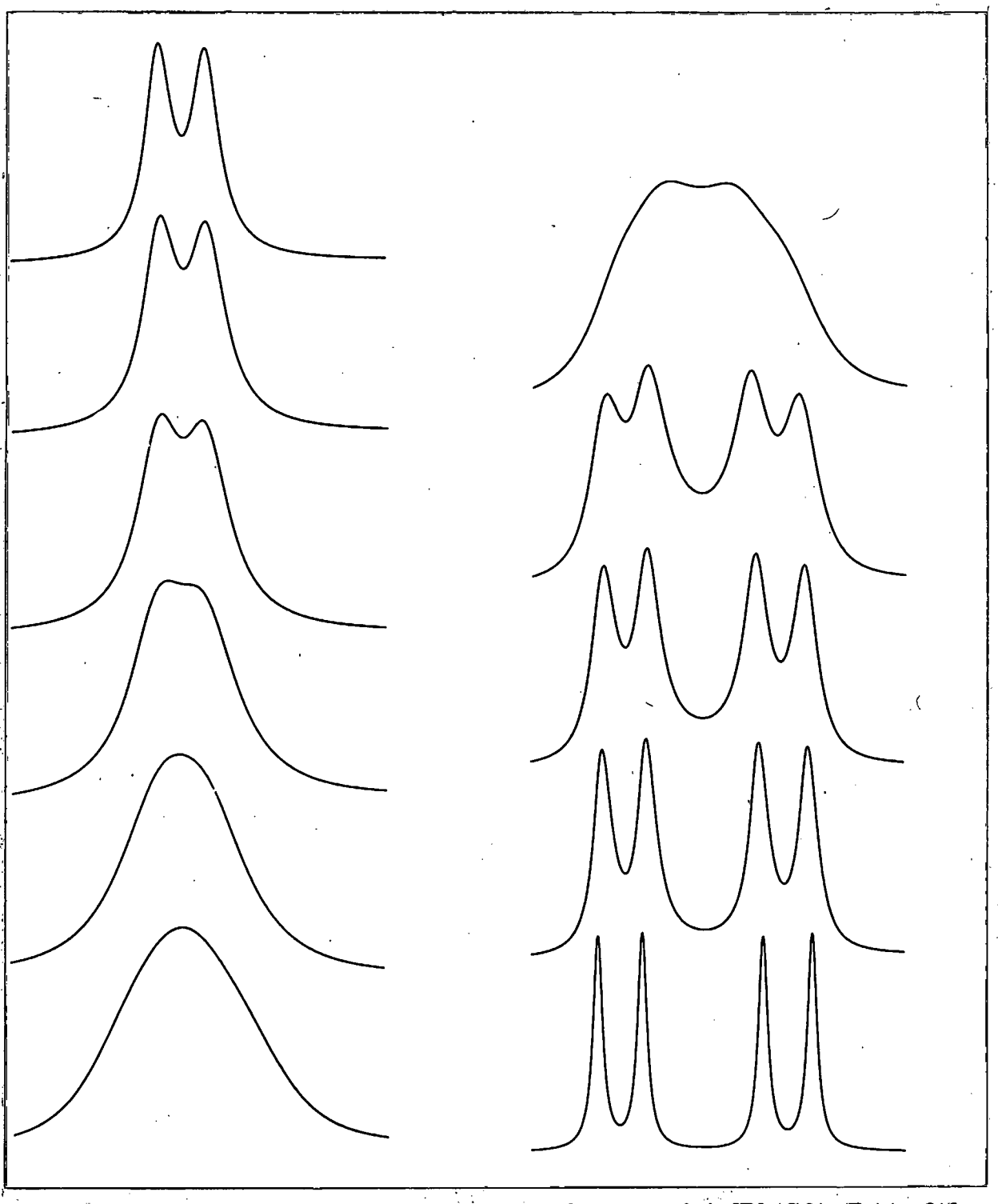

FIGURE 6.6 (a) **The computer simulated spectra of *cis*-[Rh(CO)$_2$(Br)(pyO)].**

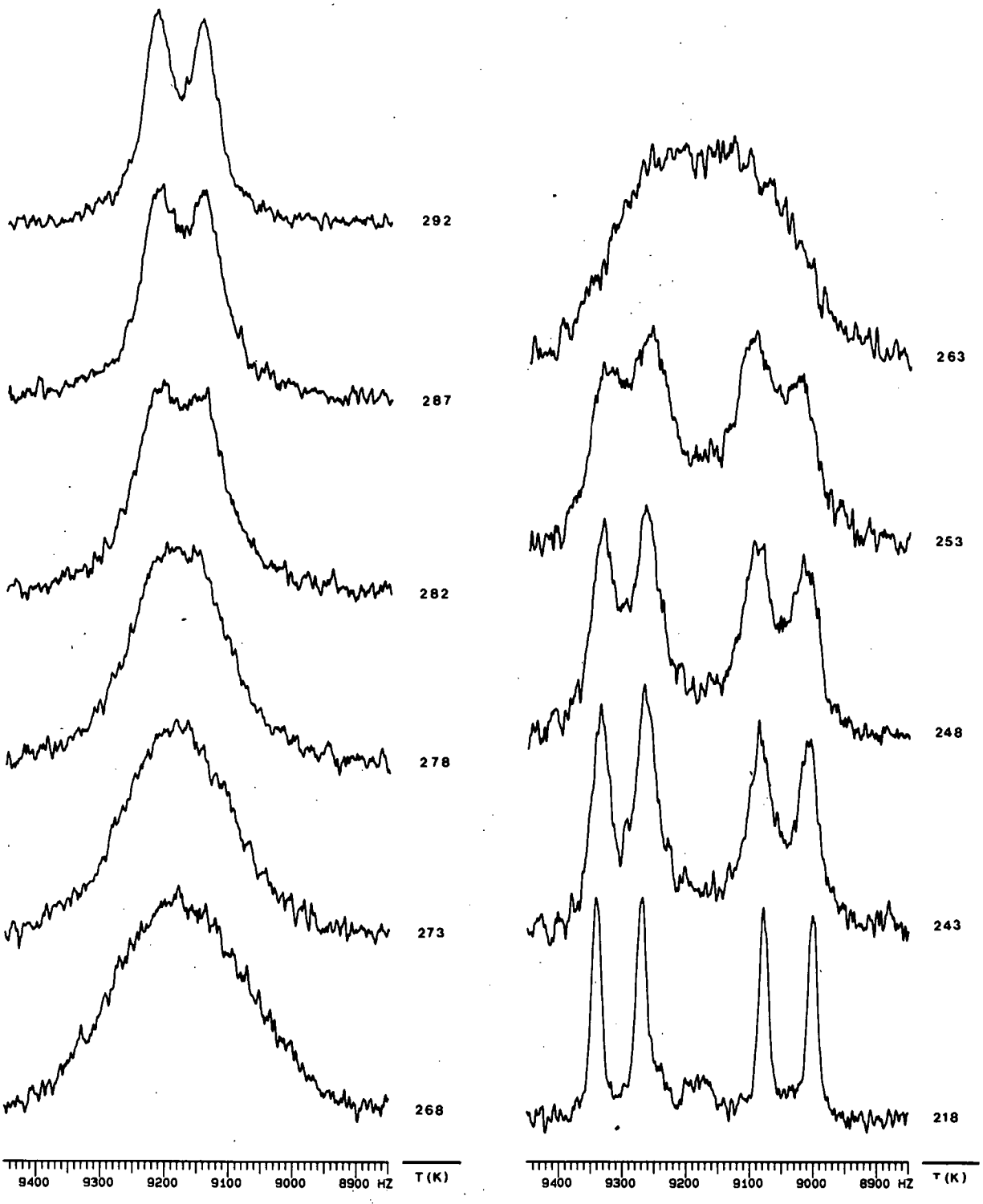

FIGURE 6.6 (b) The ^{13}C nmr (carbonyl region) temperature–dependent spectra of *cis*-$[Rh(CO)_2(Br)(pyO)]$.

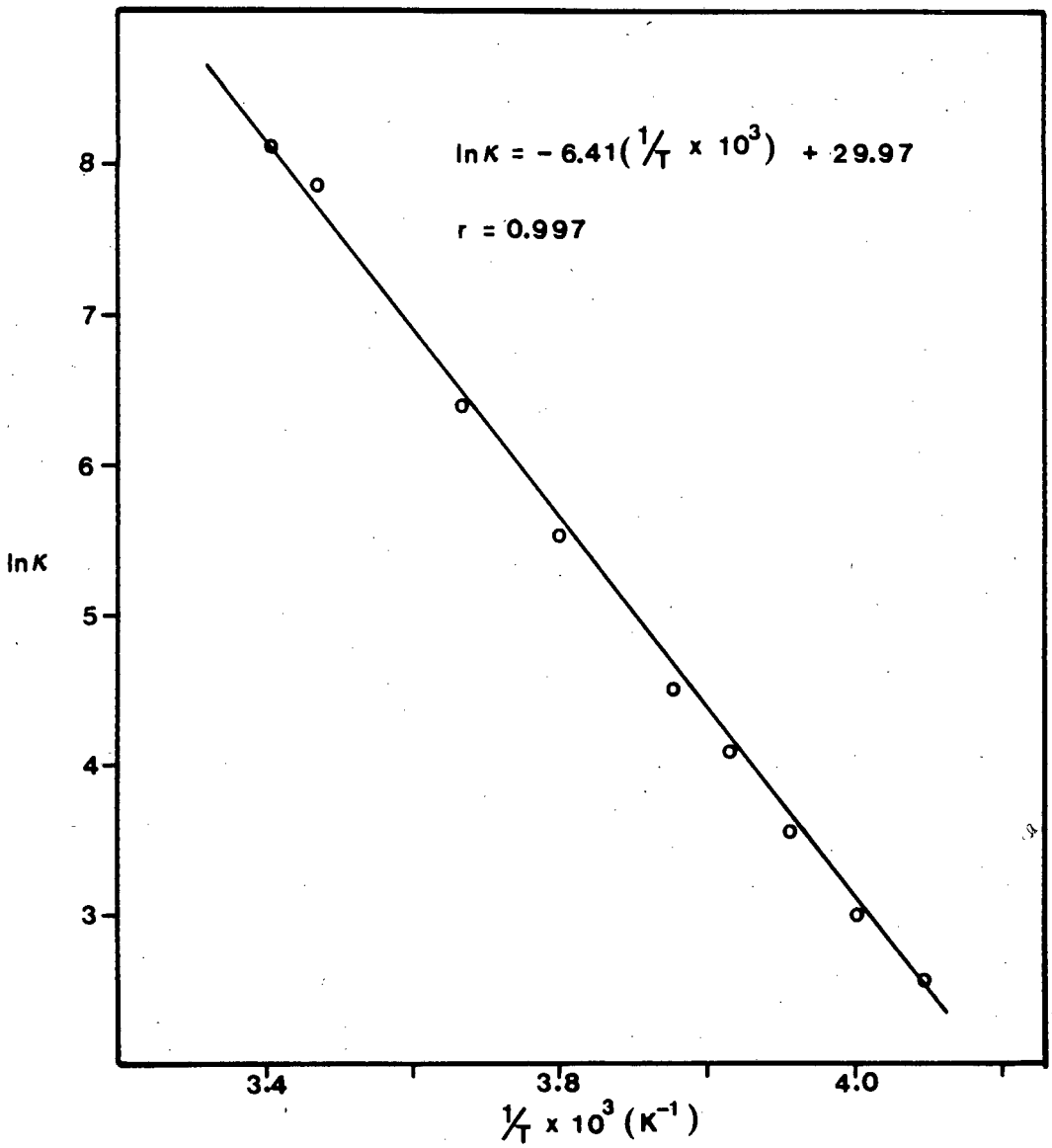

FIGURE 6.7 Plot of ln$K$ *vs* $1/T$ for *cis*-[$Rh(CO)_2(Cl)(pyO)$].

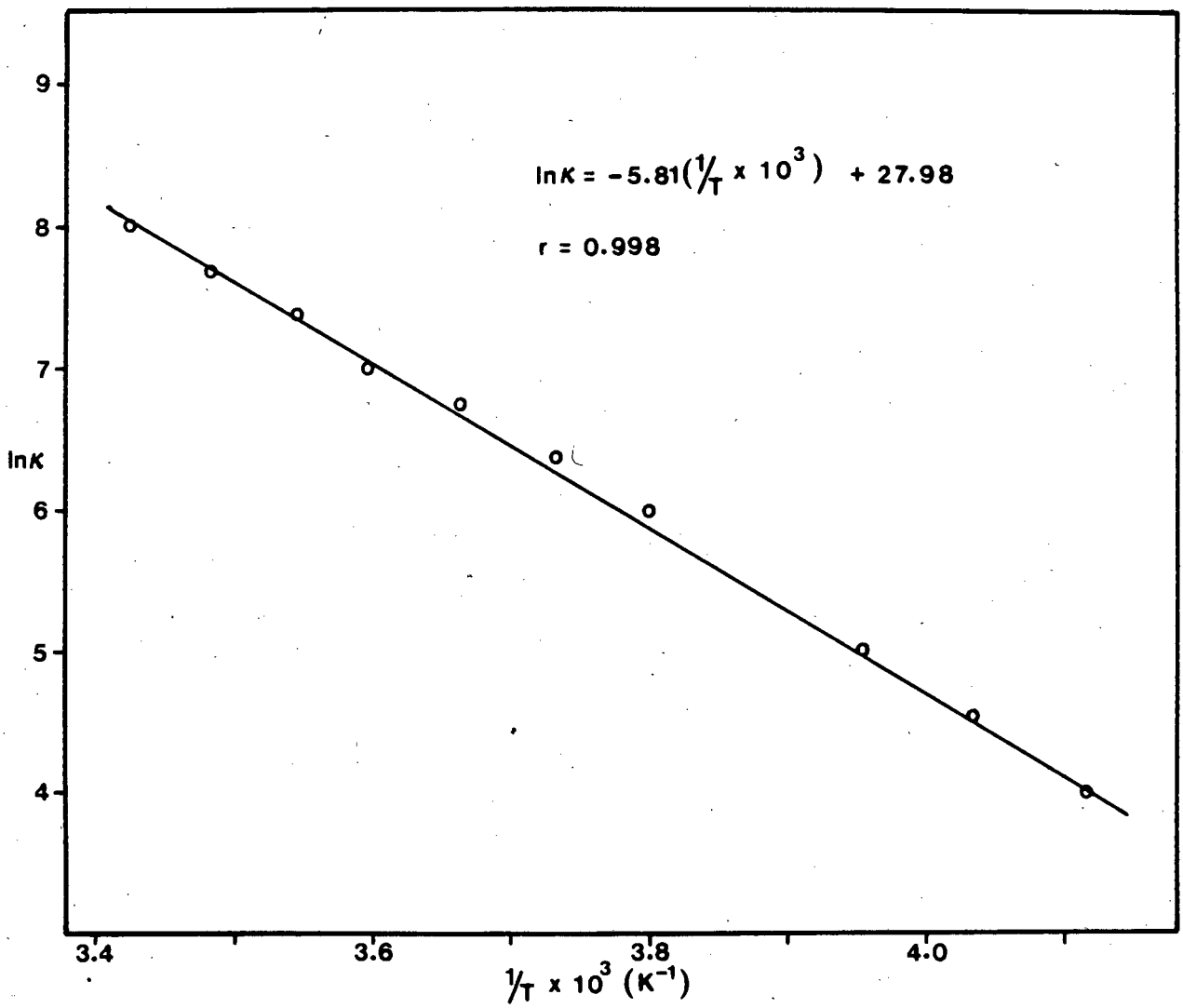

FIGURE 6.8 Plot of ln$K$ *vs* $1/T$ for *cis*-[Rh(CO)$_2$(Br)(pyO)].

TABLE 6.13 The ^{13}C nmr data (carbonyl region) of *cis*-[Rh(^{13}CO)$_2$(Cl)(pyO)] and its activation paramaters derived by band shape analysis of the carbonyl resonances.

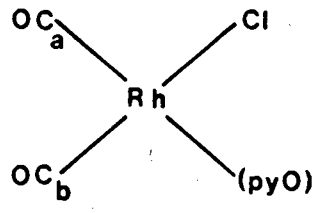

^{13}C nmr (acetone-d_6, Temp. = − 50 °C)

CO_a (184.95 ppm) $^1J(Rh–CO_a)$ = 71.59 Hz
CO_b (180.45 ppm) $^1J(Rh–CO_b)$ = 75.06 Hz
Relaxation time , T_2 = 0.017 s

T (K)	K (s^{-1})	ln$K$	Error analysis factor for ln$K$	$1/T \times 10^3$
223	~0			
233	13 ± 3	2.565 ± 0.235	0.179	4.292
238	20 ± 5	2.996 ± 0.255	0.194	4.202
243	35 ± 10	3.555 ± 0.294	0.223	4.115
248	60 ± 10	4.094 ± 0.168	0.128	4.032
253	90 ± 10	4.500 ± 0.112	0.085	3.953
263	250 ± 25	5.521 ± 0.100	0.076	3.802
273	600 ± 100	6.397 ± 0.017	0.013	3.663
288	2600 ± 200	7.863 ± 0.077	0.059	3.472
293	3400 ± 200	8.132 ± 0.059	0.045	3.413

TABLE 6.14 The ^{13}C nmr data (carbonyl region) of *cis*-[Rh(^{13}CO)$_2$(Br)(pyO)] and its activation paramaters derived by band shape analysis of the carbonyl resonances.

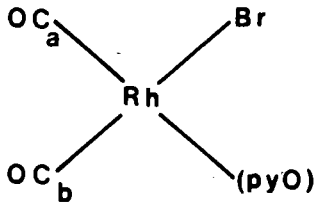

^{13}C nmr (acetone-d_6, Temp. = − 55 °C)

CO_a (184.97 ppm) $^1J(Rh–CO_a)$ = 73.70 Hz
CO_b (179.68 ppm) $^1J(Rh–CO_b)$ = 77.63 Hz
Relaxation time , T_2 = 0.017 s

T (K)	*K* (s^{-1})	ln*K*	Error analysis factor for ln*K*	$1/T \times 10^3$
218	~0			
243	55 ± 5	4.007 ± 0.091	0.191	4.115
248	95 ± 10	4.554 ± 0.053	0.097	4.032
253	150 ± 10	5.011 ± 0.067	0.111	3.953
263	400 ± 20	5.991 ± 0.050	0.070	3.802
268	600 ± 50	6.397 ± 0.084	0.109	3.731
273	850 ± 50	6.745 ± 0.059	0.073	3.663
278	1100 ± 100	7.003 ± 0.091	0.109	3.597
282	1600 ± 100	7.378 ± 0.063	0.071	3.546
287	2200 ± 200	7.696 ± 0.091	0.099	3.484
292	3000 ± 200	8.006 ± 0.067	0.069	3.425

REFERENCES

1 G.W.KING,
"Spectroscopy and Molecular Structure", Holt, Rinehart, and Winston, New York, (1964)

2 C.J.H.SCHUTTE,
"The Theory of Molecular Spectroscopy",Vol I: "The Quantum Mechanics and Group Theory of Vibrating and Rotating Molecules", North Holland, Amsterdam, (1976)

3 D.E.MANN, T.SHIMANOUCHI, J.H.MEAL AND L.FANO,
J. Chem. Phys., **27** (1975) 43

4 J.OVEREND AND J.R.SCHERER,
J. Chem. Phys., **32** (1960) 1289, 1296, 1720

5 I.M.MILLS,
Spectrochim. Acta, **16** (1960) 35

6 J.ALDOUS AND I.M.MILLS,
Spectrochim. Acta, **18** (1962) 1073

7 H.J.BECHER AND R.MATTES,
Spectrochim. Acta, **23A** (1967) 2449

8 T.SHIMANOUCHI AND I.NAKAGAWA,
Ann. Rev. Phys. Chem., **23** (1972) 217

9 W.SAWODNY, A.FADINI AND K.BALLEIN,
Spectrochim. Acta, **21** (1965) 995

10 J.HERRANZ AND F.CASTAÑO,
Spectrochim. Acta, **22** (1966) 1965

11 G.STREY,
J. Mol. Spectrosc., **24** (1967) 87

12 D.E.FREEMAN,
J. Mol. Struct., **4** (1969) 145

13 S.J.CYVIN,
"Molecular Vibrations and Mean Square Amplitudes", Elsevier, New York, (1968)

14 E.B.WILSON,
J. Chem. Phys., **7** (1939) 1047, **9** (1941) 76, **15** (1947) 736

15 E.B.WILSON, J.C.DECIUS AND P.C.CROSS,
"Molecular Vibrations", McGraw-Hill, New York, (1955)

16 J.C.DECIUS,
J. Chem. Phys., **16** (1948) 1025, **17** (1949) 1315

17 D.F.MCINTOSCH AND K.H.MICHAELIAN,
Can. J. Spectrosc., **24** (1979) 1, 35,65

18 D.STEELE,
"The Theory of Vibrational Spectroscopy",
W.B.Saunders, Philadelphia, (1971)

19 K.NAKAMOTO,
"Infrared and Raman Spectra of Inorganic and Coordination Compounds",
4th Ed., John Wiley and Sons, New York, (1986)

20 P.GANS,
"Vibrating Molecules:An Introduction to the Interpretation of Infrared and Raman Spectra", Chapman and Hall, London, (1971)

21 N.B.COLTHUP, L.H.DALY AND S.E.WIBERLEY,
"Introduction to Infrared and Raman Spectroscopy",
Academic Press, New York and London, (1964)

22 B. VAN DER VEKEN, H.O.DESSEYN AND M.HERMAN,
*Bull. Soc. Chim. Belg*es, **81** (1972) 555

23 B.S.AVERBUKH, L.S.MAYANTS AND G.B.SHALTUPER,
J. Mol. Spectrosc., **30** (1969) 310

24 A.ALIX AND L.BERNARD,
J. Mol. Struct., **20** (1974) 51

25 A.ALIX , H.EYSEL, B.JORDANOV, R.KEBABCIOGLU,
N.MOHAN AND A.MÜLLER,
J. Mol. Struct., **27** (1975) 1

26 B.VAN DER VEKEN,
Ph.D. Thesis, University of Antwerpen, Belgium, (1972)

27 L.VAN HAVERBEKE,H.O.DESSEYN, B.J.VAN DER VEKEN
AND M.A.HERMAN,
J. Mol. Struct., **25** (1975) 53

28 B.VAN DER VEKEN,
J. Mol. Struct., **15** (1973) 300

29 P.F.M.VERHOEVEN,
Ph.D. Thesis, University of Cape Town, South Africa, (1984)

30 T.SHIMANOUCHI AND I.NAKAGAWA,
Spectrochim. Acta, **18** (1962) 89, **22** (1966) 759

31 B.N.CYVIN, S.J.CYVIN, K.H.SCHMIDT, W.WIEGELER
AND A.MÜLLER,
J. Mol. Struct., **30** (1976) 315

32 B.N.CYVIN, S.J.CYVIN, K.H.SCHMIDT AND A.MÜLLER,
J. Mol. Struct., **32** (1976) 269

33 K.H.SCHMIDT AND A.MÜLLER,
Inorg. Chem., **14** (1975) 2183

34 K.H.SCHMIDT AND A.MÜLLER,
Coord. Chem. Rev., **19** (1976) 41

35 S.SUZUKI AND W.J.ORVILLE-THOMAS,
J. Mol. Struct., **37** (1977) 321

36 M.J.DECKER, D.O.K.FJELDSTED, S.R.STOBART AND M.J.ZAWAROTKO,
J. Chem. Soc. (Chem. Commun.), 1525 (1983)

37 S.PINCHAS AND I.LAUCHLICT,
"Infrared Spectra of Labelled Compounds", Academic Press, London, (1971)

38 R.G.PEARSON,
J. Chem. Educ., **45** (1968) 581, 643

39 B.F.G.JOHNSON, J.LEWIS AND P.W.ROBINSON,
J. Chem Soc., **A** (1969) 2693

40 P.L.GOGGIN AND J.MINK,
Inorg. Chim. Acta, **34** (1979) 225

41 A.ALLERHAND, H.S.GUTOWSKY, J.JONAS AND R.A.MEINZER,
J. Amer. Chem. Soc., **88** (1966) 3185

42 C.W.HAIGH,
Annu. Rep. NMR Spectrosc., **4** (1971) 311

43 D.S.STEPHENSON AND G.BINSCH,
J. Magn. Reson., **32** (1978) 145

44 R.CRAMER,
J. Amer. Chem. Soc., **86** (1964) 217

45 J.EVANS, B.F.G.JOHNSON, J.LEWIS, T.W.MATHESON AND J.R.NORTON,
J. Chem. Soc. (Dalton Trans.), (1978) 626

46 A.MAISONNAT AND R.POILBLANC,
Inorg. Chim. Acta, **29** (1978) 203

47 D.PARKER, J.M.LEHN AND J.RIMMER,
J. Chem. Soc. (Dalton Trans.), (1985) 1517

48 R.BONNAIRE, J.M.MANOLI, C.POTVIN, N.PLATZER, N.GOASDOUE AND D.DAVOUST,
Inorg. Chem., **21** (1982) 2032

49 L.M.JACKMAN AND F.A.COTTON (EDS.),
"Dynamic Nuclear Magnetic Resonance Spectroscopy",
Academic Press, New York, (1975) p.299

50 D.S.STEPHENSON AND G.BINSCH,
DNMR5, **QCPE 11** (1978) 365

51 A.ALLERHAND AND E.THIELE,
J. Chem. Phys., **45** (1966) 902

52 M.GREEN, R.M.MILLS, G.N.PAIN, F.G.A.STONE AND P.WOODWARD
J. Chem. Soc. (Dalton Trans.), (1982) 1309

53 G.A.FOULDS, G.E.JACKSON AND D.A.THORNTON,
J. Mol. Struct., **98** (1983) 323

54 G.A.FOULDS, P.S.HALL AND D.A.THORNTON,
J. Mol. Struct., **161** (1987) 237

APPENDIX 1

```
**********************************************************************
**********************************************************************
**************                          ******************************
**************    C A R T  program      ******************************
**************                          ******************************
**********************************************************************
**********************************************************************

 PURPOSE  calculation of unitvectors, carthesian coordinates
          and interatomic distances of molecules from their
          internal coordinates

   INPUT
   =====
          TITLE      maximum 80 characters                [20A4]
          NA, ND     NA  number of atoms to be read in    [20I3]
                     ND  number dummy atoms
          I1(I), I2(I), ALFA(I), BETA(I), R(I)            [2I3,10X,3F16.0]
                     I1(I)  number of concerning atom
                     I2(I)  number of atom bonded to I1(I)
                     ALFA(I)  bond angle in decimal units
                     BETA(I)  dihedral angle in decimal units
                     R(I)   distance between I1(I) AND I2(I)
          ID(I)      numbers of dummy atoms                [20I3]
          NAN(I), I=1, NAll  atomic numbers of the atoms   [20I3]
$$$$$$$$$$$$$$$$$$$$$$$$$$$$$$$$$$$$$$$$$$$$$$$$$$$$$$$$$$$$$$$$$$$$$$$$$$
 WRITTEN BY DR. B.J.VANDERVEKEN, LABO ANORGANISCHE CHEMIE, RUCA
 UNIVERSITY OF ANTWERP, BELGIUM
 MODIFIED FOR SPERRY-UNIVAC 1100
 BY PAUL VERHOEVEN, INORGANIC CHEMISTRY DEPT.,
 UNIVERSITY OF CAPE TOWN
 LITERATURE  H. BRADFORD THOMPSON, J. Chemical Physics, vol 47, nr 9, 1967
**********************************************************************
     DIMENSION I1(30),I2(30),R(435),ALFA(30),BETA(30),TRANS(480),
    1T(16),S(16),U(16),TITLE(20),IA(435),IB(435)
     DIMENSION IS(435),ID(10),RSOR(435),IDD(435)
     DIMENSION NAN(30)
000 FORMAT(20A4)
001 FORMAT(20I3)
003 FORMAT(2I3,10X,3F16.0)
000 FORMAT(1H ,1X,I3,7X,I3,8X,F14.9,7X,F14.9,8X,F8.5)
001 FORMAT(1H ,20(I3,2X))
003 FORMAT(1H ,'X',4(3X,F12.8,4X))
004 FORMAT(1H ,'Y',4(3X,F12.8,4X))
005 FORMAT(1H ,'Z',4(3X,F12.8,4X),/,/)
010 FORMAT(5(1X,I2,'-',I2,2X,F8.5,2X))
000 FORMAT(1H1,'MOLECULAR GEOMETRY',5X,20A4,/,1H ,18(1H=),/)
001 FORMAT(1H ,'DATA STRUCTURE',/,1H ,14(1H=),/)
002 FORMAT(1H ,'ATOM',3X,'ATTACHED TO',6X,'BOND ANGLE',11X,'DIHEDRAL A
   1NGLE',8X,'DISTANCE',/)
003 FORMAT(//,1H ,'DUMMY ATOMS',/,1H ,11(1H=),/)
005 FORMAT(1H1)
006 FORMAT(1H ,'ATOM',2X,I3,/,1H ,4(1H=))
007 FORMAT(1H ,2X,'UNIT VECTOR  X',5X,'UNIT VECTOR  Y',5X,'UNIT VECTOR
   1  Z',7X,'COORDINATES',/)
008 FORMAT(1H1,'DISTANCES',/,1H ,9(1H=),/)
010 FORMAT(//,1X,'ATOMIC NUMBERS',/,1X,14('='),/)
```

```
      MR = 5
      MW = 6
C
C
C  READING DATA
C
      READ(MR,1000)(TITLE(I),I=1,20)
      READ(MR,1001)NA,ND,NASH
      NA11 = NA+1
      DO 70 I = 1,NA
      READ(MR,1003)I1(I),I2(I),ALFA(I),BETA(I),R(I)
   70 CONTINUE
      READ(MR,1001)(ID(I),I=1,ND)
      READ(MR,1001)(NAN(I),I=1,NA11)
      WRITE(MW,3000)(TITLE(I),I = 1,20)
      WRITE(MW,3001)
      WRITE(MW,3002)
      DO 80 I = 1,NA
      WRITE(MW,2000) I1(I),I2(I),ALFA(I),BETA(I),R(I)
   80 CONTINUE
      WRITE(MW,3003)
      WRITE(MW,2001) (ID(I),I = 1,ND)
      WRITE(MW,3010)
      WRITE(MW,2001) (NAN(I),I = 1,NA11)
C
C  ANGLES IN RADIANT
C
      A = .017453292
      DO 90 I = 1,NA
      ALFA(I) = A*ALFA(I)
      BETA(I) = A*BETA(I)
   90 CONTINUE
C
C  INITIALIZE TRANSFORMATIONMATRIX FOR ATOM 1
C
      DO 110 I = 1,16
      TRANS (I) = .0
  110 CONTINUE
      DO 200 I = 1,NA
C
C  CONSTRUCTION TRANSFORMATIONMATRIX FOR ATOM 1
C
      ALF = ALFA(I)
      BET = BETA(I)
      RI = R(I)
      CA = COS(ALF)
      SA = SIN(ALF)
      CB = COS(BET)
      SB = SIN(BET)
      T(1) = -CA
      T(2) = SA*CB
      T(3) = SA*SB
      T(4) = .0
      T(5) = -SA
      T(6) = -CA*CB
      T(7) = -CA*SB
```

```
      T(8) = .0
      T(9) = .0
      T(10) = -SB
      T(11) = CB
      T(12) = .0
      T(13) = -RI*CA
      T(14) = RI*SA*CB
      T(15) = RI*SA*SB
      T(16) = 1.
C
C  SEARCH FOR ATOM BONDED TO ATOM 1
C
      IAT2 = I2(I)
      IF (IAT2-1) 120,115,120
  115 DO 116 J = 1,16
      U(J) = T(J)
  116 CONTINUE
      GO TO 160
C
C  SEARCH FOR PREVIOUS TRANSFORMATION
C
  120 DO 130 J = 1,16
      IR = 16*(IAT2-1)+J
      S(J) = TRANS(IR)
  130 CONTINUE
      DO 140 J = 1,16
      U(J) = .0
  140 CONTINUE
      DO 150 J = 1,4
      DO 150 K = 1,4
      JK = 4*(K-1)+J
      DO 150 L = 1,4
      JL = 4*(L-1)+J
      LK = 4*(K-1)+L
      U(JK) = U(JK)+S(JL)*T(LK)
  150 CONTINUE
C
C  STORE TRANSFORMATION OF ATOM 1
C
  160 IAT1 = I1(I)
      DO 170 J = 1,16
      IR = 16*(IAT1-1)+J
      TRANS(IR) = U(J)
  170 CONTINUE
  200 CONTINUE
C
C  SHIFT OF ORIGION
C
      IF (NASH) 209,209,201
  201 NASHX = 16*(NASH-1)+13
      NASHY = NASHX+1
      NASHZ = NASHX+2
      XNASH = TRANS(NASHX)
      YNASH = TRANS(NASHY)
      ZNASH = TRANS(NASHZ)
      DO 202 I = 1,NA11
      IXX = 16*(I-1)+13
      IYY = IXX+1
      IZZ = IXX+2
```

```
      TRANS(IXX) = TRANS(IXX)-XNASH
      TRANS(IYY) = TRANS(IYY)-YNASH
      TRANS(IZZ) = TRANS(IZZ)-ZNASH
  202 CONTINUE
  209 CONTINUE
C
C  WRITING UNITVECTORS AND COORDINATES
C
      WRITE(MW,3005)
      ITE = 0
      DO 300 I = 1,NA
      II = I+1
      ITE = ITE+1
      IF (ITE-6) 220,210,210
  210 ITE = ITE-5
      WRITE(MW,3005)
  220 WRITE(MW,3006) II
      WRITE(MW,3007)
      DO 300 J = 1,3
      IC = 16*I+J
      IX = IC
      IY = IC+4
      IZ = IC+8
      IK = IC+12
      A = TRANS(IX)
      B = TRANS(IY)
      C = TRANS(IZ)
      D = TRANS(IK)
      IF (J-1) 410,400,410
  400 WRITE(MW,2003) A,B,C,D
      GO TO 300
  410 IF (J-2) 420,415,420
  415 WRITE(MW,2004) A,B,C,D
      GO TO 300
  420 WRITE(MW,2005) A,B,C,D
  300 CONTINUE
C
C  CALCULATE DISTANCES
C
      NA = NA+1
      IT = 0
      DO 520 I = 1,NA
      J = I + 1
      DO 520 K = J,NA
      IT = IT+1
      IA(IT) = I
      IB(IT) = K
      IF (NAN(I)-NAN(K)) 515,515,516
  515 IS(IT) = 100*NAN(I)+NAN(K)
      GO TO 517
  516 IS(IT) = 100*NAN(K)+NAN(I)
  517 SUM = .0
      DO 510 L = 1,3
      IP = 16*(I-1)+12+L
      IQ = 16*(K-1)+12+L
```

```
      SUM = SUM+(TRANS(IP)-TRANS(IQ))**2.
  510 CONTINUE
      R(IT) = SQRT(SUM)
  520 CONTINUE
      IT = IT-1
C
C  WRITING DISTANCES
C
      WRITE(MW,3008)
      WRITE(MW,2010)(IA(I),IB(I),R(I),I = 1,IT)
      CALL SORB (R,IS,IT,RSOR,IA,IB,IDD,NSOR)
      WRITE(MW,3011)
 3011 FORMAT(1H1,'GESORTEERDE AFSTANDEN',/,1H ,21('='),/)
      DO 550 I = 1,NSOR
      WRITE(MW,3012)IA(I),IB(I),IDD(I),RSOR(I)
 3012 FORMAT(1H ,3(I4,3X),F12.8)
  550 CONTINUE
      STOP       'NORMAL PROGRAM TERMINATION'
      END
```

```
C*************************************************************************
C*************************************************************************
C*************************************************************************
C**************                                  *************************
C**************    G  -  M A T R I X             *************************
C**************                                  *************************
C*************************************************************************
C*************************************************************************
C*************************************************************************
C
C  PURPOSE  calculation of the coefficients of the kinetic energy
C  =======  matrix.       G = U.g.U°
C                         g = B.M-1.B°
C
C  INPUT          !!!Read operating instructions!!!
C  -----
C  K      NUMBER ATOMS IN MOLECULE
C  N      NUMBER STRETCH INTERNAL COORDINATES
C  M      NUMBER BEND INTERNAL COORDINATES
C  NOOP   NUMBER OUT-OF-PLANE WAG INTERNAL COORDINATES
C  NTOR   NUMBER TORSIONAL INTERNAL COORDINATES
C  L      NUMBER UNIT VECTORS
C  NS     TOTAL NUMBER SYMMETRY COORDINATES
C  R      VECTOR BOND LENGTHES
C  W      VECTOR ATOMIC MASSES
C  EV     UNIT VECTOR MATRIX
C
C  OUTPUT
C  ------
C  MATRIX 0  transformation matrix of internal coordinates into
C            symmetry coordinates
C  MATRIX 1  symmetrised G-matrix (dimension ns)
C  MATRIX 2  g-matrix in internal coordinates (dimension nm)
C
C$$$$$$$$$$$$$$$$$$$$$$$$$$$$$$$$$$$$$$$$$$$$$$$$$$$$$$$$$$$$$$$$$$$$$$$$$$
C WRITTEN IN THE INORGANIC CHEMISTRY LABORATORY, RUCA (BELGIUM)
C UNIVERSITY OF ANTWERP (FOR IBM 1100) BY DR. B.J. VANDERVEKEN
C MODIFIED BY PAUL VERHOEVEN
C  INORGANIC CHEMISTRY DEPT.
C  UNIVERSITY OF CAPE TOWN
C*************************************************************************
C
      DIMENSION R(10),EV(30),B(900),W(10),U(900),G(400),TITLE(20),
     1ICOF(10),COEF(10),ICOR(10),IHOEK(3)
    1 FORMAT(1H1,10X,'CALCULATION G MATRIX',5X,20A4,/,1H ,10X,20(1H=),/)
    2 FORMAT(1H ,5X,'STRETCHES',/,1H ,5X,9(1H=))
    4 FORMAT(1H1,5X,'SYMMETRY COORDINATES',/,1H ,5X,20(1H=),/)
    5 FORMAT(1H1,5X,'MATRIX U',/,1H ,5X,8(1H=))
    7 FORMAT(1H1,5X,'MATRIX G',/,1H ,5X,8(1H=))
    9 FORMAT(7F10.0)
   12 FORMAT(1H ,5X,I2,3X,I2)
   13 FORMAT(1H ,5X,I2,3X,I2,3X,I2)
   14 FORMAT(1H ,//,1H ,5X,'BENDS',/,1H ,5X,5(1H=))
   16 FORMAT(20A4)
   20 FORMAT(20I3)
   25 FORMAT(1H ,/,1H ,5X,10(F3.0,2X,I2,4X))
C
      MR = 5
      MW = 6
C
```

```
C  READING DATA
C
      READ(MR,16) TITLE
      WRITE(MW,1) TITLE
      READ(MR,20) K,N,M,NOOP,NTOR,L,NS
      NM = N+M+NOOP+NTOR
      NNM = N+M
      NNOOP = N+M+NOOP
      NL = K*3
      ISIZE = L*3
      ISIZ = NM*K*3
      READ(MR,9) (R(I),I = 1,L)
      READ(MR,9)(W(I),I = 1,K)
      CALL MATIN(ICODE,EV,ISIZE,L,3,IS,IER)
      DO 11 I = 1,ISIZ
      B(I) = 0.
   11 CONTINUE
      WRITE(MW,2)
C
C  CONSTRUCTION OF B STRETCH
C
      IF (N) 482,482,481
  481 CONTINUE
      DO 10 I = 1,N
      READ(MR,20) NA,NB,NC
      WRITE(MW,12) NA,NB
      DO 10 J = 1,3
      IJ = NM*(3*(NA-1)+J-1)+I
      IK = NM*(3*(NB-1)+J-1)+I
      IL = L*(J-1)+NC
      B(IJ) = EV(IL)
      B(IK) = -EV(IL)
   10 CONTINUE
      WRITE(MW,14)
C
C  CONSTRUCTION OF B BEND
C
  482 IF (M) 484,484,483
  483 CONTINUE
      N=N+1
      DO 400 I=N,NNM
      READ(MR,20) NA,NB,NC,ND,NE,NF
      WRITE(MW,13) NA,NB,NC
      NG = ND/IABS(ND)
      NH = NE/IABS(NE)
      ND = IABS(ND)
      NE = IABS(NE)
C
C  JUDGEMENT OF ANGLE
C
      IF (NF) 300,100,200
C
C  TETRAHEDRAL ANGLE
C
  100 S = SQRT(8./9.)
      C = -1./3.
      DO 110 J = 1,3
      IA = NM*(3*(NA-1)+J-1)+I
      IB = NM*(3*(NB-1)+J-1)+I
      IC = NM*(3*(NC-1)+J-1)+I
      NJ = L*(J-1)+ND
      NK = L*(J-1)+NE
```

```
      B(IA) = (1./(S*R(ND)))*(C*EV(NJ)*NG-EV(NK)*NH)
      B(IC) = (1./(S*R(NE)))*(C*EV(NK)*NH-EV(NJ)*NG)
      B(IB) = -B(IA)-B(IC)
  110 CONTINUE
      GO TO 400
C
C  RANDOM ANGLE
C
  200 READ(MR,20) (IHOEK(IABC),IABC = 1,3)
      HOEK = .017453292*FLOAT(IHOEK(1))+.000290888*FLOAT(IHOEK(2))+
     1.000004848*FLOAT(IHOEK(3))
      DO 210 J = 1,3
      IA = NM*(3*(NA-1)+J-1)+I
      IB = NM*(3*(NB-1)+J-1)+I
      IC = NM*(3*(NC-1)+J-1)+I
      NJ = L*(J-1)+ND
      NK = L*(J-1)+NE
      B(IA) =(1./(SIN(HOEK)*R(ND)))*(COS(HOEK)*EV(NJ)*NG-EV(NK)*NH)
      B(IC) =(1./(SIN(HOEK)*R(NE)))*(COS(HOEK)*EV(NK)*NH-EV(NJ)*NG)
      B(IB) = -B(IA)-B(IC)
  210 CONTINUE
      GO TO 400
C
C  LINEAR ANGLE
C
  300 READ(MR,20) NRA,NRB
      DO 310 J = 1,3
      IA = NM*(3*(NA-1)+J-1)+I
      IB = NM*(3*(NB-1)+J-1)+I
      IC = NM*(3*(NC-1)+J-1)+I
      NJ = L*(J-1)+ND
      NK = L*(J-1)+NE
      B(IA) = -EV(NJ)/R(NRA)
      B(IC) = -EV(NK)/R(NRB)
      B(IB) = -B(IA)-B(IC)
  310 CONTINUE
  400 CONTINUE
C
C  CONSTRUCTION OF  B OUT-OF-PLANE WAG
C
  484 IF (NOOP) 486,486,485
  485 CONTINUE
      WRITE(MW,1000)
      NNM = NNM+1
      DO 450 I = NNM,NNOOP
      READ(MR,20) NI,NJ,NK,NL,NIJ,NIK,NIL,MIJ,MIK,MIL
C  NI,NJ,NK,NL ARE ATOMIC NUMBERS
C  NIJ,NIK,NIL ARE BOND LENGTH NUMBERS
C  MIJ,MIK,MIL ARE UNIT VECTOR NUMBERS
      WRITE(MW,1010) NI,NJ,NK,NL
 1000 FORMAT(1H ,5X,'OUT-OF-PLANE BENDS',/,1H ,5X,18('='))
 1010 FORMAT(1H ,2X,(3X,I2))
      NG = MIJ/ABS(MIJ)
      NH = MIK/ABS(MIK)
      NT = MIL/ABS(MIL)
      MIJ = ABS(MIJ)
      MIK = ABS(MIK)
      MIL = ABS(MIL)
      IJX = NM*(3*(NJ-1))+I
      IJY = IJX+NM
      IJZ = IJY+NM
      IKX = NM*(3*(NK-1))+I
```

```
      IKY = IKX+NM
      IKZ = IKY+NM
      ILX = NM*(3*(NL-1))+I
      ILY = ILX+NM
      ILZ = ILY+NM
      JX = MIJ
      JY = JX+L
      JZ = JY+L
      KX = MIK
      KY = KX+L
      KZ = KY+L
      LX = MIL
      LY = LX+L
      LZ = LY+L
      B(IJX) = (EV(KY)*EV(LZ)-EV(KZ)*EV(LY))/R(NIJ)
      B(IJY) = (EV(KZ)*EV(LX)-EV(KX)*EV(LZ))/R(NIJ)
      B(IJZ) = (EV(KX)*EV(LY)-EV(KY)*EV(LX))/R(NIJ)
      B(IKX) = (EV(LY)*EV(JZ)-EV(LZ)*EV(JY))/R(NIK)
      B(IKY) = (EV(LZ)*EV(JX)-EV(LX)*EV(JZ))/R(NIK)
      B(IKZ) = (EV(LX)*EV(JY)-EV(LY)*EV(JX))/R(NIK)
      B(ILX) = (EV(JY)*EV(KX)-EV(JZ)*EV(KY))/R(NIL)
      B(ILY) = (EV(JZ)*EV(KX)-EV(JX)*EV(KZ))/R(NIL)
      B(ILZ) = (EV(JX)*EV(KY)-EV(JY)*EV(KX))/R(NIL)
      DO 440 J = 1,3
      III = NM*(3*(NI-1)+J-1)+I
      IIJ = NM*(3*(NJ-1)+J-1)+I
      IIK = NM*(3*(NK-1)+J-1)+I
      IIL = NM*(3*(NL-1)+J-1)+I
      B(IIJ) = B(IIJ)*FLOAT(NH)*FLOAT(NT)
      B(IIK) = B(IIK)*FLOAT(NG)*FLOAT(NT)
      B(IIL) = B(IIL)*FLOAT(NG)*FLOAT(NH)
      B(III) = -(B(IIJ)+B(IIK)+B(IIL))
  440 CONTINUE
  450 CONTINUE
  486 IF (NTOR) 488,488,487
  487 CONTINUE
 1060 FORMAT(7F10.0)
C
C  CONSTRUCTION OF B TORSION
C
      NNOOP = NNOOP+1
      WRITE(MW,1050)
 1050 FORMAT(1H ,5X,'TORSIES',/,1H ,5X,7('='))
      DO 480 I = NNOOP,NM
      READ(MR,20) NI,NJ,NK,NL,NIJ,NJK,NKL,MIJ,MJK,MKL
      READ(MR,1060) AIJK,AJKL
C  NI,NJ,NK,NL ARE ATOMIC NUMBERS
C  NIJ,NJK,NKL ARE BOND LENGTH NUMBERS
C  MIJ,MJK,MKL ARE UNIT VECTOR NUMBERS
C  AIJK,AJKL ARE VALENCE ANGLES
      WRITE(MW,1010) NI,NJ,NK,NL
      NG = MIJ/ABS(MIJ)
      NH = MJK/ABS(MJK)
      NT = MKL/ABS(MKL)
      MIJ = ABS(MIJ)
      NJK = ABS(MJK)
      MKL = ABS(MKL)
      IIX = NM*(3*(NI-1))+I
      IIY = IIX+NM
      IIZ = IIY+NM
      IJX = NM*(3*(NJ-1))+I
      IJY = IJX+NM
```

```
      IJZ = IJY+NM
      ILX = NM*(3*(NL-1))+I
      ILY = ILX+NM
      ILZ = ILY+NM
      IKX = NM*(3*(NK-1))+I
      IKY = IKX+NM
      IKZ = IKY+NM
      IX = MIJ
      IY = IX+L
      IZ = IY+L
      JX = MJK
      JY = JX+L
      JZ = JY+L
      KX = MKL
      KY = KX+L
      KZ = KY+L
      AI = R(NIJ)*(SIN(AIJK)**2)*FLOAT(NG)*FLOAT(NH)
      AJ =(R(NJK)-R(NIJ)*COS(AIJK))/(R(NJK)*R(NIJ)*(SIN(AIJK)**2))*FLOAT
     1(NG)*FLOAT(NH)
      BJ = COS(AJKL)/(R(NIK)*(SIN(AJKL)**2))*FLOAT(NH)*FLOAT(NT)
      AL = R(NKL)*(SIN(AJKL)**2)*FLOAT(NH)*FLOAT(NT)
      B(IIX) = -(EV(IY)*EV(JZ)-EV(IZ)*EV(JY))/AI
      B(IIY) = -(EV(IZ)*EV(JX)-EV(IX)*EV(JZ))/AI
      B(IIZ) = -(EV(IX)*EV(JY)-EV(IY)*EV(JX))/AI
      B(IJX) = (EV(IY)*EV(JZ)-EV(IZ)*EV(JY))*AJ
      B(IJX) = B(IJX)-(EV(JY)*EV(KZ)-EV(JZ)*EV(KY))*BJ
      B(IJY) = (EV(IZ)*EV(JX)-EV(IX)*EV(JZ))*AJ
      B(IJY) = B(IJY)-(EV(JZ)*EV(KX)-EV(JX)*EV(KZ))*BJ
      B(IJZ) = (EV(IX)*EV(JY)-EV(IY)*EV(JX))*AJ
      B(IJZ) = B(IJZ)-(EV(JX)*EV(KY)-EV(JY)*EV(KX))*BJ
      B(ILX) = (EV(JY)*EV(KZ)-EV(JZ)*EV(KY))/AL
      B(ILY) = (EV(JZ)*EV(KX)-EV(JX)*EV(KZ))/AL
      B(ILZ) = (EV(JX)*EV(KY)-EV(JY)*EV(KX))/AL
      B(IKX) = -(B(IIX)+B(IJX)+B(ILX))
      B(IKY) = -(B(IIY)+B(IJY)+B(ILY))
      B(IKZ) = -(B(IIZ)+B(IJZ)+B(ILZ))
  480 CONTINUE
  488 CONTINUE
      WRITE(MW,4)
C
C  CONSTRUCTION OF U MATRIX
C
      DO 70 I = 1,900
   70 U(I) = 0.
      DO 150 K = 1,NS
      READ(MR,20) (ICOF(I),ICOR(I),I = 1,10)
      DO 85 I = 1,10
   85 COEF(I) = FLOAT(ICOF(I))
      I = 1
   90 IF(COEF(I)) 120,130,120
  120 I = I+1
      GO TO 90
  130 L = I-1
      WRITE(MW,25) (COEF(J),ICOR(J),J = 1,L)
      SOM = 0.
      DO 140 J = 1,L
      SOM = SOM+COEF(J)*COEF(J)
  140 CONTINUE
      DO 150 J = 1,L
      COEF(J) = COEF(J)/(SQRT(SOM))
      IJ = NS*(ICOR(J)-1)+K
      U(IJ) = COEF(J)
```

```
  150 CONTINUE
      WRITE(MW,5)
      CALL MXOUT(0,U,NS,NM,0,40,132,1)
C
C   CALCULATION OF G MATRIX
C
      DO 520 I = 1,NS
      DO 520 J = I,NS
      IJ = NS*(J-1)+I
      JI = NS*(I-1)+J
      G(IJ) = 0.
      DO 520 IA = 1,NM
      ID = NS*(IA-1)+I
      IF (U(ID)) 600,520,600
  600 DO 520 IB = 1,NM
      IE = NS*(IB-1)+J
      IF (U(IE)) 610,520,610
  610 DO 520 IC = 1,NL
      IK = NM*(IC-1)+IA
      IL = NM*(IC-1)+IB
      IM = (IC-1)/3+1
      G(IJ) = G(IJ)+(U(ID)*U(IE)*B(IK)*B(IL))/W(IM)
      G(JI) = G(IJ)
  520 CONTINUE
C
C   WRITING OF RESULTS
C
      WRITE(MW,7)
      CALL MXOUT(1,G,NS,NS,0,40,120,1)
      STOP          'S T O P'
      END
```

```
C*****************************************************************
C*****************************************************************
C****                                                         ****
C***    M E T H O D  of  B E C H E R  and  M A T T E S        ***
C****                                                         ****
C*****************************************************************
C*****************************************************************
C     PURPOSE     CALCULATIONS OF FORCE CONSTANTS
C     =======     -------------------------------
C              INPUT
C              =====
C     TITLE                              [20A4]
C     N    ORDER OF G AND F MATRICES     [I3]
C     MO   NUMBER ITERATION S TEPS       [I3]
C     MATRIX G   (MATIN)
C     FREQ FREQUENCIES VECTOR   (IN CM-1)    [7F10.0]
C              OUTPUT
C              ======
C     MATRIX 1 G
C     FREQUENCIES   (IN CM-1)
C     MATRIX 2 FORCE CONSTANTS
C     MATRIX 3 NORMALIZED EIGENVECTORS
C     MATRIX 4 POTENTIAL ENERGY DISTRIBUTION
C$$$$$$$$$$$$$$$$$$$$$$$$$$$$$$$$$$$$$$$$$$$$$$$$$$$$$$$$$$$$$$$$
C     WRITTEN BY DR. B. VAN DER VEKEN, LABO ANORGANISCHE CHEMIE
C     UNIVERSITY OF ANTWERP (RUCA), BELGIUM (IBM 1100)
C     MODIFIED BY PAUL VERHOEVEN, INORGANIC CHEMISTRY DEPT, UCT
C     FOR THE SPERRY-UNIVAC 1100 COMPUTER
C     LITERATURE  BECHER, MATTES
C     SPECTROCHIM. ACTA, 23A(1967)2449
C*****************************************************************
      DOUBLE PRECISION G(1296), GI(1296), F(900), FA(900), EVEC(1296)
      DOUBLE PRECISION FREQ(36),EVAL(36)
      DIMENSION LA(36),LB(36),PED(36),TITLE(20)
 2000 FORMAT(I3)
 2005 FORMAT(20A4)
 2010 FORMAT(7F10.0)
 2015 FORMAT(1H1, 10X, 18H   FORCE CONSTANTS, 5X, 20A4, /,
     & 14X, 15(1H=), /)
 2020 FORMAT(7(3X, F8.2))
 2025 FORMAT(5X, 15HNUMBER OF STEPS, 5X, I2, /)
 2030 FORMAT(15X, 8HMATRIX G, /, 15X, 8(1H=))
 2035 FORMAT(////, 15X, 17HINPUT FREQUENCIES, /,
     & 15X, 17(1H=), /)
 2040 FORMAT(1H1, 15X, 15HFORCE CONSTANTS, /, 16X, 15(1H=))
 2045 FORMAT(1H1, 15X, 12HUNIT VECTORS, /, 16X, 12(1H"))
 2050 FORMAT(1H1, 15X, 29HPOTENTIAL ENERGY DISTRIBUTION, /,
     & 16X, 29(1H=), / , /)
 2055 FORMAT(1H , 'FREQUENCY', 36(4X, I2, 2X), /)
 2060 FORMAT(/, 1H , F8.2, 2X, 36(2X, F6.2))
 2065 FORMAT(1H , ' DETERMINANT IS ZERO ', /////)
```

```
*******  MR AND MW ARE THE LOGICAL UNIT NUMBERS        *******
*******  FOR THE READ AND WRITE STATEMENTS             *******
************************************************************
      MR=5
      MW=6

*******  READING AND PRINTING OF INPUTDATA             *******
************************************************************
      READ (MR, 2005) TITLE
      READ (MR, 2000) N
      READ (MR, 2000) MO
      ISIZE = N * N
      CALL MATIN  (ICODE, G, ISIZE, N, N, IS, IER)
      READ (MR, 2010) (FREQ(I), I = 1, N)
      WRITE (MW, 2015) TITLE
      WRITE (MW, 2025) MO
      WRITE (MW, 2030)
      CALL MXOUT  (1, G, N, N, 0, 40, 120, 1)
      WRITE (MW, 2035)
      WRITE (MW, 2020) (FREQ(I), I = 1, N)

*******  TRANSFORMING FREQUENCIES INTO EIGENVALUES     *******
************************************************************
      DO 10 I = 1, N
        FREQ(I) = (FREQ(I) * FREQ(I)) / (1303.16 ** 2.)
   10 CONTINUE

*******  INITIALIZE THE STARTING  Fo-MATRIX OF         *******
*******  THE UNCOUPLED VIBRATIONS                      *******
************************************************************
      DO 20 I = 1, ISIZE
        F(I) = 0.
   20 CONTINUE
      DO 30 I = 1, N
        II = N * (I-1)  +  I
        F(II) = FREQ(I) / G(II)
   30 CONTINUE

*******  START OF ITERATION CYCLE                      *******
************************************************************
      M = 0
   40 M = M + 1
      DO 50 I = 1, ISIZE
        FA(I) = F(I)
   50 CONTINUE
```

```
*******  STEPWISE INTRODUCTION OF THE NONDIAGONAL      *******
*******  G-MATRIX ELEMENTS                             *******
**************************************************************
      DO 60 I = 1, N
      DO 60 J = 1, N
        IJ = N * (J-1)  +  I
        IF (  I-J  .EQ.  0  )  THEN
            GI(IJ) = G(IJ)
            GO TO 60
        ELSE
*******     SQUARE-ROOT COUPLING FUNCTION          *************
            gi(ij) = sqrt(float(m) / float(mo)) * g(ij)
**************************************************************
        ENDIF
   60 CONTINUE

*******  COMPUTES THE EIGENVALUES AND EIGENVECTORS     *******
*******  OF THE NONSYMMETRIC  G-inverse * F  MATRIX    *******
**************************************************************
      CALL MINV  (GI, N, D, LA, LB)
      IF ( D .LE. 0 ) THEN
          WRITE (MW, 2065)
          STOP
      ELSE
          NN = N
          CALL NROOT  (NN, F, GI, EVAL, EVEC)
      ENDIF

*******  NORMALIZATION OF THE EIGENVECTORS             *******
*******  ACCORDING TO  L-transposed * F * L            *******
**************************************************************
      DO 75 I = 1, N
        SUM = 0.
        DO 70 K = 1, N
        DO 70 J = 1, N
          KI = N * (I-1)  +  K
          JI = N * (I-1)  +  J
          KJ = N * (J-1)  +  K
          SUM = SUM + EVEC(KI) * EVEC(JI) * FA(KJ)
   70   CONTINUE
      DO 75 J = 1, N
        JI = N * (I-1)  +  J
        EVEC(JI) = EVEC(JI) * SQRT(EVAL(I) / SUM)
   75 CONTINUE
```

```
*******  CALCULATION OF THE POTENTIAL ENERGY          *******
*******  DISTRIBUTION  (PED)                          *******
**************************************************************
      DO 86 J = 1, N
        DO 80 I = 1, N
          IJ = N * (J-1)  +  I
          II = N * (I-1)  +  I
          GI(IJ) = EVEC(IJ) * EVEC(IJ) * FA(II)
   80   CONTINUE
        SUM = 0.
        DO 83 I = 1, N
          IJ = N * (J-1)  +  I
          SUM = SUM + GI(IJ)
   83   CONTINUE
      DO 86 I = 1, N
        IJ = N * (J-1)  +  I
        GI(IJ) = GI(IJ) * 100./SUM
   86 CONTINUE

*******  ORDERING OF THE COORDINATES AND FREQUENCIES  *******
*******  ACCORDING TO PED                             *******
**************************************************************
      DO 99 I = 1, N
        J = 1
        K = J
   90   K = K + 1
        IK = N * (I-1)  +  K
        IJ = N * (I-1)  +  J
        IF (  GI(IJ)-GI(IK)  .LT.  0  )  THEN
            IF ( K-N .LT. 0 ) THEN
                J = K
                GO TO 90
            ELSE
                DO 93 L = 1, N
                  LK = N * (K-1)  +  L
                  LI = N * (I-1)  +  L
                  FA(LK) = EVEC(LI)
   93           CONTINUE
            ENDIF
            GO TO 99
        ELSE
            IF ( K-N .LT. 0 ) THEN
                GO TO 90
            ELSE
                DO 96 L = 1, N
                  LJ = N * (J-1)  +  L
                  LI = N * (I-1)  +  L
                  FA(LJ) = EVEC(LI)
   96           CONTINUE
            ENDIF
        ENDIF
   99 CONTINUE
```

```
*******  CALCULATION OF THE F-MATRIX                          *******
*******  F  =  (L-inverse)-transp * FREQ * (L-inverse)  *****
**************************************************************
      CALL MINV  (FA, N, D, LA, LB)
      DO 100 I = 1, N
      DO 100 J = 1, N
        IJ = N * (J-1)  +  I
        F(IJ) = 0.
      DO 100 K = 1, N
        KI = N * (I-1)  +  K
        KJ = N * (J-1)  +  K
        F(IJ) = F(IJ)  +  FA(KI) * FA(KJ) * FREQ(K)
  100 CONTINUE

*******  DECISION OF ITERATION CYCLE                          *******
**************************************************************
      IF (  MO-M  .GT.  0  )  THEN
          GO TO 40
      ELSE

*******  FINAL COMPUTATION OF THE EIGENVALUES AND      *******
*******  THE EIGENVECTORS OF   G-inverse * F           *******
**************************************************************
           DO 110 I = 1, ISIZE
             FA(I) = F(I)
  110      CONTINUE
           CALL MINV  (G, N, D, LA, LB)
           NN = N
           CALL NROOT  (NN, F, G, EVAL, EVEC)
      ENDIF

*******  FINAL NORMALIZATION OF THE EIGENVECTORS       *******
*******  ACCORDING TO   L-transposed * F * L           *******
**************************************************************
      DO 125 I = 1, N
        SUM = 0.
        DO 120 K = 1, N
        DO 120 J = 1, N
          KI = N * (I-1)  +  K
          JI = N * (I-1)  +  J
          KJ = N * (J-1)  +  K
          SUM = SUM + EVEC(KI) * EVEC(JI) * FA(KJ)
  120   CONTINUE
      DO 125 J = 1, N
        JI = N * (I-1)  +  J
        EVEC(JI) = EVEC(JI) * SQRT(EVAL(I) / SUM)
  125 CONTINUE
```

```
*******  FINAL CALCULATION OF THE POTENTIAL ENERGY     *******
*******  DISTRIBUTION                                  *******
**************************************************************
      DO 136 J = 1, N
        DO 130 I = 1, N
          IJ = N * (J-1)  +  I
          II = N * (I-1)  +  I
          GI(IJ) = EVEC(IJ) * EVEC(IJ) * FA(II)
  130   CONTINUE
        SUM = 0.
        DO 133 I = 1, N
          IJ = N * (J-1)  +  I
          SUM = SUM + GI(IJ)
  133   CONTINUE
      DO 136 I = 1, N
        IJ = N * (J-1)  +  I
        GI(IJ) = GI(IJ) * 100./SUM
  136 CONTINUE

*******  PRINTING OF OUTPUT                            *******
**************************************************************
      WRITE (MW, 2040)
      CALL MXOUT  (2, FA, N, N, 0, 40, 120, 1)
      WRITE (MW, 2045)
      CALL MXOUT  (3, EVEC, N, N, 0, 40, 120, 1)
      WRITE (MW, 2050)
      WRITE (MW, 2055) (I, I = 1, N)
      DO 140 I = 1, N
        EVAL(I) = 1303.16 * SQRT( EVAL(I) )
  140 CONTINUE
      DO 155 J = 1, N
      DO 150 I = 1, N
      IJ = N * (J-1)  +  I
  150 PED(I) = GI(IJ)
      WRITE (MW, 2060) EVAL(J), (PED(I), I = 1, N)
  155 CONTINUE
      STOP    'NORMAL TERMINATION'
      END
```

```
C*************************************************************
C*******                                              *******
C******* G F - MATRIX,  EIGENVALUES AND EIGENVECTORS *******
C*******                                              *******
C*************************************************************
C     purpose: calculation of frequencies and L-matrix
C              if the G and F matrices are given
C
C     INPUT
C     -----
C        N     ORDER OF THE G AND F MATRICES (SYMMETRIC)  [I3]
C        G-MATRIX   (READ IN BY MATINROUTINE)
C        F-MATRIX   (          "             )
C     OUTPUT
C     ------
C        MATRIX 1    G-MATRIX      (PRINTED BY MXOUTROUTINE)
C        MATRIX 2    F-MATRIX      (          "             )
C        MATRIX 3    GF-MATRIX     (          "             )
C        FREQUENCIES   (IN CM-1)
C        MATRIX 5    EIGENVECTORS                    ( " )
C        MATRIX 6    NORMALIZED EIGENVECTORS         ( " )
C$$$$$$$$$$$$$$$$$$$$$$$$$$$$$$$$$$$$$$$$$$$$$$$$$$$$$$$$$$$$
C     PROGRAMMED BY PAUL VERHOEVEN, INORGANIC CHEMISTRY DEPT.
C     UNIVERSITY OF CAPE TOWN (SPERRY-UNIVAC 1100 COMPUTER)
C*************************************************************
      DOUBLE PRECISION G(900),F(900),GF(900),EVAL(900),EVEK(900)
      DOUBLE PRECISION FA(900),FREQ(900)
      DIMENSION LA(900),LB(900)
   15 FORMAT(1H , 5X, 6F10.2, /, 6X, 6F10.2, /, 6X, 6F10.1)
   25 FORMAT(1H , 15X, 11HEIGENVALUES, /, 16X, 11(1H=), /)
   35 FORMAT(1H1, 15X, 9HGF-MATRIX, /, 16X, 9(1H=))
   45 FORMAT(1H , ' DETERMINANT IS ZERO ', /////)
   55 FORMAT(1H1, 15X, 12HEIGENVECTORS, /, 16X, 12(1H=))
   65 FORMAT(1H1, 15X, 31HEIGENVECTORS NORMALIZED BY L'FL, /,
     &16X, 31(1H=) )

*****    MR AND MW THE LOGICAL UNIT NUMBERS    **************
*****    FOR READ AND WRITE STATEMENTS         **************
*****    READING OF THE INPUTDATA              **************
*************************************************************
      MR = 5
      MW = 6
      READ (MR, 5) N
      ISIZE = N * N
      CALL MATIN  (ICODE, G, ISIZE, N, N, IS, IER)
      CALL MATIN  (ICODE, F, ISIZE, N, N, IS, IER)

*****    CALCULATES THE PRODUCT MATRIX GF      **************
*************************************************************
      DO 10 I = 1, ISIZE
        FA(I) = F(I)
   10 CONTINUE
      DO 20 I = 1, N
      DO 20 K = 1, N
        KI = N * (I-1) + K
        GF(KI) = 0.
      DO 20 J = 1, N
        JI = N * (I-1) + J
        KJ = N * (J-1) + K
        GF(KI) = GF(KI) + G(KJ) * F(JI)
```

```
   20 CONTINUE



*****    COMPUTES THE DETERMINANT D                    **************
*****    AND THE INVERSE OF G-MATRIX                   **************
*****************************************************************
      CALL MINV  (G, N, D, LA, LB)
      IF ( D .LE. 0 ) THEN
          WRITE (MW, 45)
          STOP
      ELSE

*****    COMPUTES THE EIGENVALUES AND                  **************
*****    THE EIGENVECTORS OF THE REAL                  **************
*****    NONSYMMETRIC MATRIX G-INVERSE * F             **************
*****************************************************************

          NN = N
          CALL NROOT  (NN, F, G, EVAL, EVEK)
      ENDIF

*****    NORMALIZATION OF THE EIGENVECTORS             **************
*****    BY L-TRANSPOSED * F * L                       **************
*****************************************************************
      DO 40 I = 1, N
        SUM = 0.
        DO 30 K = 1, N
        DO 30 J = 1, N
          KI = N * (I-1) + K
          JI = N * (I-1) + J
          KJ = N * (J-1) + K
          SUM = SUM + EVEK(KI) * EVEK(JI) * FA(KJ)
   30 CONTINUE
      DO 40 J = 1, N
        JI = N * (I-1) + J
        EVEK(JI) = EVEK(JI) * SQRT( EVAL(I) / SUM )
   40 CONTINUE

*****    PRINTING OF THE INPUT AND OUTPUTDATA  **************
*****************************************************************
      CALL MXOUT  (1, G, N, N, 0, 40, 120, 1)
      CALL MXOUT  (2, F, N, N, 0, 40, 120, 1)
      WRITE (MW, 35)
      CALL MXOUT  (3, GF, N, N, 0, 40, 120, 1)
      WRITE (MW, 25)
      DO 50 I = 1, N
        FREQ(I) = 1303.16 * SQRT( EVAL(I) )
   50 CONTINUE
      WRITE (MW, 15) (FREQ(I), I = 1, N)
      WRITE (MW, 55)
      CALL MXOUT  (5, EVEK, N, N, 0, 40, 120, 1)
      WRITE (MW, 65)
      CALL MXOUT  (6, EVEK, N, N, 0, 40, 120, 1)
      STOP      'stop'
      END
```

APPENDIX 2

```
      PROGRAM DNMR5(BAND,INPUT,OUTPUT,PUNCH,ZZZG67,TAPE11=BAND,
     1TAPE5=INPUT,TAPE6=OUTPUT,TAPE7=PUNCH,TAPE67=ZZZG67)

      PROGRAM FOR ITERATIVE ANALYSIS OF EXCHANGE BROADENED NMR SPECTRA

      DAVID S. STEPHENSON AND GERHARD BINSCH                MUENCHEN 1978

      COMMON/CB10/IN,IO,IOP,INT
      DATA IN,IO,IOP,INT/8,5,9,11/
      PRINT*, 'START OF RUN'
    1 CALL INITAL
      CALL DNMR3
      CALL SPECT
      GO TO 1
      INPUT IS AS FOLLOWS
      1.    TEXT                                                  (8A10)
            PROBLEM NAME, IF FIRST FIELD BLANK THEN END OF RUN
      2.    N,NE,MU,NMES,NSYM                                     (5I2)
            N=NUMBER OF NUCLEI
            NE=NUMBER OF NUCLEAR CONFIGURATIONS
            MU=1 FOR MUTUAL EXCHANGE,=0 OTHERWISE
            NMES=NUMBER OF SETS OF MAGNETICALLY EQUIVALENT NUCLEI,
            NMES MUST INCLUDE ALL SETS OF MAGNETICALLY EQUIVALENT
            NUCLEI EVEN THE TRIVIAL SETS CONTAINING ONLY ONE NUCLEUS
            THUS IF THE OPTION IS NOT TO BE USED THEN NMES=N
            NSYM=NUMBER OF SYMMETRY PAIRS. A SYMMETRY PAIR IS DEFINED
            AS TWO NUCLEI RELATED BY PERMUTATION SYMMETRY.
            NSYM=0 IF NO SYMMETRY
            NOTE.  THE SYMMETRY AND MAGNETIC EQUIVALENCE OPTIONS
            CANNOT BE USED SIMULTANEOUSLY
      3.    ITMAX,SETOUT,SCAF                                     (I5,2F10)
            ITMAX=MAXIMUM NUMBER OF ITERATIONS, IF BLANK THEN SET EQUAL
            TO 10. IF ITMAX.LT.0 THEN SIMULATION ONLY
            SETOUT=RATIO(REDUCTION IN ERROR/ERROR) AT WHICH ITERATION
            IS TERMINATED
            SCAF=STEP MULTIPLICATION FACTOR ( USUALLY=1.0 )
      4.    IDATA,IPRINT,IPLOT,IPUNCH,NO,SCAL,HEIGHT,SF(1),SF(NO)
            IDATA=0 IF SPECTRUM ON TAPE, OR 1 IF ON CARDS (4I1,I6,4F10)
            OR 2 IF USING THE TAPE SIMULATION TEST DECK
            IPRINT=1 IF INPUT AND OUTPUT SPECTRA TO BE PRINTED, ELSE 0
            IPLOT=0 IF NO PLOT OUTPUT, =1 IF PLOT OF ORIGINAL SPECTRUM
            ONLY, =2 IF PLOT OF SMOOTHED SPECTRUM ONLY, =3 IF PLOT OF
            ORIGINAL AND SMOOTHED ON SEPARATE SHEETS, =4 IF PLOT OF
            SIMULATED SPECTRUM ONLY, =5 IF PLOT OF ORIGINAL AND
            SIMULATED ON SEPARATE SHEETS, =6 IF PLOT OF SMOOTHED AND
            SIMULATED ON SEPARATE SHEETS, =7 IF PLOT OF ORIGINAL, SMOOTH
            AND SIMULATED ALL ON SEPARATE SHEETS, =8 IF PLOT OF SIMULATE
            ON ORIGINAL, AND =9 IF PLOT OF SIMULATED ON SMOOTHED.
            IPUNCH=1 IF SPECTRAL OUTPUT ON CARDS, ELSE 0
            NO=NUMBER OF SPECTRAL POINTS IN SIMULATION
            SCAL=PLOT SCALING FACTOR IN HZ/MM
            HEIGHT IS THE MAXIMUM SPECTRUM HEIGHT IN MM. FOR CARD
            INPUT OR SIMULATION THIS IS ONLY PERTINENT TO PLOT OR
            PUNCH OUTPUT. HOWEVER FOR TAPE INPUT, THE SPECTRUM
            INTENSITY VALUES ARE ALL SCALED SO THAT THE DIFFERENCE
            BETWEEN THE GREATEST AND LEAST IS EQUAL TO HEIGHT.
            THIS THEREFORE AFFECTS BALIC, BATILT, AND THE ERROR VALUE
            WHICH BECOME PROPORTIONAL TO HEIGHT.
            SF(1)=FREQUENCY OF FIRST POINT IN SIMULATED SPECTRUM
```

```
      SF(NO)=FREQUENCY OF LAST POINT IN SIMULATED SPECTRUM
      NO,SF(1),SF(NO) BLANK IF ITMAX.GE.0
      PRINT AND PUNCH OPTIONS ONLY APPLY WHEN ITMAX.LT.0
      OR IDATA.EQ.1
      PLOT OPTIONS 1 TO 9 ARE EQUIVALENT FOR ITMAX.LT.0 AND
      FOR IDATA.EQ.1 AND ALL RESULT IN PLOT OF SIMULATED SPECTRUM
5.    NNMES(I),I=1,NMES                                        (5I1)
      NUMBER OF NUCLEI IN MAGNETICALLY EQUIVALENT SET I
      OMIT IF NMES=N
6.    W(I,J),J=1,NMES                                          (5F10)
      CHEMICAL SHIFTS IN HZ FOR NUCLEAR CONFIGURATION I,
      IF NSYM.NE.0 THE LABELING MUST BE CHOSEN SO THAT ALL
      SYMMETRY PAIRS PRECEDE THOSE SPINS NOT RELATED BY SYMMETRY
7.    NEXT SET OF CARDS INPUT COUPLING CONSTANTS (HZ) FOR
      NUCLEAR CONFIGURATION I
      AJ(I,J,K),....                                           (4F10)
      FIRST CARD AJ(I,1,2),AJ(I,1,3),.....AJ(I,1,NMES)
      SECOND CARD AJ(I,2,3),AJ(I,2,4),.....AJ(I,2,NMES)
      ETC.
      LAST CARD AJ(I,NMES-1,NMES)
      SKIP 7 IF NMES=1
8.    IF MU=0 REPEAT 6 AND 7 FOR ALL NUCLEAR CONFIGURATIONS I
9.    IF MU=1 READ IN EXCHANGE VECTORS FOR MUTUAL EXCHANGE
      ONE VECTOR PER CARD
      IE(I,K),K=1,NMES                                         (5I1)
      FIRST CARD - SECOND EXCHANGE VECTOR
      SECOND CARD - THIRD EXCHANGE VECTOR
      ETC.
      THE INTEGER ELEMENTS OF THE NTH EXCHANGE VECTOR REPRESENT
      THE LABELING OF THE NUCLEI (OR THE LABELING OF THE SETS IF
      EQUIVALENCE IS USED) IN THE NTH CONFIGURATION IN TERMS OF
      THE CONSECUTIVE LABELING IN THE FIRST CONFIGURATION
10.   IF MU=0 READ IN POPULATIONS OF NUCLEAR CONFIGURATIONS
      POP(I),I=1,NE                                            (4F10)
11.   T2(I),I=1,NE                                             (4F10)
      THE RELAXATION TIMES OF THE INDIVIDUAL NUCLEAR CONFIGS.
12.   RC(I,J)                                                  (F10)
      RATE CONSTANTS IN 1/SEC ONE PER CARD
      CARD SEQUENCE IS RC(1,2),RC(1,3),...RC(1,NE),RC(2,3),..
      IF MU=1 THIS SET CONSISTS OF SINGLE CARD RC(1,2) ONLY
      SKIP IF NE.EQ.1
13.   BALIC,BATILT                                             (2F10)
      BALIC=BASELINE INCREMENT
      BATILT=BASELINE TILT
14.   IF ITMAX.LT.0 RETURN TO 1.
15.   X0,UM,SWEEPW                                             (3F10)
      X0=FREQUENCY OF ORIGIN POINT, FOR CARD INPUT THIS IS
      EQUIVALENT TO THE "ZEROTH" POINT, FOR TAPE INPUT IT IS
      THE FREQUENCY OF THE FIRST POINT ON THE TAPE
      UM=CONVERTING FACTOR, I.E. FREQUENCY SEPARATION OF TWO
      ADJACENT SPECTRAL POINTS. POSITIVE IF POINT NUMBERING IS
      IN THE NEGATIVE FREQUENCY DIRECTION, NEGATIVE OTHERWISE
      LEAVE BLANK IF IDATA.EQ.0 OR IDATA.EQ.2
      SWEEPW=FREQUENCY WIDTH OF SPECTRUM RECORDED ON TAPE
      LEAVE BLANK IF IDATA.EQ.1
16.   IF IDATA.EQ.0 OR 2 READ IN SPECTRAL CONTROLS FOR TAPE
      NS,NOF,FSNOIS,FENOIS,FSTRUN,FETRUN                       (2I5,4F10)
      NS=SMOOTHING FACTOR, WHERE INITIAL SMOOTHING OCCURS
      OVER (2*NS+1) POINTS
      NOF=NUMBER OF FINAL SMOOTHED AND TRUNCATED POINTS
      REQUIRED (LESS THAN 1025)
      FSNOIS=FREQUENCY STARTING POINT FOR NOISE MEASUREMENT
```

```
      FENOIS=FREQUENCY ENDING POINT FOR NOISE MEASUREMENT
      FSTRUN=FREQUENCY STARTING POINT FOR PRETRUNCATION
      FETRUN=FREQUENCY ENDING POINT FOR PRETRUNCATION
17.   IF IDATA.EQ.2 READ IN THE TAPE SIMULATION DECK (10200F5) OR
      IF IDATA.EQ.1 READ AN EXPERIMENTAL SPECTRUM FROM CARDS. THIS
      CONSISTS OF UP TO 1024 POINTS IN ANY ORDER, BLANKS AND
      END OF CARDS ARE IGNORED. EACH PAIR IS III.NNN+ WHERE
      III IS A POINT NUMBER, AND NNN THE HEIGHT OF THE SPECTRUM
      ABOVE THE BASELINE AT THAT POINT, III AND NNN UP TO THREE
      DIGITS AND MAY BE NEGATIVE. SPECTRUM TERMINATED BY *.
18.   IF IDATA.EQ.1 READ IN AN ESTIMATED SPECTRAL NOISE VALUE
     RNOIS                                                    (F10)
19.  NLL(I),I=1,16                                            (16I3)
      THE NUMBERS OF THE PARAMETERS TO BE VARIED INDEPENDENTLY
      WHERE THE NUMBERING IS THAT SHOWN ON THE FIRST SIMULATION
20.  NSPL(I,J),J=1,10                                         (10I3)
      THE NUMBERS OF THE PARAMETERS TO BE VARIED BUT KEPT EQUAL
      TO AN INDEPENDENT PARAMETER IN LIST 19 ( IF NSPL NEGATIVE
      THEN PARAMETER KEPT EQUAL BUT OF OPPOSITE SIGN )
      I.E. IF 4 AND 5 KEPT EQUAL TO 2 THEN CARD IS 002004005
      A BLANK CARD TERMINATES THIS SEQUENCE
21.  PLL(I),PUL(I)                                            (2F10)
      LOWER AND UPPER LIMITS ON PARAMETERS. ONE CARD PER
      VARIED PARAMETER IN THE SAME ORDER AS IN LIST 19.
22.   RETURN TO 1
END
```